Peripheral Inflammatory and Regulatory Immune Changes in HIV positive to HIV positive Renal Transplant Recipients

Stefan Rautenbach

A dissertation submitted to the Faculty of Health Sciences, University of Cape Town, for the degree of Masters in Clinical Science and Immunology

ABSTRACT

INTRODUCTION

Since 2008, 43 renal transplants have been performed from HIV positive deceased donors to HIV positive recipients with renal failure predominantly due to HIV-associated Nephropathy (HIVAN). Recipients received Anti-thymocyte globulin (ATG) induction therapy and maintenance immunosuppression. Despite transplantation across Human Leukocyte Antigen (HLA) mismatches, there were few rejection events in the first year post-transplant (PT). Recipient CD4 counts did not decrease and HIV viral load also remained undetectable at one year PT. To gain insight into immune homeostatic mechanisms after ATG induction, immunosuppression and transplantation, a subset of 10 transplant recipients were investigated. This dissertation examined levels of peripheral inflammatory and regulatory cytokines. A polychromatic flow cytometry panel was also developed to measure the phenotypic T cell proportions of T regulatory cells (Tregs) in the blood circulation.

METHODOLOGY

A multiplexed Luminex assay was used to measure the concentrations of 67 inflammatory and regulatory plasma cytokines immediately pre-transplant, at 1, 3, 6 and 12 weeks PT. Two separate manufacturers of Luminex panels were used and a series of statistical analyses were employed to identify intra- and inter-plate variation. Firstly, data was cleaned up by excluding analytes for which

>90% of measured values were outside of the observable range of the standard curve. Secondly, the measurable values were assessed for differences between replicates (intra-plate variation). A Bland-Altman plot was used to identify and exclude highly divergent replicates of the same sample. Thirdly, a Paired T-test/Wilcoxon Signed Rank Test was used to investigate differences between inter-plate controls (inter-plate variation). Fold change from baseline was calculated for all values to correct for inter-plate variability.

After correcting for variability, fold change trends in all included analytes were examined for each recipient. Trends in recipients with rejection events (rejectors) and recipients without rejection events (non-rejectors) were also compared. Fold change from baseline was assessed to identify single analytes that differed over time using a Paired T-test/Wilcoxon Signed Rank Test. A hierarchical clustering analysis (HCA) was used to identify groups of analytes for which fold change may have been significantly influenced by age, sex, baseline CD4 count at transplantation (TP), number of HLA matches, or time. A mixed effect generalised linear model (MEGLM) was constructed to calculate differences between participants for each cytokine.

A polychromatic flow cytometry panel was devised to measure Treg CD4+ T cells consisting of the following antibodies: CD3-BV650, CD4-PE/Cy5.5, CD8-HorizonV500, CD27-PE/Cy5, CD45RA-PerCP/Cy5.5, CD25-BV421, CD127-PE/CF594, and FoxP3-Alexa647. Antibody concentrations in the panel were optimised by titrating each marker on resting, or Phytohaemagglutinin (PHA)

stimulated, peripheral blood mononuclear cells (PBMCs). The median fluorescent intensity (MFI) of the positive and negative populations for each marker was used to calculate the signal:noise ratio for all titrating volumes. The optimal volumes were determined by the highest signal:noise ratio for each marker.

RESULTS

In all recipients, when compared to baseline, IL-2, IFN-α2 and IFN-γ were significantly decreased at 12-weeks PT. IL-35 was significantly decreased at weeks 1, 3, 6 and 12 PT, whilst IL-10 increased significantly at 1-week PT in 5 recipients. Hierarchical clustering showed no association with analyte fold changes due to age, sex, CD4 count, or number of HLA matches. It did show a decrease over time in IL-35, IFN-γ, IL-20, IL-28A, and IL-11 for all 10 recipients.

A mixed-effects generalized model (MEGLM) was used to identify analytes with variable concentrations between recipients. It showed that the concentrations of IL-28A, IL-6Rα, IL-6Rβ, sTNFR1, Pentraxin-3 and IFN-γ varied the most between recipients. IL-35 and TNFSF12 were shown to vary the least between recipients. These data suggest heterogeneity in the highly variable analytes, none of which were shown to differ over time. The heterogeneity is likely due to genetic diversity, history of opportunistic infections and relevant prophylaxis.

The concentrations of IL-35 did not vary between recipients, but it was shown to decline over time in all recipients. This data suggests a consistent decline in the concentration of IL-35 in all recipients over the first 12-weeks PT.

An 8-colour Regulatory T cell (Treg) flow cytometry panel was designed based on the Luminex results and optimised to phenotype peripheral T-cell subsets. It distinguished between different T-cell phenotypes, namely naïve and memory, CD4 or CD8, and activated and regulatory T cells. Antibody titrations identified the optimal volume of each marker to use in a combination cocktail. Due to time constraints, the panel was not used on patient material, but the panel and its optimisation has been described in detail.

CONCLUSIONS

Statistical investigations into the Luminex results identified variability between replicates and between plates. These differences needed to be accounted for before combining data between plates and kits to arrive at biological conclusions. By using stringent analysis, this dissertation shows that multiplex data is highly variable and a series of statistical approaches should be employed to avoid including erroneous data.

A decrease in both inflammatory and regulatory proteins was shown in the 12 weeks after transplantation and ATG induction. The transient increase in IL-10 suggested the induction of effector T-cells to become IL-10 producing Tregs

(Tr1), known to occur in response to ATG induction. Combined with the consistent decline in IL-35 in all recipients, these results suggested that there was preferential secretion of IL-10 over IL-35 in some patients early after transplantation.

Plagiarism Declaration

FORM D19

Plagiarism Declaration

"This thesis/dissertation has been submitted to the Turnitin module (or equivalent similarity and originality checking software) and I confirm that my supervisor has seen my report and any concerns revealed by such have been resolved with my supervisor."

Name: Stefan Rautenbach

Student number: RTNSTE001

Signature:

Signed by candidate

Date: 19 February 2018

Acknowledgments

To my parents who gave me the freedom to study exactly what I pleased, who helped me find my purpose in life and gave me the privilege of higher education. And for taking me back in at home during the final months of my dissertation, so that I could focus on my writing - I will forever be grateful for that.

To my ouma and oupa, without your support I would never have been able to finish my studies. Thank you for inspiring me, especially when I felt like this would task to big for me to complete. To my supervisor, Prof Clive Gray, I am deeply grateful for all the support and patience you have shown me as well the guidance in all aspects of life you have given me. Thank you to my amazing friends who have been cheering me along, especially at the end. I do not think your contribution should be underestimated. To my amazing girlfriend, Achita, I do not know how you find the ability to give me so much of yourself to me when your life as a doctor asks so much of you. To Dr Elmi Muller, Kath Manning and their team thank you for all involving me in this study and all the help and collaboration on this work as well as the funding provided. To Christian Brander, Lupe Gomes, and their respective teams, thank you for hosting me in Barcelona and making me a part of your team while I was there. Thank you also for all the collaboration that you have provided in this work. To Dr Francesca Little, thank you for the help with the biostatistics and building the MEGLM in particular. Thank you to the National Research Fund and Poliomyelitis Research Fund who funded me in this degree..

List of Figures

List of Tables

List of Abbreviations

6-MP	6-mercaptopurine
ABMR	antibody mediated rejection
ACD	anticoagulant citrate dextrose
ACTH	Adrenocorticotropic Hormone
AICD	activation induced cell death
AIDS	acquired immunodeficiency syndrome
Alexa647	Alexa Fluor® 647
ALS	antilymphocyte serum
APOL1	Apoliprotein 1
AR	acute rejection
ART	anti-retroviral therapy
atg	Anti-thymocyte globulin
AZT	3'-azido-3'-deoxythymidine
BAFF	B-cell activating factor
BCC	basal cell carcinoma
BP	band pass
BV	brilliant violet
cART	combination antiretroviral therapy
CD	cell differntiation marker
CF594	CF®594
CI	confidence interval
CKD	chronic kidney disease
CMV	cytomegalovirus
CNS	central nervous system
CTLA-4	Cytotoxic T lymphocyte-associated molecule-4
Cy	Cyanine
DCs	dendritic cells
ddC	zalcitabine
ddI	didanosine
EBV	Ebstein-Barr Virus
ELISA	enzyme-linked immunosorbent assay
ESRD	end-stage renal disease
ESRF	end-stage renal failure
FCS	fetal calf serum
FDR	false discovery rate
FI	Fusion inhibitor
FI	fluorescent intensity
FoxP3	Forkhead box Protein 3
FSC	forward scatter
FSGS	focal segmental glomerulosclerosis
GFR	glomerular filtration rate
GRID	Gay-related Immune Deficiency
Gro-α	Growth-related oncogene-α

GVHD	Graft-versus host disease
HAART	Highly Active Retroviral Therapy
HCA	Hierachical clusteringal algorithm analysis
HIV	human immunodeficiency virus
HIVAN	HIV-associated Nephropathy
HIVCK	HIV immune complex kidney disease
HIVDD	HIV deceased donors
HLA	human leukocyte antigen
HOPE	health omnibus prorams extension
HorizonV	HorizonViolet
HTLV	Human T Lymphocyte Virus
IFN	interferon
IL	interleukin
IL-1RA	IL-1 receptor antagonist
INSTI	integrase inhibitor
IP-10	Interferon-inducible Protein-10
IQR	interquartile range
LP	long pass
MAF	macrophage activation factor
MCP-1	Monocyte Chemoattractant Protein-1
MDR	multi-drug resistant
MEGLM	Mixed effects generalised linear model
MFI	median fluorescent intensity
MIF	macrohpage inhibitory factor
MIP-1β	Macrophage Inflammatory Protein 1β
MLR	mixed lymphocyte reaction
MMF	mycophenolate mofetil
MMP	Matrix Metalloproteinases
NADIs	non-AIDS-defining illnesses
NGAL	Neutrophil gelatinase-associated lipocalin
NNRTI	non-nucleoside reverse transcriptase inhibitor
NRC	National Research Conference
NRTI	nucleoside reverse transcriptase inhibitor
NVP	Nevirapine
OOR	outside of observable range
PBMCs	peripheral blood mononuclear cells
PBS	phosphate buffered saline
PCD	passive cell death
PCP	Pneumocystis carinii pneumonia
pDCs	plasmacytoid DCs
PE	phycoertyhrin
PerCP	Peridinin Chlorophyll Protein Complex
PHA	Phytohaemagglutinin
PI	protease inhibitor
PID	patient identifier

PMTCT	prevention of mother to child treatment
PT	post-transplant
PTPRC	Protein tyrosine phosphatase, receptor type, C
QC	quality control
RANTES	Regulated on Activation, Normal T cell Expressed Secreted
RBCs	red blood cells
RF	renal failure
ROS	reactive oxygen species
RRT	renal replacement therapy
RT	room temperature
SCC	squamous cell carcinoma
SD	standard deviation
SDF-1α	Stromal cell Derived Factor 1 α
SNP	single nucleotide polymorphism
SSC	side scatter
STI	Sexually transmitted infection
TBI	total body irradiation
TCMR	T-cell mediated rejection
TCR	t-cell receptor
TEC	tubular epithelial cells
Teff	effector T cell
TF	transcription factor
TGF	transforming growth factor
Th	T-helper
TNF	tumour necrosis factor
TNFSF	TNF stimulating factor
TP	transplant
Tr1	IL-10 producing Tregs
TRAIL	TNF Related Apoptosis Inducing Ligand
Treg	Regulatory T cells
TSLP	Thymic stromal lymphopoietin
TWEAK	TNF-like weak inducer of apoptosis
UNOS	United Network for Organ Sharing
VEGF	Vascular Endothelial Growth Factor
WHO	World Health Organisation
wksPT	weeks PT
XDR	extensively-drug resistant
yrsPT	years PT

Table of Contents

Stefan Rau
Deleted: 38

Stefan Rau
Deleted: 42

Stefan Rau
Deleted: 42

Stefan Rau
Deleted: 48

Stefan Rau
Deleted: 69

Stefan Rau
Deleted: 82
Stefan Rau
Deleted: 89
Stefan Rau
Deleted: 89
Stefan Rau
Deleted: 97
Stefan Rau
Deleted: 99
Stefan Rau
Deleted: 10
Stefan Rau
Deleted: 10
Stefan Rau
Deleted: 11
Stefan Rau
Deleted: 12
Stefan Rau
Deleted: 12
Stefan Rau
Deleted: 12
Stefan Rau
Deleted: 12
Stefan Rau
Deleted: 12
Stefan Rau
Deleted: 12
Stefan Rau
Deleted: 12
Stefan Rau
Deleted: 12
Stefan Rau
Deleted: 13
Stefan Rau
Deleted: 13
Stefan Rau
Deleted: 13
Stefan Rau
Deleted: 13

Stefan Rau
Deleted: 14
Stefan Rau
Deleted: 15
Stefan Rau
Deleted: 15
Stefan Rau
Deleted: 15
Stefan Rau
Deleted: 16
Stefan Rau
Deleted: 16
Stefan Rau
Deleted: 20
Stefan Rau
Deleted: 20
Stefan Rau
Deleted: 20

CHAPTER 1: LITERATURE REVIEW

1.1 Transplantation History: pre-20th Century Landmarks

The first reported case of transplantation was in the 16th century by Tagliacozzi[1], who introduced the Indian technique of skin flap transplants to Europe in Venice, Italy in 1597. At this time there was no differentiation between grafts between different individuals (homografts) and grafts from the same individual (autografts). Tagliocozzi suspected that autografts would be more successful as he used skin from the same individuals' arm to graft onto their nose. This was not confirmed until the 20th century.

In the 18th century the experimental surgeon, John Hunter, reported human teeth transplants as well as experimental animal transplants[2], seemingly unaware that homografts would be more likely to fail.

During the 19th century, the French surgeon, Jacques Louis Reverdin, improved upon Tagliocozzi's skin flap by showing that small, thin, split thickness skin grafts would be successful[3] as this promoted wound healing by encouraging angiogenesis, the growth of new blood vessels in the tissue. Two years later the first successful such skin transplant was performed in the UK[4] based on Reverdin's work. Differences between homografts and autografts were noted, as homografts were reported to have "soon disappeared". Most transplants at this time were largely unsuccessful due mainly to poor surgical technique, unsterile working conditions and a lack of knowledge regarding transplant rejection.

1.2 Transplantation History: early 20th Century Landmarks

The Lyon Chief of Surgery Mathieu Jaboulay, German surgeon Julius Dörfler and a young surgeon, Alexis Carrel, developed a technique of vascular anastomosis that allowed the suturing together of full-thickness blood vessels[5–7]. The first solid organ transplants attempted, were kidney transplants. By 1906, kidney transplants had been trialled in dogs and goats by Emerich Ullmann[8] but as a result of the new vascular anastomosis technique, Jaboulay attempted the first two renal transplants in humans[9]. Both were xenotransplants, transplants from one species to another; one kidney was transplanted from a goat and another from a pig. The kidneys were not implanted in the pelvic region; instead they were attached to more accessible vessels in the neck. Neither graft survived for more than a few hours and all the participants died. By 1910 Ernst Unger, who had performed more than 100 kidney transplants in animals, attempted two renal heterotransplants in humans, using monkey kidneys[10]. These too did not survive most likely due to the surgeons' lack of knowledge, and prevention, of transplant rejection.

Alexis Carell had left France for Chicago via Montreal and teamed up with physiologist, Charles Guthrie, to make some of the greatest advances in transplant surgery in the year they worked together. They successfully transplanted kidney, thyroid, ovary, heart, lung, and small bowel in dogs, averaging a publication every 14 days[5]. Carrell's success was partly due to the surgical technique he helped develop under Jaboulay, but further aided by his

use of finer needles and suturing material, as well as an obsession with sterile technique in the operating theatre. His successes highlighted the role that infections played in graft loss, however the role of cellular immune responses in these rejections was not known at the time. Figure 1.1 a) shows the landmarks in transplantation between 1597 and 1912.

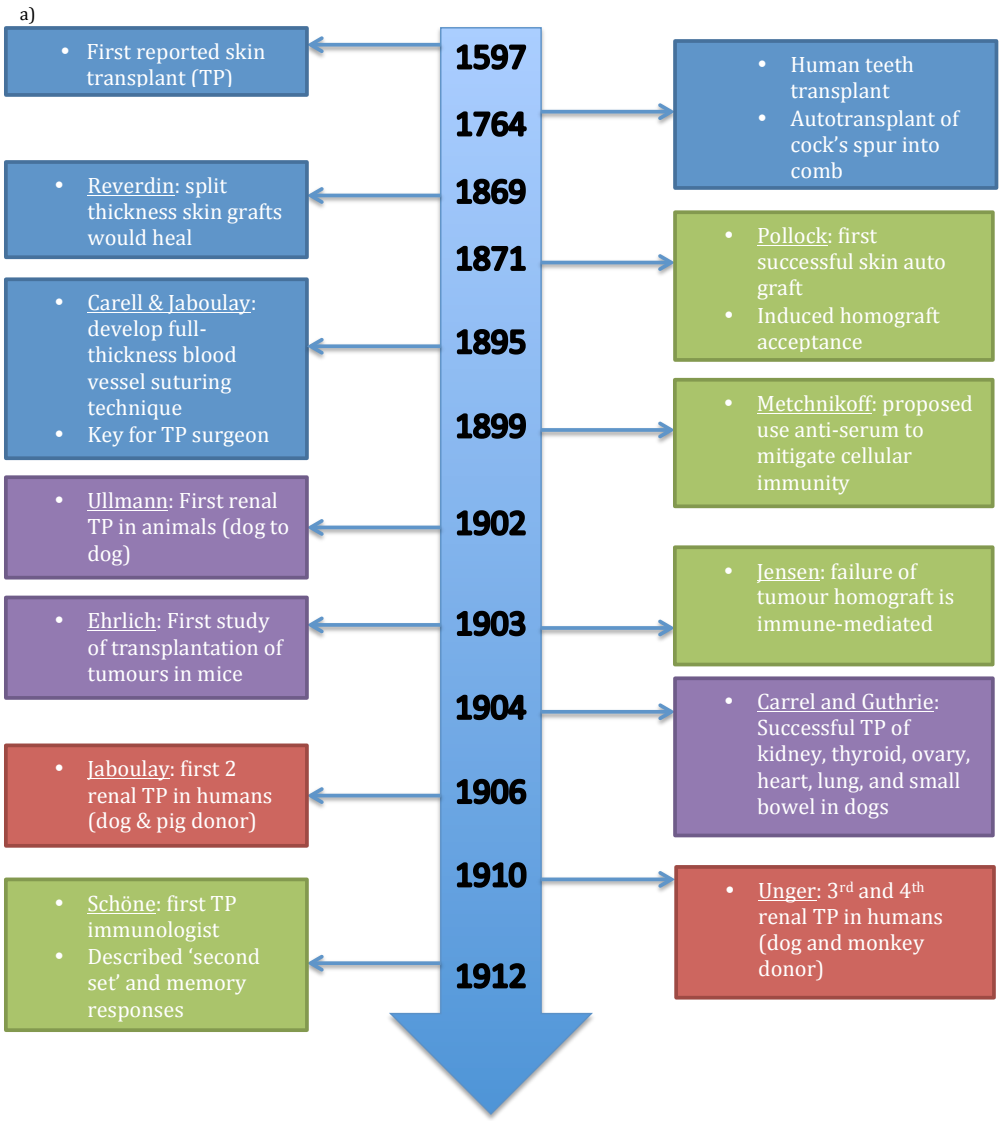

Figure 1.1a) Timeline of Landmark Events in the history of Transplantation

Colours indicate event association: In vitro (green); animal (purple); human (red); transplantation technology/ networks (orange)

1.2.1 First Transplantation Immunologist

Georg Schöne is regarded as the first transplant immunologist, and in 1912 observed in mice that skin homografts always failed and that subsequent grafts from the same donor failed more rapidly[11]. He coined the term 'Second-Set Response' to describe the phenomenon but did not relate it to cellular immune responses. In 1924, the "Second Set Response" was identified again[12]. Others had hinted at cellular involvement. As early as 1899, Élie Metchnikoff had proposed that antiserum could be developed and used therapeutically to mitigate cellular immunity[13]. At the time though the accepted dogma was that transplant rejection was solely the result of a humoral or antibody-mediated response, and did not involve a cellular component. It was only in 1914, that James B. Murphy showed that the lymphocyte was central to immunity[14,15]. He showed that graft rejection was reliant on lymphocytes and that by removing or inactivating lymphocytes (using irradiation, splenectomies, or immunosuppressants, such as benzol) rejection could be prevented or graft survival extended[16]. In the same year, Alexis Carrell showed that by irradiating skin graft recipients, their risk of rejection and loss of graft diminished[17], but this was largely a forgotten finding.

1.2.2 Cellular Nature of Rejection

In the 1930's, the German Leo Loeb dismissed the importance of lymphocyte involvement in skin graft rejection in inbred mice[18]. However, a decade later in the UK, Peter Medawar demonstrated in rabbit skin grafts the histological,

morphological and immunological nature of rejection[19]. Loeb retracted his own conclusions regarding the nature of rejection by showing that the strength and timing of homograft rejection was determined by the genetic disparity of donor and recipient lymphocytes[20].

1.2.3 First Human Renal Transplant

Despite the advances in identifying the causes of rejection and graft failure, little was done to prevent it in experimental transplants performed around the same time. It was well-known during the early 20th century that autografts were more successful than homografts but there was no consensus as to the mechanism. This did not prevent the Russian transplant surgeon, Yurii Voronoy, from attempting the first human to human renal transplants in 1933[21]. The transplant was performed across blood group mismatches and the donor organ was harvested 6 hours after death – both factors contributed to its rapid failure. In the USA, Richard Lawler performed what seemed to be the first successful human renal transplant[22]. However, his findings were misleading, as the transplant was performed on a patient whom had impaired but not terminal renal function. When the graft failed, the kidney was found to have been necrotic and shrivelled, indicative that the graft had been rejected.

1.2.4 Chimerism and Graft Acceptance

Continuing their work in skin homografts, Medawar, Billingham and Brent, investigated a phenomenon initially observed in fraternal cow twins, where homografts were far less likely to be rejected than in other transplants[23]. Their work was based on the observation in 1945 by Ray Owen, who showed that Freemartin fraternal twin cows, who shared a placenta in utero exchanged red blood cells and stem cells between each other[24], and existed in a state of chimerism, where genetically disparate cells co-existed, and did not reject homografts. This lead to the conceptual understanding by Medawar and Billingham, that chimerism explained the acceptance of skin homograft between fraternal twins because the recipient had developed tolerance to the twin in utero. At the time though it did not seem likely that chimerism could be induced in humans and there was no apparent clinical application of chimerism in humans[18]. Figure 1.1 b) shows the landmarks in transplantation between 1914 and 1951.

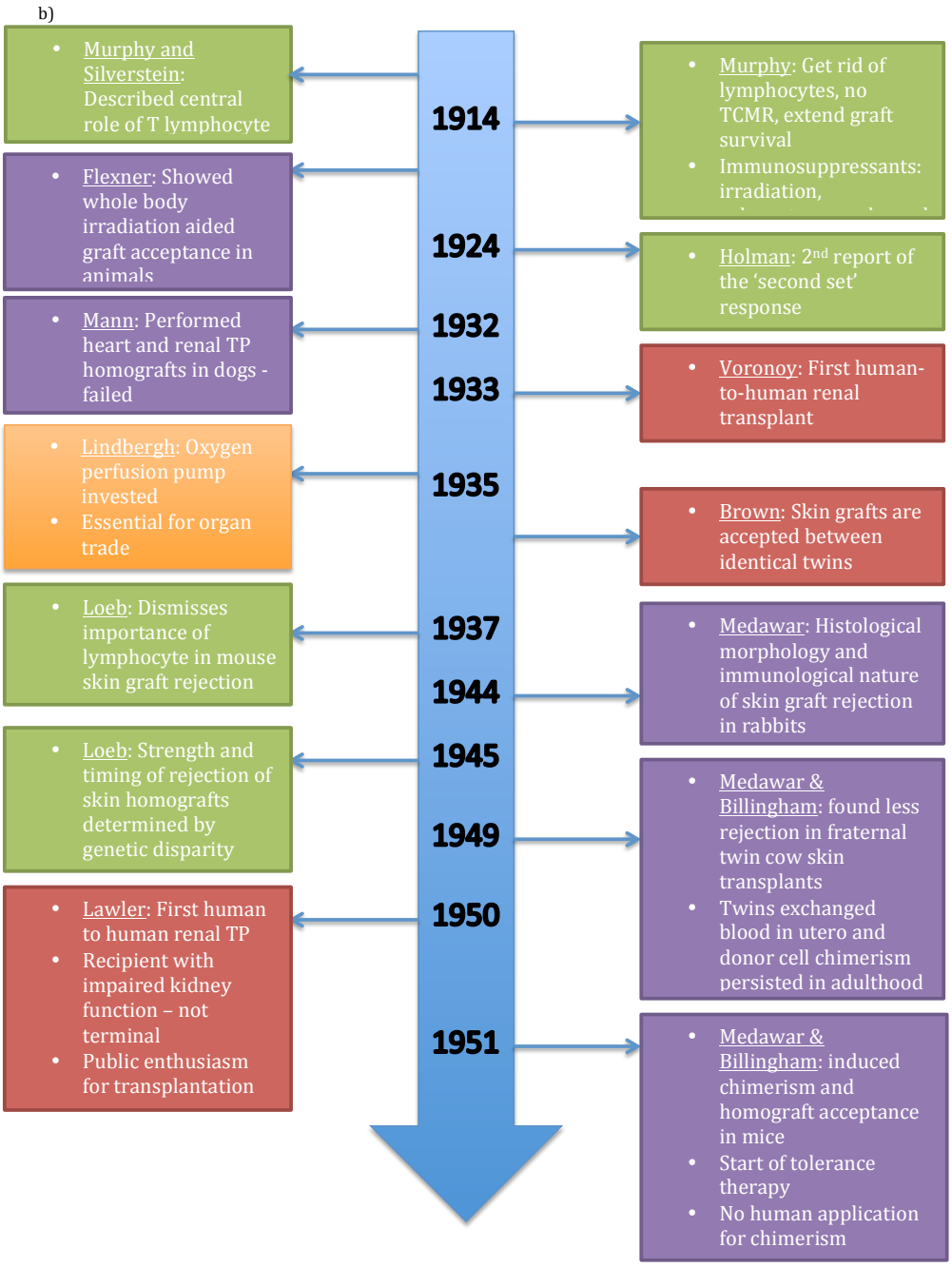

Figure 1.1b) Timeline of Landmark Events in the history of Transplantation

Colours indicate event association: In vitro (green); animal (purple); human (red); transplantation technology/ networks (orange)

1.2.5 Methods of Preventing Rejection

The nature of tolerance, at least in chimeric animal models was known but it was still not clear how either a chimeric state in animals could be induced or how to suppress rejection. One approach was to remove lymphocytes through ablative total body irradiation (TBI). TBI would deplete cell function rendering them unable to act in a host versus graft response. Carrel had already shown as early as 1914 that full body irradiation would improve skin homograft outcomes[17].

By 1951, Medawar and Billingham began investigating rodents to identify whether cortisone, which had previously been shown to have a profound influence on the activity of cells that mediate immune responses as well as those that are involved in wound healing, could improve homograft acceptance. They showed that this was indeed the case[25].

William J. Dempster used both irradiation and cortisone in dog renal recipients but neither seemed to show any improvement in graft survival or acceptance[26,27]. He concluded that neither treatment had much effect on graft survival and advised against further transplants in humans. Others were not of the same opinion; in 1951, Küss and Bomget separately performed 9 renal homografts in Paris[28]. Of the donors, 8/9 were guillotined criminals – the other was a living-related donor. They used irradiation as a means of reducing the cellular immune response to the homografts and implanted the organs retroperitoneally in the pelvis, re-vascularised with the iliac vessel – a technique

that is still in use today. Unfortunately the majority of the organs had little function and all the recipients died within days or weeks[29]. At the same time in Boston, USA, a similar transplant program was underway. David Hume performed 9 kidney transplants between 1951 and 1953[30]. The donors were all recently deceased during surgery, or in some cases, the organ had been removed from a patient with hydrocephalus whose ureter was needed to drain excess cerebrospinal fluid to the bladder. The majority of the organs were implanted in the thigh with the ureter protruding from the skin. Some, but not all of the recipients, were treated with Adrenocorticotropic Hormone (ACTH)/Testosterone in an effort to improve renal function, and cortisone to improve graft survival. Generally, the transplants were not successful; only 4/9 showed any function and in three of those, the function was very brief. One transplant did however function for 5.5 months before rejection. Joseph Murray performed a similar successful transplant in 1954 between identical twins[31,32]. The scientific success of this transplant was insignificant and it was already known that identical twins would tolerate a homograft – this added very little to the major problem in transplantation at the time: rejection. It was also not a practical advance as receiving an organ from such a donor was only an option for a very small proportion of the population. However, this transplant following on from the less successful performed in Boston and Paris maintained the slim hope that solid organ homografts could be successful in humans.

In 1955 Joan Main and Richmond Prehn induced experimental chimerism by irradiating mice and then inoculating the recipient of a skin graft with bone marrow from the donor[33], which was also later confirmed in dogs[34].

The "Main-Prehn" technique was later used in human renal transplants for the first time[35,36]. Murray et al (1958) transplanted two patients using this chimeric technique and a further ten who were only treated with TBI. Over 90% (11/12) of patients died within a month, and the one who survived received bone marrow from his semi-allogeneic fraternal twin. This was the first time the genetic barrier had been breached. The recipient survived for more 20 years.

Shortly after Murray's transplants, Jean Hamburger used the same irradiation treatment in another fraternal twin donor-recipient pair – the recipient also survived for more than 20 years and died of unrelated causes[37]. To show that these fraternal twin cases were not caused by chimerism induced in utero, Hamburger & Küss (1962) performed a further four irradiation-conditioned renal transplants with non-related donors[38]. These findings justified the continuation of solid organ transplant research and also demonstrated that chimerism was not a requirement for a successful transplant.

1.2.6 Graft-Versus Host Disease

The mechanisms leading to transplanted tissue and cell rejections were becoming clearer at this time. In the late 1950s Billingham and Brent first

identified Graft-Versus Host Disease (GVHD) in mice in which they had induced chimerism through bone marrow inoculation in neonates. They identified certain chimeric mice as sickly runts and found that this was because immunocompetent cells in the neonatal inocula had migrated to, and attacked, the hosts' lymphoid tissue. Shortly thereafter, Simonsen demonstrated how GVHD occurred in chickens in which he had injected allogenic lymphoid cells as embryos[39]. He also demonstrated that lymphocytes, previously thought to remain static in tissue, were in fact mobile[40]. Gowans later showed that not only were lymphocytes mobile, but they recirculated from the blood to the lymph and back[41]. This was the first report showing that cells from the donor graft, namely stem cells, could recognize and reject the host.

The mechanism by which cells recognised allogeneic antigen was later discovered to be due to the Human Leukocyte Antigen (HLA)[42,43] system. These "transplantation antigens" were discovered by Jean Dausset, building on the work of Rose Payne[44] and Jon van Rood[45] using leukocyte agglutination in human sera from pregnant women. These serological HLA phenotyping techniques, which were used for decades, have now been superseded by DNA technologies.

1.2.7 Immunosuppressant Advances

Cortisone had been shown to be ineffective in preventing rejection[30] and there was no other more effective immunosuppressant available in 1958. In an effort

to induce immune tolerance in a rabbit model, Schwartz and Dameshek found that 6-mercaptopurine (6-MP) was effective in reducing the antibody response to bovine albumen[46]. They went on to show that 6-MP extended the survival of skin homografts[47]. Calne and Hume then both independently tested the effect of 6-MP on the rejection of renal homografts in dogs[48,49]. They found that 6-MP significantly prolonged graft survival. It was still not clear how best to make use of this new immuno-suppressant in human transplants though. Figure 1.1 c) shows the transplantation landmarks between 1951 and 1959.

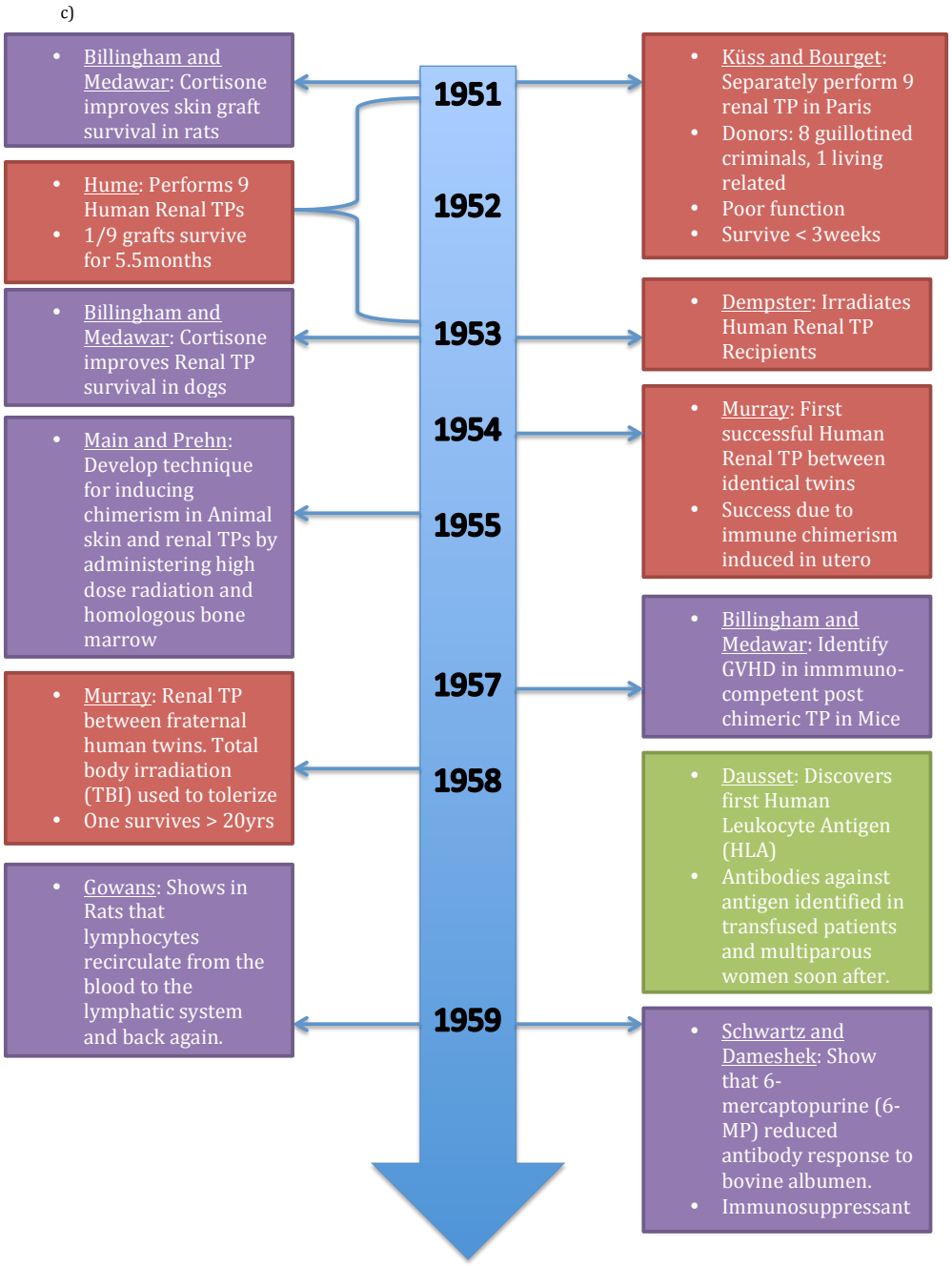

Figure 1.1c) Timeline of Landmark Events in the history of Transplantation

Colours indicate event association: In vitro (green); animal (purple); human (red); transplantation technology/ networks (orange)

1.3 Transplantation History: late 20th Century landmarks

1.3.1 First National Research Conference on Transplantation

In 1963 the first National Research Conference (NRC) on transplantation took place and the majority of research showed poor results for solid organ transplantation. Hundreds of transplants had been performed yet less than 10% of the recipients had survived for up to 3 months[50]. Of all the recipients who had been treated with an irradiation conditioning regimen, only 6 had approached or achieved 1 year survival[51]; of the ten recipients that Murray et al had treated with a combination of 6-MP and azathioprine (a new immunosuppressant) instead of irradiation, only one survived for a year and at the time of the conference, the graft was failing – others all died within 6 months[52].

1.3.2 Starzl's Immunosuppressant Protocol Success

Tom Starzl then described a new immunosuppressant protocol that had resulted in 70% graft survival at 1 year[53]. He had more surviving transplant recipients than the rest of the 1963 NRC attendees combined[51]. Starzl had observed that rejection usually occurred in patients on azathioprine alone. He had found that this rejection was reversible when the patients were treated with prednisone and in most patients on the combination therapy, drug doses could be diminished without provoking rejection. His findings were initially met with scepticism but as the inquiries progressed, more and more people became

convinced that the results were believable[18,51]. Many of the conference attendees promptly visited Starzl in Denver to learn how to adopt the new immunosuppressant protocol[54]. The new protocol allowed the success of future transplants in many centres globally.

1.3.3 Technical Advances in Transplant Services

The success of transplantation was not due only to surgical and immunosuppressive advances. Many other discoveries were needed in order for transplantation to become practical, and for organ procurement and transplantation networks to be established. The first of these was an invention by Charles Lindbergh[55]. He invented an oxygen perfusion pump originally to be used for open heart surgery[55]. The pump allowed for the reperfusion of donor organs, so making organ transportation a possibility. The advent of infusing organs with cold solution in order to preserve tissue from necrosis improved the viability of organs and prolonged transplant survival[56] and in 1969, this was accepted as common practice. Donor organs could now be preserved and transportation between locations was possible[57]. Figure 1.1 d) shows the landmarks in transplantation between 1960 and 1964.

d)

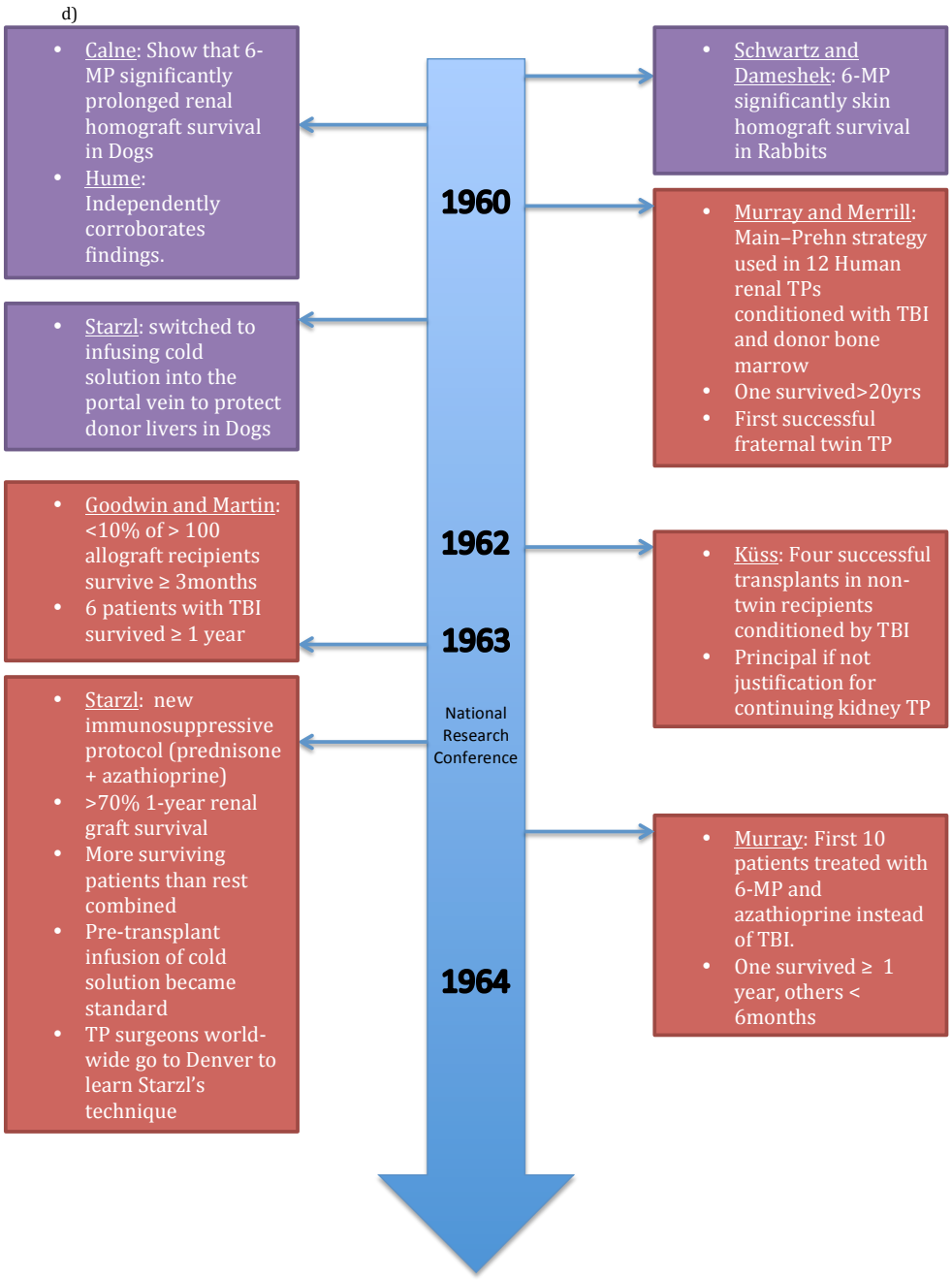

Figure 1.1d) Timeline of Landmark Events in the history of Transplantation

Colours indicate event association: In vitro (green); animal (purple); human (red); transplantation technology/ networks (orange)

1.3.4 Organ Sharing Networks

Within a year of Starzl's new immunosuppressive protocol being introduced, 50 new transplant programs had begun in the United States alone[58]. In 1967, Paul Terasaki started the first organ-sharing network[59], meaning that donors from one hospital could supply organs to a recipient at another – this increased the numbers of organs available to potential recipients. Shortly after, Harvard Medical School made the recommendation that loss of brain function in an irreversible coma should be accepted as death[60] – not only did this further increase the number of available donors but it was much easier to successfully harvest organs from donors whose vitals were still functioning. By 1969 the South Eastern Organ Procurement Foundation was established[61]. This was to be precursor for the national network in the United States, the United Network for Organ Sharing (UNOS)[61].

1.3.5 Histocompatibility in Transplantation Success

In 1964, Paul Terasaki developed the first microcytotoxicity assay[62]. This assay mixed donor lymphocytes with recipient serum in micro-wells to test for the presence of donor-specific antibodies[62]. It improved upon the cumbersome and inconsistent agglutination assays previously used. The assay could identify donor-specific antibodies in the serum that could predict hyper acute rejection as well as aiding the identification of optimal living-related donors. At the time it was thought that histocompatibility (matches between the different HLA alleles)

between donor and recipient was necessary for optimal graft survival. Terasaki later showed that when examining his database of kidney transplant recipients (1216 transplants across 52 centres) that there was no correlation with matching tissue types and allograft survival[59] during the first 3 months. Later studies showed that long-term (>10 years) graft survival is related to the number of HLA matches[63,64]. The more mismatches in between donor and recipient in either class I or II, and in HLA-B and HLA-DR in particular, the poorer is long-term acceptance[63–65].

1.3.6 T-cell Depletion Therapies

There are numerous factors that lead to the rejection of an allograft. These are initiated during the revascularisation of the graft, where ischemia-reperfusion injury induces the production of cytokines and chemokines as well as the activation of both donor and recipient APCs[66]. These processes not only attract allo-specific memory T cells to the graft, but also cause the differentiation of naïve T cells to become allo-specific effector T cells. These cells can act to reject the allograft and the initial response is large, polyclonal, local and systemic and predominantly T-cell mediated[66].

Antilymphocyte serum (ALS) had been proposed as a solution to cellular immunity by Metchnikoff[13] but was ignored at the time of initial reporting. However, in 1966, Woodruff et al[67] reported that ALS was remarkably effective in extending the survival of skin allografts in rodents. Later that year, Starzl was

the first to demonstrate that ALS could improve the outcomes of solid organ transplants by using it in renal and liver transplants in canines[68]. He credited ALS for allowing him to perform the first successful human liver transplant[69]. In 1981, Cosimi et al, introduced the use of monoclonal derivatives of ALS that were first directed at all T lymphocytes (marked by CD3) and CD4+ and CD8+ subsets[70]. This laid the platform for the use of antithymocyte globulins (ATG), polyclonal antibodies directed at thymocytes, as a means of preventing GVHD in bone marrow transplant recipients[71] or treating those experiencing cellular rejection[72].

ATG therapy is now used as a means of depleting lymphocytes in order to avoid early rejection in the majority of heart, lung, pancreas and renal transplants[73,74]. The antibodies are primarily directed at T-cells but due to its polyclonal nature, ATG has also been shown to deplete NK cells, B cells, and plasma cells[75–77]. Figure 1.1 e) shows the landmarks in transplantation between 1964 and 1978.

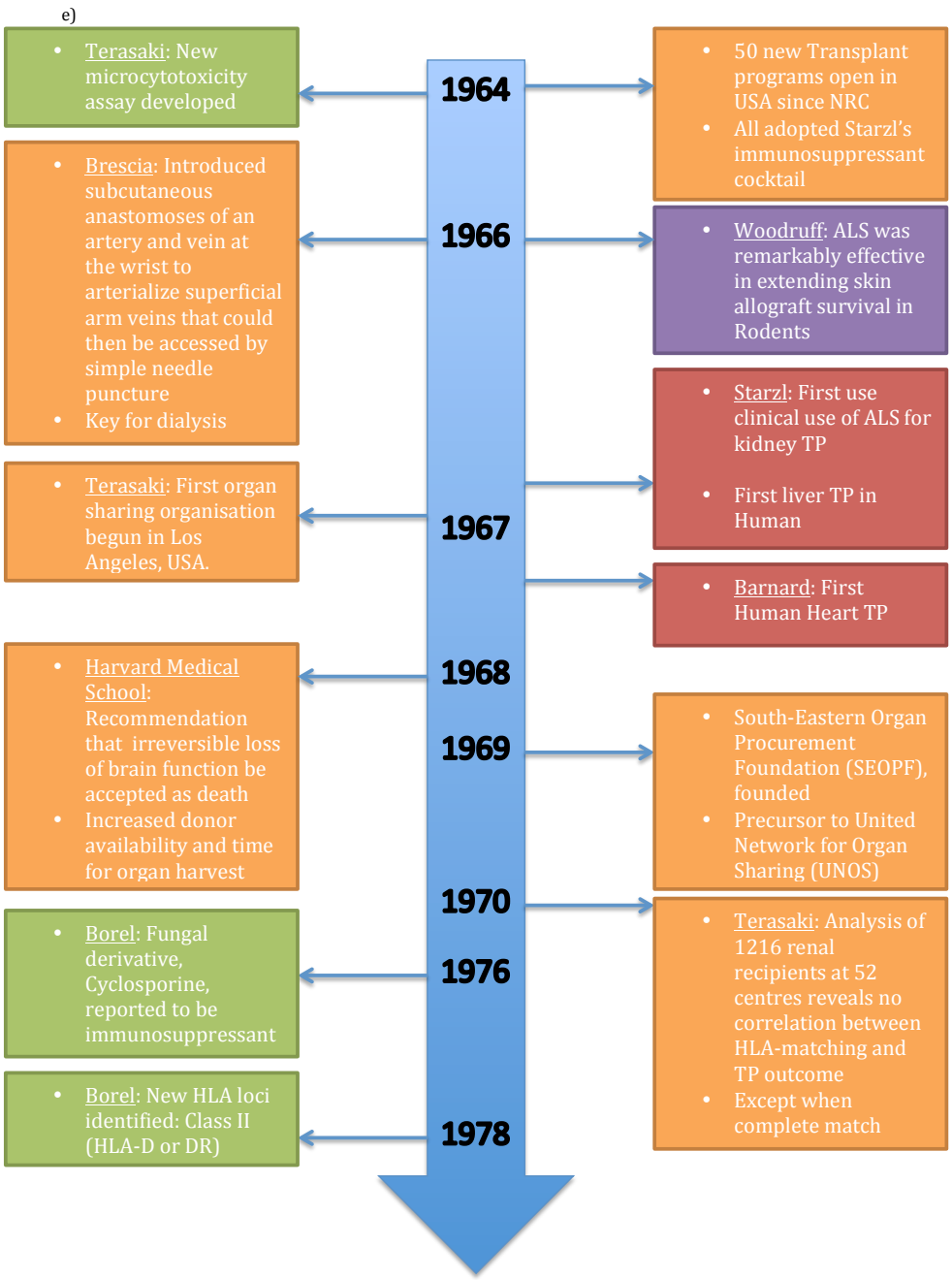

Figure 1.1e) Timeline of Landmark Events in the history of Transplantation

Colours indicate event association: In vitro (green); animal (purple); human (red); transplantation technology/ networks (orange)

1.3.7 First Heart Transplant

In addition to the first human liver transplant, in 1967 the first human heart transplant was performed in South Africa at Groote Schuur Hospital. Chris Barnard performed the transplant[78] , but the recipient only survived 18 days. Barnard also performed a second heart transplant which was far more successful; this recipient survived for several years[78,79].

1.3.8 Immunosuppressive Protocols Improvements

During the 1970s two new immune-suppressive drugs also came to the market. Cyclosporine A, a fungal derivative, was first identified by Jean-François Borel in 1976 to have immunosuppressive qualities[80], and then used by Calne as a single agent in the treatment of 34 human kidney transplant recipients[81] in 1979. Calne found it to be more potent than azathioprine but it was also toxic in higher doses, leading to infections, lymphoma and renal failure.

Starzl improved his own immunosuppressive protocol by using cyclosporine, instead of azathioprine, combined with prednisone[82]. Of the first time kidney transplant recipients, 17/18 survived for at least a year; only one patient died, due to a cardiac failure. The new protocol improved the outcomes of kidney transplant recipients[82]. Using the same protocol he also improved the outcomes of human liver[83], heart[84] and lung transplants[85,86]. Solid organ transplants were

brought to the level of a practical clinical service and became a viable treatment option for various organ failures[51].

In the late 1980s, Starzl further improved immunosuppressive drug protocols. He found that some solid organ transplant recipients experiencing rejection did not respond to treatment by cyclosporine, steroids or ATG and that by using a new more potent immunosuppressive drug, FK 506 (Tacrolimus), the rejection in these patients could be reversed[87]. Tacrolimus soon replaced cyclosporine as the standard baseline immunosuppressive agent. Figure 1.1 d) shows the landmarks in transplantation between 1979 and 2008.

f)

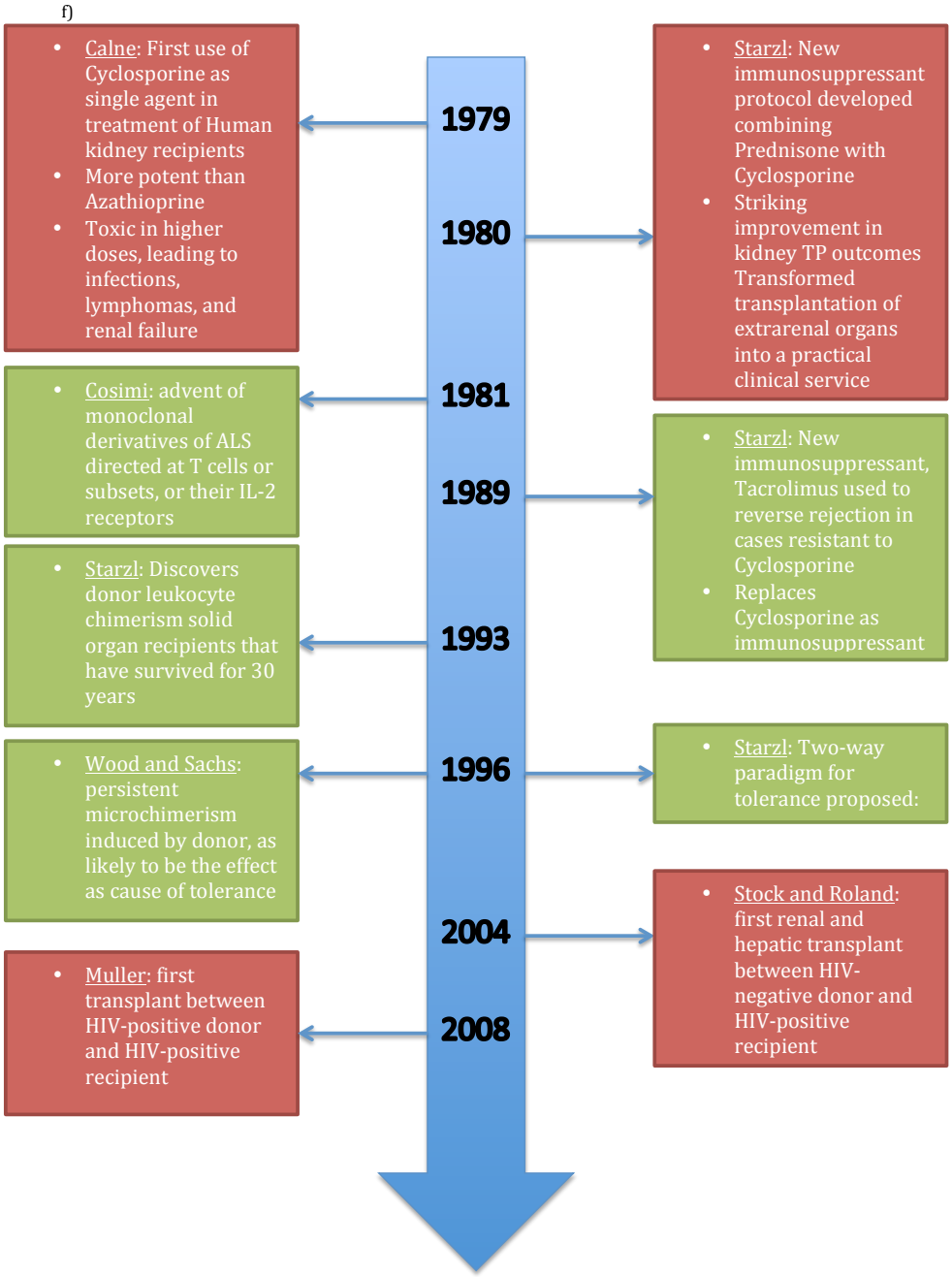

Figure 1.1f) Timeline of Landmark Events in the history of Transplantation

Colours indicate event association: In vitro (green); animal (purple); human (red); transplantation technology/ networks (orange)

1.3.10 Mechanisms of Tolerance

In the 1990s solid organ transplantation programs were routine throughout the world. Starzl identified that patients who had maintained successful kidney or liver grafts for up to 27-29 years had a level of donor chimerism[88]. He postulated that chimerism was a cause and not a consequence of prolonged allograft survivial[89]. He proposed a hypothesis that a two-way mechanism existed for inducing tolerance; successful engraftment is the result of the responses of co-existing donor and recipient cells each to the other, causing reciprocal clonal exhaustion followed by peripheral clonal deletion. This was rebutted by Kathryn Wood and David Sachs, who argued that persistent microchimerism induced by the donor organ, as observed in long-term survivors, is likely to cause tolerance[90].

1.4. Human Immunodeficiency Virus (HIV) and Transplantation

1.4.1. Discovery of Acute Immunodeficiency Syndrome (AIDS)

In the 1980s, of large number of otherwise healthy young men were dying of rare diseases such as a Kaposi's sarcoma[91], and Pneumocystis carinii pneumonia (PCP)[92,93]. Other opportunistic infections were often also found in these patients such as the bacteria, *Mycobaterium tubcercolisis*, *Mycobaterium avium-intracellulare*, *Klebisella pneumonia*, and other gram-negative aerobic bacteria as well as fungi such as *Candida albicans*[94], and *Cryptoccocus neoformans*, and

protozoans *Toxoplasma gondii* and *Entamoeba histolytica*[95]. This was concerning as a healthy, intact immune system would normally protect against these infections[92,94]. Many of these men were drug users and all were homosexual. As a result, the condition afflicting this group was initially given the clumsy title of 'Gay Compromise Sydrome'[96] and later the New York Times started referring to it as "Gay-related Immune Deficiency (GRID)"[97]. The CDC started using the term "Acquired Immunodeficiency Syndrome" or AIDS to describe the condition[93].

Initially, the only links between the patients suffering from AIDS were that they were mostly homosexual, engaging in risky sexual behaviour, as evidenced by the high numbers of sexually transmitted infections (STIs) found in combination with AIDS; many were drug users and all lived in metropolitan areas[98–100]. Patients presented with a decrease in T lymphocyte numbers, which seemed to be the basis of AIDS. A year after it was first identified, more than 278 patients had died as a result of AIDS in the USA[101] and one to three new cases were reported per day[102]. Amongst these new cases, there were also heterosexual men and women (mostly intravenous drug users)[103], Haitians who had recently immigrated to the USA[104] and haemophiliacs[105]. In 1982, there was the first case of a 20-month infant contracting AIDS from a blood transfusion. These epidemiologic findings indicated that the causal agent of AIDS was likely a blood borne infection.

The disease was not restricted to the USA either. There were reports of homosexual men with AIDS appearing in Europe[106,107] in France, Denmark and

the UK, some, but not all of whom, had sexual partners in the USA. Reports also started appearing for cases in Uganda of a new wasting disease called 'slim disease' which was later to be shown to be AIDS[108], and later reports of AIDS in Zaire[109] and Rwanda[110]. The first reports of AIDS in South Africa were in 1983[111]. With the growing number of cases worldwide, it became evident that the disease was an epidemic and could soon develop into a global pandemic. In order to combat the disease, the causal agent needed to be identified.

1.4.2 Identifying the causal agent of AIDS

Between 1983 and 1984, three separate groups independently showed that it was a retrovirus - an RNA virus that inserts a DNA copy of its genome into the host cell - later called the Human Immunodeficiency Virus (HIV), that caused AIDS[112–114]. Françoise Barré-Sinoussi, working in Luc Montagnier's group at the Pasteur Institut in Paris, suspected the causal agent of AIDS to be a similar retrovirus to the Human T Lymphocyte Viruses (HTLV-I & HTLV-II)[115,116]. They confirmed the presence of a retrovirus, in a culture of cells from a lymph node of a patient with AIDS-like symptoms[117]. They showed that this retrovirus was serologically different to HTLV-I & HTLV-II[114]. Robert Gallo's group used their already existing system of human T-cell cultures and antibodies to HLTV to detect, isolate and continuously produce a new retrovirus from a patient who had been identified as having pre-AIDS; they called the new virus, HTLV-III[113]. They later showed that this was the same retrovirus that had been identified by Barré-Sinoussi under Montagnier[118]. Jay Levy's group confirmed what Gallo's

group found, as well as confirming that Lymphadenopathy Associated Virus (LAV) and HTLV-III were the same retrovirus[112] – they named it AIDS-associated retrovirus.

Gallo's group managed to grow three different strains of the virus in a continuous culture[119] - as a result, they developed the first blood test for the virus and methods for its continuous production, isolated the new retrovirus, performed analyses of its proteins, and provided evidence to show that it was the cause of AIDS[119]. By 1985, blood tests were patented and developed so that patients, as well as donated blood, could now be tested for the virus[119].

A panel of experts in retrovirology was assembled by Harold Varmus to settle the naming of the virus[120]. Montagnier, Gallo and Levy were included in the panel. Only by May 1986, did the panel formally declare that the virus would be known as Human Immunodeficiency Virus (HIV)[121].

1.4.3 The State of the Epidemic in the 1980s

The United States CDC published a report in 1986 detailing their goals for dealing with the AIDS epidemic. At the time, there were >19000 cases reported, and >9000 deaths that had been attributed to AIDS in the USA[122]. They estimated that there were 1 – 1,5 million people infected with the virus. Cases had been identified in 50 different states and numerous countries worldwide. They were confident that they could eliminate the transmission of the virus causing AIDS by

the year 2000[122]. There was growing public fear and hysteria surrounding the disease and those infected with it, in particular due to its associations with sex, homosexuals, drug use and immigrants[123].

1.4.4 Antiretroviral Drug Discoveries

In 1987, the anti-retroviral therapy (ART) for the treatment of HIV was brought to market, 3'-azido-3'-deoxythymidine (AZT)[124]. The drug acted by inhibiting the action of the viral reverse transcriptase. It was rushed through the standard safety protocols to meet the demands of the epidemic[125]. Single therapy with AZT was found to be largely ineffective due to short generation time of HIV and its high mutagenicity resulting in the appearance of drug-resistant variants[126–128]. It was also shown to be toxic and many reports suggested it was safer not to take AZT[127]. Although AZT increased survival rates at 24 weeks[126] as well as increased CD4 counts[129], at 48 weeks the plasma RNA viral loads were comparable to placebos[129]. Only when AZT started being used in combination with other ART drugs was it found to be effective in preventing disease progression without the development of drug resistance[130]. The invention of AZT started an era in which HIV infection became a treatable chronic disease[131].

In 1992, didanosine (ddI), a new nucleoside reverse transcriptase inhibitor (NRTI) was approved by the FDA and made available to the public[132,133]. An alternative to AZT was needed due to the toxic effects of AZT[127]. Patients failing AZT could switch to ddI treatment[132]. In 1994, another NRTI, zalcitabine (ddC),

was introduced to the market. Alternating AZT with ddC was shown to reduce the toxicity associated with either drug, while still maintaining a strong antiretroviral activity[134].

1.45 The Highly Active Retroviral Therapy (HAART) Era

In 1996 a double-blind randomized trial of AZT monotherapy versus combination NRTI therapy of AZT plus ddI or ddC[135] demonstrated that combination regimens prolonged life and delayed disease progression. The 1996 AIDS conference saw the introduction of combinatorial ART therapy and a turning point in the management of HIV/AIDS[131]. In the following years, several new antiretrovirals were put into trial and FDA approved, including the new classes of protease inhibitors (PIs), non-nucleoside reverse-transcriptase inhibitors (NNRTIs), integrase inhibitors (INSTIs), Fusion inhibitors (FIs) and chemokine receptor antagonists (CCR5 antagonists)[136]. Highly active antiretroviral therapy (HAART) was introduced when two NRTIs could be combined with a PI[137–139], although it has been continually updated based on the most effective combinatorial ART available[136]. HAART has been shown to be the most effective treatment for HIV[131].

1.4.6 The Impact of HIV on Transplantation Services

There were a number of safeguards established to prevent the unintentional spread of HIV through public health services, such as preventing high risk individuals from donating blood/plasma, and screening donated blood/plasma for HIV-specific antibodies[140] using an enzyme-linked immunosorbent assay (ELISA). This ELISA was not highly sensitive, and as a result there were still transmissions observed in blood transfusions from HIV-antibody negative donors[141]. In 1988, a public health service act was passed in the United States known as the Health Omnibus Programs Extension (HOPE) Act of 1988 – also known as the AIDS Amendment Act. It outlined research programs, changes to health services, HIV prevention programs and the establishment of a national commission on AIDS[142]. This act also made it illegal to transplant organs from an HIV-positive donor. Transplantation requires that the recipient receive chronic immunosuppression in order to prevent the loss of immune suppression. HIV infection can cause the reactivation of many other viruses, such as cytomegalovirus (CMV) and Epstein-Barr Virus (EBV). These viruses can lead to transplant rejection. These factors, combined with life-long ART and the implications of the HOPE Act of 1988, meant that HIV-positive patients were ineligible for organ donation, as well as considered to be poor candidates for organ transplantation[143–145] – and in the case of renal transplantation, it was recommended that HIV-seropositive patients with ESRD would be better treated with dialysis than transplantation[145,146]. If transplantation was absolutely necessary, it should only be performed in centres that had extensive experience

in organ transplantation and HIV/AIDS management[145,146], of which at the time, there were almost none. These changes effectively made organ transplantation impossible for HIV-positive patients.

1.4.6 HIV-related Kidney Pathologies

HIV has been shown to affect many organs, such as the kidney, liver, heart and brain[147–150]. In 1985, 5.4% of AIDS patients in had organ failure and it one of the leading causes of death in patients with late-stage AIDS[151]. These deaths were often attributed to secondary infections, which occurred due to the immunocompromisation caused by HIV. HIV was known to affect the kidney's functioning as early as 1984[152]. Multiple causes for kidney failure in HIV infection have since been identified, these are summarised in Table 1.1

Table 1.1 Differential diagnosis of kidney disease in HIV-infected patients[153–156]

Acute kidney injury
Common HIV non-specific causes
Opportunistic infections[a]
Kidney hypoperfusion and ischaemia
Acute interstitial nephritis
Rhabdomyolysis
Urinary tract obstruction: blood clots, fungus balls or crystalluria[b]
HIV-specific glomerulopathies[a]
Drugs[b]
Chronic kidney disease
HIV-specific glomerulopathies[a]
HIV-associated nephropathy (HIVAN)
HIV immune complex kidney disease (HIVICK)
Immune complex-mediated glomerulonephritis
Post-infectious glomerulonephritis
Immunoglobulin A nephritis
Mixed sclerotic/inflammatory disease
Membranous glomerulopathy
Lupus-like disease
Thrombotic microangiopathy
Common HIV non-specific glomerulopathies[b]
HCV-related membranoproliferative glomerulonephritis/cryoglobulinemia
Amyloidosis
Classic FSGS
Diabetic nephropathy
Minimal change disease
Nephroangiosclerosis
Drugs[c]
Fluid and electrolyte disorders
Disorders of osmolality
Potassium disorders
Acid-based disorders
Antiretroviral nephrotoxicity[c]
AKI: abacavir, atazanavir, didanosine, indinavir, ritonavir, saquinavir, tenofovir
CKD: abacavir, atazanavir, indinavir, lopinavir, tenofovir
Acute interstitial nephritis: abacavir, atazanavir, indinavir
Fanconi syndrome: tenofovir, didanosine, abacavir
Renal tubular acidosis: lamivudine, stavudine,
Crystalluria, lithiasis: indinavir, atazanavir and (rare): nelfinavir, amprenavir
Nephrogenic diabetes insipidus: didanosine, tenofovir
Others

HIV, human immunodeficiency virus; HCV, hepatitis virus C; FSGS, focal segmental glomerulosclerosis; AKI, acute kidney injury; CKD, chronic kidney disease. [a]Less common since combination antiretroviral therapy (cART) introduction. [b]More common since cART introduction.[c]Including antiretroviral drugs listed in Antiretroviral nephrotoxicity.

After the introduction of HAART, there were sustained reductions in AIDS-related deaths and opportunistic infections across diverse patient populations[157–163]. HAART also resulted in prolonged disease-free survival, durable HIV virologic suppression (as determined by reduced plasma viral load), immunologic ($CD4^+$ T cell) recovery, and reductions in hospitalization rates[164]. Between 1996 and 2004 there was a decrease in HIV-positive patients dying from AIDS-related causes, and as a result, proportionately more HIV-infected patients were dying from more non-AIDS-defining-illnesses (NADIs)[131]; the percentage of deaths due to NADIs rose from 13.1% pre-HAART (1996) to 42.5% in 2004[131]. Renal and hepatic diseases were both NADIs that proportionately increased during this period. The treatment for end-stage renal and hepatic disease in the general population was transplantation and there was a rapidly increasing population on both kidney and liver transplant waiting lists as a result of comorbidities associated with HIV[165].

1.4.7 Renal Transplantation in HIV-positive Patients

A 1990 study investigating the outcomes of transplant recipients who were undiagnosed as HIV-positive or seroconverted as result of transplantation, indicated that transplantation in the HIV-positive population would be possible once deaths due to AIDS-related complications were reduced[166]. Further studies showed that both patient and graft survival were similar in HIV-negative and HIV-positive transplant recipients[167]. Due to these findings and the advances in HAART, Peter Stock, a transplant surgeon at the University of California San

Francisco initiated a pilot study[168] and eventually a multi-centre, prospective trial to examine the safety and efficacy of renal transplantation between HIV-negative donors and HIV-positive recipients. Between 2003 and 2009, 150 participants underwent HIV-negative to HIV-positive renal transplants[169]. The outcomes indicated that these transplants were safe and effective as mean graft-survival rates fell between those reported in the national database for older kidney-transplant recipients (≥65 years) - who are offered transplantation selectively because they are at increased risk for graft loss or death- and those reported for all kidney-transplant recipients. Transplant recipients also showed no acceleration in their HIV disease progression profiles despite the immunosuppression and drug interactions[169]. They did however find that there were higher rates of rejection in the HIV-positive population as compared to the HIV-negative control transplants in this study as well as their pilot study[167,169]. They therefore recommended a T-cell depletion induction therapy (anti-thymocyte globulin, ATG) in patients at very high risk of immunologic rejection as well as close monitoring of, and swift response to, potential rejection events.

1.4.9 HIV Epidemic In South Africa

As mentioned in Section 1.4.1 (pg. 25), the first patients with AIDS in South Africa were reported in 1983. During the 1980s the majority of HIV cases were only found in homosexual males. By the end of 1989 surveillance studies showed high rates of HIV infection in the heterosexual population, predominantly mine workers[170] and blood donors[171]. Between 1990 and 1994 it became apparent

that the heterosexual epidemic was exceeding the homosexual epidemic in South Africa. The National HIV prevalence rates, based on annual antenatal surveys, increased from 0,76% in 1990, to 10,44% in 1994 and to 22,4% by 2000[172]. Age categorized prevalence data from antenatal clinics gave an indication of incidence in sexually active women. The first South African household survey of HIV prevalence, incidence and behavioural risks of men, women and children older than two years, was performed in 2002. It reported that the HIV prevalence in the general population in 2002 was 11.4% (Confidence Interval [CI] 10.0% - 12.7%)[173]. The report also showed that was a higher HIV prevalence in adult (15-49 years old) females (17.7%) than males (12.8%).

By 2000, the epidemic was spread throughout Africa, with Sub-Saharan Africa bearing the burden of disease – there were an estimated 36.1million people living with HIV of which 25.3 million were in Sub-Saharan[174]. Sub-Saharan Africa differed from the rest of the world in that there was a higher prevalence of women with HIV, and dying from AIDS-related illnesses, than men[174] – this may be due to the main source of prevalence data coming from antenatal surveys. 2000 was the first year that the regional HIV incidence in Sub-Saharan Africa was stabilizing, with an estimated 3.8 million new infections as opposed to 4 million the year before[174]. This was largely due to education campaigns and the initiation of HAART in most countries.

1.4.10 Delay of HAART and PMTCT in South Africa

Many Sub-Saharan African countries initiated public HAART and Prevention of Mother to Child Treatment (PMTCT) programs between 2000 and 2007 - South Africa delayed these interventions. According to UNAIDS, by 2007 South Africa had the highest number of people living with HIV in the world with 5.7 million people [4.9 million–6.6 million][175], an increase from 4.7million [4 million – 5.million] from 2001[175].

The South African HIV/AIDS/STD National Strategic Plan for 2000 – 2005 included investigating the potential use of antiretrovirals only for PMTCT and occupational exposure (e.g. needle stick injuries), but not as a treatment option for people living with HIV[176]. In 2001, South Africa announced that it would make ART available to pregnant mothers as part of PMTCT[177,178]. Initially PMTCT consisted of single therapy with Nevirapine (NVP). Only in 2008 did the South African government announce that it would provide HAART to people with late stage HIV-related complexes (WHO stage 3 or 4)[179] and expand combination ART to the PMTCT program[180]. At the time the prevalence of HIV in the general population was 10.9% (CI: 10.0% – 11.9%)[181]. This had increased to 12.2% (CI: 11.4% – 13.1%) by 2012[182].

1.4.11 HIVAN and HIV-related Kidney Disease in South Africa

As a probable result of the delay in providing HAART, South Africa still has the highest HIV prevalence in the world[183]. There are also a large number of patients suffering from secondary conditions related to HIV infection of which HIV-Associated Nephropathy (HIVAN) is of particular importance. HIVAN is by far the most common kidney complication in people living with HIV[184–186]. It is the result of viral infection and replication in the kidney[187–189]. Characteristic focal segmental glomerulosclerosis (FSGS) and tubular interstitial disease is diagnosed by biopsy[186,190]. Clinically, it presents as a rapid decrease in the glomerular filtration rate (GFR), heavy proteinuria and rapid progression to End-Stage Renal Disease (ESRD)[191]. HIVAN is particularly problematic in the African context as there is evidence to suggest that people of African descent are genetically more susceptible to developing HIVAN[190,192] due to a specific single-nucleotide polymorphism (SNP) in the Apoliprotein L1 (APOL1) gene, found in a high prevalence in West African descendants[193,194]. A biopsy study at the Chris Hani Baragwanath Hospital in Soweto, South Africa showed that HIVAN was present in 27.3% (27/99) of biopsied patients with HIV[195]. This does not account for other forms of non-collapsing FSGS nor other chronic kidney diseases. At present, the standard treatment for HIVAN is HAART.

1.4.12 HIV-positive to HIV-positive Renal Transplants

Patients with HIV and kidney failure require dialysis for continued renal function and eventually require Renal Replacement Therapy (RRT). In a resource-limited setting such as South Africa, the availability of dialysis as well as RRT is very limited. Spurred on by the outcomes of the pilot study by Stock et al[168], Elmi Muller, a transplant surgeon at Groote Schuur Hospital in Cape Town, South Africa made history by performing the first 4 renal transplants between HIV positive deceased donors and HIV positive recipients[196] in November 2008. The rationale behind the study and some immunological results of the follow-ups of these transplants will be explored in this dissertation.

1.5 Aim of the dissertation

Transplantation success is determined by a balance between inflammation and tolerance. This balance needs to be maintained in order to achieve graft acceptance without inducing dysfunctional immunity. In operational tolerance (tolerance in the absence of immunosuppression) regulatory T cells have been suggested to control the effect of allo-reactive T cells, preventing rejection without immunosuppression[197–199]. In HIV positive patients a balance is also required between regulatory and effector cells so that the viral load can be controlled while maintaining a functional immune system. Regulatory T cells have been shown to be involved in maintaining this balance[200]. There is little known about the impact of T-cell depletion therapy on HIV disease progression

but it has been shown to reduce the risk of acute rejection in HIV-positive kidney transplant recipients[201]. ATG has been shown to alter the proportions of different T-cells populations in such a way that a higher proportion of regulatory T cells to effectors T cells exists at post treatment[202–204]. There is however no evidence as to what effect T-cell depletion will have in a HIV-positive patient receiving renal transplantation on the T-cell repertoire and Regulatory T cells in particular.

The aim of this dissertation is to investigate the impact of T-cell depletion therapy combined with maintenance immunosuppression and renal transplantation on the relative proportion of peripheral regulatory T cells in HIV-positive patients receiving renal transplants from HIV-positive donors.

This aim was achieved by completing several objectives:

1) Use a Luminex assay to measure the concentrations of inflammatory and regulatory peripheral proteins in plasma over the first 3 months post ATG and transplantation
    a. Investigate the changes in inflammatory and regulatory proteins in selected recipients over time
    b. Compare the changes in the inflammatory and regulatory peripheral proteins in selected recipients with acute rejection to those with no acute rejection

c. Identify proteins that changed in concentration over time in all recipients
d. Correlate the concentrations of the inflammatory and regulatory proteins with clinical and biological factors of the recipients
e. Identify which of the inflammatory and regulatory proteins differed between patients and to what extent

2) Build a polychromatic flow cytometry panel to phenotype T cells in the periphery post-transplant based on the results from the Luminex assay
    a. Phenotype T cell subsets at one year post-transplant
    b. Phenotype T cell subsets at baseline
    c. Compare changes in the T cell proportions at baseline to one year post transplant.

CHAPTER 2: Details of the HIV+-to-HIV+ transplant cohort and selected patients

2.1 Background and Aims

The increased coverage of anti-retroviral therapy (ART) in South Africa has been successful in extending the lives of individuals living with HIV[131,205]. HIV-infected patients now live longer than before[206] as a result they are at a greater risk of developing chronic conditions long term ART and prophylactic medications use, or causes unrelated to HIV[207]. South Africa has the highest prevalence of HIV in Africa[183,208] and as much as 22% of the HIV-infected population may develop chronic kidney diseases (CKD)[185,209,210]. Biopsy studies have reported that ±30% of CKD in HIV-infected patients is attributed to HIV-associated Nephropathy (HIVAN)[211–213] which can lead to end-stage renal disease (ESRD) and death particularly in resource-limited settings where dialysis treatment options are limited. Stock et al., showed that renal transplants from an uninfected donor to a HIV-infected recipient are safe and successful in treating ESRD[169]. However, an increasing number of HIV-infected patients are waiting for transplants[214].

Organs from HIV-infected deceased donors (HIVDD) can create a new source of expanded organ availability for HIV-infected patients in need of a transplant. The use of these organs, that would otherwise be discarded, could also benefit the HIV-uninfected population by removing HIV-infected individuals from transplant waiting lists. An exploratory study to assess the safety and efficacy of HIV-

positive to HIV positive renal transplants was started in 2008 in South Africa at Groote Schuur Hospital. To date, 43 HIV-infected individuals have been transplanted with kidneys from HIVDD. The preliminary data as well as the 3-to-5 year follow-ups show that these transplants are safe and effective[196,215]

This chapter describes the cohort and which samples from the deceased donors and transplant recipients were used in this dissertation.

2.2 Inclusion and Exclusion Criteria

2.2.1 Inclusion Criteria

To be a candidate for the Renal Replacement Program at GSH, HIV-infected patients must have been diagnosed with CKD and approaching Stage V of the disease. The candidate needed to be on a stable HAART regimen for at least 6 months prior to screening, unless there had been changes made due to toxicity/drug-drug interactions in which case the candidate needed to be show excellent adherence for at least 3 months. Their viral load needed to be undetectable (<50copies/ml) and $CD4^+$ T cell counts greater than 200cells/μL at 16 weeks prior to transplantation. If the candidate had opportunistic infections or neoplasms (see Table 1.1 for details) then they needed to be on appropriate acute and maintenance therapy with no sign of active disease.

Table 2.1 Opportunistic infections/Neoplasms and treatment required for inclusion

Opportunistic Infection/	Treatment Required for Inclusion
Candidiasis of Esophagus or Vagina	Response to treatment with no recurrence in the last 6 months on HAART.
Encephalopathy (HIV related)	Diagnosed prior to HAART, resolved on HAART and no evidence of progression.
Isopsoriasis (chronic intestinal)	Good response to treatment without history of recurrence in the last 6 months on HAART
Mycobacterium tuberculosis	Completed treatment with clinical, radiological and microbiological response. Must be on INH secondary prophylaxis.
Non-tuberculosis Mycobacteria	Completed treatment with clinical, radiological and microbacterial response, with no recurrence in the last 6 months on HAART.
Pneumocystis pneumonia (PCP)	Completed treatment with clinical and radiological response. Must be on / restart secondary cotrimoxazole prophylaxis
Recurrent bacterial infections	Completed treatment with clinical, ±radiological and microbacterial response with no recurrence in the last 6 months on HAART
Non-typhodial Salmonella Septicemia	Completed treatment with clinical response and no recurrence in the last 6 months on HAART
Toxoplasmosis (CNS)	Completed therapy and CT/MRI shows signs of resolution without active disease and is on secondary cotrimoxazole prophylaxis

2.2.2 Exclusion Criteria

Candidates were not considered for inclusion into the study cohort if they had any opportunistic infections or malignancies that are not included in Table 2.1 or

treated as in Table 2.1. If the candidate had the following malignancies/opportunistic infections then they were not considered for inclusion: Kaposi's sarcoma, lymphoma, or other EBV- or HHV8-associated Lymphoproliferative diseases; any other neoplasm except for anogenital carcinoma in situ, adequately treated basal/squamous cell carcinoma (BCC/SCC) or SCC of skin, or solid tumour disease free at 5 years; cytomegalovirus disease: retinitis or disseminated infection; deep fungal infection (Cryptococcus; histoplasmosis; candidiasis at a site other than the esophagus or vagina sporotrichosis, aspergillosis, fusariosis); any other disseminated fungal infections; Disseminated Herpes Simplex virus infection; Multi-drug resistant (MDR) or extensively-drug resistant (XDR) tuberculosis; Progressive multifocal leukoencephalopathy; Chronic intestinal cryptosporidiosis of > 1 month duration; Untreated hepatitis B or hepatitis C co-infection with active viral replication, where treatment for hepatitis B or C should be considered first. No candidates with advance cardiac or pulmonary disease were considered. If candidates had documented HIV resistance to all 3 antiretroviral classes (NRTIs, NNRTIs and PIs) or an inability to comply with the immunosuppressive protocol or advanced cardiac or pulmonary disease then they were also not included in the study.

2.3 Details cohort of all HIV$^+$ to HIV$^+$ Recipients

Since 2008, there have been a total of 43 recipients from 24 deceased donors. All recipients met the inclusion criteria. All recipients received ATG induction

therapy for 5 days post transplant due to the increased risk of rejection in HIV positive renal transplant recipients[201] and were placed on maintenance immunosuppression of prednisone, mycophenolate mofetil and Tacrolimus. The summary of the numbers of recipients, donors, and their sex, age, pre-transplant CD4 count and the median follow up time was recorded (Table 2.2). Viral loads were undetectable for all recipients at TP. The number of patients that lost their grafts or died with a functional graft was included as was the number of recipients that had biopsy-confirmed T-cell mediated rejection (TCMR) and Antibody mediated rejected (ABMR). The number of recipients in which HIVAN was the cause of renal failure (RF) before transplantation (pre-TP), as well as the number of recipients that developed HIVAN after transplantation (post-TP) was also included.

Table 2.2. Summary Data for all participants in HIV+ to HIV+ transplants

Number of recipients	43
Number of donors	24
Male	29
Female	14
Median Age (IQR)	43 (33-49)
Median Baseline CD4 count/µL (IQR)	420 (332-513)
Median months followed up (IQR)	38 (11-63)
Number of grafts lost	7
Died with functional graft	7
TCMR	2
ABMR	8
HIVAN as cause of RF (pre-TP)	24
HIVAN post-TP	5

2.4 Sample Collection

Samples were collected shortly before transplantation (Visit 000) then at regular intervals during the first year post-transplant (Visit 101 – 126). At Visit 000, blood was drawn from the recipient as well as the donor. From this blood, plasma and peripheral blood mononuclear cells (PBMCs) were isolated and stored. Two renal biopsy cores were removed from the donor kidney; one was sent for pathological scoring and the other saved for further work. At the other visits during the first year, blood was drawn from the recipients from which plasma and PBMCs were isolated and cryopreserved. At annual visits thereafter in years 2 – 5 (Visit 200 – Visit 500), the recipients had blood drawn and protocol biopsies performed. Non-protocol biopsies were also taken when a change in renal function was indicated.

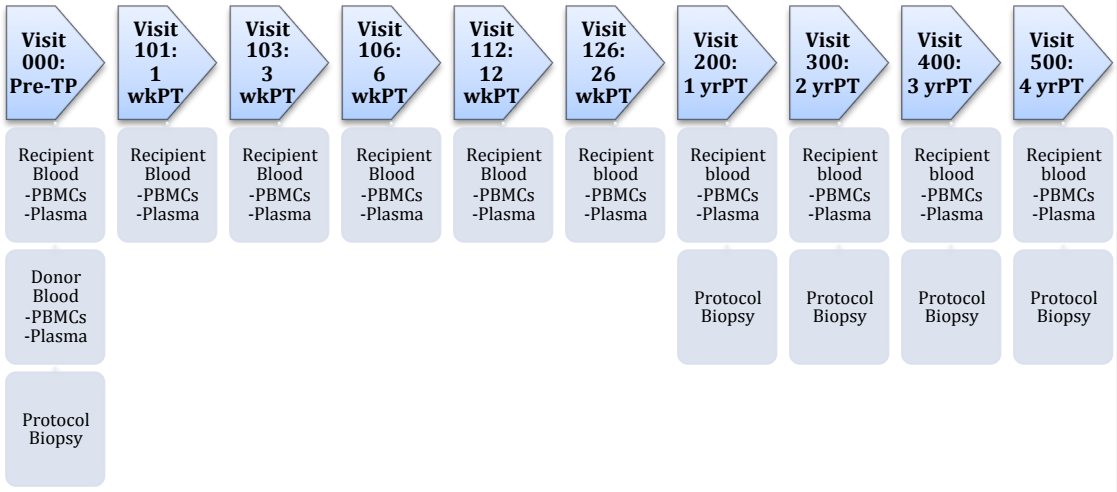

Figure 2.1 . Sequence of Events for Sample Collection. The visit time codes showing the time at which samples were collected are shown in Figure 2.1. Any

pre-transplant timepoints is designated Visit 000. Visits in the first year are named according to the weeks post transplant (PT) as V101 – V126. The post-transplant (PT) timepoints are designated as weeks PT (wksPT) or years PT (yrPT). The different samples collected and saved at each visit are shown.

2.5 Clinical Details of Selected Recipients and Donors

Of the 43 recipients, 10 were selected for investigation in this dissertation to identify changes in the peripheral immune and regulatory factors within the first 12 weeks post-transplant. These recipients were selected because there was both stored plasma and PBMCs available for Visits 000, 101, 103, 106 and 112. Table 2.3 shows the clinical details for these participants. This table uses the patient identifier (PID) for the study, the KID-PID, for the 10 selected recipients as well as their donors. There were 6 donors for these 10 recipients. The majority of the selected participants (8/10) were black, one was mixed race, and one white. There was an equal split of male (5/10) and female (5/10) participants. Their median age at transplant was 34.5 years (range: 27 to 52 years). CD4 counts were recorded in the week prior to transplantation for 9/10 participants. The median CD4 count was of 441 cells/µl (range: 233 to 973 cells/µl). The participants had protocol renal core biopsies taken as indicated in Figure 2.1 (pg. 48), as well as when the clinical signs suggested a decrease in renal function. From these biopsies, acute and chronic rejection was diagnosed. Recipients in which acute rejection was clinically indicated were treated with additional Tacrolimus and plasmapheresis. Only 2/10 of the recipients (KID-131

and KID-132) experienced acute rejection during the 12-week period. KID-131 had ABMR and KID-132 had a borderline change related to TCMR. There were no cases of graft loss or death in the 10 participants. The HLA-serotypes for the recipients are also included. Not all of the HLA-genes were sequenced for all recipients or donors. The HLA allele genotypes (indicated by '*') and serotypes (indicated by no '*') are displayed – where a dash is shown neither the genotype nor serotype is available for the HLA allele. It is not routine practice at GSH to HLA match deceased donors with recipients due to the small donor pool and large numbers of patients awaiting kidney transplants. The trigger for transplant allocation is based on being crossmatch negative using the most recent patient serum and two historical samples from the preceding 12 months. In the 10 patient samples selected, there were, however, a number of HLA matches between donors (highlighted in green), which was by chance. The numbers for the total matched HLA –alleles between the recipients and donors are summarised for each recipient.

Table 2.3 Clinical details of Luminex-assayed patients

Recipient KID PID	111	112	114	125	131	132	135	136	137
Donor KID PID	5007	5007	5008	5014	5018	5018	5020	5020	5021
Race	Black	Black	Mixed	Black	Black	Black	White	Black	Black
Sex	Female	Female	Female	Male	Male	Male	Male	Male	Fema
Age at Tx	34	31	39	33	27	45	35	52	32
Pre-op CD4	517	441	378	473	521	-	233	256	973
AR <12wkPT	No	No	No	No	Yes	Yes	No	No	No
ART Rx1	EFV	LPV/r	EFV	LPV/r	LPV/r	LPV/r	NVP	EFV	EFV
ART Rx2	ABC	TDF	ABC	TDF	ABC	ABC	ABC	ABC	ABC
ART Rx3	3TC	3TC	3TC	3TC	3TC	3TC	3TC	3TC	3TC
HLA-A1	A23	A23	-	A28	A23	A29	A*01	A*29	A28
HLA-A2	A10	A28	-	A23	A30	A30	A*26	A*68	A29
HLA-B1	B08	B7	-	B08	B17	B17	B*18	B*13	B70
HLA-B2	B70	B14	-	B45	B70	B70	B*27	B*58	-
HLA-DR1	DR*0302	DR*04	DR*13	DR*01	DR*13	DR*11	DR*14	DR*13	DR*0
HLA-DR2	DR*11	DR*13	DR*15	DR*03	DR*15	DR*1112	DR*03	DR*12	DR*1
HLA-DQ1	DQ*0402	DQ*0302	DQ*06	DQ*05	DQ*06	DQ*05	DQ*02	DQ*05	DQ*0
HLA-DQ2	DQ*06	DQ*06	-	DQ*02	-	DQ*02	DQ*05	DQ*06	DQ*0
HLA Matches (total)	1	2	2	3	2	2	3	2	1

CHAPTER 3: MATERIALS AND METHODS

3.1 Standard Procedures

3.1.1 Plasma isolation from whole blood

As mentioned in Chapter 2 (Section 2.4, page 48), blood was collected at various study visits. For each participant, a total of 80ml of blood was collected in ten 8ml Anticoagulant Citrate Dextrose (ACD) tubes. In a Class II Biological safety cabinet, the blood was pooled and then layered onto a 50ml Leucosep™ tubes containing 15ml of Histopaque solution. The Leucosep™ tubes were then centrifuged at 2200 rpm for 18 min with the brakes off. When the spin was complete, separate layers were visible (Figure 3.1).

The plasma layer was first removed using a sterile serological pipette. Twenty 1ml aliquots of plasma were dispensed into labelled 2ml "o-ring" screw cap tubes. These were frozen at -80°C and their positions recorded.

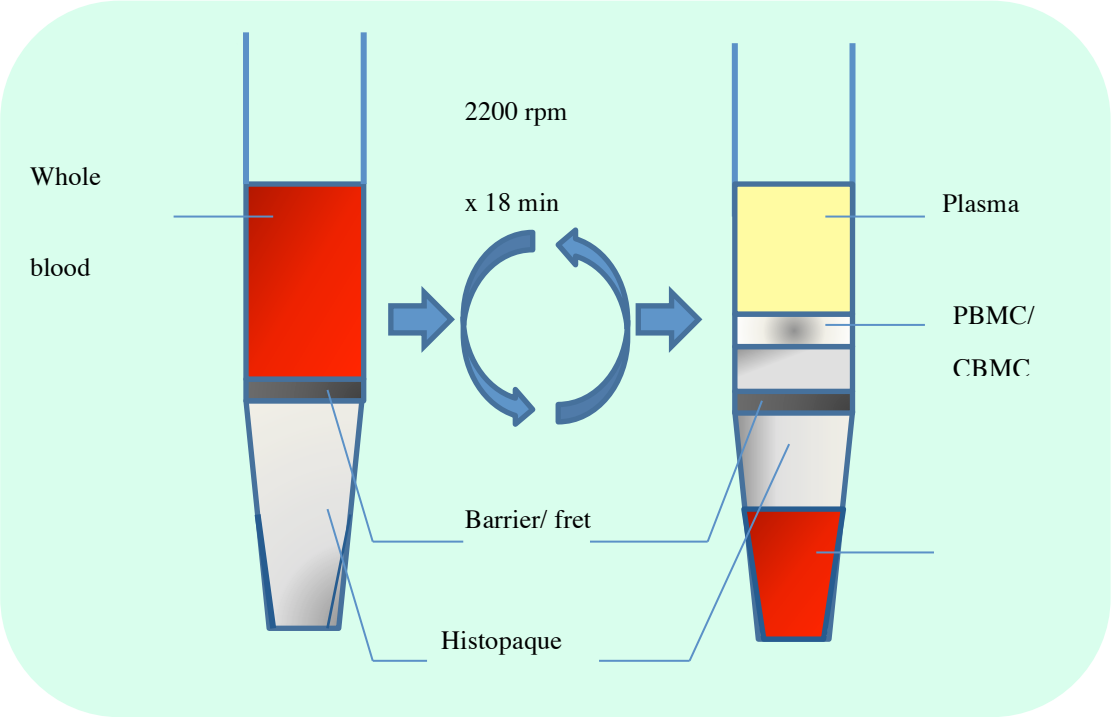

Figure 3.1. Leucosep™ Tubes used for Separation of Plasma and PBMCs

A total of 25ml of whole blood was added on top of the barrier and centrifuged to separate the blood into layers of plasma, PBMC, Histopaque and Red Bloods Cells (RBCs).

3.1.2 PBMC isolation from whole blood

The PBMC layer in the Leucosep™ was carefully removed using a sterile Pasteur pipette. This was added to a 50ml polypropylene tube and topped up to 30ml with a wash buffer consisting of Phosphate Buffered Saline (PBS) solution and 2% Fetal Calf Serum (FCS). The PBMCs were washed twice. Each wash step included centrifugation of the PBMC solution at 1500 rpm for 10min with brakes on, discarding the supernatant and re-suspension of the pellet by the re-addition

of 30ml of the wash buffer for the next wash. After the second wash was completed, the PBMC pellet was resuspended in 10ml of wash buffer for counting. The count was performed by first mixing 10µl of the wash buffer cell suspension with 10µl of trypan blue in a 96-well plate well. A total of 10µl of this mixture was added to an automatic cell counting slide compatible with the TC20 Automatic Cell Counter and counted twice. For each count, the viability and live cells/ml was recorded. The total live cells in 10ml were calculated and a mean viability and live cells numbers was calculated for the sample. The cell suspension was topped up to 20ml with wash buffer and centrifuged at 1500 rpm for 10min again. The pellet was resuspended at a concentration of $20x10^6$ cells/ml in cold FCS. Into cold, labelled cryovials, 500µl of the FCS cell suspension was added. A total of 500µl of 20% DMSO in FCS was added drop by drop while gently swirly each cryovial on ice to make the cell density 10×10^6 cells/ml. The cryovials containing $1x10^6$ PBMCs in 1ml of 10% DMSO and FCS were moved to a Mr. Frosty™ Freezing Container (Thermo Scientific). The Mr Frosty™ Freezing Container was moved to the -80°C freezer overnight and the following day, the cryovials were moved to Liquid Nitrogen and their positions recorded.

3.1.3 Thawing PBMCs

When thawing PBMCs, the cryovials were removed from liquid nitrogen and 75% thawed in a 37°C water bath. Drop by drop, warm RPMI containing 10% FCS (R10) was added to the cryovials while gently shaking. This was transferred to a 50ml polypropylene tube and topped up to 30ml with warm R10. The R10

cell suspension was centrifuged at 1500 rpm for 10min with the brakes on. The pellet was resuspended in 2% FCS in PBS (wash buffer) and centrifuged at the same speed again. This wash step was then repeated after which the pellet was resuspended in 10ml wash buffer and counted as during freezing. The cell suspension was centrifuged as before and the pellet resuspended in a 2% FCS in PBS solution at a concentration of $20x10^6$ cells/ml.

3. 2 Luminex Assay Procedures

3.2.1 Luminex Concept

In order to determine the changes in peripheral proteins in plasma related to inflammation, regulatory activities of T cells and kidney-related injury, a luminex assay was developed to measure the concentrations of these proteins over time.

Luminex is a multiplex bead-based assay, similar to an enzyme-linked immunoassay (ELISA). It uses micro-beads linked to multiple antibodies specific to proteins of interest attached to the beads. The capture antibodies are located on a specific area of the bead, known as the bead region. The sample is incubated with the beads in a 96-well plate, in order for the proteins of interest to adhere to the capture antibodies attached to the beads. After an incubation period, the unbound sample is washed from the beads. A secondary detection antibody linked to biotin is incubated with the beads, where the addition of the secondary detection antibody greatly increases the specificity and sensitivity of the assay.

After washing, the beads are incubated with a Streptavidin-Phycoerythrin (PE) reporter. Each biotin molecule can bind up to five Streptavidin-PE molecules, amplifying the signal generated. A laser of 488nm excites the Streptavidin-PE. The median fluorescence intensity (MFI) of the emitted light is measured for each bead region using The Luminex 200 system (Luminex Corp., Austin, TX, USA). This can identify each of the unique bead regions to which specific antibodies are attached. By using a serially diluted standard of known concentrations of all the proteins of interest, one can determine the concentration of each analyte from the MFI.

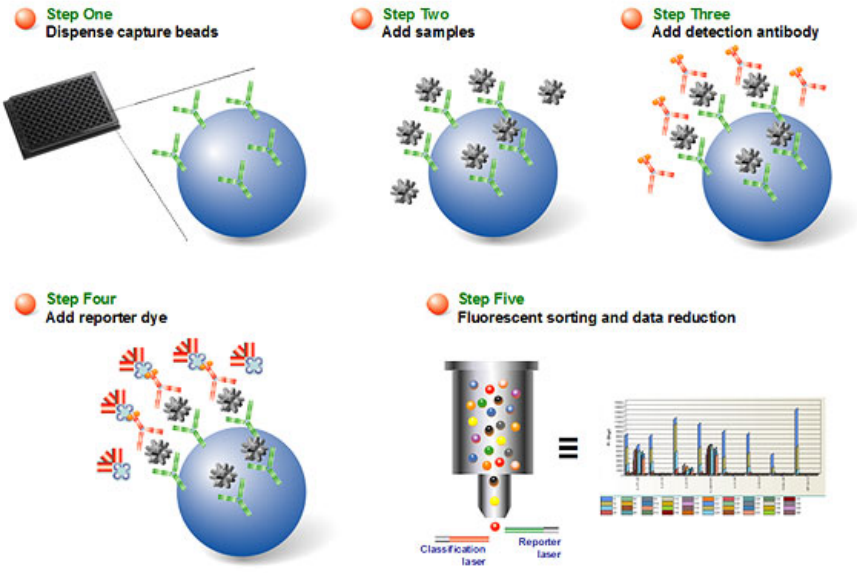

Figure 3.2. Schematic representation of multiplexed microbead-based Luminex Assay.[216] The figure shows the step-by-step procedure of the Luminex assay. Step one shows the samples added to the 96-well plates used for the luminex assay. Step two shows the inside of the well with the capture that bind the protein of interest. Step three shows the addition of the sandwich antibody

that binds to capture antibody/protein. In Step four, a reporter dye is added. The laser shown in Step five excites and the fluorescent intensity is recorded.

3.2.2 Luminex Assay Design

The Luminex 200 system was used to measure the concentrations of 67 different plasma proteins using two different kits for the selected recipients outlined in Chapter 2 (table 2.2, section 2.5, page 47). The plasmas assayed were isolated from blood drawn at different visits; Visit 000, 101, 103, 106 and 112 (Figure 3.3).

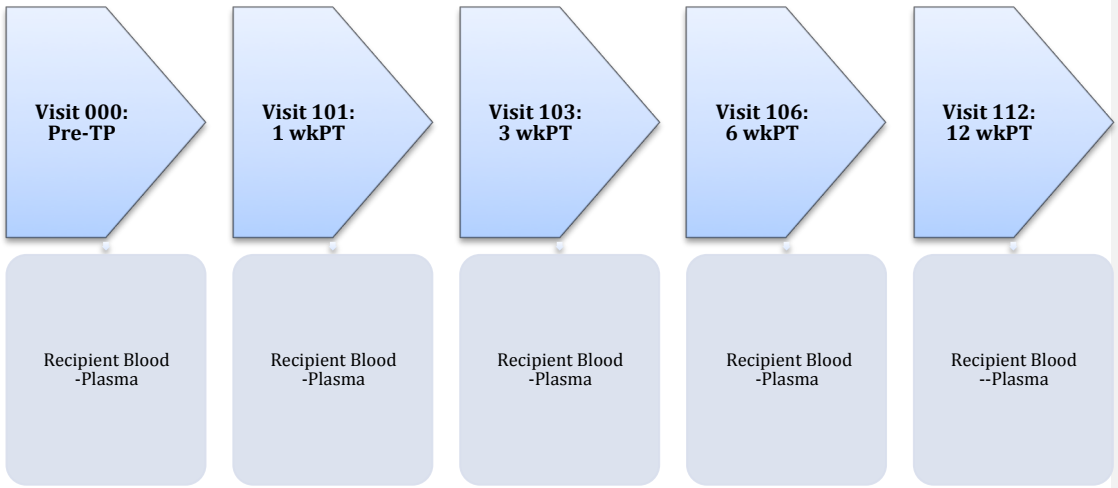

Figure 3.3. Study visits where plasma protein concentrations were measured for 10 participants. The visits used for the Luminex assay are shown in the figure. These included the visits prior to transplantation (V000), 1 week post-transplant (V101), 3 weeks post-transplant (V103), 6 weeks post-transplant (V106) and 12 weeks (V112) post-transplant where the Luminex assay was

performed. At each visit, blood was drawn and plasma extracted and stored.

These time-points were selected to give an indication of the acute changes in inflammatory and regulatory proteins in response to ATG treatment for 5 days immediately after transplantation and then maintenance immunosuppression. Plasma samples were thawed overnight at 4°C on ice to minimize heat shock to the plasma proteins and maximise protein recovery. Once thawed, the plasma was divided into 200µl aliquots and refrozen to ensure that assayed samples would have the same number of freeze-thaw cycles; in this case each had been through 2 freeze-cycles, the maximum permitted cycles before loss of cytokine protein concentration has been observed[217].

Two separate Luminex kits were used. The first was the Bio-Rad 37-plex Inflammation Panel (Bio-Rad, Hercules, California, USA). The analytes of which are shown in in Table 3.1 along with the classification of their mode of action as either Inflammatory, Regulatory of Dual Action, which was used for downstream analysis. The second panel was a custom 30-plex kit (Table 3.2) from eBioscience (San Diego, California, USA) that included inflammatory and regulatory proteins not included in the 37-plex kit as well as markers of tissue damage and remodelling. There were 3 cytokines (IL-2, IL-10 and IFN- γ), which were common between the two plates. These acted as inter-kit controls.

Table 3.1. Bio-Rad 37-plex Panel grouped according to primary mechanism of action

Inflammatory		**Regulatory**	**Inflammatory/Regulatory**
APRIL/TNFSF13	IL-8	IL-10	gp130/sIL-6Rbeta
BAFF/TNFSF13B	IL-12(p40)	IL-20	sIL-6Ralpha
sCD30/TNFRSF8	IL-12(p70)	IL-35	IL-11
sCD163	IL-26	sTNF-R1	IL-19
Chitinase 3-like1	IL-27	sTNF-R2	IL-22
IFN-a2	IL-28A/IFN-λ2	TSLP	MMP-1
IFN-beta	IL-29/IFN-λ1		MMP-2
IFN- γ	IL-34		MMP-3
IL-2	LIGHT/TNFSF14		TWEAK/TNFSF12
	Osteocalcin		
	Osteopontin		
	Pentraxin-3		

Table 3.2. eBioscience 30-plex Panel grouped according to primary mechanism of action

Inflammatory		**Regulatory**	**Inflammatory/Regulatory**
IL-1α	IL-2	IL-1RA	IL-9
IL-1β	IL-23	IL-10	IL-13
IL-4	IP-10	IL-21	MIF
IL-6	BLC		
IL-15	MCP-1		
IL-16	sCD40L		
IL-17	MIP-1β/CCL4		
IL-18	Eotaxin		
Gro-α	Fractalkine		
IFN- γ	TNF- α		
VEGF-α	SDF-1 α		
sFAS-L	TRAIL		

3.2.3 Luminex Plate Layout

For both kits, the samples from each participant were divided into 2 plates so that all visits from one participant were on one plate (Figure 3.4). The same plate layout was used for both Luminex kits. In order to control for variability between 2 plates of the same kit, 10 samples were chosen at random to serve as interplate controls, and from which interplate variability for each analyte could be measured. The samples were tested in duplicate on every plate and these were randomly assigned to wells on the plate to avoid assay bias. The procedure was performed according to the protocols provided by the manufacturer. Data were analysed using five-parametric-curve fitting with Bio-Rad Analyst software. The concentration of each cytokine was determined by the mean fluorescence intensity (MFI), which was subsequently converted to a cytokine concentration (ng/ml) using a simultaneously generated standard curve.

A

PLATE 1

	1	2	3	4	5	6	7	8	9	10	11	12
A	S1	S1	B	B	111 V101	135 V112	131 V000	112 V112	114 V103	111 V103	136 V103	114 V112
B	S2	S2	QC1	QC1	131 V101	114 V000	111 V000	114 V112	125 V103	114 V101	112 V112	135 V112
C	S3	S3	QC2	QC2	138 V106	111 V103	125 V101	114 V101	112 V106	125 V101	125 V000	131 V112
D	S4	S4	125 V000	132 V112	112 V000	131 V112	112 V112	114 V106	137 V106	111 V101	114 V000	131 V112
E	S5	S5	111 V101	136 V103	137 V106	131 V106	138 V106	131 V103	125 V106	114 V101	112 V112	111 V000
F	S6	S6	114 V106	131 V101	112 V101	125 V112	112 V103	125 V103	132 V112	112 V101	HIV-1	HIV-1
G	S7	S7	131 V106	112 V106	111 V101	125 V106	125 V106	114 V103	111 V112	131 V000	HIV-2	HIV-2
H	S8	S8	125 V106	131 V112	114 V101	111 V112	131 V103	112 V103	125 V112	112 V000	HIV-3	HIV-3

B

PLATE 2

	1	2	3	4	5	6	7	8	9	10	11	12
A	S1	S1	B	B	132 V000	135 V112	132 V112	136 V000	135 V103	136 V101	136 V103	136 V112
B	S2	S2	QC1	QC1	138 V106	137 V101	132 V106	135 V101	132 V106	114 V101	112 V112	135 V112
C	S3	S3	QC2	QC2	138 V106	136 V000	135 V106	114 V101	135 V101	136 V103	135 V112	136 V112
D	S4	S4	132 V112	138 V101	132 V000	138 V106	112 V112	137 V106	137 V106	132 V101	137 V103	131 V112
E	S5	S5	136 V103	132 V112	137 V106	138 V000	138 V106	136 V103	135 V106	137 V101	HIV+1	HIV+1
F	S6	S6	135 V000	138 V101	138 V103	135 V000	132 V103	138 V103	132 V112	138 V000	HIV+2	HIV+2
G	S7	S7	136 V101	137 V000	136 V000	132 V101	125 V106	135 V103	132 V000	136 V106	HIV+3	HIV+3
H	S8	S8	125 V106	131 V112	136 V106	137 V000	132 V103	137 V103	137 V106	135 V112	HIV+4	HIV+4

KEY

Standards
Quality Control
Blank
Interplate Controls
Samples
Other controls

Figure 3.4. Plate Layout for Luminex Assays. The plate layout shows the wells in which samples on the 96-well plate in the Luminex assay. The wells are coloured according to the key. The recipients' plasma is shown in green. The 3-digit KID-PID is included for these samples, followed by the visit code loaded into that well (V000 – V112). The serially diluted standards are indicated in dark blue as S1 to S8 where S1 is the neat standard protein cocktail and it is diluted 1:2 until S8. The blanks are indicated in white as B. The Quality Controls provided with the kit are indicated in orange as QC1 or QC2. The samples highlighted in yellow are the interplate controls and appear on both plates. The samples in turquoise are the control plasmas included from either an HIV negative cohort in Barcelona, Spain or an HIV positive cohort in Lima, Peru.

3.3 Development of a Regulatory T cell Flow Cytometry Panel

3.3.1 Flow Cytometry Antibodies and Fluorochromes

An 8-colour flow cytometry panel was developed with the intention of phenotyping the Tregs in the periphery. The panel was designed to assess what proportion of T cells ($CD3^+$), $CD4^+$ or $CD8^+$, which of these were memory cells (CD27/CD45RA), activated ($CD25^{+,)}$ and which of these had a T regulatory cell phenotype ($CD4^+$, $CD25^{high}$, $CD127^{low}$, $FoxP3^+$). The final panel included a live/dead marker (Zombie-NIR) as well for the discrimination of live cells.

Table 3.3 shows all the surface markers and Table 3.4, all the intracellular markers used in the panel.

Table 3.3. Surface markers of Treg Flow Cytometry Panel

Antibody	Fluorescence	Clone	Isotype	Company
Zombie-NIR	-	-	-	Biolegend
Anti-human CD3	BV650	OKT3	Mouse IgG2a,k	Biolegend
Anti-human CD4	PECy5.5	S3.5	Mouse IgG2a	Invitrogen
Anti-human CD8	V500	RPA-T8	Mouse IgG1,k	BD Biosciences
Anti-human CD25	BV421	M-A251	Mouse IgG1,k	BD Biosciences
Anti-human CD27	PECy5	O323	Mouse IgG1,k	eBiosciences
Anti-human CD45RA	PerCP-Cy5.5	HI100	Mouse IgG2b,k	BD Biosciences
Anti-human CD127	PE-CF594	HIL-7R-M21	Mouse IgG1,k	BD Biosciences

Table 3.4. Intracellular markers of Treg Flow Cytometry Panel

Antibody	Fluorescence	Clone	Isotype	Company
Anti-human FoxP3	Alexa647	259D/C7	Mouse IgG1	BD Biosciences

3.3.2 Staining PBMCs

In a 96 well plate, 1 x 10^5 of thawed PBMCs (50µl) was added to a well for each staining condition. Each well was topped up with 150µl of staining buffer (2% FCS in PBS) and centrifuged at 2200 rpm for 3 min. After centrifugation, the supernatant was discarded, and the cells resuspended in 50µl of staining buffer containing the titrated optimal volume of Zombie-NIR. The plate was covered with foil and incubated at room temperature (RT) for 30 min. After incubation, 150µl staining buffer was added to each well and the plate centrifuged as before. The cell pellet was then resuspended in a surface marker mix containing the conjugated-antibodies for all the surface markers at their titrated volumes in a total of 50µl. The plate was covered and incubated at 4°C for 30-45min. After incubation the plate was washed as before. The pellet was resuspended in 100ul of cold stain buffer and transferred to a 5ml Polystyrene FACS tube. An additional 1.9ml of cold stain buffer was added to the tube, which was then centrifuged at 1500rpm for 10min and the supernatant aspirated off. The pellet was resuspended in 1ml Transcription Factor (TF) Fixation/Permeabilisation (fix/perm) buffer (BD Biosciences), added while vortexing. This was incubated at 4°C for 45 min and then 1ml of the TF Permeabilisation/Wash (perm/wash) buffer (BD Biosciences) was added and the tube was centrifuged as before. Another 1ml perm/wash buffer was added and the tube centrifuged again. After aspirating the supernatant, the titrated volumes of the intracellular markers were added in 100ul of the perm/wash buffer and the tube incubated at 4°C for 45 min. Two washes were performed with 2ml of the perm/wash buffer,

centrifuging in between and the pellet was resuspended in 350µl and was ready for acquisition.

3.3.3 Acquisition on the LSRII Flow Cytometer

The samples were acquired on the LSRII Flow Cytometer. The configuration of the detectors and their Band pass (BP) and Long Pass (LP) filters are shown in Figure 3.5. For each fluorochrome included in the panel, a compensation tube was included with anti-mouse compensation beads and the relevant antibody. Compensation tubes were acquired to correct for the spill-over of emission spectra of some fluorochromes into other channels. After the compensation tubes and the samples were acquired, the data were exported as FCS files and analysed on FlowJo software v9.9.4 (TreeStar, Oregon, USA).

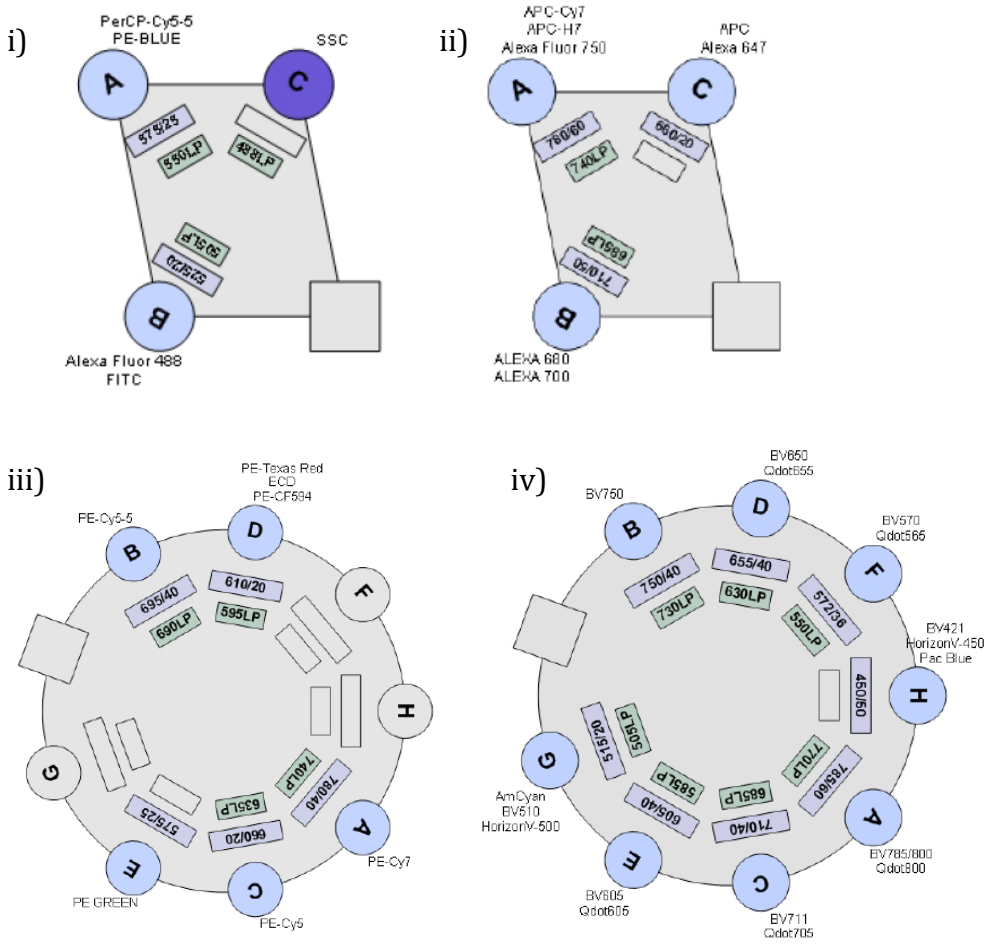

Figure 3.5. Configuration of the Detection filters on the LSRII Flow Cytometer. The detection filters for the different lasers are shown in the figure. The long pass (LP) filters shown in green only allow light above the specific wavelength and reflects all light that is below. The band pass (BP) filters highlighted in blue allow light between a set wavelength to pass through and reflects light above and below the set wavelength – the wavelength range is equal to the first number ± the number after the slash. The detection filters for all the markers excited by the different colour lasers are shown in i-iv; (i) the blue laser (488nm) as well as the Side Scatter detector (SSC); (ii) the red laser (633nm); (iii) the green laser (532nm) as well as the Forward Scatter detector

(FSC); (iv) the violet laser (405nm). The commonly used fluorescent markers detected by each filter are also shown.

3.4 Statistical Analysis

3.4.1 Luminex Data Clean Up

The data generated from the Bio-Rad software was an MFI and calculated concentration based on the automatically generated standard curve for each analyte in the kit. This was produced in an excel sheet for each sample shown in Figure 3.4. These data also indicated if an MFI fell Outside of the Observable Range (OOR) of the Standard Curve for a particular analyte. For all values that were OOR it was also indicated if they were above (>OOR) or below (<OOR) that analyte's range. Clean-up of Luminex data commenced by excluding all analytes for which >90% of measured values were <OOR. As all samples from each patient were run as duplicates on the plate, the variability between duplicates (intra-plate variability) was initially assessed.

3.4.2 Intra-plate variability

The intra-plate variability was assessed to identify replicates that were outliers. This was done to control for excessive variability between replicates on the same plate. This was assessed using a Bland-Altman plot, also known as a difference plot, a graphical method for determining the difference of two values from the

mean. The difference between the two duplicates was plotted on the Y-axis, and the average of the two measurements on the X-axis.

The Bland Altman plots were generated using the raw concentrations for a single analyte. The analysis was performed using Graphpad Prism 5 by Graphpad Software (Graphpad Software Inc, California, USA). The software provides a 95% Confidence Interval (>2 Standard Deviations [SD] from the mean) and if a duplicate fell outside of that range, then that duplicate was excluded as an outlier. New datasets were generated of all analytes excluding the outliers. The mean was taken of duplicates and normality assessed by means of a histogram and Shapiro-Wilks test.

3.4.3 Inter-plate variability

Five recipients were plated on one plate (plate 1), and the other five, on a second plate (plate 2). For each recipient, plasma from all visits was included on the same plate. This was true for both kits. Inter-plate controls were included on both plates 1 and 2 for both panels. There were 9 inter-plate controls, plated in duplicate on both plates. In order to test whether the measured values on plate 1 were comparable with those on plate 2, the difference between the inter-plate controls was assessed. A Paired T-test or Wilcoxon signed rank (depending on distribution of the analyte) was used to test the difference between the inter-plate controls on the two plates for each analyte. If the difference was significant, the plates were analysed separately.

3.4.4 Inter-panel variability

The two panels used to measure plasma protein concentrations differed except for 3 analytes, IL-2, IL-10 and IFN-y, which were included as inter-panel controls. The concentrations of these analytes were used as controls for the variability between the two panels in order to assess whether the panels could be combined for analysis. This difference was tested using a t-test or Wilcoxon Rank Sum Test based on the distribution of each analyte. If there were significant differences in the inter-panel controls, then the panels were analysed separately.

3.4.5 Fold Change from Baseline

In order to compare highly variable data between plates, the fold change from baseline (V100) was calculated for each visit. For each participant, fold change was determined as the fold-difference at V101, V103, V106, or V112 from V100 and expressed as a decimal of V100 per analyte; a fold change of 1 had the same concentration as baseline; a fold change of 2 had double the concentration of baseline; and fold change of 0.5 was half the concentration of baseline. Fold change data was assessed for normality as before and if not normally distributed, it was log-transformed and reassessed.

3.4.6 Difference in Fold Change over Time

The fold change from baseline at each visit was assessed for significant change, on a per plate and per panel basis. This was tested using a t-test or Wilcoxon-Rank-Sum Test based on distribution of the log-transformed fold change data and corrected for multiple comparisons using a Bonferroni Correction. The difference was considered significant when p-value < 0.5 after multiple comparison correction. The median for the different modes of action groups (inflammatory, regulatory and dual action) was also taken and fold change for each mode of action was also calculated.

3.4.7 Hierarchical Clustering Algorithm (HCA) Analysis

Qlucore Omics Explorer software was used to apply a hierarchical clustering algorithm to the data and visualise it as a heat map. HCA groups the most similar pairs of objects together according to their measurements. In this case the most similar participants' visits were paired together based on the fold changes (log_2 transformed) of the different analytes. The goal of the clustering algorithm is to partition the participants' visits into homogeneous groups, such that the within-group similarities are large compared to the between-group similarities. This is represented as a dendogram as well as heat map. The relative increase or decrease from baseline for each analyte was represented as a colour change in the heat map; red indicated an increase, green, a decrease and the median for that analyte was represented by black. The HCA was also used to test which

analytes differed for all participants according to the clinical variables, time (visit), age, gender, ethnicity, pre-operative CD4 count, and the number of HLA-matches between recipient and donor. For this analysis, a two-group test (T-test) is used for dichotomous or binary variables and a multi-group comparison (F-test) is used for categorical or continuous variables. The final heat map is then filtered to display only those analytes that had a false discovery rate (FDR) of 10% (q-value < 0.1). The FDR is the probability of type I errors in the null hypothesis and it controls the expected proportion of analytes being falsely identified as differing between participants.

3.4.8 Mixed Effects Generalized Linear Model (MEGLM)

The Mixed Effect Generalised Linear Model (MEGLM) is a regression analysis for which certain covariates are modelled as fixed effects and other covariates are modelled as random effects. The covariates that are modelled as fixed effects are those that are assumed to have the same influence on all measured values. The variables that are modelled as random effects are those that are assumed to vary between subjects.

In this analysis an MEGLM was built for each analyte. The model was used to quantify the difference in concentration between recipients for that analyte. Visit was modelled as a fixed effect. The effect of visit on concentration was assumed to be equal for all recipients in the model. The recipients' unique identifier, the KID-PID, was modelled as a random effect. The effect of KID-PID on

concentration was assumed to vary for all recipients in the model. The results from the MEGLM were used to calculate the percentage of variation between recipients for a specific analyte. This differed from the previous analyses which all investigated differences over time - the MEGLM calculated differences in the concentrations of one analyte, between recipients, irrespective of time. A MEGLM was used instead of an ANOVA as it allowed for the identification of inter-subject differences while including missing values. It was also more reliable for the analysis of such a small number of subjects.

The concentrations were used instead of fold changes to avoid having the same value for all recipients at baseline. The models could therefore not use the combination of both plates and were built on a per plate basis - five participants were included in each model. Normality of the raw concentrations was assessed using a histogram. The means of the replicates were taken, and distribution re-assessed. Non-normally distributed analytes were log-transformed, and normality reassessed. The model could only be fitted to normally distributed data. A line graph was generated to visualise the log concentration over time. The model was then fitted to the data. The goodness-of-fit was checked by plotting the predicted linear model with the mean log concentrations over time, and ensuring that the distribution of the residuals was normal. The output from the model was recorded, in particular the variance of the level-two errors (random intercept) and the variance of the level-one errors (residuals). The values for the random intercept and the residual could be used to calculate the percentage of the inter-subject variability for a particular analyte.

The percentage calculated gave an indication of how different recipients' concentrations were from each other. A large variability (>65%) between recipients indicated that there were substantial differences in concentration between recipients for that analyte. A small variability (<10%) between recipients indicated that there were minimal differences in concentration between recipients for that analyte. The model was built in STATA SE 12 (StataCorp, Texas, USA).

CHAPTER 4: Changes in Peripheral Plasma Inflammatory and Regulatory Cytokines

4.1 Introduction

Cytokines are small, secreted, signalling proteins released by cells that have specific effects on the interaction and communication between cells[218]. They can act on the cells that secrete them (autocrine), on nearby cells (paracrine) or on distant cells (endocrine)[218] and are crucial mediators of inflammatory and anti-inflammatory (regulatory) processes[219].

Several studies have outlined the roles that cytokines can play in various forms of chronic kidney diseases (CKD), kidney transplant rejection and tolerance. This introduction will outline cytokines, and other proteins, found in the blood plasma that are associated with renal disease progression, renal function/dysfunction, renal transplant rejection and tolerance, and the effect of ATG and immunosuppression on those cytokines. Changes in inflammatory and regulatory cytokines can be used to gain insight into the changes in the T cell repertoire as a result of ATG, immunosuppression and transplantation.

4.1.1 Cytokines in Chronic Kidney Disease

Chemotactic cytokines (chemokines) are a family of cytokines that predominantly induce the migration of monocytes, lymphocytes and other cells

to the site of inflammation. Inflammatory processes in kidney disease stimulate various cell types to release chemokines. Chemokines such as Interleukin-8 (IL-8), Growth-related oncogene-α (Gro-α), Interferon-inducible Protein-10 (IP-10), Monocyte Chemoattractant Protein-1 (MCP-1), Fractalkine, Stromal cell Derived Factor 1 α (SDF-1α), Eotaxin, Macrophage Inflammatory Protein 1β (MIP-1β) are secreted by renal tissue, and in plasma can attract monocytes, lymphocytes and other innate immune cells to the kidney[220,221].

The Matrix Metalloproteinases (MMP) are a family of enzymes that are involved in the remodelling of the extra-cellular matrix and cleavage of a number of surface proteins[222]. MMP-2 and MMP-3 are produced in the kidney and serum levels of MMP-2 has been correlated with kidney function in CKD[222,223].

sTNFR1 is one of the soluble receptors for the TNF cytokines. It is considered an anti-inflammatory cytokine as it binds TNF and limits its pro-inflammatory activity[224]. It has been indicator of the progression of chronic kidney disease (CKD)[225] and in these recipients the variable concentrations between them may be related to the progression of their CKD pre-transplant.

Pentraxin-3 is an acute phase protein produced during inflammation that activates the classical complement pathway[226]. Plasma levels of Pentraxin-3 are increased when glomerular filtration rate (GFR) declines in chronic kidney disease[227] and much the same as sTNFR1, the concentration is related to the severity of CKD.

One of the consequences of end-stage renal disease (ESRD) is the calcification of vascular structures, which significantly increases the risk factor of cardiovascular mortality in these patients. Vascular calcification is the result of various factors but one of significance is the reduced clearance of circulating non-collagenous bone matrix proteins including, Osteocalcin and Osteopontin[228]. High plasma levels of Osteocalcin and Osteopontin are indicative of ESRD. Osteopontin has also been shown to be upregulated in proximal and distal renal tubules in glomerulonephritis[229] and plasma levels of Osteopontin have been shown to have an inverse relationship with glomerular filtration rate (GFR) and can be used to monitor kidney dysfunction[230].

Soluble TNF-like weak inducer of apoptosis (TWEAK) is a pleiotropic cytokine and its receptor (Fn-14) is found on a variety of organs. TWEAK plasma levels are correlated with a decrease in GFR due to its effect on endothelial cells in the kidney[231] and is therefore also a marker for renal dysfunction.

CD163 is a haptoglobin-haemoglobin scavenger receptor molecule that is found on the surface of monocytes and macrophages[232]. The soluble form is shed in plasma by activated macrophages[232]. In HIV positive patients with a high level of sCD163, the risk of developing chronic kidney disease is 11-times higher compared to patients with a low level[233].

4.1.2 Cytokines in Transplant Rejection and Tolerance

Several studies have investigated cytokines in plasma as early predictors of rejection in renal transplantation: Neutrophil gelatinase-associated lipocalin (NGAL) and IP-10 in serum have been identified in as predictors of acute rejection at day 1 post-transplant[234]; a combination of IL-1RA, IL-20 and sCD40L in serum was shown to predict acute cellular rejection with >90% sensitivity and specificity[235] during the first month post-transplant; IL-6 levels have been shown to identify acute rejectors in renal recipients presenting with acute graft dysfunction with >90% sensitivity[236]. Screening gene expression profiles in plasma/serum[237–241] and urine[242–246] has identified additional markers that are more predictive of acute rejection in renal transplants than plasma concentrations.

Vascular Endothelial Growth Factor (VEGF) is a cytokine primarily involved in angiogenesis and plays a variety of roles in the pathophysiology of a number of renal diseases[247]. Certain single gene polymorphisms are associated with an increase in the risk allograft rejection in renal transplantation[247].

Allo-specific T-cells and APCs prime B-cells to release donor-specific antibodies which can lead to antibody-mediated rejection (ABMR)[248]. B-cell activating factor (BAFF/TNFSF13B) and A Proliferation Inducing Ligand (APRIL/TNFSF13) play key roles in B-cell activation, maturation and survival[249,250]. Renal recipients

with higher levels of BAFF have significantly higher risk of developing donor-specific antibodies[251].

IFN-α2 and IFN-β are inflammatory type I interferons that are produced are in large amounts by plasmacytoid dendritic cells (pDCs) in response to viral antigens[252], such as cytomegalovirus (CMV). In immunosuppressed transplant recipients, and HIV-infected patients, CMV levels can increase to pathological levels resulting numerous complications including rejection[253,254]. One of the reasons for this is the increased levels type I interferons produced in response to the virus[255,256]. Increased type I interferon levels are a risk factor for renal rejection. IFN-α2, however, has also been shown to act in combination with IL-10 to induce the conversion of activated CD4+ T cells to IL-10 producing T-reg-like cells[257].

The T-cell growth factor, IL-2, plays an important role in rejection and tolerance[258]; it contributes to the deletion of allospecific T-cells through activation induced cell death (AICD) and its depravation can result in passive cell death (PCD) of activated T cells. Tregs also help to deplete the levels of IL-2 by binding it using CD25[259].

IFN-γ a plays a role in both inflammation and regulation at the site of the allograft[260]. IFN-γ drives inflammatory responses in lymphocytes, APCs, macrophages, epithelial and endothelial cells[261]. In transplant rejection, it is produced by allospecific T cells and NK cells and drives a Th1 host versus graft

response in combination with other cytokines such as IL-6 and Chitinase-3-like-1[262,263]. IFN-γ was shown to be produced by Tregs in order to induce tolerance[264–267] and it is critical for long-term graft survival as it blocks co-stimulatory signals[268].

The Macrophage Migratory Inhibitory Factor (MIF) is a pleiotropic lymphocyte and macrophage produced cytokine, with enzymatic properties[269]. Its expression is increased in acute and chronic renal allograft rejection.

IL-1α and IL-1β are produced predominantly by activated monocytes/macrophages. High levels IL-1β have been found in rejecting renal allografts[270] and recipients with lower levels of IL-1β relative to its regulating cytokine, IL-1 receptor-antagonist (IL-RA) are less prone to rejection[271].

IL-18 and IL-12 are also produced by activated macrophages. They act synergistically to stimulate the production of IFN-γ and other pro-inflammatory cytokines from macrophages, T-cells and NK cells[272]. IL-18 is significantly increased in renal allograft rejection[273].

IL-19 and IL-20 are predominantly produced by monocytes and are both involved in the autoimmune skin conditions, psoriasis[274]. IL-19 can stimulate the release of pro-inflammatory cytokines such as IL-6, TNF-α and reactive oxygen species (ROS)[274] which are known to affect allograft rejection. IL-20 plays a role in angiogenesis and may promote allograft survival[274].

Allospecific cytotoxic CD8+ T cells are involved in the rejection of the allograft. These can induce apoptosis in allograft cells by the release of perforin, granzymes, Fas Ligand and TNF Related Apoptosis Inducing Ligand (TRAIL)[275]. Increased FasL expression has been identified as a marker of allograft rejection[276].

T-helper 2 (Th2) cytokines (IL-4, IL-13) can be protective in renal allografts as T-cells are shifted to the Th2 phenotype instead of the allospecific Th1 cells that mediate TCMR[277]. IL-4 is protective when it is produced prior to transplantation, and shortly after, but a prolonged increase in IL-4 after transplantation results in an increase in acute rejection events[219]. IL-13 promotes allograft survival by inhibiting macrophages and/or dendritic cell cytokine production[278]. IL-4 and IL-13 can also induce the alternatively activated macrophages that are involved in regulatory processes associated with long term graft survival[279].

sIL-6Rα and sIL-6Rβ are soluble forms of the two subunits of the receptor for the dual action inflammatory/regulatory cytokine IL-6. The IL-6R binds IL-6 and serve as a carrier protein by forming a complex with the cytokine, increasing its half-life in plasma and facilitating its many functions[280]. It is unknown whether sIL-6R is affected is involved in rejection or tolerance but, as mentioned previously, IL-6 has been shown to be a predictor of acute rejection[236] and this effect may be enhanced by IL-6R.

IL-11 is a cytokine in the IL-6 family. It has pleiotropic effects on multiple tissues but most common effects have been identified as hematopoietic and thrombopoietic[281]. In terms of transplantation, it has been shown to prevent graft versus host disease (GVHD)[282] and separates GVHD from graft-versus-leukaemia in bone marrow transplants[283].

IL-17 and IL-23 are cytokines produced by T-helper 17 cells. IL-17 is expressed by tubular epithelial cells (TEC) in ABMR[284–286]. IL-17 is not only produced by TEC but acts synergistically with sCD40L in an autocrine manner on TEC to stimulate the production of the pro-inflammatory cytokines, IL-6 and pro-inflammatory chemokines, IL-8 and Regulated on Activation, Normal T cell Expressed Secreted (RANTES)[287]. IL-23 is a pro-inflammatory cytokine in the IL-12 family[288]. IL-23 has been shown to be involved in the Th17-mediated inflammation in experimental glomerulonephritis in mice[289]. It is also elevated in plasma during CMV reactivation after renal transplantation in humans and indicative of CMV status[290].

IL-21 is produced predominantly by follicular helper T cells. It acts synergistically with Transforming Growth Factor β (TGF-β) in the germinal centre of lymph nodes to cause the conversion of Naïve B cells to mature B cells required for renal allograft tolerance[291,292].

IL-28A and IL-29 are type III interferon. They can be produced by most nucleated cells, but in particular by dendritic cells (DCs), following viral or

activation by bacterial components and its targets are predominantly epithelial cells and hepatocytes[274,293]. IL-28A treated DCs have been shown to induce proliferation of Tregs in vitro[294].

Thymic stromal lymphopoietin (TSLP) is produced in the thymus and plays a key role in the induction of Tregs from naïve CD4+ T cells. TSLP activates plasmacytoid DCs (pDCs) to induce the generation of FOXP3+ regulatory T cells with a different cytokine production potential – pDC-induced Tregs produce more IL-10 than TGF-β.

The main cytokines produced by Tregs are Transforming Growth Factor (TGF-β), IL-10 and IL-35. TGF-β plays a number of key roles in transplantation; it activates the FoxP3+ Tregs that prevent allograft rejection[291] and is required to maintain the expression of FoxP3 in the peripheral Tregs and therefore maintains their suppressor function[295]. Together with IL-10, TGF-β suppresses the activity and cytokines of allospecific effector T cells[296] and both are required by Tregs to mediate tolerance to alloantigens[297]. IL-35 is anti-inflammatory and immunoregulatory cytokine[298]. IL-35 can be produced by DCs and can it can act to induce a unique population of potent immunosuppressive regulatory-like T cells that produces IL-35 but not IL-10 or TGF-β, and does not require or express FoxP3[299]. These differ from conventional Tregs as they only produce IL-35 and do not express FoxP3. Conventional Tregs can also produce IL-9. IL-9 recruits mast cells to the allograft that are also required for T-reg mediated immune suppression[300].

4.1.3 Effect of Anti-Thymocyte Globulin (ATG) induction on cytokines

One of the major side effects of monoclonal lymphocyte depleting antibodies, such as the anti-CD3, OKT3, is the risk of cytokine release syndrome, a sudden release of cytokines from activated T cells, predominantly TNFα and IFN-γ[301,302]. This occurs when the antibody binds to CD3 and results in symptoms that range from a mild flu-like reaction to and a life-threatening shock-like reaction[302].

ATG contains polyclonal lymphocyte-specific antibodies and does not have the same risk of cytokine release syndrome[302]. Cytokine release syndrome is still listed as potential adverse event on the package insert[303,304].

Cytokines that are produced by the cells depleted by ATG, namely T-cells, B-cells, NK cells and to a lesser extent, DCs, will be decreased. Monocyte/macrophage-related cytokines should be less affected[304].

4.1.4 Effect of Immunosuppression on Cytokines

All the renal transplant recipients in this cohort are placed on maintenance immunosuppression of prednisone, Tacrolimus and mycophenolate mofetil (MMF). Immunosuppression dampens the inflammatory response to the allograft but also suppresses systemic inflammation. MMF non-competitively inhibits the enzyme, inosine monophosphate dehydrogenase on which B and T

cells rely for the synthesis of purines required for DNA synthesis[302,305]. MMF will not affect expression of cytokines by surviving lymphocytes.

Prednisone is a corticosteroid. It is analogous to endogenous cortisol but more four times more potent in efficacy[302]. It binds to intercellular steroid hormone receptors and the steroid-receptor complex binds to DNA to down regulate the expression of cytokines, IL-1, IL-6, IFN-γ and TNF-α[302]. Prednisone also blocks IL-2 production and binding to its receptor[302]. Additionally, prednisone suppresses MIF and the Macrophage Activation Factor (MAF), which results in reduced macrophage migration and activation[302].

The aim of this chapter was to assess the impact of ATG induction therapy, renal allograft transplantation and maintenance immunosuppression in HIV positive recipients with End-Stage Renal Disease on peripheral regulatory T cells. This was addressed by measuring peripheral cytokine changes using Luminex. The Luminex assay was used to investigate changes in plasma cytokines and other proteins involved in inflammatory and regulatory processes.

This chapter investigates whether peripheral inflammatory and regulatory cytokines and other proteins changed over time during the first 3 months post ATG induction and transplantation in 10 selected HIV positive renal recipients. The influence of demographic and clinical characteristics on the cytokines changes, and cytokines that differed between recipients, were also investigated.

These investigations were used to gain insight into the changes in the T cell repertoire.

4.2 Luminex Assay Results

A Luminex assay, consisting of two panels, covering 67 proteins, was used to measure the concentrations of inflammatory, regulatory and dual action inflammatory/regulatory cytokines and other proteins. This chapter will focus on assessing the levels of variability within the Luminex plates that differentiates between assay "noise" from biological variability before investigating changes over time and between recipients. This was achieved using several steps: a) cleaning up the raw data; b) assessing variability between replicates of the same sample within one plate (intra-plate); c) assessing variability of controls between plates (inter-plate); d) normalising inter-plate variability to combine data for analysis, e) identifying analytes that significantly differed over time; f) identifying groups of analytes that associated with clinical criteria or time; g) calculating the difference between recipients irrespective of time for each analyte.

4.2.1 Raw Data Clean Up

Panel 1 consisted of 37 analytes, and Panel 2, 30 analytes. Analytes for which >90% of samples' concentrations were found to lie outside of the observable range (OOR) as determined by the standard of known concentrations, were

excluded from the analysis. In Panel 1, 5/37 cytokines were excluded, and in Panel 2, 12/30 analytes were excluded (Table 4.1). Table 4.1 also shows the analytes retained for downstream analysis. In order to avoid having concentrations values equal to zero, all concentrations that were <OOR were replaced with a value that was half of the lowest detectable concentration for that analyte on that plate. There were no concentrations that were >OOR.

Table 4.1. Analytes from Panel 1 and 2 which were excluded (>90% values <OOR) or included (<90% values OOR) for downstream analysis

Excluded		**Included**	
Panel 1	Panel 2	Panel 1	Panel 2
IL-26	BLC	Chitinase-3-like1	Eotxain
IL-27	IFN-γ	IFN-α2	Fractalkine
IL-32	IL-1α	IFN-β	GRO-α
IL-34	IL-1RA	IFN-γ	IL-1β
LIGHT/TNFSF14	IL-10	IL-10	IL-16
	IL-13	IL-11	IL-17a
	IL-15	IL-12p40	IL-18
	IL-23	IL-12p70	IL-21
	IL-2	IL-19	IP-10
	IL-4	IL-2	MCP-1
	IL-6	IL-20	MIF
	IL-9	IL-22	MIP-1β
	sFASligand	IL-28A	sCD40L
		IL-29	SDF-1α
		IL-35	TNFα
		IL-8	TRAIL
		MMP-1	VEGFα
		MMP-2	
		MMP-3	
		Osteocalcin	
		Osteopontin	
		Pentraxin-3	
		sCD163	
		sIL-6Rα	
		sIL-6Rβ	
		sTNFR1	

	sTNFR2
	TNFRSF-8
	TNFSF-12
	TNFSF-13
	TNFSF-13b
	TSLP

4.2.2 Intra-plate variability

Intra-plate variation was investigated in order to identify highly divergent pairs of the sample duplicates using a Bland-Altman plot as outlined in Chapter 3, (section 3.4.2, pg 67). A representative figure for analytes, APRIL/TNFSF13 and BAFF/TNFSF13B, is included in Figure 4.1. All duplicates for which one of the pair fell outside 2 x SD could be excluded as an outlier with 95% confidence. A mean was taken for the remaining replicates and a new dataset for each analyte was generated, and used for further analysis. On the representative plot for APRIL/TNFSF13, the duplicates for which the difference from the mean was greater than 2 x SD were excluded; in this case KID-125 V100, KID-131 V103, and KID-111 V100 were excluded.

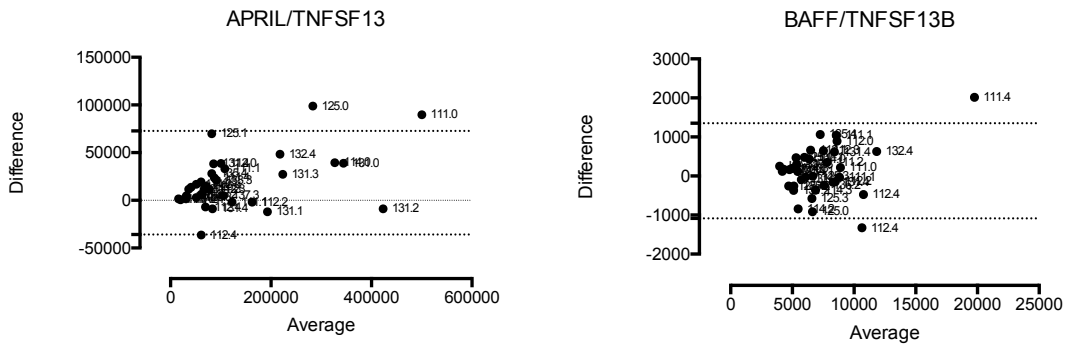

Figure 4.1. Representative Bland-Altman Plots for Intra-plate variability.

Representative plots are shown for two analytes, APRIL/TNFSF13 and BAFF/TNFSF13B. The mean average of two duplicates is on the x-axis (Average) and the difference from the mean is represented on the y-axis (Difference). The duplicates that fell outside of 2 x SD (represented as dotted line) could be excluded as an outlier with 95% confidence. The points are labelled with the KID-PID and the visit number (0-4) as KID-PID.Visit

4.2.3 Inter-plate variability

Due to the number of samples included in the analysis and the limited number of wells on the luminex plate, only five participants' samples (all visits) could be plated on one plate and two plates were assayed in total. In order to assess whether the samples on different plates could be combined for comparison, the inter-plate variability was assessed using the 9 inter-plate controls plated in duplicate. This was done to ensure that there was not unnecessary variability introduced by running samples on different plates. Depending on the distribution, a Paired T-test or Wilcoxon Signed-Rank Test was used to

determine whether there was a significant difference between plates for the interplate controls. This was done for Panel 1 and Panel 2.

For Panel 1 there were significant differences between the interplate controls for all analytes. For Panel 2, not all analytes were significantly different but because many of the interplate controls' values were OOR, these results could not be trusted. Therefore it was not possible to combine the plates' data. The plates were analysed separately or the data was normalised so that plates could be combined.

4.2.4 Inter-panel variability

There were 3 analytes in common between the two panels, IL-2, IL-10 and IFN-γ. These were included as inter-panel controls and the concentrations of those analytes across all samples were to be used to assess whether the panels could be combined. As can be seen in Table 4.1, IL-2, IL-10 and IFN- γ were excluded from Panel 2. Therefore no comparison could be made between Panel 1 and Panel 2 and they could not be combined.

4.3 Luminex Data Analysis

4.3.1 Normalisation by Fold Change from Baseline

For both panels, the absolute values on the different plates could not reliably be combined without first normalising the differences between the plates. Calculating the fold change from baseline for visits V1-V4, where V0 was taken as the baseline, allowed for the data to be normalised. This was done for all participants and all analytes and the fold change data for both plates was combined. The combined fold change data was then log transformed to normalise the distribution of the data. The log fold change data was plotted for each participant against the visits to assess trends in the cytokine changes over time (Figure 4.2).

4.3.2 Trends in Analytes over Time per Participant

The graphs in Figure 4.2 A and B are qualitative plots of the fold changes of all analytes over time per participant. There was no statistical analysis applied to these. The graphs on the left show the changes of all the analytes in each panel per participant. The graphs on the right show the medians of the analytes as grouped into either inflammatory, regulatory and dual action functions in the periphery (Table 3.1, pg 59). It should be noted that for Panel 2, the median for the regulatory group and dual-action group is calculated from only one analyte each, IL-21 and MIF respectively. Panel 2 only had one regulatory (IL-21) and

one dual-action analyte (MIF) included (Table 3.1, pg 59) after the exclusion of OOR analytes.

The general trend for 8 of the 10 participants on Panel 1 is that analytes decrease in comparison to baseline up until 21 or 42 days post-transplant and then remain low or increase marginally to week 12 but still remain below baseline.

As mentioned above, many of the values for Panel 2 were <OOR. As a result, of those analytes that were not excluded (Table 4.1), many had samples that were <OOR and therefore replaced with a value which was ½ of the lowest detectable value. As a result the data from Panel 2 is less reliable as there were many samples with the same concentration. This is illustrated by a trend where many of the values remain at a fold change near 0 over the 12-week (84 day) follow up. The graphs of the medians of the mode of action groups further illustrate this; only minor changes were observed in the inflammatory cytokines by 84 days post transplant, with only two transplant recipients, KID-137 and KID-138, achieving a Log fold change difference of ±0.4. The only participant in whom the median inflammatory analytes increased was recipient KID-114.

a)

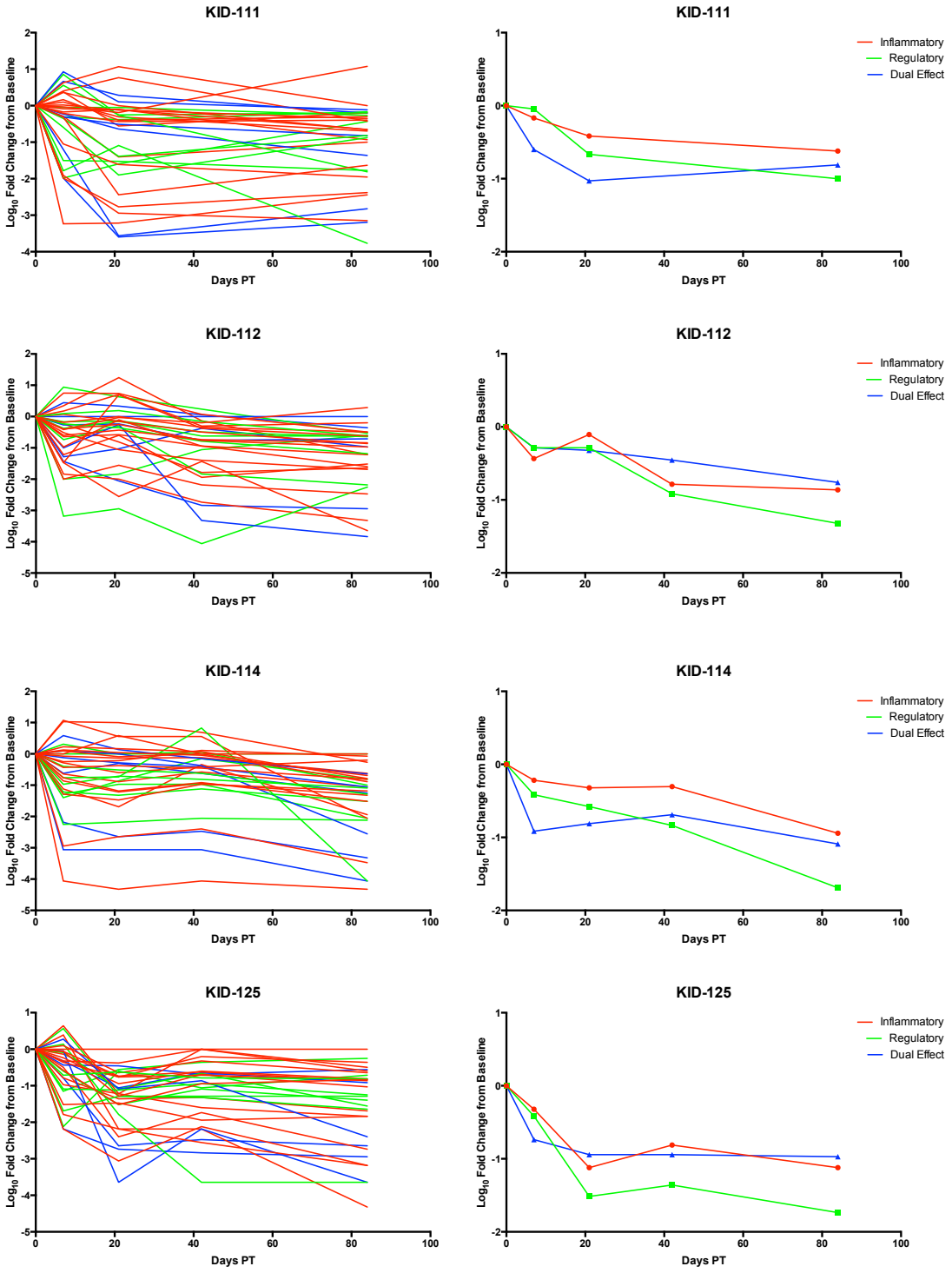
KID-111
KID-111
KID-112
KID-112
KID-114
KID-114
KID-125
KID-125
Log10 Fold Change from Baseline
Days PT
Inflammatory
Regulatory
Dual Effect

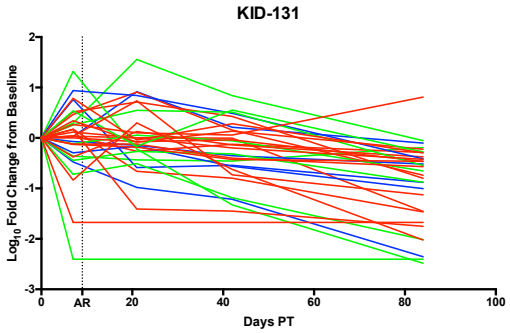
KID-131
Log10 Fold Change from Baseline
Days PT
AR

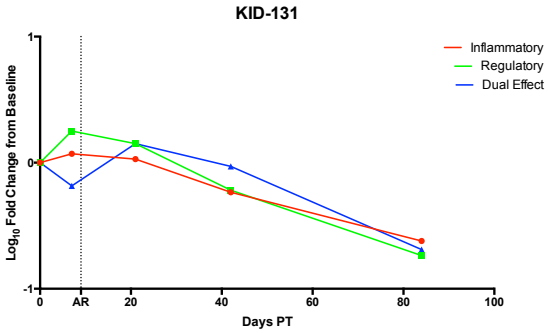
KID-131
Inflammatory
Regulatory
Dual Effect
Log10 Fold Change from Baseline
Days PT
AR

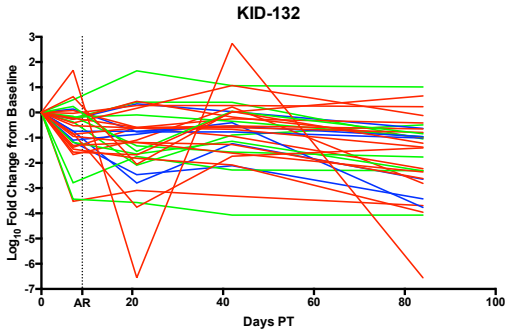
KID-132
Log10 Fold Change from Baseline
Days PT
AR

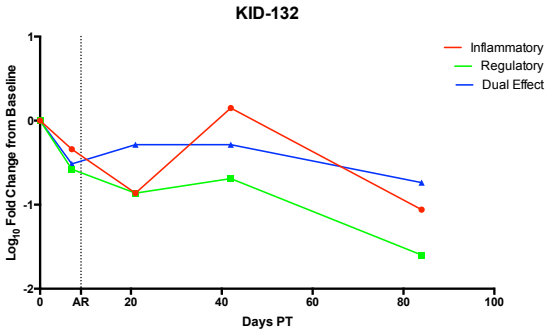
KID-132
Inflammatory
Regulatory
Dual Effect
Log10 Fold Change from Baseline
Days PT
AR

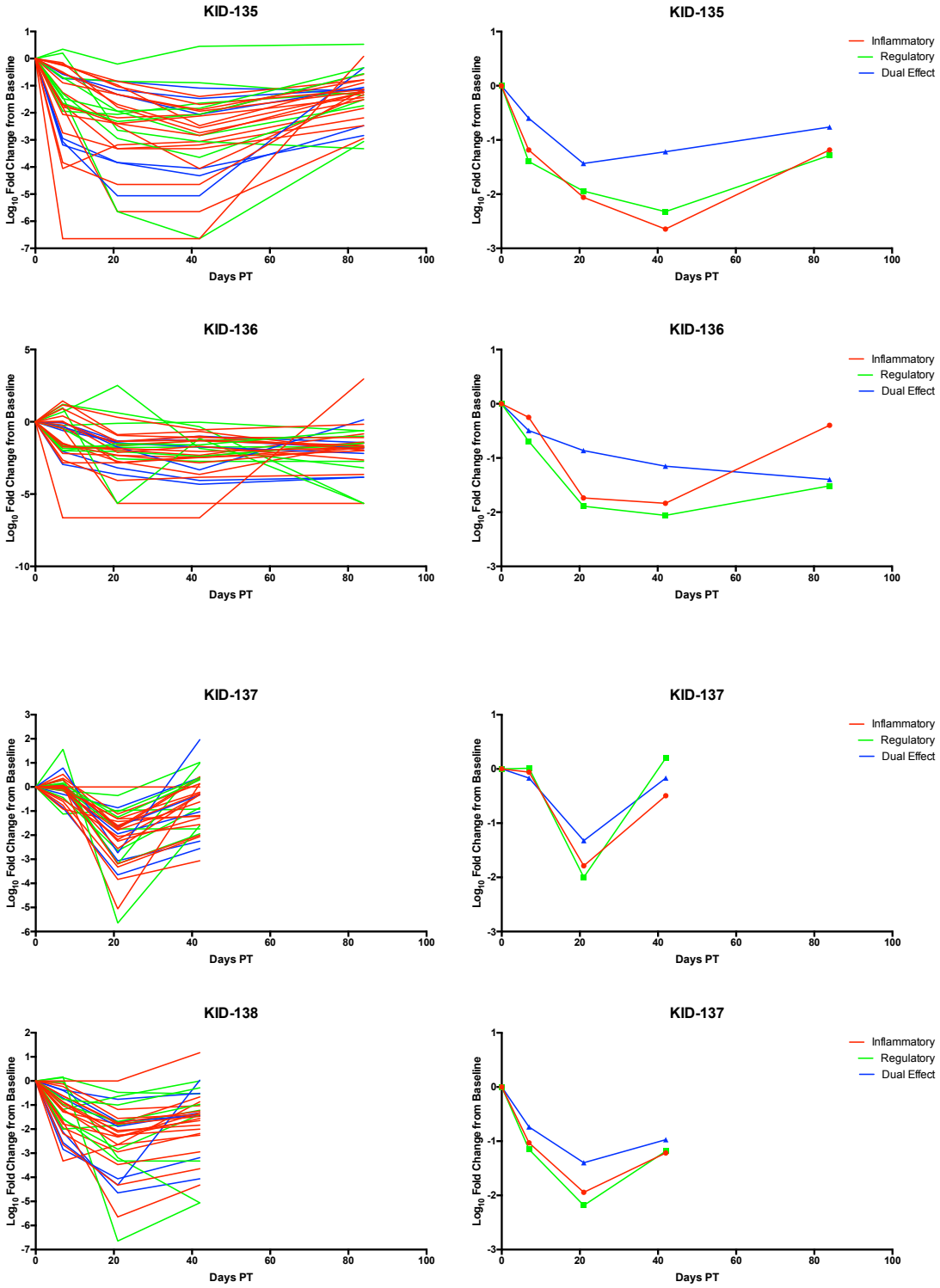
KID-135
KID-135
KID-136
KID-136
KID-137
KID-137
KID-138
KID-137
Log10 Fold Change from Baseline
Days PT
Inflammatory
Regulatory
Dual Effect

b)

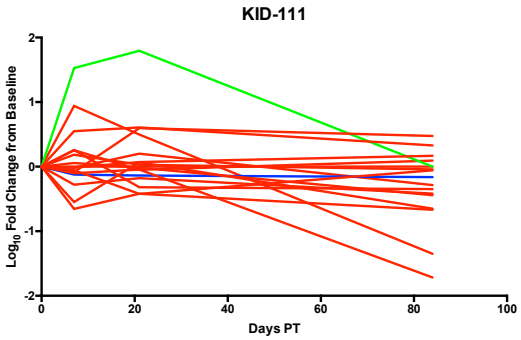
KID-111
Log10 Fold Change from Baseline
Days PT

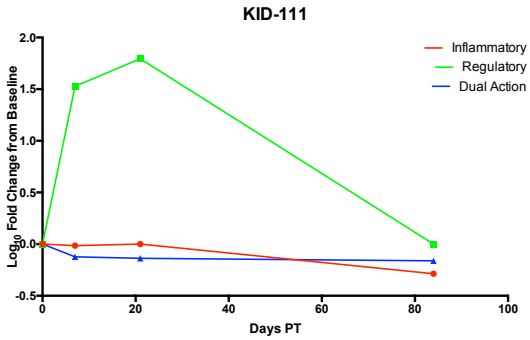
KID-111
Inflammatory
Regulatory
Dual Action
Log10 Fold Change from Baseline
Days PT

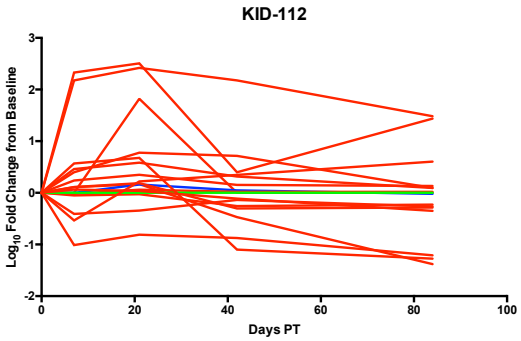
KID-112
Log10 Fold Change from Baseline
Days PT

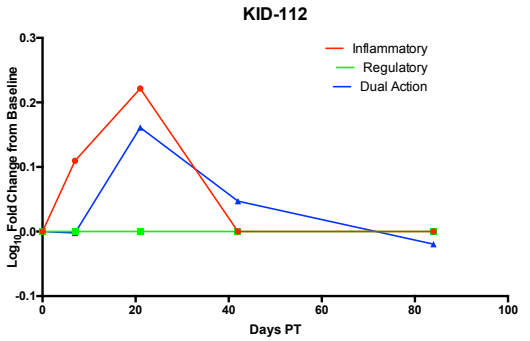
KID-112
Inflammatory
Regulatory
Dual Action
Log10 Fold Change from Baseline
Days PT

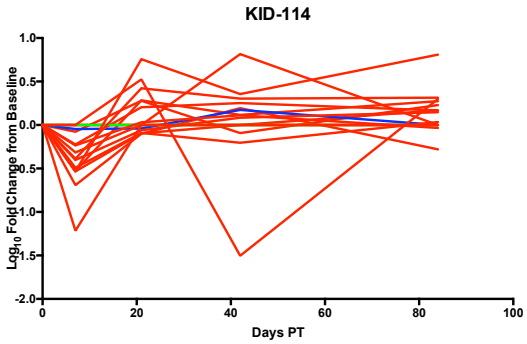
KID-114
Log10 Fold Change from Baseline
Days PT

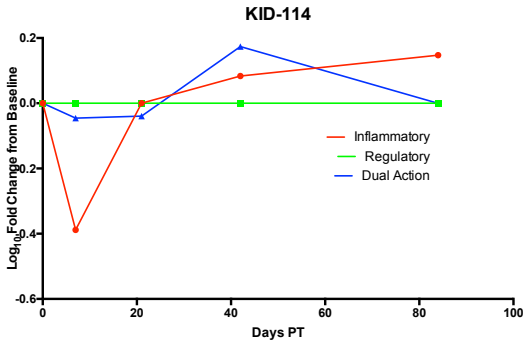
KID-114
Log10 Fold Change from Baseline
Days PT
Inflammatory
Regulatory
Dual Action

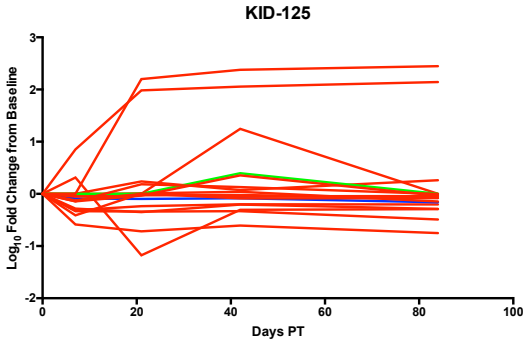
KID-125
Log10 Fold Change from Baseline
Days PT

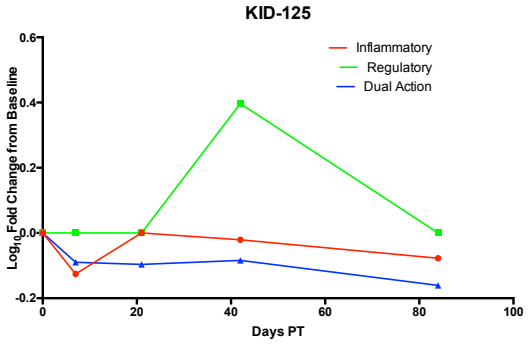
KID-125
Log10 Fold Change from Baseline
Days PT
Inflammatory
Regulatory
Dual Action

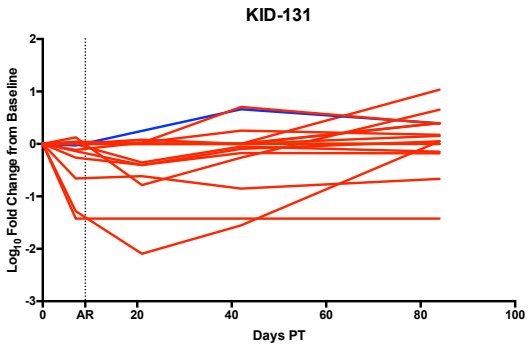
KID-131
Log10 Fold Change from Baseline
AR
Days PT

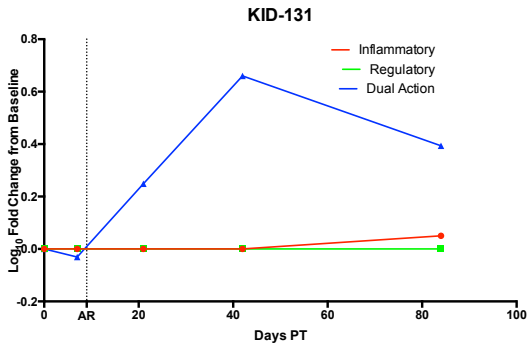
KID-131
Log10 Fold Change from Baseline
AR
Days PT
Inflammatory
Regulatory
Dual Action

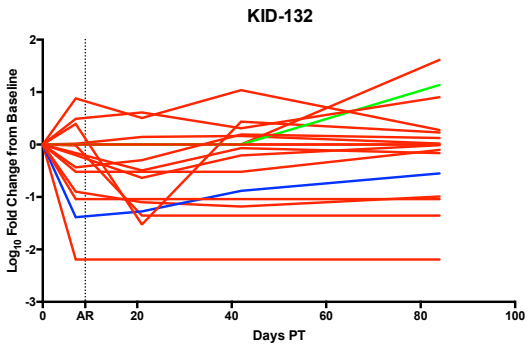
KID-132
Log10 Fold Change from Baseline
AR
Days PT

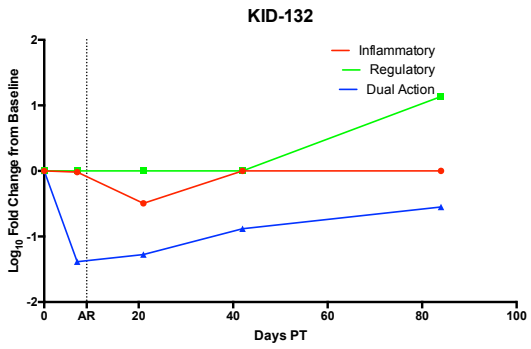
KID-132
Log10 Fold Change from Baseline
AR
Days PT
Inflammatory
Regulatory
Dual Action

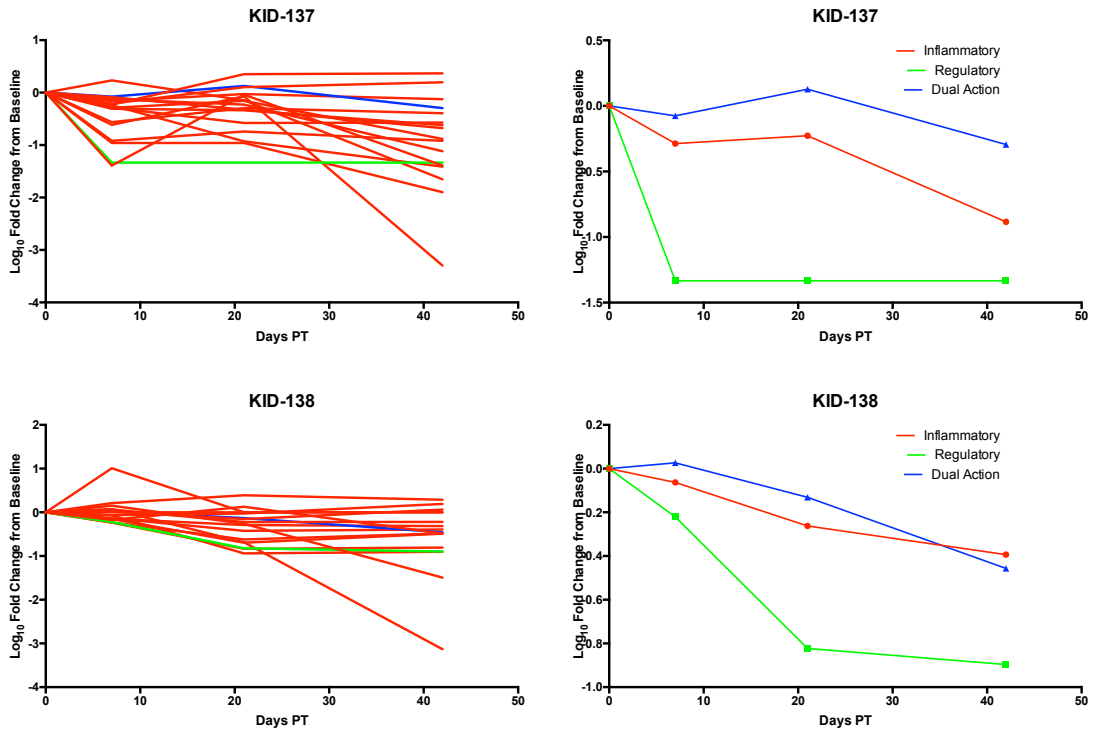

Figure 4.2. Log Fold Change over time of Grouped Cytokines and Median Grouped Cytokines per participant.

On the left, each graph represents the log fold changes from baseline (V100) of all analytes of one participant at V100, V101, V103, V106 and V112. The analytes are coloured according to their mode of action: inflammatory analytes are in red, regulatory in green, and analytes with a dual mode of action are in blue. On the right, each graph represents the median log fold changes from baseline (V100) for each mode of action of one participant at V100, V101, V103, V106 and V112. KID-137 and KID-138 only had V100-V106. KID-111 is missing V106. (a) All figures for Panel 1 and (b) All figures for Panel 2.

4.3.3 Influence of Acute Rejection Events on Fold Changes

The two participants who do not follow this trend are recipients KID-131 and KID-132. These two patients both experienced an acute rejection event; KID-131 (ABMR) and KID-132 (Borderline change, TCMR) on day 9 post-transplant. This event is indicated as acute rejection (AR) by a dotted line on the graphs (Figure 4.2a). For Panel 1, these two participants differ in the trends of their mode of action groups. KID-131 showed an increase in both the regulatory and inflammatory analytes at 7 days post-transplant, and then a gradual decline in all groups until a minimum at the last assayed time-point. KID-132 had a decline in inflammatory and regulatory analytes until day 21 PT but the dual action analytes show a lesser decline, with an increase between day 7 and 21 PT but not to baseline levels, and a further decline to the end of the assayed time-points. The inflammatory and regulatory analytes increase between days 21 and 42 post-transplant with the inflammatory surpassing the baseline levels; these then also gradually declined to a minimum at 84 days post-transplant.

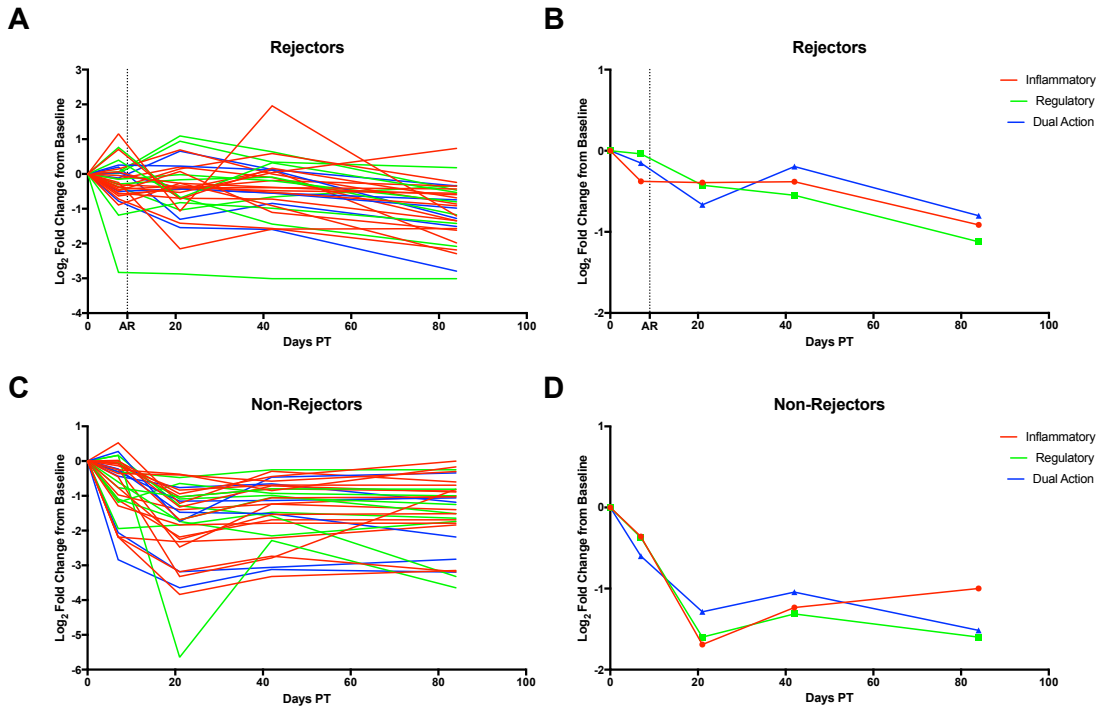

Figure 4.3. Panel 1 Analyte changes over time of participants with acute rejection compared to those without

The top graphs (A-B) show the median fold changes of Panel 1 analytes for participants who experienced at least one acute rejection event (rejectors) (KID-131; KID-132) at the different assayed timepoints. The bottom (B-D) graphs show the Panel 1 median fold changes of all participants who experienced no rejection at all (non-rejectors) (KID-111; KID-112; KID-114; KID-125; KID-135; KID-136; KID-137; KID-138) at the different assayed timepoints. The graphs on the left show the median for each analyte measured for the rejectors (A) and non-rejectors (C). The graphs on the right show the median of the groups of mode action for rejectors (B) and non-rejectors (D). In all the graphs, analytes are coloured according to their mode of action: inflammatory analytes are in red,

regulatory in green, and analytes with a dual mode of action are in blue.

Figure 4.3 compares the medians of participants with acute rejection (rejectors) to those that did not experience any rejection (non-rejectors). A difference in the decline of the grouped analytes (Figure 4.3 B & D) can be seen between baseline and day 21 PT; the rejectors (Figure 4.3b) regulatory group at 21 days PT has decreased to 0,97 of baseline, whereas in the non-rejectors at the same time PT the regulatory analyte group had decreased to 0,77 of baseline. The inflammatory and regulatory analytes in the non-rejectors follow a matching trend in their decline until day 42 PT, at which point the inflammatory analytes increase and the regulatory analytes decrease- but neither groups reaches baseline level again.

4.3.4 Analytes that differ over time for all participants

Section 4.3.2 and 4.3.3 showed descriptive plots of the analytes' and medians of the grouped analytes' fold changes over time as well as comparing rejectors to non-rejectors. The next stage was to statistically evaluate the changes in single analytes.

The fold change difference from baseline V100 at each visit (V101, V103 V106, V112) was tested for statistical significant as described in Chapter 3 (section 3.4.5, page 69). This was done for each measurable analyte found on both Panel 1 and Panel 2. The difference from baseline was tested using the dataset

generated from the combination of all 10 recipients as well as those datasets for the 5 recipients on the plate 1 and the 5 recipients on plate 2. This was done to ensure that any inter-plate variability that may have been introduced during the combination of the fold change data of the two plates did not affect the findings.

There were no analytes in Panel 2 for which the fold change was significantly different from baseline at any visit, after correcting for multiple comparisons.

For Panel 1 (Figure 4.4), there were significantly different fold changes found in 4/32 of the analytes in the 10 participants after combining plate 1 and 2 (Figure 4.4 A-D). Only IL-10 was significantly different after correcting for multiple comparisons when the 5 participants on plate 1 were tested (Figure 4.4F).

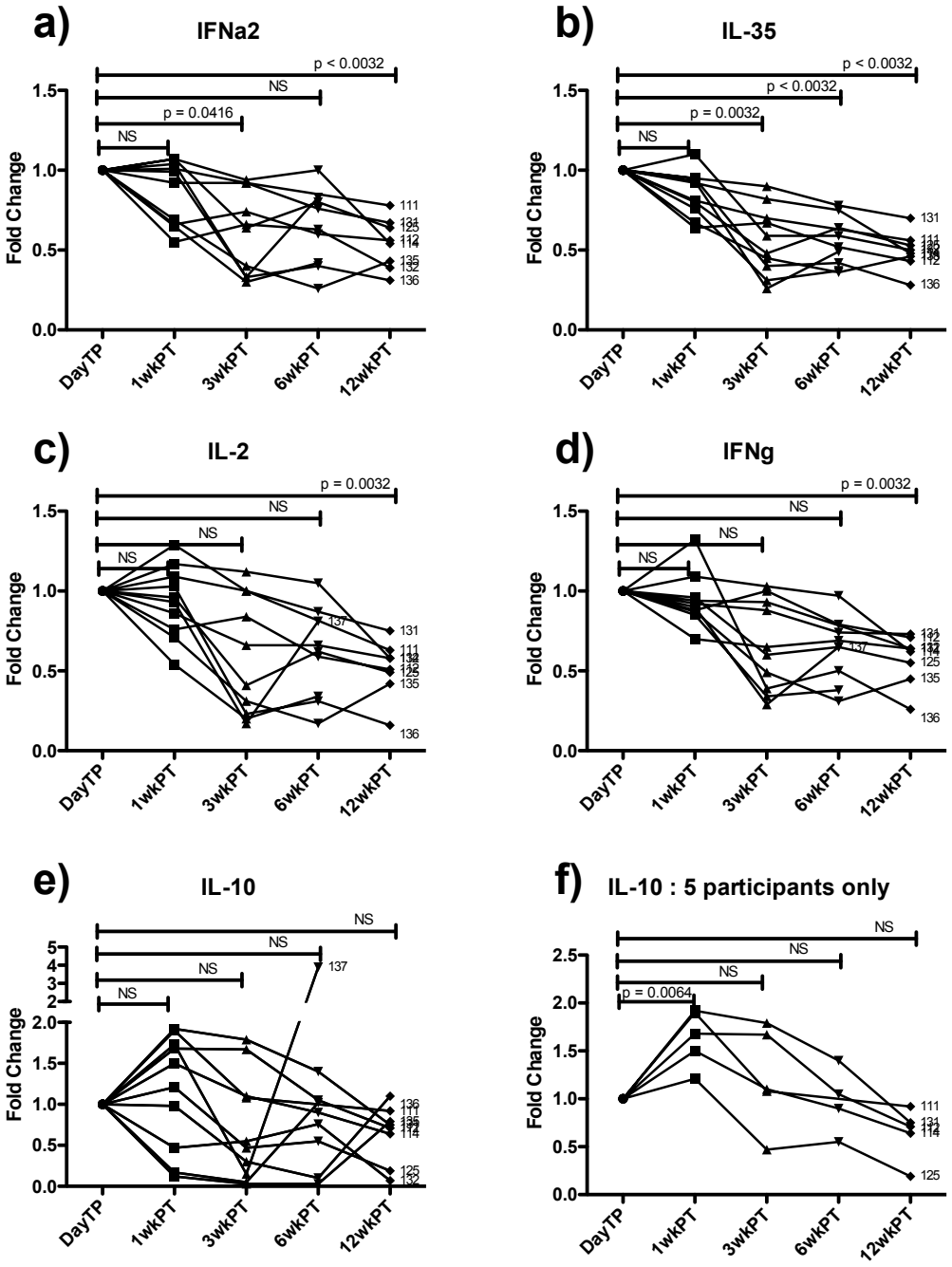

Figure 4.4 Single Analyte Fold Change from Baseline.

Each graph indicates an analyte for which there was a significant fold change from baseline. The fold change is on the y-axis and the different visits are on the x-axis. The lines connect the fold change from baseline at each visit for an

individual recipient. The lines are labelled with the KID-PID. Depending on the distribution, either a Paired T-Test or Wilcoxon Signed Rank Test was used. The p-values generated were adjusted for multiple comparisons using a Bonferonni correction. P-values <0.05 after adjusting for multiple comparisons were considered significantly differed from baseline. The p-value for significantly different analytes is indicated above the visit at which the fold change was found to be differnet. P-values >0.05 are marked as non-significant (NS). The graphs for IFNα2 (a), IL-35 (b), IL-2 (c), IFNγ (d) and IL-10(e) were generated from the fold changes for all 10 recipients. The graph for IL-10: 5 recipients only (f) was generated using only the particpants on plate 1.

The analytes, IFNα2, IL-35, IL-2 and IFN-γ were shown to be significantly lower than baseline by week 12-weeks PT (Figure 4.4 A-D). IFNα2 was also significantly lower at 3-weeks PT (Figure 4.4A) and IL-35 was significantly decreased at 1-week, 3-weeks, 6-weeks and 12 weeks-post transplant (Figure 4.4B). IL-10 significantly increased at 1-week PT compared to baseline in the five recipients (KID-111; KID-112; KID-114; KID-125; KID-131) on plate 1 only (Figure 4.4F). When all ten recipients were analysed, there were no significant differences identified for the fold changes in IL-10 (Figure 4.4E).

4.3.5 Hierarchical Clustering Analysis (HCA) and Heat Maps

Where previously, Figure 4.1 and 4.2 investigated trends of analytes over time per participant, and Figure 4.4 identified differences for individual analytes over

time for all participants, a hierarchical clustering analysis (HCA) was used to identify cytokine groups that changed across all recipients due to the influence of time and other potential confounding factors (age, sex, ethnicity, pre-operative CD4 count, the number of HLA-matches). Heat maps were used to visualise the HCA so that combinations of analytes that differ due to the influence of time, or confounding factors, could be identified. The heat map showing the unsupervised HCA heat maps for Panel 1 and Panel 2 is shown in Figure 4.5.

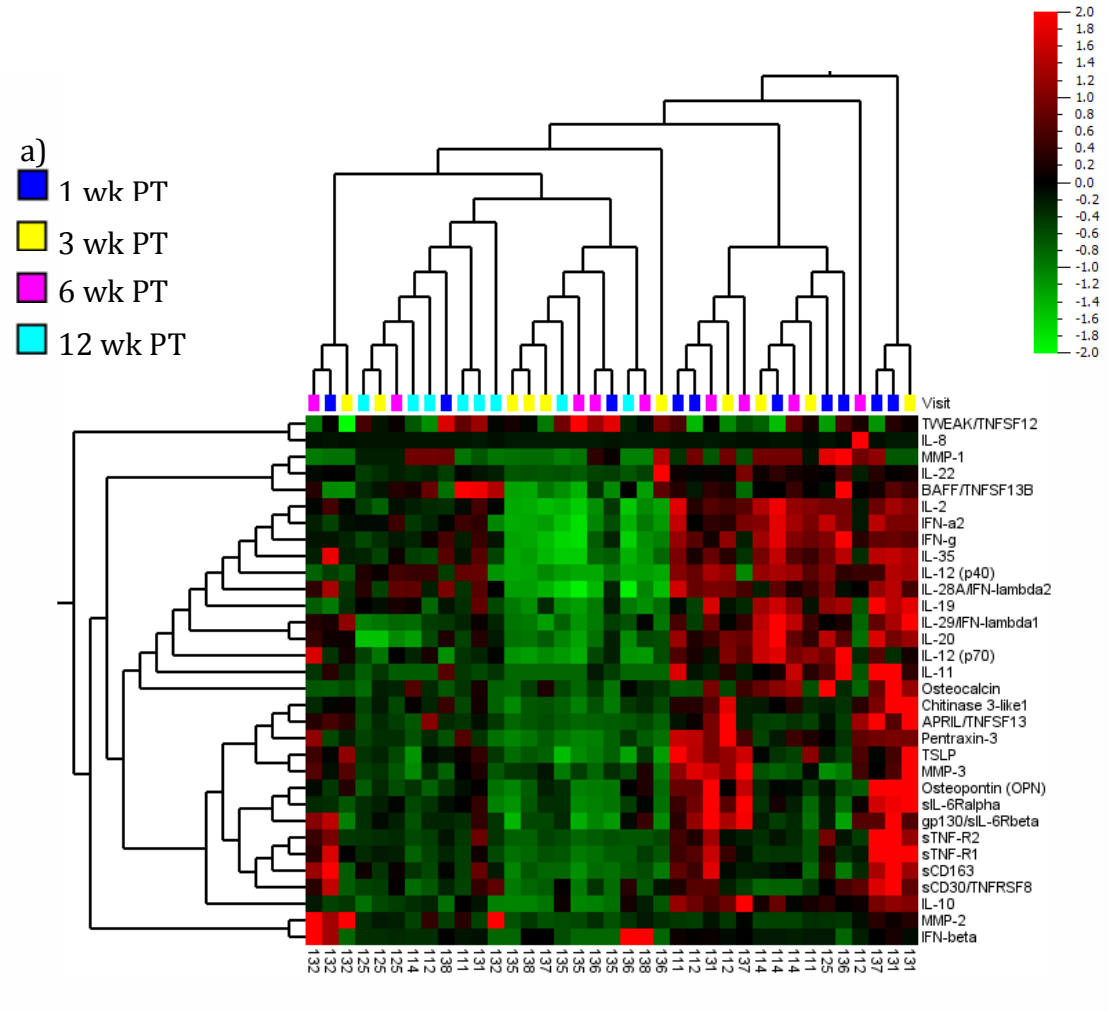
a)
1 wk PT
3 wk PT
6 wk PT
12 wk PT
2.0
1.8
1.6
1.4
1.2
1.0
0.8
0.6
0.4
0.2
0.0
-0.2
-0.4
-0.6
-0.8
-1.0
-1.2
-1.4
-1.6
-1.8
-2.0
Visit
TWEAK/TNFSF12
IL-8
MMP-1
IL-22
BAFF/TNFSF13B
IL-2
IFN-a2
IFN-g
IL-35
IL-12 (p40)
IL-28A/IFN-lambda2
IL-19
IL-29/IFN-lambda1
IL-20
IL-12 (p70)
IL-11
Osteocalcin
Chitinase 3-like1
APRIL/TNFSF13
Pentraxin-3
TSLP
MMP-3
Osteopontin (OPN)
sIL-6Ralpha
gp130/sIL-6Rbeta
sTNF-R2
sTNF-R1
sCD163
sCD30/TNFRSF8
IL-10
MMP-2
IFN-beta
132 132 132 125 125 114 112 138 111 131 132 135 138 137 135 135 136 135 136 138 136 111 131 112 137 114 114 111 125 136 112 137 131

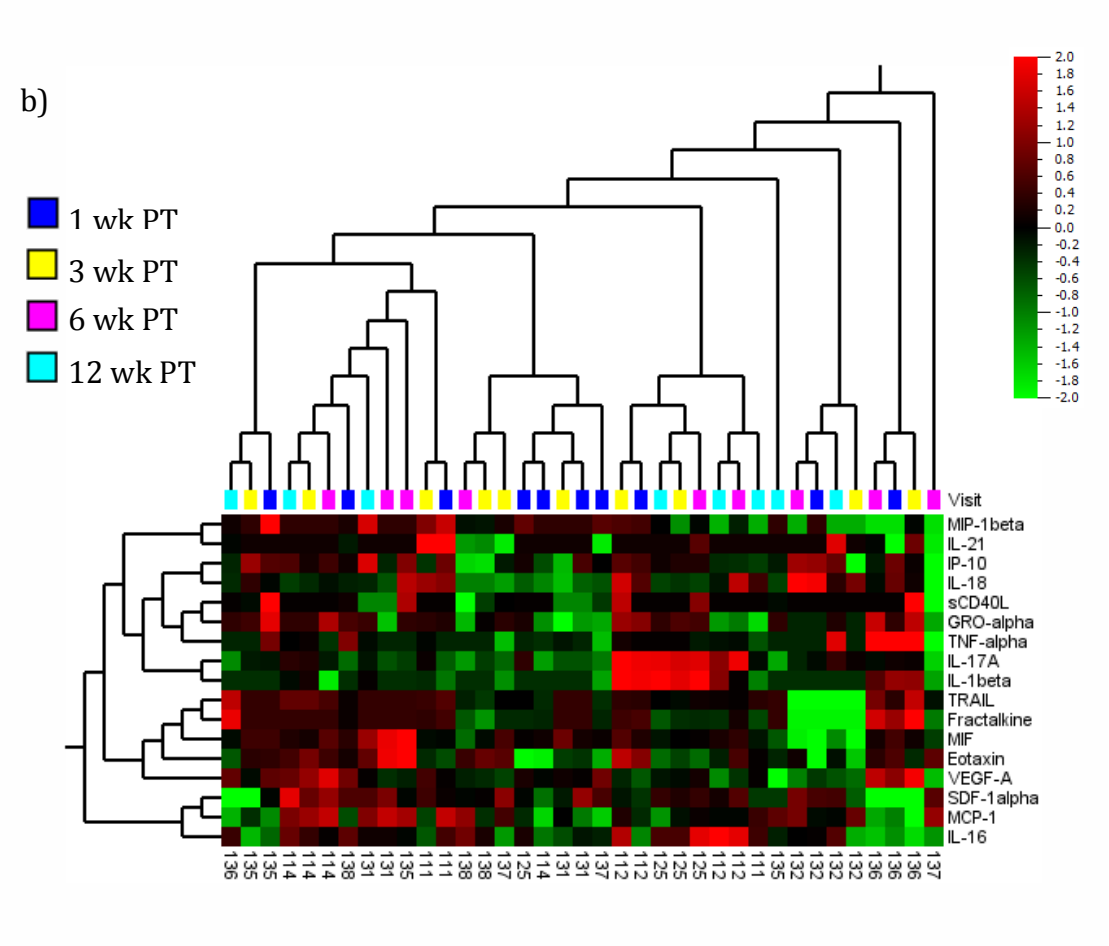

Figure 4.5. Unsupervised Hierarchical Clustering Analysis (HCA) Heat Maps for the two panels (a and b).

All recipients' log-transformed analyte fold changes were included in the HCA except for baseline values. Each visit is shown by coloured blocks (1, 3, 6 and 12 weeks PT) and the rows represent the analytes measured. The heat map indicates the relative fold change increase/decrease from the median for each analyte. Red is increased and green is decreased according to the colour scale.

The unsupervised heat maps (Figure 4.5) do not account for false discovery rate or for the influence of any confounding factors. The most similar analytes and recipients' visits have been grouped together. In order to determine if a fold

change difference is influenced by time or another confounding factor, a two-group or multi-group comparison was applied. The two-group analysis was used for binary variables and the multi-group comparison for categorical variables. For both types of tests, a p-value <0.05 and a false discovery rate (q-value) <0.1 indicated a significant influence of that variable on fold change.

Panel 2 showed no differences in analyte fold change according to any confounding factor used in the comparison (age, sex, ethnicity, pre-operative CD4 count, the number of HLA-matches) or time.

For Panel 1, the comparisons testing whether there was an association of fold change of analytes with age, gender, ethnicity, pre-operative CD4 count, or the number of HLA-matches, showed there was no difference attributed to those variables. There was a significant difference identified when using a multi-group comparison of the visits for Panel 1 analyte fold changes. It showed that there was a group of analytes for which fold change was significantly affected by time (visits) (Figure 4.6).

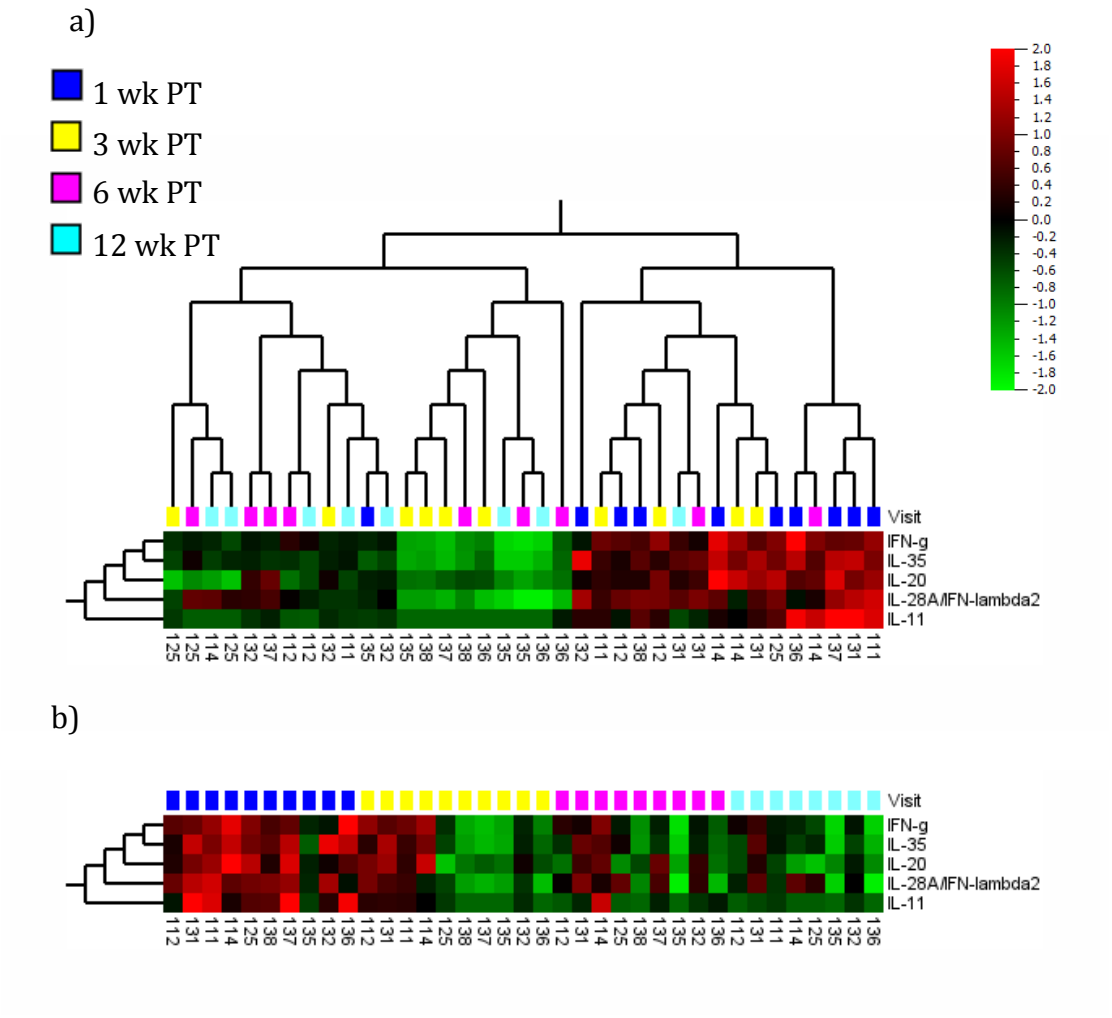

Figure 4.6. Hierarchical Clustering Analysis (HCA) Heat Maps comparison of Visits for the Panel 1.

All Panel 1 recipients' log-transformed analyte fold changes were included in the HCA except for baseline values. Each visit is shown by coloured blocks (1, 3, 6 and 12 weeks PT) and the rows represent the analytes measured. The heat map indicates the relative fold change increase/decrease from the median for each analyte. Red is increased and green is decreased according the colour scale. The analytes that significantly differ over time ($q < 0.1$) are displayed using an unsupervised hierarchical clustering of the visits and analytes (a) and ordered according to visit (b).

Figure 4.6(a) shows the heat map where a multi-group comparison of visits has been applied. Five cytokines, IFNγ, IL-35, IL-20, IL-11 and IL-28A, show a decline in fold change values over the 12-week period. IFN-γ and IL-35 were also found to significantly differ in the fold change over time analysis (Figure 4.4.) There is a trend that the highest fold change was observed at 1 week post-transplant, with the median level at 3-weeks or 6-weeks post-transplant and the lowest at the 6-weeks or 12-weeks time point. This is further emphasized in Figure 4.6B where the heat map is supervised by time.

Patient KID-135 is the only participant to show lower than median fold changes at 1-week post-transplant for the five cytokines (Figure 4.6B). KID-112, KID-131, KID-111, KID-114 show higher than median values at 3 weeks post-transplant. KID-131 and KID-114 are the only to show above median fold changes at 6-weeks PT for all five cytokines, and KID-125 and KID-137 only two of the cytokines are above the median at 6-weeks PT. At 12-weeks PT, only two cytokines are above the median for KID-131 and one for KID-114. The general trend shown is one of a decline in these 5 cytokines over time, in particular during the period from 1 week to 12 weeks post-transplant.

The fold change comparison in Figure 4.4 reflected a significant difference over time for five analytes, which was reinforced in the five analytes identified in Figure 4.6, two of which were common in both analyses.

4.3.6 Mixed Effects Generalised Linear Model (MEGLM)

A mixed generalized linear model (MEGLM) was built for each analyte in order to quantify the difference in concentration between recipients as outlined in Chapter 3 (section 3.4.8, pg 71-73). The visits were modeled as a fixed effect and KID-PID as a random effect. This allowed for the calculation of a percentage of the variation between recipients' in the concentration of a specific analyte. The previous analyses in sections 4.3.4 and 4.3.5 showed that the analytes measured were significantly different over time (Figure 4.4; Figure 4.6b). Neither analysis, however, could identify whether there was a difference in concentration between recipients that was not due to time.

The confidence intervals for the goodness of fit and the percentages calculated from all accepted MEGLMs for both Panel 1 and Panel 2 is represented in Table 4.2.1 and Table 4.2.2 respectively.

Table 4.2.1 Differences in Concentration between recipients from Mixed Effects Generalized Linear Model Panel 1

	Plate 1			Plate 2		
Analyte	Variation between recipients (%)	95% Confidence Interval		Variation between recipients (%)	95% Confidence Interval	
Chitinase3like1	1.97	0	0.36	2.39	0	0.46
IFNα2	40.22	0	0.09	10.04	0	0.36
IFNβ	69.6	0.01	0.14	-	-	-
IFN-γ	51.89	0	0.06	-	>1	>1
IL-10	32.53	0.01	0.24	0.08	0	>1
IL-11	18.71	0.03	>1	-	-	-
IL-12p40	34.16	0	0.05	3.85	0.01	>1
IL-12p70	2.83	0	0.23	0	-	-
IL-19	8.15	0	0.14	82.7	0.07	>1
IL-2	13.96	0	0.08	0.81	0	>1
IL-20	27.11	0.03	1	0.05	0	>1
IL-22	52.46	0.01	0.17	-	-	-
IL-28A	88.21	0.01	0.12	-	-	-
IL-29	47.81	0.03	0.72	-	-	-
IL-35	21.17	0	0.06	6.51	0	0.18
IL-8	0	-	-	0	-	-
MMP-1	31.83	0.04	>1	10.56	0.03	>1
MMP-2	5.84	0	0.41	0.11	0	>1
MMP-3	52.7	0.03	0.56	18.78	0.01	0.47
Osteocalcin	55.44	0.07	>1	31.29	0.04	>1
Osteopontin	52.95	0.02	0.45	-	-	-
Pentraxin-3	73.87	0.05	0.9	-	-	-
sCD163	17.99	0.01	0.32	-	-	-
sIL-6Rα	74.53	0.04	0.6	23.55	0.02	0.57
sIL-6Rβ	68.31	0.02	0.34	-	-	-
sTNFR1	73.99	0.05	0.8	32.59	0.02	0.62
sTNFR2	40.46	0.03	0.59	19.26	0.02	0.79
TNFRSF-8	35.71	0.04	0.89	27.26	0.04	1.12
TNFSF-12	1.42	0	0.36	0.51	0	1.58
TNFSF-13	15.94	0.02	0.86	86.04	0.14	2.11
TNFSF-13b	66.36	0.01	0.14	-	-	-
TSLP	4.74	0	0.1	25.81	0.01	0.3

Table 4.2.2 Differences in Concentration between recipients from Mixed Effects Generalized Linear Model Panel 2

	Plate 1			Plate 2		
Analyte	Variation between recipients (%)	95% Confidence Interval		Variation between recipients (%)	95% Confidence Interval	
Eotxain	55.11	0.05	>1	57.86	0.09	>1
Fractalkine	99.28	0.19	>1	74.79	0.23	>1
GRO-α	15.55	0.18	>1	0	0	0
IL-1β	8.8	0.14	>1	5.23	0.02	>1
IL-16	0.26	0	>1	1.02	0	0.91
IL-17a	8.64	0.14	>1	6.51	0.01	>1
IL-18	76.44	0.1	>1	55.38	0.12	>1
IL-21	9.1	0.03	>1	94.53	>1	>1
IP-10	29.94	0.05	>1	0	0	0
MCP-1	16.23	0	0.15	8.02	0	0.24
MIF	99.41	0.42	>1	86.45	0.46	>1
MIP-1β	30.96	0.21	>1	38.67	0.33	>1
sCD40L	-	0	0	2.56	0.05	>1
SDF-1α	23.63	0.01	0.33	91.01	0.19	>1
TNFα	42.77	0.03	0.69	0.39	0	>1
TRAIL	99.75	0.35	>1	94.37	>1	>1
VEGFα	22.97	0.02	0.66	10.73	0.07	>1

The Tables 4.2.1 and 4.2.2 show the results from the MEGLM for Panel 1 and Panel 2 respectively. The models were built on a per plate basis and therefore separate results columns are included for each plate. A MEGLM was fitted for each analyte. For each model, the 95% confidence interval (CI) is a measure of whether the model fits the data; if the 95% CI is between 0 and 1 then the model can be accepted to fit the data with 95% confidence. The inter-subject variability is the percentage by which the values for that analyte differ amongst the participants included in the model. A high percentage (>65%) indicates a large variability between participants and a low percentage (<10%) indicates near identical values for the different participants.

For Panel 1, 26/32 of Plate 1 MEGLMs fit the data. Of these, IL-28A showed the highest variation in concentration between recipients (88,21%). Other cytokines with highly variation in concentration between recipients (>65%) were sIL-6Rα (74,53%), sTNFR1 (73,99%), Pentraxin-3 (73,87%), IFN-β (69,60%) and sIL-6Rβ (68,31%). Analytes with low variation in concentration between recipients (<10%) were IL-19 (8,15%), MMP-2 (5,84%), TSLP (4,74%), IL-12p70 (2,83%), Chitinase-3-like-1 (1,97%) and TNFSF12 (1,42%); these analytes' concentrations varied minimally between recipients.

For plate 2, fewer MEGLMs could be fitted to the data. Only 9/30 of the plate 2 MEGLMs fit the data. Of those that did, the only cytokines with high variation in concentration between recipients (>65%) on this plate were TNFSF-13 (86,04%) and IL-19 (82,70%). The cytokines with low variation in concentration between recipients (<10%) were TNFSF12 (0,51%), Chitinase-3-like1 (2,39%) and IL-35 (6,51%).

The data from Panel 2 was shown to be less sensitive as the inter-panel controls (IL-2, IL-10 & IFN-γ), which were detected within the observable range for Panel 1, were <OOR for Panel 2 (Section 4.2.1, Table 4.1). These data were shown to be less accurate as far more replicates were excluded from the analysis (Section 4.2.1, Table 4.1) for being <OOR. This was further emphasised by the fact that only 6/22 of plate 1 MEGLMs and 2/22 of plate MEGLMs fit the data (Table 4.2.2). Of these, only IL-23 on plate 1 (98,56%) had high inter-subject variability,

and IL-16 (1,02%) and MCP-1 (8,02%) on plate 2, had low inter-subject differences.

4.4 Discussion

This chapter focussed on investigating the changes in peripheral inflammatory and regulatory proteins in HIV positive renal recipients in the first 12 weeks post ATG induction and transplantation. This was done to address the first aim of this dissertation which was to use a Luminex assay to measure the concentrations of 67 inflammatory and regulatory peripheral proteins in plasma at 5 visits, immediately pre-transplant and 1, 3, 6, 12 weeks PT.

The Luminex assay had various levels at which unnecessary variability could have been introduced into the data ('noise') which may be interpreted for biologically relevant variability if not properly assessed and accounted for. The difference between 'noise' and biological variability was accounted for by, a) eliminating analytes for which more than 90% of measured values were outside the observable range (<OOR) of the standard curve, b) assessing differences between replicates of the sample (intra-plate variability) and excluding outliers, c) assessing differences between plates (inter-plate variability) using inter-plate controls and normalising the differences, d) assessing difference between panels (inter-panel variability) using 3 analytes found in both panels and only combining panels if not difference were identified.

The data clean up results from section 4.2.1 showed the cytokines and other proteins that were excluded from further analysis (Table 4.1, Section 4.2.1, pg. 86). The difference between the two panels in terms of the number of analytes excluded implied that Panel 2 was less sensitive than panel 1. There were more <OOR values than in panel 2 compared to panel 1. The lower sensitivity of panel 1 was confirmed by the exclusion of the 3 inter-panel controls, which also limited the total number of analytes that could not be analysed together and that weakened the assay design. As the panels were from different manufacturers, the difference in sensitivity may be due to manufacturing processes, shipping conditions, or antibody, detector or bead design. The panels were also acquired on 2 different Luminex 200 machines and machine variability and error could have contributed to the reduced sensitivity observed in panel 2 compared to panel 1.

In the Luminex system, in each well of the 96-well plate, the observed fluorescence intensity (FI) of the fluorphore bound to the protein captured by the bead-bound antibodies was measured for each bead region. Each bead region was specific for one protein of interest. The background FI, measured in the blank, was subtracted from the observed FI to calculate the relative median fluorescent intensity (MFI). The 5-parameter standard curve was constructed using the FI of the serial dilutions of the standards containing known concentrations of all measured proteins. The standard curve was used to calculate the absolute concentration values from the MFI.

Breen et al[306] showed that the subtraction of background FI and subsequent calculation of absolute concentration often results in negative values and variable results due to the variability in the dilution of the standards. They developed a new approach that used MFI to calculate statistical analysis of Luminex data, which reduced the number of Out of Range (OOR) values by 50% without any change in statistical differences between samples. If this approach were employed then more of the analytes excluded in section 4.2.1 could have been retained in the analysis and fewer <OOR values would have had to be replaced an arbitrary value. Considering fold changes were used for all analyses except the MEGLM (Section 4.3.6) this approach would have significantly improved the quality of the data and the results.

Most Luminex assays or similar multiplexed assays do not assess the variability between replicates of the same sample. Replicates of the same sample are used in biological assays to increase the precision of the measured value of a sample but replicates should be assessed before averaging so that aberrant results, or significantly outlying replicates, can be identified and excluded[307]. In the Luminex assay the aberrant result of replicates, like those excluded in section 4.2.2, could have been caused by the impact of freeze-thaw cycles, sample homogeneity, variable antibody binding or bead numbers in a well, and the impact of heterophilic antibodies (endogenous antibodies that interfere with the luminex antibodies) in the samples, amongst other uncontrolled factors, could significantly alter the concentrations measured for the same sample in two different wells[217,308]. Including adequate numbers of replicates of all samples, to

account for intra-plate variability has been shown to increase the precision of luminex results[309]. By excluding outliers in section 4.2.2, the mean of each sample was a more precise representation of the biological concentration of that analyte.

The variation between the plates identified in in section 4.2.3 meant that the plates could not be combined. Using the fold changes instead of concentration minimized inter-plate differences. One weakness of this analysis is that the inter-plate differences were never assessed for the fold changes, which is why all single analytes were analysed on a per-plate basis so that plate differences would not cause erroneous results to be reported. Fang et al.,[310] proposed an analytical approach of quantifying the between-plate effect in multiplex assays and reducing it. The approach used a log transformation of the measured linear values, and inter-plate controls of known values to calculate a between-plate effect and then corrected that effect. Fang et al., also only included 5 analytes in the microarray, which made it easier for differences to be assessed and corrected.

If samples with known concentrations were included as inter-plate controls in this analysis in Chapter 4, the between-plate effect could have been quantified using this approach. But as the inter-plate controls used in Section 4.2.3 were unknown and intra-plate variability had been identified between replicates, it would have been risky to use this method to correct the inter-plate differences

using unknown samples. There is also the possibility, that additional variability would be introduced by this approach – this was not investigated by Fang et al.

The trend in almost all analyte fold changes was a decrease from baseline (Figure 4.2, Section 4.3.1). This trend was likely the result of the cytokine release during the first 6 hours post-ATG[311,312] (Section 4.1.3) followed by a decline in those cytokines further accelerated by the cytokine suppression by Tacrolimus and prednisone[302] (Section 4.1.4). The biggest decrease in fold change for most analytes was at 3 or 6 weeks PT after which there was a trend where most fold changes increased until the 12-week visit, but not to the baseline level. This pattern could be indicative of the homeostatic proliferation of T-cells and APCs after the cessation of ATG therapy[313,314].

It is difficult to draw conclusions from different trends in the fold changes of the rejectors compared to the non-rejectors in Figure 4.3 (Section 4.3.3) .The biggest limitation was that there were only 2 rejectors included in the analysis and they experienced two different types of acute rejection (ABMR and TCMR).

Considering that both rejection events occurred at day 9 PT, the changes observed in between day 7 and 21 might have been the cause, or the result, of rejection. If the rejectors did not have different causes of rejection or there were more rejectors included in the analysis, then the changes in cytokines that correlate with acute rejection outlined in Section 4.1.2 could have been identified.

The differences in single analytes over time were (section 4.3.4) were corrected for multiple comparisons using a Bonferroni correction, a stringent method of correcting for multiple comparisons. This stringent correction method was used because with such a small sample size the false positive report probability was large[315] and the most stringent approach was required to avoid reporting false results.

The cytokines IL-2, IFN-α2, IFN-γ and IL-35 were all decreased at one or more visits during the 12-weeks PT (Figure 4.4, section 4.3.4, pg. 101). IL-10 showed a transient increase at one week for 5 recipients. The decreases in IL-2, IFN-α2, and IFN-γ at 12 weeks post-transplant are indicative of effective immune suppression; Tacrolimus inhibits the mRNA expression of all 3 cytokines in activated T-cells[316,317] (Section 4.1.4).

The different roles played by IFN-γ, in rejection and tolerance, are outlined in Section 4.1.2. The decrease in IFN-γ at 12-weeks may be due to a reduction in allospecific T-cells that produce it[262], a reduction in its production by Tregs or the induction of an immunoregulatory environment[264,265,267] – from these data it is not clear which role it is playing. Investigating the phenotypes and functions of the T cells in the periphery with a focus on allospecific regulatory T cells would resolve the ambiguity in these results.

The transient increase in IL-10 is the clearest indicator of an induction or expansion of Tregs, either by the ATG therapy, or in response to the allograft. The function of IL-10 (Section 4.1.2) is immunoregulatory and suppresses allograft rejection. It produced by Tregs[318] in the regulation of allospecific T cells[297] and can also be increased without an increase in Treg cell numbers[319,320]. IL-10 can be produced by tolerogenic DCs, and IL-10 from either Tregs or DCs can induce CD4+ FoxP3- T cells to become IL-10 producing T-reg-like cells (Tr1)[257,321]. The production of IL-10 can therefore work in a feedback loop maintaining its suppressive function. The peak in allospecific Treg proliferation has been shown to be 5 days in vitro[322].

The IL-10 increase was shown in only 5/10 recipients, likely because of the stringency of the statistical approach, the small number of recipients that were analysed and the earliest time PT at which cytokines were measured was 7 days PT, two days after the peak IL-10 production would have taken place[322].

IL-35 is another immunoregulatory cytokine produced predominantly by Tregs[323] (Section 4.1.2). The reduction in IL-35 at all visits post-transplantation may be due to a number of reasons. IL-35 secretion is dependent on surface contact stimulation by conventional T cells[324]. As numbers of conventional T cells are reduced due to ATG and immunosuppression this would reduce IL-35 levels. IL-10 is also produced by Tregs in the same contact-dependent manner[324] but IL-10 is also produced by tolerogenic DCs and other allo-specific Tregs in response to the allograft[257,321]. IL-10 can convert CD4+ FoxP3- T cells into Treg-

like cells (Tr1) cells that only produce IL-10[321] and promote positive feedback loop that leads to preferential IL-10 production. This also further reduces the numbers of conventional T cells available for IL-35 contact-dependent secretion. IL-35 can similarly cause the differentiation of conventional CD4+ FoxP3- T cells into a subset of regulatory-like T cells that produce only IL-35 (Tr35)[299] but this is not known to be influenced by ATG or transplantation.

The hierarchical clustering analysis (HCA) (section 4.3.6) failed to identify analytes the influenced by age, sex, ethnicity, pre-transplant CD4 count or number of HLA-matches. The small number of recipients and large variation in their demographic and clinical criteria likely reduced the association that could be identified by the HCA.

Only time was shown to be associated with fold changes in five analytes (IL-35, IFN-γ, IL-20, IL-28a and IL-11) (Figure 4.6, section 4.3.5, pg. 107) in the HCA. A similar trend over time was shown in Figure 4.6b as was shown as the general trend in Figure 4.2 (section 4.3.2).

Of the analytes' fold changes that were influenced by time, IL-35 and IFN-γ were also identified as significantly different over time in Section 4.3.4. This reaffirmed the findings of the single analyte analysis and shows the reproducibility of these findings. This also strengthened the argument that ATG and immunosuppression was responsible for these trends and that there was a need to phenotype the T cells with a particular focus on Tregs.

The other analytes shown to differ over time (IL-20, IL-28A and IL-11) are not directly involved in transplantation although they are predominantly inflammatory and their decrease is indicative of effective ATG induction and immunosuppression. IL-20 is a known predictor of acute rejection[235] (Section 4.1.2), and its reduction is consistent with the few acute rejection events in these 10 recipients. IL-28A is a viral response cytokine and its reduction suggests effective screening and prophylaxis to prevent viral reactivation in these recipients. Increased IL-11 is implicated in graft versus host disease (GVHD) and its decrease is likely due to control of GVHD by ATG and immunosuppression.

The MEGLM identified IL-28A, sIL-6Rα, sIL-6Rβ, sTNFR1, Pentraxin-3, IFN-β, IL-19 and IL-23 as the cytokines for which the concentrations differed the most between recipients (Table 4.2.1 and Table 4.2.2, section 4.3.6). Only IL-28A was identified as differing over time as well (section 4.3.6). The reason the majority of these analytes were not identified in the previous analyses was that those tested differences over time, whereas the MEGLM investigated differences between recipients. Therefore these cytokines had consistent concentrations over time in each recipient but the concentrations were different between the recipients. The reasons for the different cytokine levels between recipients depend on the function of the cytokine (functions outlined in Section 4.1). In general, there are patient-specific factors that were not controlled for by the inclusion/exclusion criteria (Section 2.2.1, pg 44) or altered the factors that were common between recipients, namely, ATG, transplantation or

immunosuppression. These include but are not limited to the severity of the chronic kidney disease of the native kidney (Pentraxin-3[227], sTNFR1[224]), history of recipients' opportunistic infections and relevant prophylaxis (IL-28A[274,293], IFNβ[252]) and autoimmune conditions (IL-19[274]), levels of pathogenic antigens in the donor kidney (IL-23[296]), variable binding of the capture antibodies to cytokine/receptor complexes (sIL6Rα, sIL6Rβ, sTNFR1) or natural genetic variation between individuals.

The analytes that were shown to have minimal difference in concentration between recipients (IL-19, MMP-2, TSLP, IL-12p70, Chitinase-3-like-1, TNFSF12, IL-35) are not biologically relevant in this analysis except if they were shown to differ over time (Section 4.3.2 and Section 4.3.4). The fact that some of the plates' results do not agree with each other, such as IL-19 showing high variation between plate 1 recipients but low variation between on plate 2 recipients is the result of one or two individuals on a plate with a large difference in concentration compared to the rest. Therefore those individuals are introducing the higher variation identified in that model, resulting in a higher percentage which is not seen for the other plate.

IL-35 was the only analyte that was identified as significantly over time (Section 4.3.2 and 4.3.4) that also showed minimal difference in concentration between recipients (Section 4.3.5). This shows that IL-35 was consistently decreased from baseline in all recipients at week 1, 3, 6, and 12 weeks PT. The reduction of IL-35 was therefore most likely the result of factors that were common between all

recipients, name of ATG and immunosuppression. This further emphasises the need for phenotypic and functional analysis of the peripheral T cells focusing on differentiating between conventional T cells and Tregs to understand whether differences in IL-35 can be explained by this analysis.

One of the biggest weaknesses of the Luminex panel was the omission the suppressive Treg cytokines, TGF-β1, TGF-β2 and TGF-β3[291,295,325]. It could not be included in a multiplex assay, as all three TGF-β isoforms require activation by acid treatment before they can be bound by capture antibodies[326].

These results could be used to answer the objectives of this chapter. The trends in cytokine changes suggested effective T-cell depletion by ATG and immunosuppression by MMF, prednisone and Tacrolimus. No significant differences could be identified between rejectors and non-rejectors but trends did suggest a difference in the regulatory and inflammatory cytokines measured albeit. Significant deceases were shown in several inflammatory cytokines, IL-2, IFN-γ, IFNα2, IL-20, IL-28A and IL-11 and one regulatory cytokine, IL-35. A transient increase in one key immunosuppressive, regulatory cytokine, IL-10 was identified. IL-35 was shown at a consistent between recipients indicated an alteration in regulatory T cells that secrete it. It is not clear from these data whether the changes in regulatory cytokines were due to the induction of Tregs from conventional $CD4^+$ T cells or the expansion of a pre-existing allo-specific Treg population in response to the transplanted organ, or another mechanism.

Further investigations into the phenotypes of the T cell repertoire at baseline as well as various time points post-transplant could clarify this.

These findings suggest that there were changes in peripheral immune cells, in particular changes in the T-cell repertoire, which shifted the balance between inflammation and regulation towards more of a regulatory environment. Further investigations into the phenotypes and functions of T cells were therefore needed to make conclusions regarding the effect of ATG and immunosuppression on peripheral immnunity in HIV positive renal recipients.

Chapter 5: Optimisation of 8-Colour Flow Cytometry Panel

5.1 Introduction

The results from Chapter 4 suggested that there were changes in the T cell repertoire that may be related to changes in Regulatory T cells in particular. This introduction outlines the phenotypes and functions of regulatory T cells, their role in transplantation, how they are affected by ATG induced T cell depletion therapy and how they can be identified using flow cytometry.

5.1.1 Regulatory T cell phenotype

Regulatory T-cells (Tregs) maintain immune tolerance to self[327–330], prevent autoimmune conditions[331], limit bystander damage in response to pathogens by regulating inflammatory responses. Tregs were initially identified by the expression of the surface markers, CD4 and CD25, and later it was shown that the intracellular transcription factor, Forkhead box Protein 3 (FoxP3)[332], was key to their development. A subset of regulatory $CD8^+$ T-cells has also been identified[333]. Although the $CD25^+FoxP3^+$ T-cell phenotype appears to be associated with suppressive regulatory cells, CD25 and FoxP3 can also be expressed transiently on activated cells[334] which have an inflammatory rather than regulatory function. Therefore other markers to identify functional Tregs have been investigated such as: the inhibitory cell surface molecule, Cytotoxic T lymphocyte-associated molecule-4 (CTLA-4)[335,336]; CD127, which has low

expression on Tregs[337]; and markers of suppressive regulatory activity, such as the ectonucleotidases CD39[338,339] and CD73[340].

5.1.2 Regulatory T cell function

Tregs suppress the activity of $CD4^+$ or $CD8^+$ T-cells and antigen-presenting cells (APCs). Tregs can suppress T-cell proliferation by acting as a sink for the proliferative cytokine, IL-2, when binding it using CD25 (IL-2Rα). They can down-regulate inflammatory processes in T-cells[21–24] or induce the conversion of effector T-cells to Treg-like cells through the expression of IL-10[297], TGF-β[325] or IL-35[299] on their cell surface or as soluble regulatory mediators[21–24]. Tregs directly induce apoptosis in their targets through the production of perforin[342] and granzymes[343] as well as indirectly through the consumption of IL-2 dependent on the pre-apoptotic factor *Bim*[344].

Tregs constitutively express the regulatory marker, Cytotoxic T Lymphocyte–associated Antigen 4 (CTLA-4 [CD152])[336]. It is a homologue of the co-stimulatory marker found on conventional T-cells, CD28, which interacts with CD80 or CD86 expressed on APCs, which in combination with the TCR initiate immune responses. But unlike CD28, CTLA-4 causes a down-regulation of T-cell-mediated immune responses in APCs[335]. Tregs can therefore attenuate immune responses via CTLA-4 by affecting the potency of APCs to activate other T-cells[345]. Tregs can also decrease the costimulation of APCs by the expression of

ATPases on their surface, such as CD39 and CD73. These ATPases inactivate the inflammatory extracellular ATP which have deleterious effects on APCs.

5.1.3 Regulatory T cells in Transplantation

Alloreactive Tregs play a key role in tolerance and acceptance of allografts[346–348]. They maintain the balance between inflammation and regulation, and in effect, the balance between allograft rejection and survival. Tregs specific to the allograft promote a regulatory environment that aids in the graft survival by regulating the anti-graft activity of allospecific effector T-cell (Teff) both locally and systemically and has been well studied in renal transplantation[198,349]. In transplant recipients, there are usually insufficient Tregs present at the time of transplantation to prevent the rejection of the allograft[350]. The Tregs are not ineffective; they simply represent too small a proportion of the T-cell repertoire for them to have a significant suppressive impact on allo-specific Teff. These Tregs could increase in number as the population expands in response to the allospecific stimulus by the transplanted organ.

5.1.4 Effect of T-cell Depletion on Regulatory T cells

As discussed in Chapter 1 (section 1.3.6, pg 19), ATG T-cell depletion therapy ablates almost all T-cells, B-cells and NK-cells[351,352]. Tregs however, appear to be either resistant to this depletion[353], and/or undergo rapid homeostatic proliferation after the cessation of the ATG therapy[354], or cause the conversion of

$CD4^+CD25^-FoxP3^-$ cells to $CD4^+CD25^+FoxP3^+$ Tregs[202,355]. As a result, ATG therapy results in an increase in the ratio of Tregs:Teff by one year post-transplant, as compared to pre-therapy levels[203,204,352,353,355,356]. Higher proportions of Tregs allow the Tregs to suppress the allospecific T cells, improve allograft survival and potentially attenuate transplant tolerance.

ATG therapy has been the mode of immunosuppressive induction in the cohort studied in this dissertation. ATG was provided to HIV infected patients receiving kidneys from deceased HIV^+ kidney donors (Chapter 2, section 2.3, pg 46), and the effect of T-cell depletion in these patients is unknown. This could mean that depleted T-cells would result in fewer target CD4+ cells for HIV to infect, or the emergent Treg population that proliferates after cessation of ATG may represent a reservoir of latent HIV[357]. Nevertheless, the higher proportions of Tregs may be beneficial to the transplant recipients, as a reduction in activated T-cells would result in fewer target CD4+ cells for HIV and facilitate a state of elite control[358]. Tregs have also been identified as a reservoir of latent HIV[357], and a rapidly proliferating population of T-cells latently infected with HIV could result in an uncontrolled increase in viral load. There are therefore many roles that Tregs would play in these patients. It is still unknown how the combination of HIV, transplantation and immunosuppression will alter the proportion of Tregs, especially in the first 3 months post-ATG induction as well as more than one year post-transplant.

5.1.5 Phenotyping T cells using Flow Cytometry

Flow cytometry is a technology that analyses the physical and chemical characteristics of cells in a fluid as they pass through numerous lasers. It allows for the quantification of the numbers and proportions of different cell-types based on their size, granularity and the presence of phenotypic surface or intracellular proteins. Before the cell suspension enters the flow cytometer, cells are labelled using antibodies specific to the proteins of interest, tagged with different fluorescent markers. In the flow cytometer, cells are passed in front of numerous lasers in a sheath fluid. Cells of different sizes and granularity scatter light in a forward direction (Forward scatter, FSC) and orthogonally (side scatter, SSC). The fixed wavelength lasers excite the fluorescent probes, which emit a spectrum of light that can be collected through a series of long-pass and short pass filters and then detected by the photomultiplier tubes (PMTs). The emitted spectra allows for the identification of cells that stain positively for the proteins of interest. By selecting cells based on their size and granularity and including multiple antibodies in one stain, phenotypes at the single cell level can be identified.

As shown in Chapter 4, the Luminex assay investigated the changes in inflammatory and regulatory cytokine levels in the first 3 months post-transplant. The results were used to guide the markers that were included in the flow cytometry panel. There was a decrease in inflammatory cytokines, IL-2, IFN-γ and IFN-α2, across all 10 participants, as well as a transient increase in a

regulatory cytokine, IL-10, in five of the participants (Chapter 4, Section 4.3.2 and Section 4.3.2). This may suggest that there is a decrease in the effector T cell numbers, as would be expected from the ATG therapy and immunosuppression but also an expansion of Treg-like cells in at least five of the participants. There is also a decrease shown in the other regulatory T cell cytokine, IL-35 (Chapter 4, Section 4.3.2).

As the T-cells during the first 3-months had not yet recovered to pre-ATG levels and were functionally suppressed, the T-cells phenotypes and function 1-year post-transplant were to be compared to baseline (pre-transplant) to investigate what effect the combination of ATG, transplantation and immunosuppression had on the T-cell proportions in the long term and how this was influenced by the changes observed in cytokine levels in the first 3 months.

The 8-colour flow cytometry panel was designed with the intention of phenotyping the T cell population in the peripheral blood mononuclear cells (PBMCs) of the HIV+ renal transplant recipients, with a particular focus on differentiating between effector T cells (Teff) and regulatory T cells (Tregs). The panel was designed to assess what proportion of T cells ($CD3^+$) were $CD4^+$or $CD8^+$, which of these were memory or naïve cells (CD27/CD45RA), activated ($CD25^+$), or had a Treg phenotype ($CD4^+$, $CD25^{high}$, $CD127^{low}$, $FoxP3^+$). The final panel (Chapter 3, Table 3.3 and Table 3.4) included a dead cell marker to discriminate live/dead cells.

In this dissertation, the aim was to assess the impact of ATG treatment along with kidney allograft transplantation in HIV positive recipients. The overall objective was to use the Luminex assay to investigate changes in plasma cytokines involved in inflammation and regulatory processes to guide the development of a polychromatic flow cytometry panel.

This chapter aimed to develop and optimise a polychromatic flow cytometry panel that could be used to phenotype and differentiate between Regulatory T cells in transplantation, to compare T cell repertoires pre-transplant to those at one-year post ATG therapy and transplantation in 10 HIV positive recipients.

5.2 Optimisation of the panel

When the flow cytometry panel was compiled, the first step was to determine the optimal volume or titre of the antibodies used in the panel. The aim was to determine the optimal volume of the conjugated-antibody required to generate a positive fluorescent emission while minimising non-specific fluorescence. The optimal volume was determined by comparing the mean fluorescence intensities (MFI) of emission of the population that stain positive for the antibody to those which were negative for the different titrating volumes. The ratio between positive MFI and negative MFI was used show ratio of signal to noise (Signal:Noise). The optimal titre was determined for each conjugated antibody by the best Signal:Noise ratio but although this is sometimes misleading so the optimal titre was also assessed by separation of the positive and negative

populations by eye, ensuring that the MFI of the positive was not too high as this could lead to a spill over of fluorescence from one channel into another. The panel was then slowly combined, adding each antibody marker one by one so that the titres could be adjusted to avoid spill over of the emission of one fluorescent marker into the emission spectra of others. The titres for each antibody used for the titrations are shown in Table 5.1. All staining was done using the antibodies and staining buffer (2% FCS in PBS) in a total staining volume of 50µl.

Table 5.1. Flow Cytometry Antibody Markers and Titres used in Titrations

Group	**Marker**	**Titrating Volumes (µl) in 50µl staining buffer**					
Dead	Zombie	1	0.5	0.25	0.12	0.062	0.031
Anchor	CD3	1.2	0.6	0.31			
	CD4	1.6	0.8	0.4	0.2		
	CD8	1.6	0.8	0.4	0.2		
Memory/Naïve	CD27	5	2.5	1.25	0.62	0.31	
	CD45RA	4	2	1	0.5		
Activation	CD25	5	2.5	1.25	0.61		
Tregs	CD127	1.2	0.6	0.3	0.15		
	FoxP3	6	3	1.5			

5.2.1 Dead Cell Marker Titrations

Zombie-Near Infrared Red (Zombie-NIR) is a dead cell marker that stains dead cells but not viable cells. It was included as dead cells can bind antibodies non-specifically and the positive Zombie-NIR, considered as dead cells, could be excluded from the analysis. The dye is excited by the red laser (632nm) and the

emission spectra (max at 746nm) is detected by detector A (780/60nm BP) (Chapter 3, Figure 3.5 ii, pg 66).

The titrations for the dead cell marker were performed as described in Chapter 3 using the volumes shown in Table 5.1. Figure 5.1 shows a representative gating strategy (A), the flow cytometry density plots (B-D), the MFIs and signal:noise (E-G). For the purposes of titrating a live/dead marker and to ensure there were detectable dead cells, half of the PBMCs were killed using two different methods: cell lysis with the addition of Reverse Osmosis (RO) H_2O for 3 minutes, or incubation at 60°C for 3 minutes. The dead cells were added back to resting PBMCs before staining.

The optimal staining titre was identified using the methods outlined in Chapter 3. The optimal titre of Zombie-NIR was found to be 0.625µl in a staining volume of 50ul.

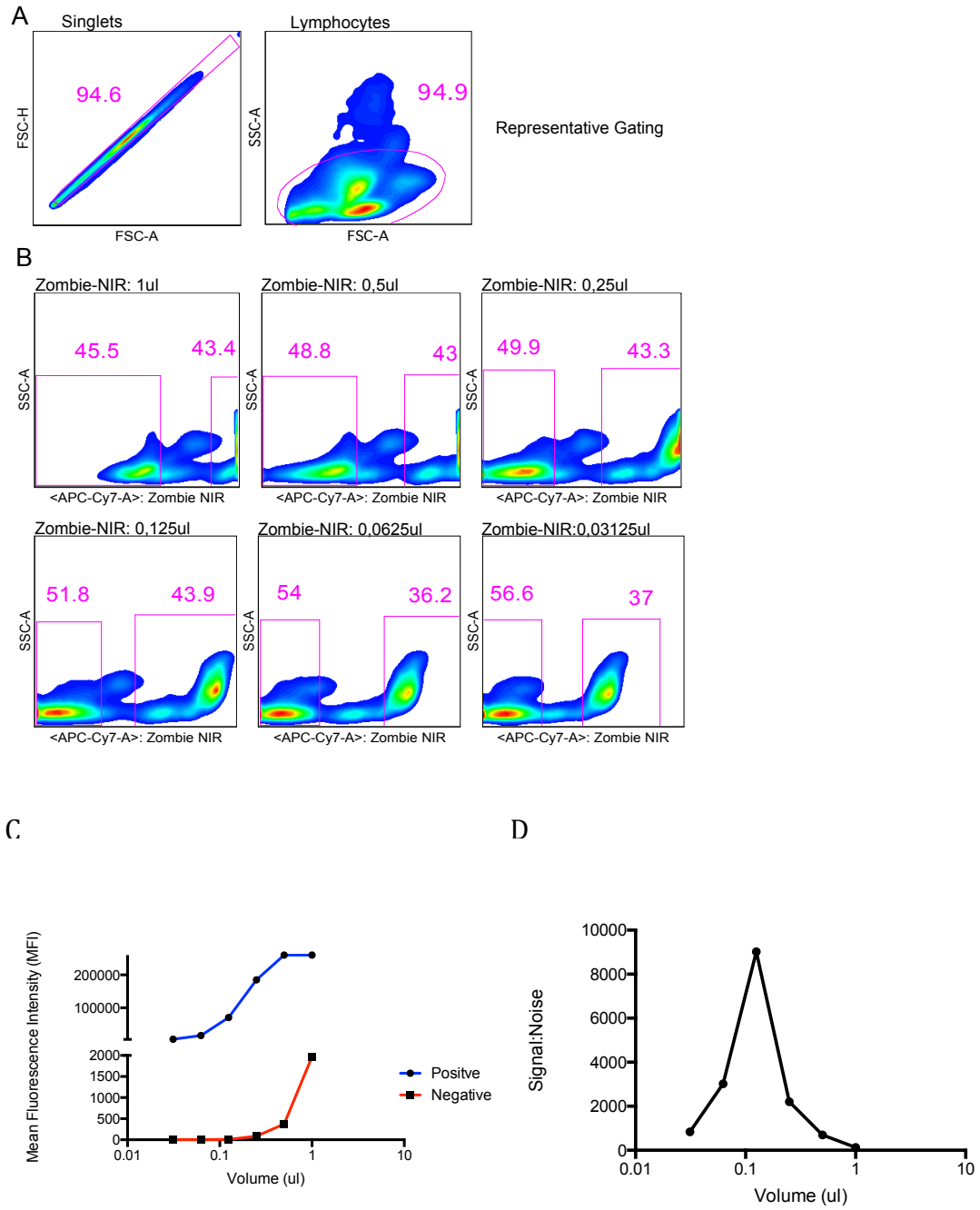

Figure 5.1. Flow Cytometry Density Plots, MFIs and Signal:Noise for Zombie-NIR titrations on thawed PBMCs spiked with Lysed PBMCs.

The flow cytometry pseudo-colour density plots are shown for the representative gates used for each Zombie-NIR titration (A). The label above and the pink shapes indicate the population gated upon. The numbers in pink

indicate the percentage of the parent population represented within that gate. The titrations of the different volumes of Zombie-NIR are shown (B). The pink gates indicate the percentage of Zombie-NIR negative and Zombie-NIR positive lymphocytes. The MFI of the Zombie-NIR positive (blue) and negative (red) populations are shown for the different Zombie-NIR volumes used (C). The Signal:Noise ratio of MFI positive: MFI negative is shown for the different Zombie-NIR volumes (D).

5.2.2 Anchor Marker Titrations

CD3 is a complex of proteins found in conjunction with the T-cell receptor (TCR) on all T cells[359]. It serves as a co-receptor that helps to transduce antigen-specific signal from TCR/MHC interactions on both $CD8^+$ and $CD4^+$ T cells[359]. When staining PBMCs, all $CD3^+$ cells are considered T cells.

CD4 is a glycoprotein predominantly found on $CD3^+$ helper T cells[360]. It interacts with the TCR to recognise the class II Major Histocompatibility Complex (MHC II) antigen complex[361]. Naive CD4+T cells are activated after this interaction and differentiate into specific subtypes depending on the mainly cytokine milieu of the microenvironment[362,363]. These subtypes included the T helper (Th1, Th2, Th9, Th17) subsets as well as Tregs. When staining PBMCs, all $CD3^+$ $CD4^+$ cells are considered helper T cells.

CD8 is a glycoprotein found on a subset of $CD3^+$ T cells, which can be cytotoxic. It interacts with the TCR to recognise the class I MHC antigen complex[361]. These cells can cause cytotoxicity through several mechanisms: secretion of perforin/granzymes, FasLigand/Fas interactions, and production of tumor necrosis factor α (TNFα)[364]. When staining PBMCs, all $CD3^+$ $CD8^+$ cells are considered $CD8^+$ T cells.

In the panel under development, the anti-CD3 antibody was conjugated to Brilliant Violet 650 (BV650). It fluoresces when excited with the violet laser

(405nm); the emission max is 407nm and is detected by detector D (655/40nm BP) (Chapter 3, Figure 3.5 1 iv, section 3.3.3, pg 65). The anti-CD4 antibody is linked to Phycoerythrin/Cyanine5.5 (PE/Cy5.5). It fluoresces when excited with the green laser (488nm); the emission max is 690nm and is detected by detector B (575/25nm BP) (Chapter 3, Figure 3.5. iii, section 3.3.3, pg 65). The anti-CD8 antibody is linked to HorizionViolet500 (HorizonV500). It fluoresces when excited with the violet laser (405nm); the emission max is 415nmm and is detected by detector G (515/20nm BP)(Chapter 3, Figure 3.5 iv, section 3.3.3, pg 65).

The titrations for all anchor markers were performed as described in Chapter 3 (Section 3.3.2, pg 64) using the volumes in Table 5.1. The representative gating strategy (A), the flow cytometry density plots (B-D), the MFIs (E-G) and signal:noise (H-J) are shown in Figure 5.2.

The optimal titre for each antibody was determined using the method outlined in Chapter 3 (Section 3.3.2, pg 64). The optimal titre for CD3-BV650 was 1.25µl in a staining volume of 50ul, for CD4-PE/Cy5.5 it was 0.8µl in a staining volume of 50ul, and for CD8-HorizonV500 it was 0.4µl in a staining volume of 50ul. Figure 5.2 shows the flow plots for CD3, CD4 ad CD8 titrations.

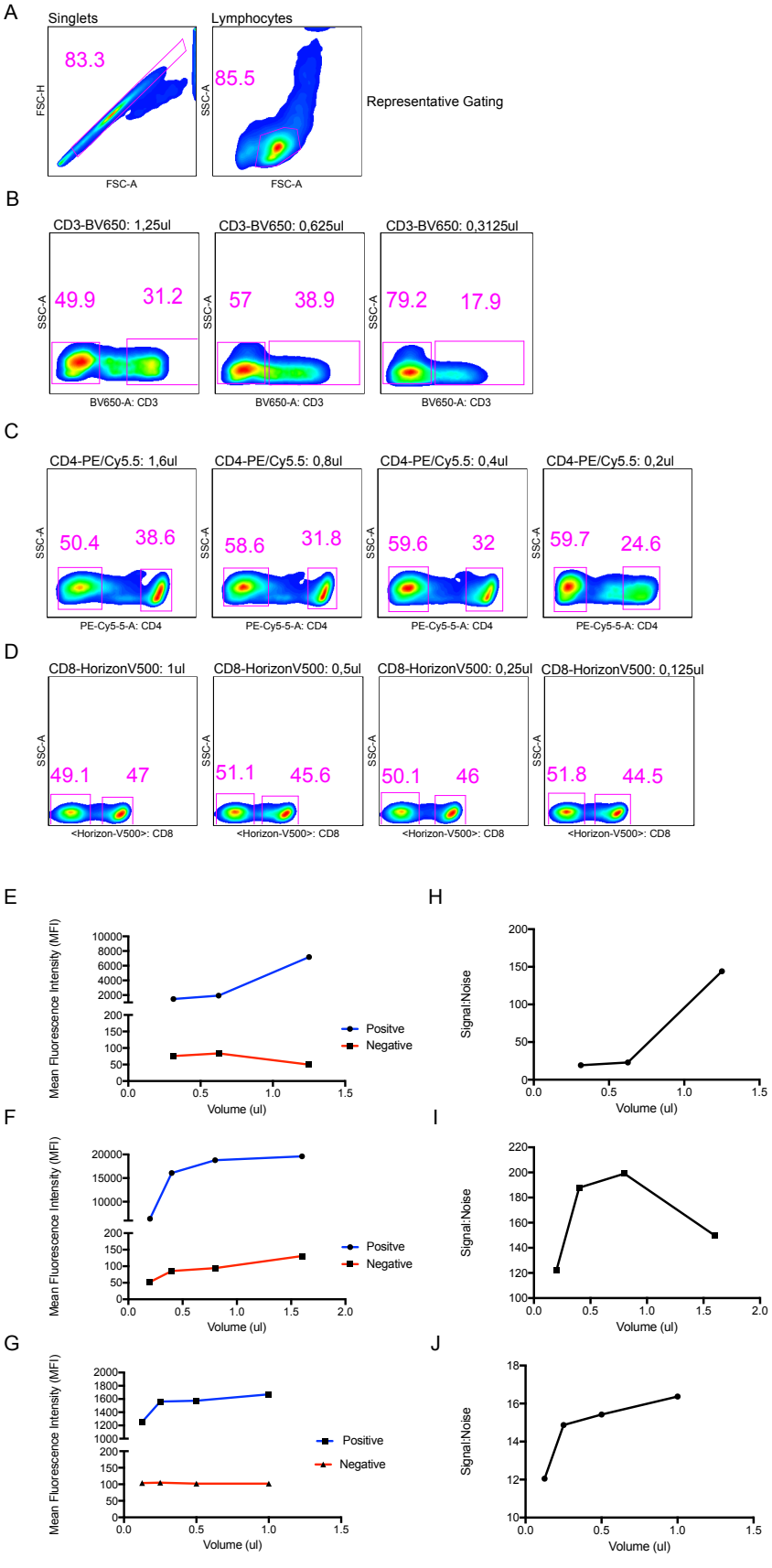
A
Singlets
Lymphocytes
83.3
85.5
FSC-H
SSC-A
FSC-A
FSC-A
Representative Gating
B
CD3-BV650: 1,25ul
CD3-BV650: 0,625ul
CD3-BV650: 0,3125ul
49.9
31.2
57
38.9
79.2
17.9
SSC-A
BV650-A: CD3
C
CD4-PE/Cy5.5: 1,6ul
CD4-PE/Cy5.5: 0,8ul
CD4-PE/Cy5.5: 0,4ul
CD4-PE/Cy5.5: 0,2ul
50.4
38.6
58.6
31.8
59.6
32
59.7
24.6
PE-Cy5-5-A: CD4
D
CD8-HorizonV500: 1ul
CD8-HorizonV500: 0,5ul
CD8-HorizonV500: 0,25ul
CD8-HorizonV500: 0,125ul
49.1
47
51.1
45.6
50.1
46
51.8
44.5
<Horizon-V500>: CD8
E
F
G
H
I
J
Mean Fluorescence Intensity (MFI)
Signal:Noise
Volume (ul)
Positve
Negative
Positive

Figure 5.2. Flow Cytometry Density Plots, MFIs and Signal:Noise for Anchor Marker on thawed PBMCs.

The flow cytometry pseudo-colour density plots are shown for the representative gates used for CD3-BV650, CD4-PE/Cy5.5, CD8-HorizonV500 titrations (A). The label above and the pink shapes indicate the population gated upon. The numbers in pink indicate the percentage of the parent population represented within that gate. The titrations of the different volumes of each marker are shown (B). The pink gates indicate the percentage of antibody positive and antibody negative lymphocytes. The MFI of the antibody positive (blue) and antibody negative (red) populations are shown for the different volumes used for CD3-BV650 (E), CD4-PE/Cy5.5 (F) and CD8-HorizonV500. The Signal:Noise ratio of MFI positive: MFI negative is shown for the different volumes corresponding to the MFI graphs (H-J).

5.2.3 Memory/Naïve Markers

CD27 is a co-stimulatory molecule found on T cells. It interacts with its ligand CD70 as co-stimulatory signals, especially in $CD4^+$ $CD45RA^+$ Naïve T cells[365].

CD45RA is an isoform of the enzyme Protein tyrosine phosphatase, receptor type, C (PTPRC/CD45). CD45RA acts as a signalling molecule and regulates a variety of cellular processes.

CD27 and CD45RA can be used together to identify populations of naïve, effector and memory T cells. When staining PBMCs, the different naïve, effector and memory population that are identifiable using CD27 and CD45RA are shown in Figure 5.3A. Figure 5.3A shows an adapted flow cytometry dot plot from Hamann et al[366], comparing cord blood to adult blood using a triple stain of CD45RA, CD27 and CD4 or CD8. Four populations are identified in the CD8+ Adult blood and these are illustrated in Figure 5.3B. The cell population identified in the cord blood ($CD45RA^+/CD27^+$) is naïve-like and the other populations' effector/memory profiles were determined by their function.

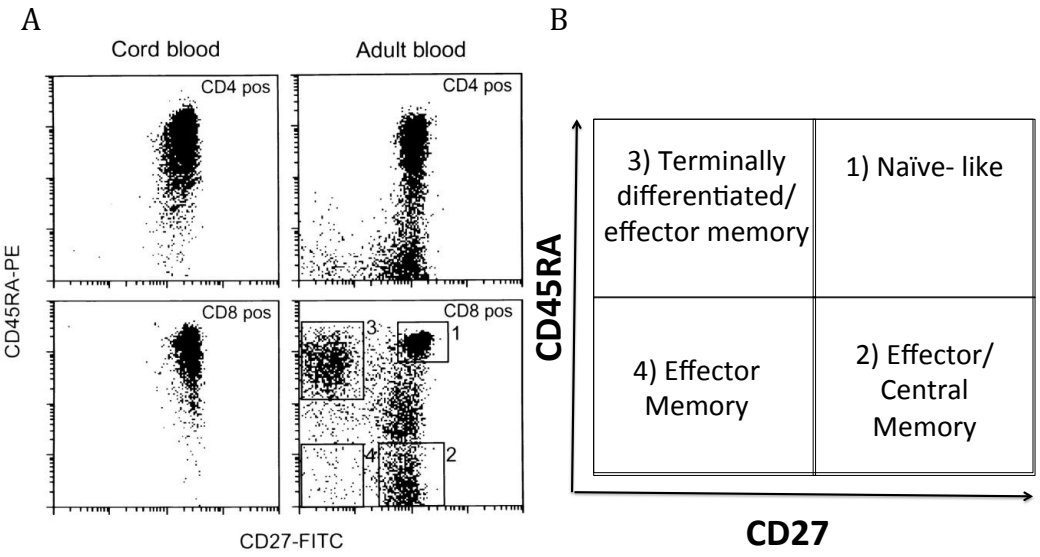

Figure 5.3. Different Naive, Effector or Memory Populations Identifiable using markers for CD45RA and CD27 in Flow Cytometry[366]

A comparison of Cord Blood and Adult blood when stained with CD27, CD45RA, and CD4 or CD8. (A). The four populations identified are summarised (B): 1) $CD45RA^+/CD27^+$ = Naïve-like; 2) $CD45RA^+/CD27^-$ = Effector/central memory; 3)

$CD45RA^-/CD27^+$ = terminally differentiated/effector memory 4) $CD45RA^-/CD27^-$ = Effector Memory.

The anti-CD27 antibody is linked to Phycoerythrin/Cyanine5.5 (PE/Cy5), which fluoresces when excited with the blue laser (488nm); the emission max is 670nm and is detected by detector C (660/20nm BP) (Chapter 3, Figure 3.5 iii, section 3.3.3, pg 65). The anti-CD45RA antibody is linked to Peridinin Chlorophyll Protein Complex/Cyanine5.5 (PerCP/Cy5.5), which fluoresces when excited with the blue laser (488); emission max is 695nm and is detected by detector B (575/25nm BP) (Chapter 3, Figure 3.5 iii, section 3.3.3, pg 65).

CD27-PE/Cy5 was titrated by gating only on the viable T cells (Figure 5.3A) by co-staining the titrating PBMCs with Zombie-NIR negative cells and CD3-BV650 positive cells. The optimal staining volume for CD27-PE/Cy5 was calculated using the methods outlined in Chapter 3. The optimal titre was found to be 1.25µl in a staining volume of 50ul (Figure 5.3B, F &K).

The titrated volume of CD27-PE/Cy5 was included as a co-stain along side Zombie-NIR, CD3-BV650, CD4-PE/Cy5.5 and CD8-HorizonV500 to titrate CD45RA-PerCP/Cy5.5. The optimal titre was determined using the same gating as CD27-PE/Cy5 (Figure 5.3A) with additional gating on $CD4^+$ or $CD8^+$ Live T cells (Figure 5.3C). The MFIs of CD45RA-PerCP/Cy5.5 were calculated for the $CD27^+$ and $CD27^-$ populations both the $CD4^+$ and $CD8^+$ T cells. The optimal titre for CD45RA-

PerCP/5.5 was based on the $CD8^{+}CD27^{+}$ population (Figure 5.3E, I & N) and was found to be 1µl in a staining volume of 50ul.

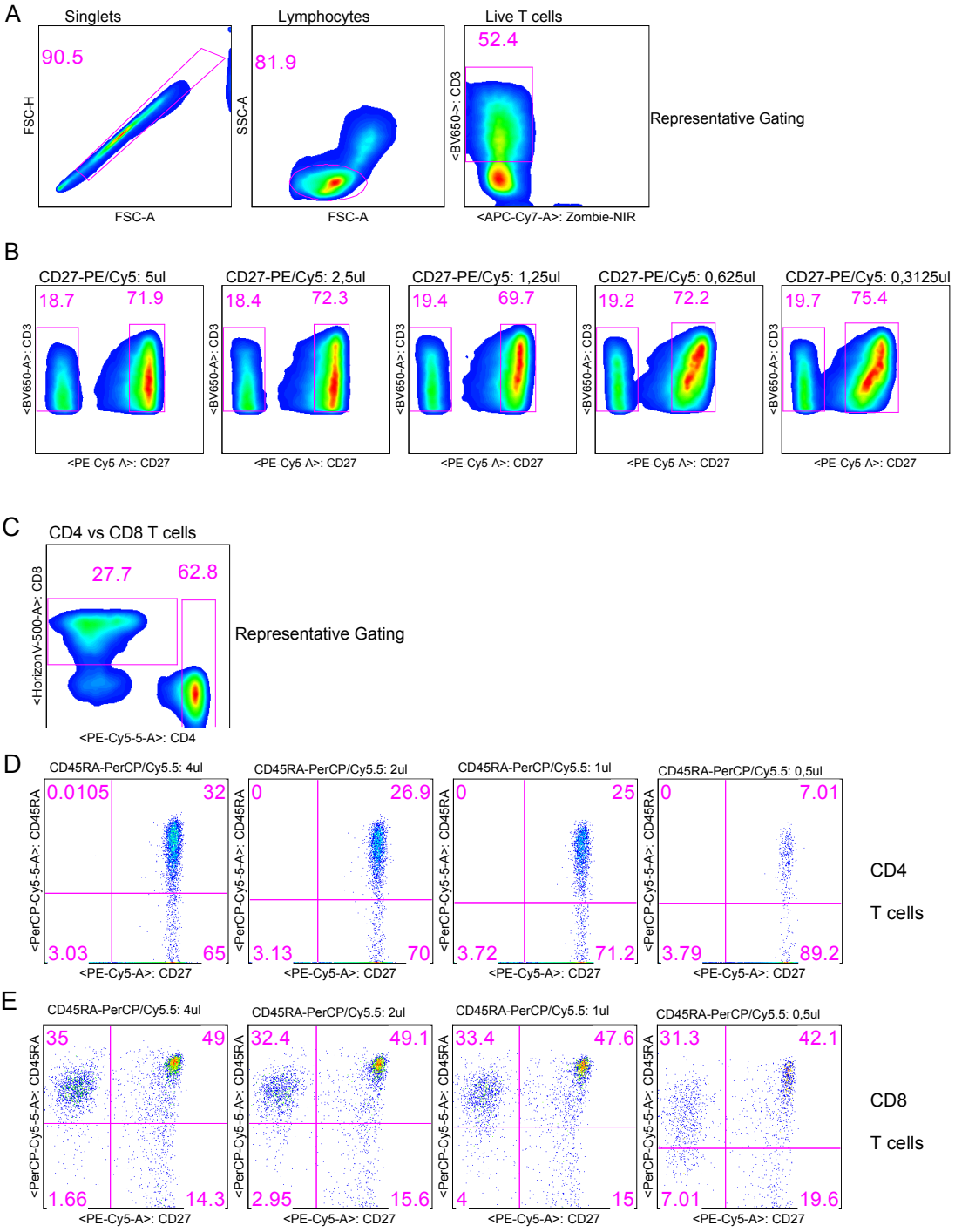

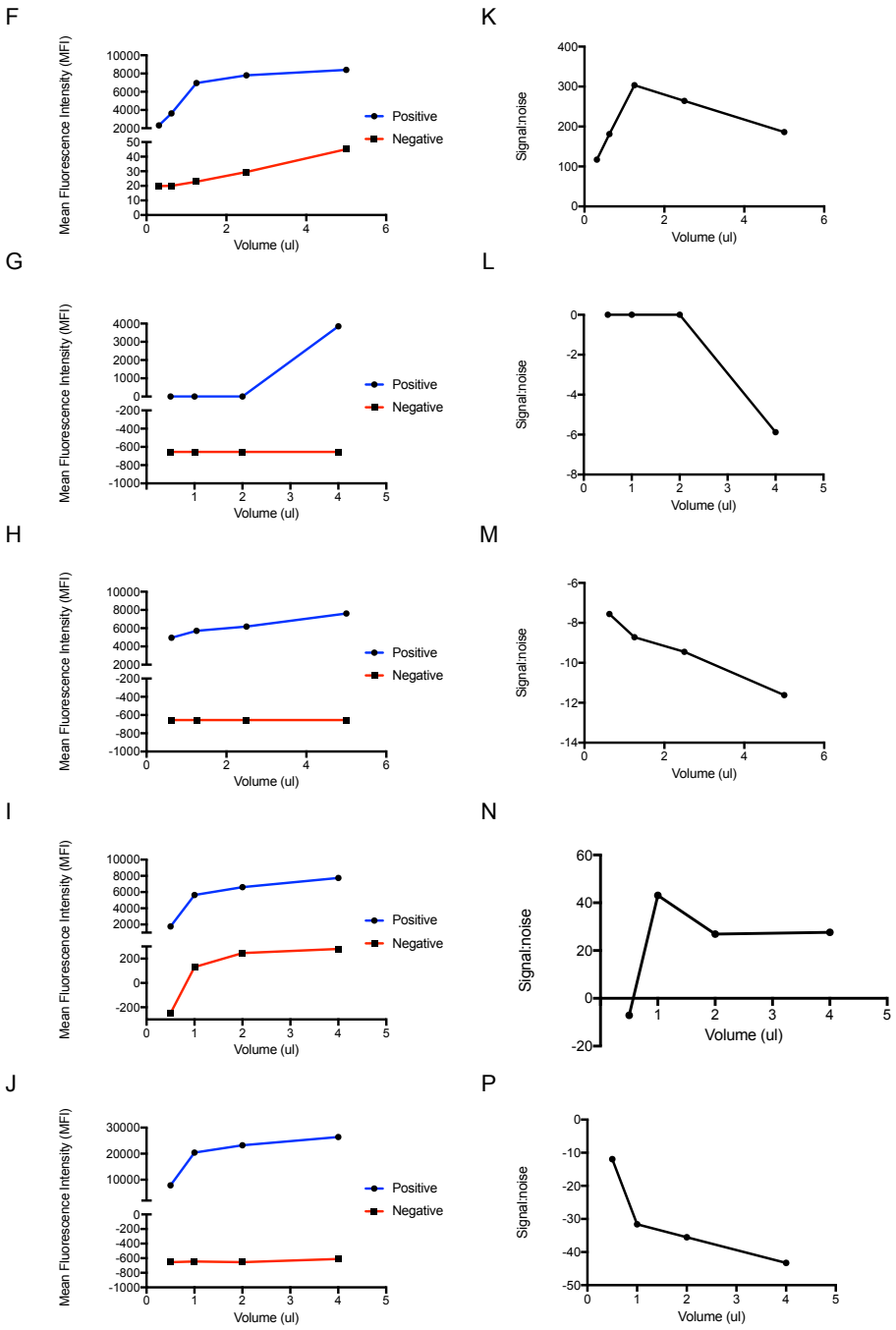

Figure 5.4. Flow Cytometry Density And Dot Plots, MFIs and Signal:Noise for Memory/Naïve markers on thawed PBMCs The flow cytometry pseudo-colour density plots are shown for the representative gates used for the CD27-PE/Cy5 titrations (A) and the additional gates that were applied for CD45RA-

PerCP/Cy5.5 (C). The label above and the pink shapes indicate the population gated upon. The numbers in pink indicate the percentage of the parent population represented within that gate. The titrations of the different volumes of CD27-PE/Cy5 are shown (B) and the different volumes CD45RA-PerCP/Cy5.5 titrations gated on $CD4^+$ (D) and $CD8^+$(E). The pink gates or grids indicate the percentage of the parent population within that shape. The MFI of the CD27-PE/Cy5 positive (blue) and negative (red) populations for the different volumes used are shown (F). The MFIs for the $CD4RA^+$ (blue) and $CD45RA^-$ (red) are show for the $CD4^+CD27^-$ (G), $CD4^+CD27^+$ (H), $CD8^+CD27^-$ (I) and $CD8^+CD27^+$ (J). The Signal:Noise ratio of MFI positive: MFI negative is shown for the different volumes corresponding to the MFI graphs (K-P).

5.2.4 Regulatory T cell Markers

CD25 is also known as the interleukin-2 (IL-2) receptor α-chain. IL-2 was initially identified as a T-cell growth factor and plays key roles in both inflammation and tolerance. CD25 is upregulated on activated T-cells but it was the first marker that was identified on suppressive $CD4^+$ T cells with a Treg-like function[330,367].

Forkhead box P3 (FoxP3) is a transcription factor expressed in Tregs and key to their development. FoxP3 was used to identify Tregs in the $CD4^+CD25^+$ T cell population[368]. FoxP3 is however also transiently upregulated during T cell activation[334] and all $CD4^+CD25^+FoxP3^+$ T cells may not have a regulatory function.

CD127 plays a critical role during lymphocyte development, specifically during V(D)J recombination, the process of somatic recombination which results in the highly diverse repertoire of immunoglobulins and TCRs found on B-cells and T-cells, respectively[369,370]. It is expressed at a low level on $CD4^+CD25^+FoxP3^+$ regulatory T cells[337] and helps to identify functional, suppressive Tregs from transiently activated $CD4^+$ T cells that can also express $CD25^+$ or $FoxP3^+$[337]. When staining PBMCs, all $CD4^+$ $CD25^{high}$ $CD127^{low}$ $FoxP3^+$ T cells are considered Tregs.

The anti-CD25 antibody is linked to BrilliantViolet421 (BV421), which fluoresces when excited with the violet laser (405nm); the emission max is 421nm and is detected by detector H (450/50nm BP)(Chapter 3, Figure 3.5 iv, section, 3.3.3). The anti-FoxP3 antibody is linked to Alexa Fluor® 647 (Alexa647), which fluoresces when excited with the red laser (633nm); emission max is 665nm and is detected by detector C (660/20nm BP) (Chapter 3 Figure 3.5 1 ii, section 3.3.3, pg 65). The anti-CD127 antibody is linked to Phycoerythrin/CF®594 (PE/CF594), which fluoresces when excited with the green laser (532nm); emission max is 612nm and is detected by detector D (610/20nm BP) (Chapter 3, Figure 3.5 iii, secton 3.3.3, pg 65).

The representative gating strategies (A & C), the flow cytometry density/dot plots (B, D & E) and, MFIs (F), and Signal:Noise (H) for the Treg markers are shown in Figure 5.4. The titrations for CD127-PE/CF594 were performed on thawed, resting PBMCs, whereas the CD25-BV421 and FoxP3-Alexa647 titrations were performed on 24 hour Phytohaemagglutinin (PHA) stimulated PBMCs. PHA is a

mitogen which upregulates activation markers in lymphocytes. The CD127-PE/CF594 titrations included the co-stain of only Zombie-NIR. The CD25-BV421 titrations included co-stains of Zombie-NIR, CD3-BV650 and CD4-PE/Cy5.5, and the FoxP3-Alexa647 titrations included the full panel of titrated antibodies (Table5.1). For the full panel, the PBMCs were gated as with the CD25-BV421, on singlets, lymphocytes then live T cells (Figure5.4 C). The live T cells were gated on either the $CD4^+$ T cells or the $CD8^+$ T cells. The $CD4^+$ and $CD8^+$ T cells were gated on the $CD25^{high}CD127^{low}$ population. The MFI for the $CD4^+$ $CD25^{high}CD127^{low}$ FoxP3 positive and FoxP3 negative populations was calculated and used to generate the signal:noise. Representative plots of the memory/naïve gates are also included.

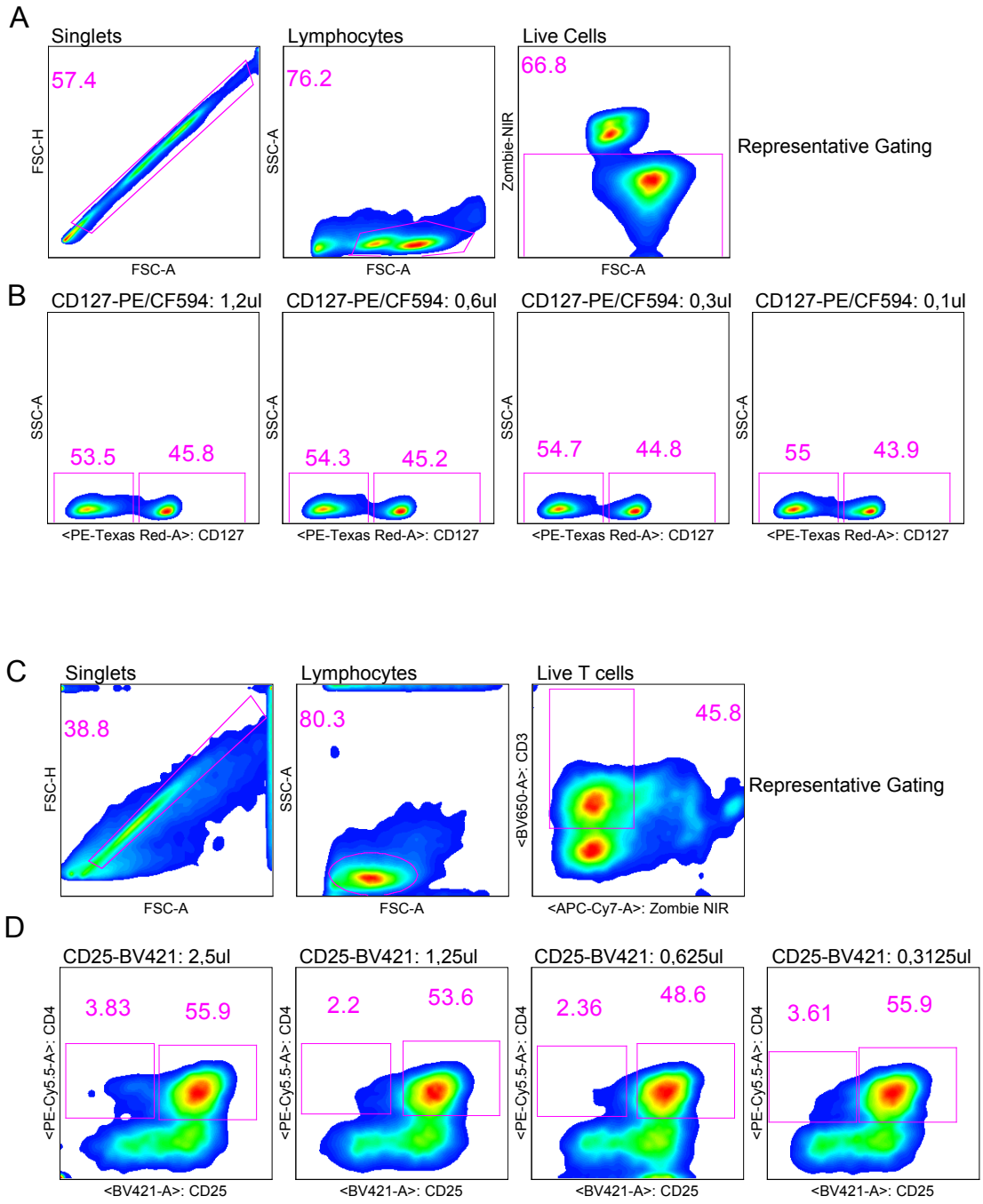
A
Singlets
57.4
FSC-H
FSC-A
Lymphocytes
76.2
SSC-A
FSC-A
Live Cells
66.8
Zombie-NIR
FSC-A
Representative Gating
B
CD127-PE/CF594: 1,2ul
53.5
45.8
SSC-A
<PE-Texas Red-A>: CD127
CD127-PE/CF594: 0,6ul
54.3
45.2
SSC-A
<PE-Texas Red-A>: CD127
CD127-PE/CF594: 0,3ul
54.7
44.8
SSC-A
<PE-Texas Red-A>: CD127
CD127-PE/CF594: 0,1ul
55
43.9
SSC-A
<PE-Texas Red-A>: CD127
C
Singlets
38.8
FSC-H
FSC-A
Lymphocytes
80.3
SSC-A
FSC-A
Live T cells
45.8
<BV650-A>: CD3
<APC-Cy7-A>: Zombie NIR
Representative Gating
D
CD25-BV421: 2,5ul
3.83
55.9
<PE-Cy5.5-A>: CD4
<BV421-A>: CD25
CD25-BV421: 1,25ul
2.2
53.6
<PE-Cy5.5-A>: CD4
<BV421-A>: CD25
CD25-BV421: 0,625ul
2.36
48.6
<PE-Cy5.5-A>: CD4
<BV421-A>: CD25
CD25-BV421: 0,3125ul
3.61
55.9
<PE-Cy5.5-A>: CD4
<BV421-A>: CD25

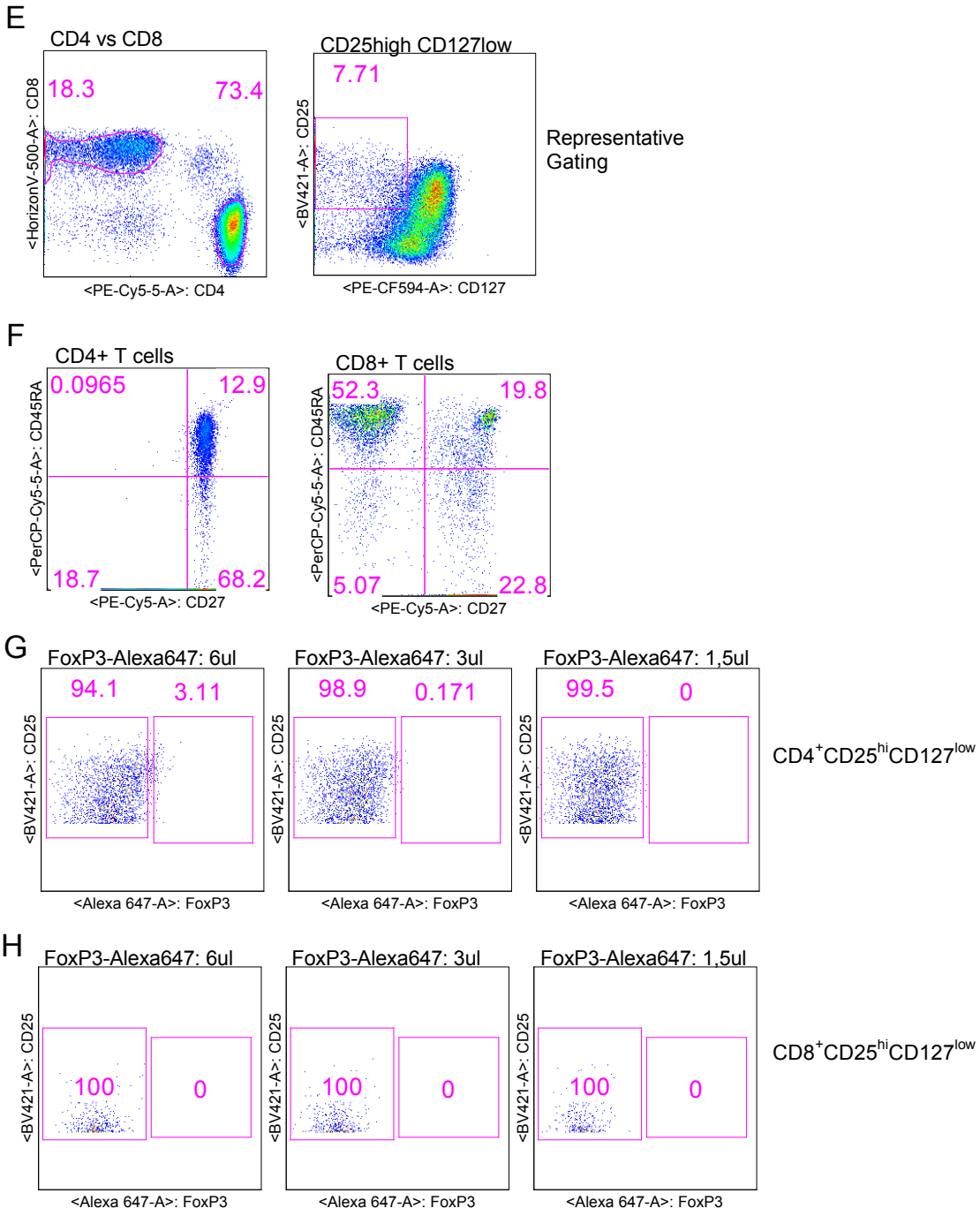
E
CD4 vs CD8
18.3
73.4
<HorizonV-500-A>: CD8
<PE-Cy5-5-A>: CD4
CD25high CD127low
7.71
<BV421-A>: CD25
<PE-CF594-A>: CD127
Representative Gating
F
CD4+ T cells
0.0965
12.9
18.7
68.2
<PerCP-Cy5-5-A>: CD45RA
<PE-Cy5-A>: CD27
CD8+ T cells
52.3
19.8
5.07
22.8
<PerCP-Cy5-5-A>: CD45RA
<PE-Cy5-A>: CD27
G
FoxP3-Alexa647: 6ul
94.1
3.11
FoxP3-Alexa647: 3ul
98.9
0.171
FoxP3-Alexa647: 1,5ul
99.5
0
<BV421-A>: CD25
<Alexa 647-A>: FoxP3
CD4+CD25hiCD127low
H
FoxP3-Alexa647: 6ul
100
0
FoxP3-Alexa647: 3ul
100
0
FoxP3-Alexa647: 1,5ul
100
0
<BV421-A>: CD25
<Alexa 647-A>: FoxP3
CD8+CD25hiCD127low

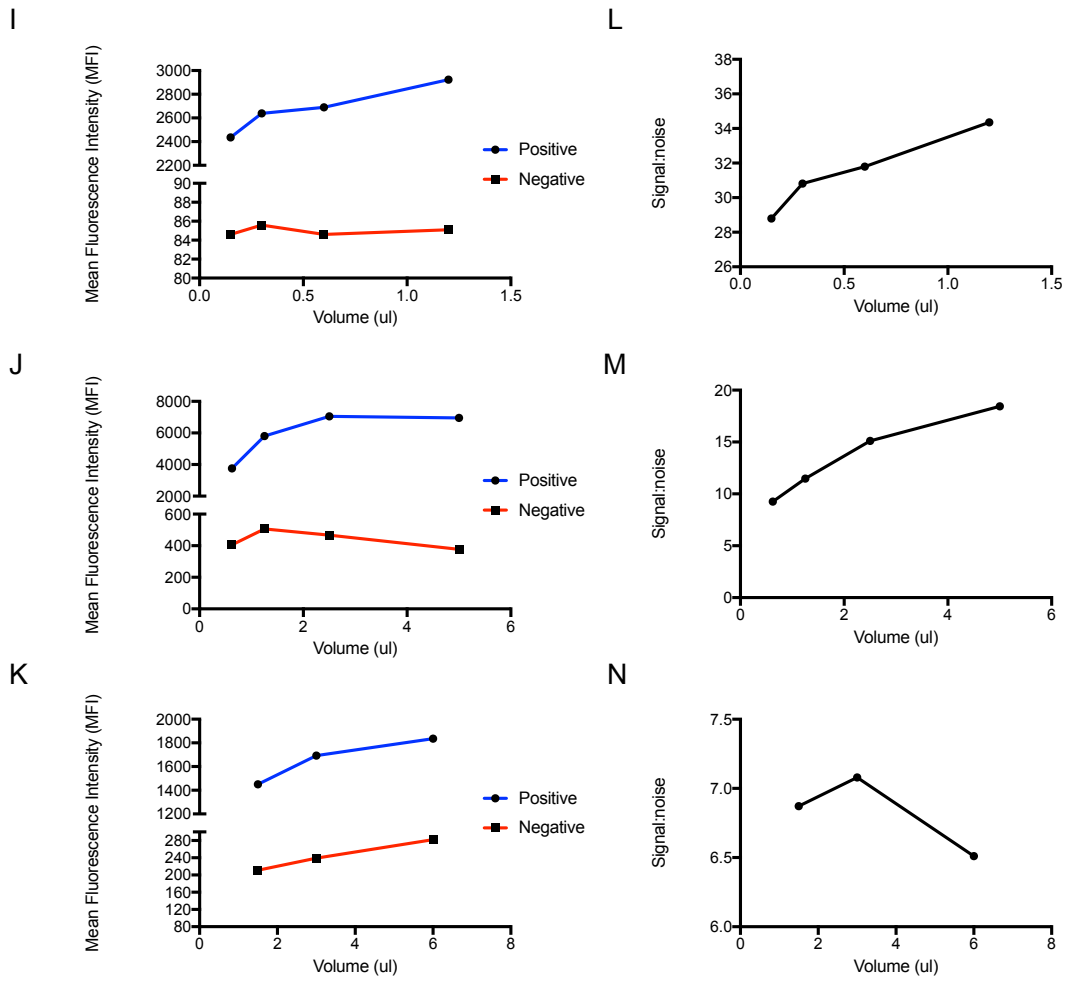

Figure 5.4. Flow Cytometry Density And Dot Plots, MFIs and Signal:Noise for Treg Markers on thawed and PHA-stimulated PBMCs The flow cytometry pseudo-colour density plots are shown for the representative gates used for the CD127-PE/CF594 titrations (A) and the additional gates that were applied for CD25-BV421 (C) and FoxP3-Alexa647 (E). The label above and the pink shapes indicate the population gated upon. The numbers in pink indicate the percentage of the parent population represented within that gate. The titrations of the different volumes of each CD127-PE/CF594 (B) and CD25-BV421 (D) are shown. Representative gating of the memory/naïve markers

on the $CD4^+$ and $CD8^+$ T cells (F). The different volumes of FoxP3-Alexa647 titrations gated on $CD4^+$ (G) and $CD8^+$(H) T cells are also shown. The pink gates or grids indicate the percentage of the parent population within that shape. The MFIs of the CD127-PE/CF594 (I), CD25-BV421 (J), and CD4+ FoxP3 (K) positive (blue) and negative (red) populations for the different volumes used are shown. The Signal:Noise ratio of MFI positive: MFI negative is shown for the different volumes corresponding to the MFI graphs (L-N).

The titrations for CD127-PE/CF594 were performed as described in Chapter 3. The optimal titre was identified as 1,2µl (Figure5 I, L) in a staining volume of 50ul. The titrations for CD25-BV421 and FoxP3-Alexa647 was performed on PHA-stimulated PBMCs. The optimal titre for CD25-BV421 was found to be 1µl (Figure 5 J, M) and FoxP3-Alexa647 (Figure K, N) in a staining volume of 50ul.

Table 5.2. Final titres for use in 50µl staining volume for all antibodies included in Final Flow Cytometry Panel

Antibody	Fluorescence	Optimal Titre (µl)
Zombie-NIR	-	0,0625
Anti-human CD3	BV650	1,25
Anti-human CD4	PECy5.5	0,8
Anti-human CD8	HorizonV500	0,4
Anti-human CD25	BV421	1
Anti-human CD27	PECy5	1,25
Anti-human CD45RA	PerCP-Cy5.5	1
Anti-human CD127	PE-CF594	1,2
Anti-human FoxP3	Alexa647	*

The final panel (Table 5.2) shows the titres for all antibodies used. These were assembled in figure 5.4 and were used to identify live $CD4^+$ and $CD8^+$ T cells, which have a memory or naïve phenotype, as well as being able to identify $CD4^+$ $CD25^{high}$ $CD127^{low}$ cells. The FoxP3-Alexa647 titrations could not be completed.

5.3 Discussion

The intention of this chapter was to optimise a polychromatic flow cytometry panel to phenotype regulatory T cells. The titrations for the dead cell marker, Zombie-NIR (section 5.2.1) the anchor markers, CD3-BV650, CD4-PE/Cy5.5 and CD8-HorizonV500 (section 5.2.2), and the memory/naïve markers, CD27-

PE/Cy5.5 and CD45RA-PerCP (section 5.2.3) were successful in identifying optimal titres of the fluorescent-tagged antibodies for use in a combination cocktail (Figure 5.4F and Table 5.2). The titrations for the regulatory T cell markers were successful for CD127-PE/CF594 but mixed success was achieved for CD25-BV421 and FoxP3-Alexa647 was not successful. An example of good staining of CD25-BV421 vs CD127 in $CD3^+$ $CD4^+$ T cells from cryopreserved PBMCs from an HIV positive patient is shown in Figure 5.5[371]. The same clone of anti-CD25 (M-A251) was used in this stain.

In the representative example shown in Figure 5.5, no stimulations were performed on the PBMCs prior to staining. As opposed to the healthy donors used for the titration of CD25-BV421 (Figure 5.4 C and D), the donor used was HIV-positive. The difference between the CD25 vs CD127 plot in Figure 5.5 and Figure 5.4E is that there is a much clearer-defined, distinct CD25 high and CD127 low population in Figure 5.5 compared to the scattered events with variable levels of both CD25 and CD127 within the gate. The gate was kept very loose in Figure 5.4E to maximise the likelihood of detecting FoxP3 in the gated population.

The CD25-BV421 titrations could have been improved by staining using a different stimulation protocol in which there are more likely to be a higher number of activated cells. The stimulation by PHA should have ensured this but it does not seem that to have increased the CD25-BV421 but the 24 hour stimulation or PHA concentration used may not have been optimal.

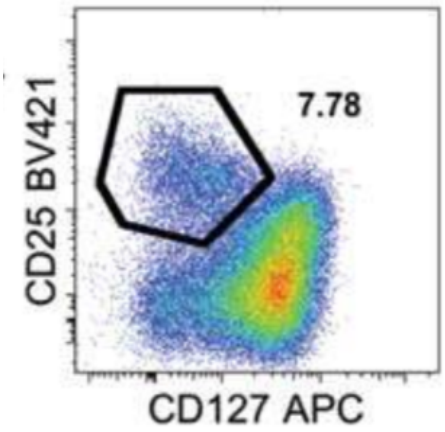

Figure 5.5. Flow Cytometry Pseudo colour Dot Plot of CD25-BV21 (clone: M-A251) vs CD127-APC from OMIP-024.

Cryopreserved PBMCs from an HIV positive patient were thawed and stained for flow cytometry. The flow cytometry plot shown has been gated on singlets, lymphocytes, CD3+ T cells and then CD4+CD8- T cells. Shown in this figure is CD25-BV421 vs CD127-APC plot, gated on CD3+ CD4+ CD8- T cells. The gate for the CD25high CD127low population is indicated in black. The percentage of CD3+ CD4+ CD8- T cells that are CD25hi CD127low is shown by the number in black.

The FoxP3 titrations could also have been improved by using samples in which FoxP3+ Treg cells have been upregulated. Levitsky et al.,[322] optimised a Mixed Lymphocyte Reaction (MLR) protocol, called the 'Human Treg MLR' to generate $CD4^{+}CD25^{high}CD127^{low}FoxP3^{+}$ suppressive Tregs *in vitro.* The 'Human Treg MLR' used PBMCs from 2 HLA-DR mismatched donors, where one donor's PBMCs were irradiated to act as stimulator and the other acted as a responder. Using

this protocol, the titrations of FoxP3 could have been performed on a cell sample enriched for Tregs.

The other advantage of this protocol would have been to use it as a means to measure allospecific Tregs in the HIV positive renal transplant cohort. Donor cells would have been irradiated and recipient cells PBMCs rested in media. The MLR would allow donor-specific Tregs to be phenotyped. Comparing the MLR-stimulated Tregs to thawed, unstimulated Tregs could have given an indication of the proliferative response to donor alloantigen and the suppressive ability of the donor-specific Tregs.

The Treg panel optimised in this chapter could also have been improved by addition of several other markers. The T cells most likely to proliferate after the cessation of ATG induction are the memory T cells that are resistant to ATG-mediated depletion.[372–375]. The memory/naïve markers CD27 and CD45RA are not ideal for differentiating naïve from naïve-like cells, or for differentiating between the different memory populations (Figure 5.3, section 5.4, pg 140). The addition of CD28, CCR7 and CD62L would have allowed for the differentiation of naïve from memory and between phenotypic memory subsets[366,375–377].

It is difficult to identify functional Tregs without any functional markers (section 5.1.2) included in the panel. The addition of the cytokines, IL-10[297] or IL-35[299], could have linked the panel to the results found in Chapter 4. The addition of the suppressive Treg cytokine, TGF-β[325], could also have added value to the panel,

especially considering its omission from Chapter 4. Additionally, other functional markers such as CTLA-4, CD39 or CD73 could have been used to measure Treg function.

The full 8-colour flow cytometry panel could not be optimised, as the titrations of FoxP3-Alexa647 could not identify an optimal volume. As a result of time constraints, the flow cytometry panel was not used on transplant recipient samples. This meant that the flow cytometry objectives for the dissertation of identifying the changes in the peripheral T cell repertoire at one-year post-transplant compared to pre-transplant could not be completed. The optimisation of the flow cytometry panel was however shown in detail and the panel could be successfully used to identify T cells (CD3+) that were CD4+ or CD8+ T cells, had either a naïve-like (CD27+CD45RA+), effector/central memory (CD27+CD45RA), terminally differentiated/effector memory (CD27-CD45RA+) or effector memory (CD27-CD45RA-) phenotype, as well as CD4+CD25highCD127low cells that were potentially also FoxP3+ Tregs. The intent is to complete the panel and utilize it for the identity of Treg cells in the HIV positive transplant cohort.

Chapter 6: Summary and Conclusions

6.1 Summary of Dissertation

This dissertation focuses on the intersection of two fields, transplantation and HIV. A brief history of both fields is outlined in Chapter 1. The history of transplantation was outlined up until the time at which the field was influenced by the emerging HIV epidemic. The history of the HIV epidemic is outlined with a focus on the epidemic in South Africa, the influence of HIV infection and its treatment on the development of chronic kidney diseases, and the need for transplantation in this population. The advances in transplantation between HIV negative donors and HIV positive recipients, and between HIV positive donors and HIV positive recipients, for the treatment of end-stage renal disease were outlined providing the rationale for this dissertation. This dissertation examined the impact of rejection prevention therapies and renal transplantation, in the first 12 weeks after HIV positive patients received an allograft from an HIV positive deceased donor on, peripheral immune responses that maintain the balance between rejection and tolerance. The work focused on a subset 10 recipients with follow-up samples.

The known history of transplantation started in the 16th century where crude skin transplants were performed with a complete lack of knowledge regarding in the influence the cellular and humoral immunity on the balance between inflammation and tolerance, and the role that they both play in transplant

outcomes. Chapter 1 details the discoveries and advances in surgical and sterile techniques in the 20th century that were used to improve experimental transplantation in animals, and later in humans. Cellular rejection was difficult to control because the initial immune response to an allograft was shown to be predominantly T-cell mediated, large, polyclonal, local, systemic and redundant. Antilymphocyte serum (ALS) were been shown to be an effective means of controlling the cellular immune response to allografts, especially in HLA-mismatched transplants. Polyclonal derivatives of ALS directed at thymocytes, known as antithymocyte globulin (ATG), were then used for effective lymphocyte depletion, enhancing the prevention and treatment of rejection and GVHD. ATG has since been used as induction therapy in the majority of solid organ transplants.

ATG was shown to effectively deplete T cells in experimental and animal models, but memory T cells were shown to be depletion resistant. Regulatory T cells (Tregs) were also shown to be either resistant to ATG depletion, undergo rapid homeostatic proliferation after the cessation of the ATG therapy, and/or cause the conversion of effector T cells to Treg-like cells. As a result, after T-cell depletion the proportion of T cells that were Tregs, was found to increase. Tregs were shown to play an integral role in transplant tolerance and an increase in Tregs relative to allospecific effector T cells could shift the balance between inflammation and regulation so that effective tolerance could be achieved. As discussed in Chapter 1 and formed the basis of investigating a panel of cytokines and analytes related to immune regulation and Treg cells.

The most common chronic kidney disease in the HIV positive population was shown to be HIV-associated nephropathy (HIVAN). HIVAN was of particular importance in South Africa because of the increased likelihood of its development in people of African descent. The high prevalence of HIV increased the risk of developing HIVAN, and lack of dialysis treatment for chronic kidney conditions due to resource limitations, indicated a need for kidney transplantation in the HIV positive population in South Africa. Prior to 2003 transplantations were not performed in patients with HIV experiencing organ failure. A clinical study performed between 2003 and 2009 in the USA showed that transplantation of kidneys from HIV negative donors was safe and effective.

Following on from the success with HIV negative donors, the first HIV positive to HIV positive kidney transplants were performed in 2008 at Groote Schuur Hospital in South Africa. These were shown to be safe and effective and provided the rationale for the initiation of a clinical study investigating transplantation between HIV positive donors and HIV positive recipients. Between 2008 and 2017 there were 43 HIV positive to HIV positive transplants performed as part of the clinical study. The details of the study are included in Chapter 2 of this dissertation. This chapter includes the aims for the clinical study, the inclusion and exclusion criteria for patients, summary statistics of the transplant recipients and their outcomes. Ten patients were selected from the cohort for further investigations into the changes in the peripheral immune system related

to the balance between rejection and tolerance. Their demographic and clinical characteristics were also included in this chapter.

These recipients all received ATG induction therapy for the first 5 days due to the increased risk of rejection identified in HIV positive renal recipients and were placed on maintenance immunosuppression post-transplant. As mentioned above, this dissertation focussed on the effect of ATG induction, immunosuppression and kidney transplantation in HIV positive recipients on peripheral inflammatory and regulatory immune changes over time that control the balance between rejection and tolerance.

The methods by which these changes were identified were outlined in Chapter 3. The methods included were: the standard procedures for processing and storing recipient samples; the Luminex assay procedure that measured concentrations of peripheral inflammatory, regulatory, or dual inflammatory/regulatory cytokines in the selected recipients at 5 different visits during the first 12 weeks post-transplant; procedures used to optimise the polychromatic flow cytometry panel that was intended to be used to phenotype regulatory T cells; and the statistical methods used in the Luminex assay analysis to control for variability introduced at various levels, to test significant differences in cytokine changes over time, to identify associations of cytokine changes with demographic and clinical criteria, and to identify cytokines that differed in concentration between recipients .

The results from the Luminex assay that investigated changes in peripheral inflammatory and regulatory cytokines was shown in Chapter 4. This guided the construction of the 8-colour polychromatic flow cytometry panel that was optimised in Chapter 5 to differentiate between naïve, activated or memory, CD4+ or CD8+, or regulatory T cells subsets.

Chapter 4 showed the there was variability between replicates and plates in the Luminex assay. It was shown that there was a need for this to be assessed and controlled prior to data analysis to avoid reporting false or erroneous results and it was suggested that this should be standard practice for all multiplex immunoassays.

Significant differences over time were shown for cytokines involved in inflammatory and regulatory processes using two different methods. Decreases were identified in the levels of several inflammatory cytokines (IL-2, IFN-γ, IFN-α2, IL-28A, IL-20 and IL-11) and one regulatory cytokine (IL-35) compared to baseline. A transient increase from baseline in one regulatory (IL-10) was identified in five recipients. There were no associations of cytokine changes with the demographic and clinic criteria used.

The differences between recipients in cytokines that were not shown to change over time indicated that patient-specific factors influenced the differences measured in those cytokines. The regulatory cytokine, IL-35, was the only cytokine shown not to differ between recipients that also decreased over time.

This indicated that the decrease in IL-35 over time was due to factors common to all the recipients, likely the effect of ATG induction and immunosuppression after transplantation on effector and regulatory T cell populations. Combined with the change in IL-10, these results suggested a change in the numbers or function of regulatory T cells in response to the ATG induction and immunosuppression in these recipients that needed to be further investigated.

The optimisations for the polychromatic flow cytometry panel and different T cells populations that could be identified using this panel, was shown in Chapter 5. Due to time constraints, the panel was not used on patient samples. Several methods for improving the optmisations and suggestions for the use of the panel to identify functional allo-specific Tregs were provided. The panel will still be used to identify Tregs in the HIV postive renal transplant cohort.

6.2 Conclusions

The decreased rejection events in HIV positive transplant recipients observed in other cohorts and the relatively low numbers of acute rejection events in this cohort can likely be attributed to the positive impact of ATG on regulatory T cells. Regulatory T cells play a vital role in promoting tolerance at the site of the allograft . An increase in peripheral Treg numbers or in their suppressive function due to ATG could shift in the balance between tolerance and rejection in the HIV postive renal recipients. The shift could favour tolerance over rejection

by the creation of an immunosuppressive, regulatory environment in the periphery of these recipients.

References

1. Tagliacozzi, G. *Decurtorum cirugia per insitionum. Bindonum, Venice, Italy.* (1597).
2. Martin, C. E. John Hunter and tissue transplantation. *Surg. Gynecol. Obstet.* **131,** 306—310 (1970).
3. Reverdin, J. Greffe épidermique. *Bull Soc Chir Paris* **10,** 511–515 (1869).
4. Pollock, G. D. Cases of skin grafting and skin transplantation. *Trans Clin Soc L.* **4,** 37 (1871).
5. Malinin, T. I. *Surgery and life: the extraordinary career of Alexis Carrel*. (Houghton Mifflin Harcourt P, 1979).
6. Jaboulay, M. & Briau, E. Recherches expérimentales sur la suture et la greffe artérielles. *Lyon méd* **81,** 97–99 (1896).
7. Dörfler, J. Über die Naht von Arterienwunden. *Chirurgie* **22,** 1113 (1895).
8. Ullman, E. Tissue and organ transplantation. *Ann. Surg.* **60,** 195 (1914).
9. Jaboulay, M. Kidney grafts in the antecubital fossa by arterial and venous anastomosis. *Lyon Med* **107,** 575–592 (1906).
10. Unger, E. Nierentransplantationen. *Klin Wochenschr* **47,** 573–582 (1910).
11. Schöne, G. *Die heteroplastische und homöoplastische Transplantation*. (Springer, 1912).
12. Holman, E. Protein sensitization in isoskingrafting. Is the latter of practical value? *Surg Gynecol Obs.* **38,** 100–106 (1924).
13. Metchnikoff, E. Etudes sur la resorption des cellules. *Ann Inst Pasteur* **13,** 737–769 (1899).

14. Murphy, J. B. Factors of resistance to heteroplastic tissue-grafting. *J. Exp. Med.* **19,** 513–522 (1914).

15. Silverstein, A. M. The lymphocyte in immunology: from James B. Murphy to James L. Gowans. *Nat. Immunol.* **2,** 569–71 (2001).

16. Murphy, J. B. Heteroplastic tissue grafting effected through roentgen-ray lymphoid destruction. *J. Am. Med. Assoc.* **LXII,** 1459 (1914).

17. Flexner, S. *Report on Cancer. Report of the Director of Laboratories to the Scientific Directors. RURG 439. Rockefeller Archives. Rockefeller Archives Center, Sleepy Hollow, NY. Gibson*. (1914).

18. Hamilton, D. *A History of Organ Transplantation: Ancient Legends to Modern Practice*. (University of Pittsburgh Press, 2012).

19. Medawar, P. B. The behaviour and fate of skin autografts and skin homografts in rabbits (A report to the War Wounds Committee of the Medical Research Council). *J. Anat.* **78,** 176–99 (1944).

20. Loeb, L. *The biological basis of individuality*. (CC Thomas, 1945).

21. Voronoy, U. Blocking the reticuloendothelial system in man in some forms of mercuric chloride intoxication and the transplantation of the cadaver kidney as a method of treatment for the anuria resulting from the intoxication [In Spanish]. *Siglo Med* **97,** 296 (1937).

22. Lawler, R. H., West, J. W., McNulty, P. H., Clancy, E. J. & Murphy, R. P. Homotransplantation of the kidney in the human. *J. Am. Med. Assoc.* **144,** 844–845 (1950).

23. Billingham, R. E., Brent, L. & Medawar, P. B. 'Actively acquired tolerance'of foreign cells. *Nature* **172,** 603–606 (1953).

24. Owen, R. D. Immunogenetic consequences of vascular anastomoses between bovine twins. *Science (80-.).* **102,** 400–401 (1945).

25. Billingham, R. E., Krohn, P. L. & Medawar, P. B. Effect of cortisone on survival of skin homografts in rabbits. *Br. Med. J.* **1,** 1157 (1951).

26. Dempster, W. J. Kidney homotransplantation. *Br. J. Surg.* **40,** 447–465 (1953).

27. Dempster, W. J. The effects of cortisone on the homotransplanted kidney. *Arch. Int. Pharmacodyn. Ther.* **95,** 253–282 (1953).

28. Küss, R. & Bourge, P. *An illustrated history of organ transplantation: the great adventure of the century*. *Rueil-Malmaison, France: Laboratoires Sandoz* (1992).

29. Kuss, R., Teinturier, J. & Milliez, P. Quelques essais de greffe de rein chez l'homme. *Mem Acad Chir* **77,** 755 (1951).

30. Hume, D. M., Merrill, J. P., Miller, B. F. & Thorn, G. W. Experiences with renal homotransplantation in the human: report of nine cases. *J. Clin. Invest.* **34,** 327 (1955).

31. Murray, J. E., Merrill, J. P., Harrison, J. H. & Carpenter, C. B. Renal homotransplantation in identical twins. *J Am Soc Nephrol* **12,** 201–204 (2001).

32. Merrill, J. P., Murray, J. E., Harrison, J. H. & Guild, W. R. Successful homotransplantation of the human kidney between identical twins. *J. Am. Med. Assoc.* **160,** 277–282 (1956).

33. Main, J. M. & Prehn, R. T. Successful skin homografts after the administration of high dosage X radiation and homologous bone marrow. *J.*

Natl. Cancer Inst. **15,** 1023–1029 (1955).

34. Mannick, J. A., Lochte, H. L., Ashley, C. A., Thomas, E. D. & Ferrebee, J. W. A functioning kidney homotransplant in the dog. *Surgery* **46,** 821–828 (1959).

35. Merrill, J. P. *et al.* Successful homotransplantation of the kidney between nonidentical twins. *N. Engl. J. Med.* **262,** 1251–1260 (1960).

36. Murray, J. E. *et al.* Kidney transplantation in modified recipients. *Ann. Surg.* **156,** 337 (1962).

37. Hamburger, J. *et al.* Transplantation of a kidney between nonmonozygotic twins after irradiation of the receiver. Good function at the fourth month. *Press. méd* **67,** 1771–1775 (1959).

38. Kuss, R., Legrain, M., Mathe, G., Nedey, R. & Camey, M. Homologous human kidney transplantation: experience with six patients. *Postgrad. Med. J.* **38,** 528 (1962).

39. Simonsen, M. The impact on the developing embryo and newborn animal of adult homologous cells. *Acta Pathol. Microbiol. Scand.* **40,** 480 (1957).

40. Simonsen, M. Graft-versus-Host-Reactions: The History that never Was, and the Way Things Happened to Happen. *Immunol. Rev.* **88,** 5–24 (1985).

41. Gowans, J. L. The effect of the continuous re-infusion of lymph and lymphocytes on the output of lymphocytes from the thoracic duct of unanaesthetized rats. *Br. J. Exp. Pathol.* **38,** 67 (1957).

42. Dausset, J. Iso-leuco-anticorps. *Acta Haematol.* **20,** 156–166 (1958).

43. Groth, C. G. *et al.* Historic landmarks in clinical transplantation: Conclusions from the consensus conference at the University of California,

Los Angeles. *World J. Surg.* **24,** 834–843 (2000).

44. Payne, R. Leukocyte agglutinins in human sera: correlation between blood transfusions and their development. *AMA Arch. Intern. Med.* **99,** 587–606 (1957).

45. Van Rood, J. J., Leeuwen, A. van & Eernisse, J. G. Leucocyte antibodies in sera of pregnant women. *Vox Sang.* **4,** 427–444 (1959).

46. Schwartz, R. & Dameshek, W. Drug-induced immunological tolerance. *Nature* **183,** 1682–1683 (1959).

47. Schwartz, R., Dameshek, W. & Donovan, J. The effects of 6-mercaptopurine on homograft reactions. *J. Clin. Invest.* **39,** 952 (1960).

48. Zukoski, C. F., Lee, H. M. & Hume, D. M. The prolongation of functional survival of canine renal homografts by 6-mercaptopurine. in *Surgical forum* **11,** 470 (1960).

49. Calne, R. Y. The rejection of renal homografts. *Lancet* **275,** 417–418 (1960).

50. Goodwin, W. E. & Martin, D. C. Transplantation of the Kidney. *Urol. Surv.* **13,** 229–248 (1963).

51. Starzl, T. E. History of clinical transplantation. *World J. Surg.* **24,** 759–782 (2000).

52. Murray, J. E., Merrill, J. P., Harrison, J. H., Wilson, R. E. & Dammin, G. J. Prolonged survival of human-kidney homografts by immunosuppressive drug therapy. *N. Engl. J. Med.* **268,** 1315–1323 (1963).

53. Starzl, T. E., Marchioro, T. L. & Waddell, W. R. The reversal of rejection in human renal homografts with subsequent development of homograft

tolerance. *Surg. Gynecol. Obstet.* **117,** 385 (1963).

54. Starzl, T. E. The development of clinical renal transplantation. *Am. J. kidney Dis.* **16,** 548–556 (1990).

55. Lindbergh, C. A. *Autobiography of values*. (Harcourt, 1978).

56. Marchioro, T. L., Huntley, R. T., Waddell, W. R. & Starzl, T. E. Extracorporeal perfusion for obtaining postmortem homografts. *Surgery* **54,** 900 (1963).

57. Collins, G. M., Bravo-Shugarman, M. & Terasaki, P. I. Kidney preservation for transportation: initial perfusion and 30 hours' ice storage. *Lancet* **294,** 1219–1222 (1969).

58. Brent, L. *A history of transplantation immunology*. (Academic Press, 1996).

59. Terasaki, P. I. *History of transplantation : thirty-five recollections*. (UCLA Tissue Typing Laboratory, 1991).

60. Beecher, H. K. Report of the ad hoc committee of the Harvard Medical School to examine the definition of brain death: The definition of irreversible coma. *Transplantation* **7,** 204 (1969).

61. McDonald, J. C. The national organ procurement and transplantation network. *JAMA* **259,** 725–726 (1988).

62. Terasaki, P. I. & McClelland, J. D. Microdroplet assay of human serum cytotoxins. *Nature* **204,** 998–1000 (1964).

63. Williams, R. C., Opelz, G., McGarvey, C. J., Weil, E. J. & Chakkera, H. A. The risk of transplant failure with HLA mismatch in first adult kidney allografts from deceased donors. *Transplantation* **100,** 1094–1102 (2016).

64. Coupel, S. *et al.* Ten-year survival of second kidney transplants: impact of immunologic factors and renal function at 12 months. *Kidney Int.* **64,** 674–

680 (2003).

65. Althaf, M. M., El Kossi, M., Jin, J. K., Sharma, A. & Halawa, A. M. Human leukocyte antigen typing and crossmatch: A comprehensive review. *World J. Transplant.* **7,** 339 (2017).

66. Rosenblum, J. M. & Kirk, A. D. Recollective homeostasis and the immune consequences of peritransplant depletional induction therapy. *Immunol. Rev.* **258,** 167–182 (2014).

67. Woodruff, M. F. A. & Anderson, N. A. Effect of lymphocyte depletion by thoracic duct fistula and administration of antilymphocytic serum on the survival of skin homografts in rats. *Nature* **200,** 702 (1963).

68. Starzl, T. E., Marchioro, T. L., Porter, K. A., Iwasaki, Y. & Cerilli, G. J. The use of heterologous antilymphoid agents in canine renal and liver homotransplantation and in human renal homotransplantation. *Surg. Gynecol. Obstet.* **124,** 301 (1967).

69. Starzl, T. E. *et al.* Orthotopic homotransplantation of the human liver. *Ann. Surg.* **168,** 392 (1968).

70. Cosimi, A. B. *et al.* Use of monoclonal antibodies to T-cell subsets for immunologic monitoring and treatment in recipients of renal allografts. *N. Engl. J. Med.* **305,** 308–314 (1981).

71. Ramsay, N. K. C. *et al.* A randomized study of the prevention of acute graft-versus-host disease. *N. Engl. J. Med.* **306,** 392–397 (1982).

72. Cosimi, A. B. *et al.* Treatment of acute renal allograft rejection with OKT3 monoclonal antibody. *Transplantation* **32,** 535–540 (1981).

73. Harmon, W. E., MacDonald, R. A. & Reyes, J. D. SRTR report on the state of

transplantation. *Pediatr. Transplant.* 887–903 (2003).

74. Department of Health and Human Services. OPTN/SRTR 2010 Annual Data Report. *Am. J. Transplant.* **12,** 1–156 (2012).

75. Popow, I. *et al.* A comprehensive and quantitative analysis of the major specificities in rabbit antithymocyte globulin preparations. *Am. J. Transplant.* **13,** 3103–3113 (2013).

76. Préville, X. *et al.* Mechanisms Involved in Antithymocyte Globulin Immunosuppressive Activity In A Nonhuman Primate Model 1. *Transplantation* **71,** 460–468 (2001).

77. Bonnefoy-Bérard, N., Vincent, C. & Revillard, J. Antibodies against functional leukocyte surface molecules in polyclonal antilymphocyte and antithymocyte globulins. *Transplantation* **51,** 669–673 (1991).

78. Barnard, C. N. Human cardiac transplant: an interim report of a successful operation performed at Groote Schuur Hospital, Cape Town. *South African Med. J.* **41,** 1271–1274 (1967).

79. Barnard, C. N. Human cardiac transplantation: an evaluation of the first two operations performed at the Groote Schuur Hospital, Cape Town. *Am. J. Cardiol.* **22,** 584–596 (1968).

80. Borel, J., Feurer, C., Gubler, H. U. & Stähelin, H. Biological effects of cyclosporin A: a new antilymphocytic agent. *Agents Actions* **6,** 468–474 (1976).

81. Calne, R. Y. *et al.* Cyclosporin A initially as the only immunosuppressant in 34 recipients of cadaveric organs: 32 kidneys, 2 pancreases, and 2 livers. *Lancet* **314,** 1033–1036 (1979).

82. Starzl, T. E. *et al.* The use of cyclosporin A and prednisone in cadaver kidney transplantation. *Surg. Gynecol. Obstet.* **151,** 17 (1980).

83. Starzl, T. E., Klintmalm, G. B. G., Porter, K. A., Iwatsuki, S. & Schröter, G. P. J. Liver transplantation with use of cyclosporin A and prednisone. *N. Engl. J. Med.* **305,** 266 (1981).

84. Griffith, B. P., Hardesty, R. L., Deeb, G. M., Starzl, T. E. & Bahnson, H. T. Cardiac transplantation with cyclosporin A and prednisone. *Ann. Surg.* **196,** 324 (1982).

85. Cooper, J. D. The evolution of techniques and indications for lung transplantation. *Ann. Surg.* **212,** 249 (1990).

86. Reitz, B. A. *et al.* Heart-lung transplantation: successful therapy for patients with pulmonary vascular disease. *N. Engl. J. Med.* **306,** 557–564 (1982).

87. Starzl, T. *et al.* FK 506 for human liver, kidney and pancreas transplantation. *Lancet* **2,** 1000–1004 (1989).

88. Starzl, T. E. *et al.* Chimerism and donor-specific nonreactivity 27 to 29 years after kidney allotransplantation. *Transplantation* **55,** 1272 (1993).

89. Starzl, T. E. *et al.* The lost chord: microchimerism and allograft survival. *Immunol. Today* **17,** 577–584 (1996).

90. Wood, K. & Sachs, D. H. Chimerism and transplantation tolerance: cause and effect. *Immunol. Today* **17,** 584–587 (1996).

91. Friedman-Kien, A. E. *et al.* Kaposis sarcoma and Pneumocystis pneumonia among homosexual men--New York City and California. *MMWR. Morb. Mortal. Wkly. Rep.* **30,** 305–308 (1981).

92. Masur, H. *et al.* An outbreak of community-acquired Pneumocystis carinii pneumonia: initial manifestation of cellular immune dysfunction. *N. Engl. J. Med.* **305,** 1431–1438 (1981).

93. Gottlieb, M. S. *et al.* Pneumocystis pneumonia--Los Angeles. *MMWR. Morb. Mortal. Wkly. Rep.* **30,** 250–252 (1981).

94. Gottlieb, M. S. *et al.* Pneumocystis carinii pneumonia and mucosal candidiasis in previously healthy homosexual men: evidence of a new acquired cellular immunodeficiency. *N. Engl. J. Med.* **305,** 1425–1431 (1981).

95. Durack, D. T. Opportunistic infections and Kaposi's sarcoma in homosexual men. (1981).

96. Brennan, R. & Durack, D. Gay compromise syndrome. *Lancet* **318,** 1338–1339 (1981).

97. Altman, L. K. New Homosexual Disorder Worries Health Officials. *New York Times [Internet]* 20–23 (1982).

98. Siegal, F. P. *et al.* Severe acquired immunodeficiency in male homosexuals, manifested by chronic perianal ulcerative herpes simplex lesions. *N. Engl. J. Med.* **305,** 1439–1444 (1981).

99. Phillips, S. C., Mildvan, D., William, D. C., Gelb, A. M. & White, M. C. Sexual transmission of enteric protozoa and helminths in a venereal-disease-clinic population. *N. Engl. J. Med.* **305,** 603–606 (1981).

100. Marmor, M. *et al.* Risk factors for Kaposi's sarcoma in homosexual men. *Lancet* **319,** 1083–1087 (1982).

101. Centers for Disease Control. Current trends update on acquired immune

deficiency syndrome (AIDS). *Morb. Mortal. Wkly. Rev.* **24,** (1982).

102. Quagliarello, V. The Acquired Immunodeficiency Syndrome: current status. *Yale J. Biol. Med.* **55,** 443 (1982).
103. Masur, H. *et al.* Opportunistic infection in previously healthy women: initial manifestations of a community-acquired cellular immunodeficiency. *Ann. Intern. Med.* **97,** 533–539 (1982).
104. Centers for Disease Control. Opportunistic infections and Kaposi's sarcoma among Haitians in the United States. *MMWR. Morb. Mortal. Wkly. Rep.* **31,** 353 (1982).
105. Ehrenkranz, N. J. *et al.* Pneumocystis carinii pneumonia among persons with hemophilia A. *MMWR. Morb. Mortal. Wkly. Rep.* **31,** 365–367 (1982).
106. Gerstoft, J. *et al.* Severe acquired immunodeficiency in European homosexual men. *Br Med J (Clin Res Ed)* **285,** 17–19 (1982).
107. Rozenbaum, W. *et al.* Multiple opportunistic infection in a male homosexual in France. *Lancet* **319,** 572–573 (1982).
108. Lwegaba, A. Preliminary report of an 'unusual wasting disease'complex nicknamed 'Slim'–a slow epidemic in Rakai District, Uganda. *Unpubl. typescript, Gov. Uganda* (1984).
109. Piot, P. *et al.* Acquired immunodeficiency syndrome in a heterosexual population in Zaire. *Lancet* **324,** 65–69 (1984).
110. Van de Perre, P. *et al.* Acquired immunodeficiency syndrome in Rwanda. *Lancet* **324,** 62–65 (1984).
111. Anderson, R. *et al.* Immunological abnormalities in South African homosexual men. *South african Med. J.* **64,** 119–122 (1983).

112. Levy, J. A. *et al.* Isolation of lymphocytopathic retroviruses from San Francisco patients with AIDS. *Science (80-.).* **225,** 840–843 (1984).

113. Popovic, M., Sarngadharan, M. G., Read, E. & Gallo, R. C. Detection, isolation, and continuous production of cytopathic retroviruses (HTLV-III) from patients with AIDS and pre-AIDS. *Science (80-.).* **224,** 497–500 (1984).

114. Barre, F. S. *et al.* Isolation of a T-lymphotropic retrovirus from a patient at risk for acquired immune deficiency syndrome (AIDS). *Science (80-.).* **220,** 868–871 (1983).

115. Poiesz, B. J., Ruscetti, F. W., Reitz, M. S., Kalyanaraman, V. S. & Gallo, R. C. Isolation of a new type C retrovirus (HTLV) in primary uncultured cells of a patient with Sezary T-cell leukaemia. *Nature* **294,** 268–271 (1981).

116. Kalyanaraman, V. S. *et al.* A new subtype of human T-cell leukemia virus (HTLV-II) associated with a T-cell variant of hairy cell leukemia. *Science (80-.).* **218,** 571–573 (1982).

117. Poiesz, B. J. *et al.* Detection and isolation of type C retrovirus particles from fresh and cultured lymphocytes of a patient with cutaneous T-cell lymphoma. *Proc. Natl. Acad. Sci.* **77,** 7415–7419 (1980).

118. Gallo, R. C. The early years of HIV/AIDS. *Science (80-.).* **298,** 1728–1730 (2002).

119. Kulstad, R. AIDS: papers from Science, 1982-1985. (1986).

120. Bakal, C. 1982 Award Winner-Harold E. Varmus. (1982).

121. Coffin, J. *et al.* Human immunodeficiency viruses. *Science (80-.).* **232,** 697 (1986).

122. (CDC), C. for D. C. Coolfont report: a PHS plan for prevention and control of

AIDS and the AIDS virus. *Public Health Rep.* **101,** 341–348 (1986).

123. Rogers, E. M., Dearing, J. W. & Chang, S. AIDS in the 1980s: The agenda-setting process for a public issue. *Journal. Commun. Monogr.* **126,** (1991).

124. Yarchoan, R. *et al.* Administration of 3'-azido-3'-deoxythymidine, an inhibitor of HTLV-III/LAV replication, to patients with AIDS or AIDS-related complex. *Lancet* **327,** 575–580 (1986).

125. Molotsky, I. US Approves Drug to Prolong Lives of AIDS Patients. *New York Times* **1,** 32 (1987).

126. Fischl, M. A. *et al.* The efficacy of azidothymidine (AZT) in the treatment of patients with AIDS and AIDS-related complex. *N. Engl. J. Med.* **317,** 185–191 (1987).

127. Richman, D. D. *et al.* The toxicity of azidothymidine (AZT) in the treatment of patients with AIDS and AIDS-related complex. *N. Engl. J. Med.* **317,** 192–197 (1987).

128. Larder, B. A., Darby, G. & Richman, D. D. HIV with reduced sensitivity to zidovudine (AZT) isolated during prolonged therapy. *Science (80-.).* **243,** 1731–1735 (1989).

129. Niu, M. T. *et al.* Zidovudine treatment in patients with primary (acute) human immunodeficiency virus type 1 infection: a randomized, double-blind, placebo-controlled trial. *J. Infect. Dis.* **178,** 80–91 (1998).

130. Jablonowski, H. Studies of zidovudine in combination with didanosine and zalcitabine. *J. Acquir. immune Defic. Syndr. Hum. retrovirology Off. Publ. Int. Retrovirology Assoc.* **10,** S52-6 (1994).

131. Palella Jr., F. J. *et al.* Mortality in the highly active antiretroviral therapy

era: changing causes of death and disease in the HIV outpatient study. *J Acquir Immune Defic Syndr* **43,** 27–34 (2006).

132. Cooley, T. P. *et al.* Once-daily administration of 2′, 3′-dideoxyinosine (ddI) in patients with the acquired immunodeficiency syndrome or AIDS-related complex: results of a phase I trial. *N. Engl. J. Med.* **322,** 1340–1345 (1990).

133. Lambert, J. S. *et al.* 2′, 3′-Dideoxyinosine (ddI) in patients with the acquired immunodeficiency syndrome or AIDS-related complex: a phase I trial. *N. Engl. J. Med.* **322,** 1333–1340 (1990).

134. Skowron, G. *et al.* Alternating and intermittent regimens of zidovudine and dideoxycytidine in patients with AIDS or AIDS-related complex. *Ann. Intern. Med.* **118,** 321–330 (1993).

135. Darbyshire, J. H. & Committee, D. C. Delta: a randomised double-blind controlled trial comparing combinations of zidovudine plus didanosine or zalcitabine with zidovudine alone in HIV-infected individuals. *Lancet* **348,** 283–291 (1996).

136. Rathbun, R. C., Liedtke, M. D. & Lockhart, S. M. Antiretroviral Therapy for HIV Infection. *Medscape* (2017).

137. Hammer, S. M. *et al.* A controlled trial of two nucleoside analogues plus indinavir in persons with human immunodeficiency virus infection and CD4 cell counts of 200 per cubic millimeter or less. *N. Engl. J. Med.* **337,** 725–733 (1997).

138. Gulick, R. M. *et al.* Treatment with indinavir, zidovudine, and lamivudine in adults with human immunodeficiency virus infection and prior antiretroviral therapy. *N. Engl. J. Med.* **337,** 734–739 (1997).

139. Gulick, R. M. *et al.* Simultaneous vs sequential initiation of therapy with indinavir, zidovudine, and lamivudine for HIV-1 infection: 100-week follow-up. *Jama* **280,** 35–41 (1998).

140. (CDC), C. for D. C. Provisional Public Health Service inter-agency recommendations for screening donated blood and plasma for antibody to the virus causing acquired immunodeficiency syndrome. *MMWR. Morb. Mortal. Wkly. Rep.* **34,** 1 (1985).

141. Ward, J. W. *et al.* Transmission of human immunodeficiency virus (HIV) by blood transfusions screened as negative for HIV antibody. *N. Engl. J. Med.* **318,** 473–478 (1988).

142. Law, P. *Health Omnibus Programs Extension of 1988*. **100–607,** 3048–3173 (1988).

143. Spital, A. Should all human immunodeficiency virus-infected patients with end-stage renal disease be excluded from transplantation?: the views of US transplant centers. *Transplantation* **65,** 1187–1191 (1998).

144. Boyd, A. S. Organ transplantation in HIV-positive patients. *N Engl J Med* **323,** 1492 (1990).

145. Rubin, R. H. & Tolkoff-Rubin, N. E. The problem of human immunodeficiency virus (HIV) infection and transplantation. *Transpl. Int.* **1,** 36–42 (1988).

146. Rubin, R. H. *et al.* The acquired immunodeficiency syndrome and transplantation. *Transplantation* **44,** 1–4 (1987).

147. Alexaki, A., Liu, Y. & Wigdahl, B. Cellular reservoirs of HIV-1 and their role in viral persistence. *Curr. HIV Res.* **6,** 388–400 (2008).

148. Price, R. W. *et al.* The brain in AIDS: central nervous system HIV-1 infection and AIDS dementia complex. *Science (80-.).* **239,** 586–592 (1988).

149. Glassock, R. J., Cohen, A. H., Danovitch, G. & Parsa, K. P. Human immunodeficiency virus (HIV) infection and the kidney. *Ann. Intern. Med.* **112,** 35–49 (1990).

150. Cao, Y. *et al.* Identification and quantitation of HIV-1 in the liver of patients with AIDS. *Aids* **6,** 65–70 (1992).

151. Turner, B. J., Kelly, J. V & Ball, J. K. A severity classification system for AIDS hospitalizations. *Med. Care* 423–437 (1989).

152. Sreepada Rao, T. K. *et al.* Associated focal and segmental glomerulosclerosis in the acquired imunodefiency syndrome. *N. Engl. J. Med.* **310,** 669–673 (1984).

153. Rosenberg, A. Z., Naicker, S., Winkler, C. A. & Kopp, J. B. HIV-associated nephropathies: epidemiology, pathology, mechanisms and treatment. *Nat. Rev. Nephrol.* **11,** 150–160 (2015).

154. Bigé, N. *et al.* Presentation of HIV-associated nephropathy and outcome in HAART-treated patients. *Nephrol. Dial. Transplant.* **27,** 1114–1121 (2011).

155. Campos, P., Ortiz, A. & Soto, K. HIV and kidney diseases: 35 years of history and consequences. *Clin. Kidney J.* sfw104 (2016).

156. Mallipattu, S. K., Wyatt, C. M. & He, J. C. The new epidemiology of HIV-related kidney disease. *J. AIDS Clin. Res.* 1 (2012).

157. Palella Jr, F. J. *et al.* Declining morbidity and mortality among patients with advanced human immunodeficiency virus infection. *N. Engl. J. Med.* **338,** 853–860 (1998).

158. Detels, R. *et al.* Effectiveness of potent antiretroviral therapies on the incidence of opportunistic infections before and after AIDS diagnosis. *Aids* **15,** 347–355 (2001).

159. Palella Jr, F. J., Chmiel, J. S., Moorman, A. C., Holmberg, S. D. & Investigators, H. I. V. O. S. Durability and predictors of success of highly active antiretroviral therapy for ambulatory HIV-infected patients. *Aids* **16,** 1617–1626 (2002).

160. Moore, R. D. & Chaisson, R. E. Natural history of HIV infection in the_era of combination antiretroviral therapy. *Aids* **13,** 1933–1942 (1999).

161. Vittinghoff, E. *et al.* Combination antiretroviral therapy and recent declines in AIDS incidence and mortality. *J. Infect. Dis.* **179,** 717–720 (1999).

162. Mocroft, A. *et al.* Changing patterns of mortality across Europe in patients infected with HIV-1. *Lancet* **352,** 1725–1730 (1998).

163. Mocroft, A. *et al.* Decline in the AIDS and death rates in the EuroSIDA study: an observational study. *Lancet* **362,** 22–29 (2003).

164. Fleishman, J. A. & Hellinger, F. H. Recent trends in HIV-related inpatient admissions 1996–2000: a 7-state study. *JAIDS J. Acquir. Immune Defic. Syndr.* **34,** 102–110 (2003).

165. Selik, R. M., Byers Jr, R. H. & Dworkin, M. S. Trends in diseases reported on US death certificates that mentioned HIV infection, 1987-1999. *J. Acquir. Immune Defic. Syndr.* **29,** 378–387 (2002).

166. Tzakis, A. G. *et al.* Transplantation in HIV+ patients. *Transplantation* **49,** 354 (1990).

167. Roland, M. E., Carlson, L. L., Frassetto, L. A. & Stock, P. G. Solid Organ

Transplantation : Referral , Management , and Outcomes in HIV-Infected Patients. (2006).

168. Roland, M. E. *et al.* HIV-infected liver and kidney transplant recipients: 1- and 3-year outcomes. *Am. J. Transplant.* **8,** 355–365 (2008).
169. Stock, P., Barin, B. & Murphy, B. Outcomes of kidney transplantation in HIV-infected recipients. *… Engl. J. …* **363,** 2004–2014 (2010).
170. Sher, R. Acquired immune deficiency syndrome (AIDS) in the RSA. *South African Med. J.* 23–26 (1986).
171. Crookes, R. L. & Heyns, A. P. HIV seroprevalence--data from blood transfusion services. *South African Med. journal= Suid-Afrikaanse Tydskr. vir Geneeskd.* **82,** 484 (1992).
172. Department of Health South Africa. *Eleventh National HIV and syphilis sero-prevalence survey of women attending public antenatal clinics in South Africa*. (2000).
173. Shisana, O. & Simbayi, L. C. *Nelson Mandela/HSRC study of HIV/AIDS: South African national HIV prevalence, behavioural risks and mass media: household survey 2002*. (HSRC Press, 2002).
174. Joint United Nations Programme on HIV/AIDS UNAIDS. AIDS epidemic update: December 1999. *AIDS Anal. Afr.* **10,** 2 (2000).
175. UNAIDS. Report on the global AIDS epidemic. *Nov. York Jt. United Nations Progr. HIV/AIDS (UN AIDS)* (2008).
176. Department of Health South Africa. *HIV/AIDS/STD Strategic Plan For South Africa 2000 - 2005*.
177. Hussain, A., Moodley, D., Naidoo, S. & Esterhuizen, T. M. Pregnant women's

access to PMTCT and ART services in South Africa and implications for universal antiretroviral treatment. *PLoS One* **6,** (2011).

178. Stinson, K., Boulle, A., Coetzee, D., Abrams, E. J. & Myer, L. Initiation of highly active antiretroviral therapy among pregnant women in Cape Town, South Africa. *Trop. Med. Int. Heal.* **15,** 825–832 (2010).
179. Department of Health South Africa. Operational Plan For Comprehensive HIV And AIDS Care, Management And Treatment For South Africa. (2003).
180. Department of Health of South Africa. Policy and Guidelines for the Implementation of the PMTCT Program South Africa. (2008).
181. Shisana, O., Rehle, T., Simbayi, Lc., Zuma, K. & Jooste, S. South African national HIV prevalence incidence behaviour and communication survey 2008: a turning tide among teenagers? (2009).
182. Human Sciences Research Council. South African National HIV Prevalence, Incidence and Behaviour Survey, 2012. (2012).
183. United Naitons Joint Programme on HIV/AIDS (UNAIDS). *Global AIDS Update 2016*. (2016). doi:10.1073/pnas.86.15.5781
184. Fabian, J., Katz, I. & Gerntholtz, T. Chronic kidney disease in human immunodeficiency virus infection. *Panminerva …* **49,** 51–66 (2007).
185. Winston, J. *et al.* Kidney disease in patients with HIV infection and AIDS. *Clin. Infect. Dis.* **47,** 1449–1457 (2008).
186. Han, T. M., Naicker, S., Ramdial, P. K. & Assounga, a G. A cross-sectional study of HIV-seropositive patients with varying degrees of proteinuria in South Africa. *Kidney Int.* **69,** 2243–50 (2006).
187. Bruggeman, L. a *et al.* Renal epithelium is a previously unrecognized site of

HIV-1 infection. *J. Am. Soc. Nephrol.* **11,** 2079–87 (2000).

188. Winston, J. & Bruggeman, L. Nephropathy and establishment of a renal reservoir of HIV type 1 during primary infection. *N. Engl. J. Med.* **344,** (2001).

189. Marras, D. *et al.* Replication and compartmentalization of HIV-1 in kidney epithelium of patients with HIV-associated nephropathy. *Nat. Med.* **8,** 522–6 (2002).

190. Atta, M. G. Diagnosis and natural history of HIV-associated nephropathy. *Adv. Chronic Kidney Dis.* **17,** 52–8 (2010).

191. Szczech, L. A. *et al.* The clinical characteristics and antiretroviral dosing patterns of HIV-infected patients receiving dialysis. *Kidney Int.* **63,** 2295–2301 (2003).

192. Mallipattu, S. K., Salem, F. & Wyatt, C. M. The changing epidemiology of HIV-related chronic kidney disease in the era of antiretroviral therapy. *Kidney Int.* **86,** 259–65 (2014).

193. Kasembeli, A. N. *et al.* APOL1 Risk Variants Are Strongly Associated with HIV-Associated Nephropathy in Black South Africans. *J. Am. Soc. Nephrol.* ASN.2014050469- (2015). doi:10.1681/ASN.2014050469

194. Genovese, G. *et al.* Association of Trypanolytic ApoL1 Variants with Kidney Disease in African-Americans. **329,** 841–845 (2010).

195. Gerntholtz, T. E., Goetsch, S. J. W. & Katz, I. HIV-related nephropathy: a South African perspective. *Kidney Int.* **69,** 1885–91 (2006).

196. Muller, E., Mendelson, M. & Kahn, D. Renal Transplantation between HIV-Positive Donors and Recipients. *South African Med. J.* (2010).

doi:10.1056/NEJMc0900837

197. Braza, F. *et al.* Central Role of CD45RA- Foxp3hi Memory Regulatory T Cells in Clinical Kidney Transplantation Tolerance. *J. Am. Soc. Nephrol.* **4,** ASN.2014050480- (2015).

198. Leventhal, J. R. *et al.* Nonchimeric HLA-Identical Renal Transplant Tolerance: Regulatory Immunophenotypic/Genomic Biomarkers. *Am. J. Transplant.* 221–234 (2015). doi:10.1111/ajt.13416

199. Feng, G., Chan, T., Wood, K. J. & Bushell, A. Donor reactive regulatory T cells. *Curr. Opin. Organ Transplant.* **14,** 432–8 (2009).

200. Kinter, A. L. *et al.* CD25(+)CD4(+) regulatory T cells from the peripheral blood of asymptomatic HIV-infected individuals regulate CD4(+) and CD8(+) HIV-specific T cell immune responses in vitro and are associated with favorable clinical markers of disease status. *J. Exp. Med.* **200,** 331–343 (2004).

201. Locke, J. E. *et al.* Immunosuppression regimen and the risk of acute rejection in HIV-infected kidney transplant recipients. *Transplantation* **97,** 446–450 (2014).

202. Lopez, M., Clarkson, M. R., Albin, M., Sayegh, M. H. & Najafian, N. A Novel Mechanism of Action for Anti-Thymocyte Globulin : Induction of CD4+CD25+Foxp3+ Regulatory T Cells. *J. Am. Soc. Nephrol.* 1–10 (2006). doi:10.1681/ASN.2006050422

203. Valdez-Ortiz, R. *et al.* Induction of suppressive allogeneic regulatory T cells via rabbit antithymocyte polyclonal globulin during homeostatic proliferation in rat kidney transplantation. *Transpl. Int.* **28,** 108–119

(2015).

204. Sewgobind, V. D. *et al.* Characterization of rabbit antithymocyte globulins-induced CD25+ regulatory T cells from cells of patients with end-stage renal disease. *Transplantation* (2010).

205. Nattrass, N. South Africa's' rollout' of highly active antiretroviral therapy: a critical assessment. *JAIDS J. Acquir. Immune Defic. ...* **43,** 618–623 (2006).

206. Bor, J., Herbst, A., Newell, M. & Bärnighausen, T. Increases in adult life expectancy in rural South Africa: valuing the scale-up of HIV treatment. *Science (80-.).* 961–965 (2013).

207. Cornell, M. *et al.* Twelve-year mortality in adults initiating antiretroviral therapy in South Africa. *J. Int. AIDS Soc.* **20,** (2017).

208. UNAIDS. *GLOBAL REPORT: UNAIDS report on the global AIDS epidemic 2013*. *Unaids* (2013). doi:JC2502/1/E

209. Lucas, G. M. *et al.* Chronic Kidney Disease Incidence, and Progression to End-Stage Renal Disease, in HIV-Infected Individuals: A Tale of Two Races. *J Infect Dis* **197,** 1548–1557 (2008).

210. Wyatt, C. M. *et al.* Chronic kidney disease in HIV infection: an urban epidemic. 226–227 (2005). doi:10.1093/tropej/fmi104

211. Wearne, N., Swanepoel, C. R., Boulle, A., Duffield, M. S. & Rayner, B. L. The spectrum of renal histologies seen in HIV with outcomes, prognostic indicators and clinical correlations. *Nephrol. Dial. Transplant.* **27,** 4109–4118 (2012).

212. Okpechi, I. *et al.* Patterns of renal disease in Cape Town South Africa: A 10-year review of a single-centre renal biopsy database. *Nephrol. Dial.*

Transplant. **26,** 1853–1861 (2011).

213. Laurinavicius, A., Hurwitz, S. & Rennke, H. G. Collapsing glomerulopathy in HIV and non-HIV patients: A clinicopathological and follow-up study. *Kidney Int.* **56,** 2203–2213 (1999).

214. Ahuja, T. S., Grady, J. & Khan, S. Changing trends in the survival of dialysis patients with human immunodeficiency virus in the United States. *J Am Soc Nephrol* **13,** 1889–1893 (2002).

215. Muller, E., Barday, Z., Mendelson, M. & Kahn, D. HIV-Positive–to–HIV-Positive Kidney Transplantation — Results at 3 to 5 Years. *N. Engl. J. Med.* **372,** 613–620 (2015).

216. Bio-Rad. Bio-Plex® Multiplex Immunoassays. (2017). at <http://www.bio-rad.com/en-za/applications-technologies/bio-plex-multiplex-immunoassays>

217. de Jager, W., Bourcier, K., Rijkers, G. T., Prakken, B. J. & Seyfert-Margolis, V. Prerequisites for cytokine measurements in clinical trials with multiplex immunoassays. *BMC Immunol.* **10,** 52 (2009).

218. Zhang, J.-M. & An, J. Cytokines, inflammation and pain. *Int. Anesthesiol. Clin.* **45,** 27 (2007).

219. Karczewski, J., Karczewski, M., Glyda, M. & Wiktorowicz, K. Role of TH1/TH2 Cytokines in Kidney Allograft Rejection. *Transplantation Proceedings* **40,** 3390–3392 (2008).

220. Segerer, S., Nelson, P. J. & Schlöndorff, D. Chemokines, chemokine receptors, and renal disease: from basic science to pathophysiologic and therapeutic studies. *J. Am. Soc. Nephrol.* **11,** 152–176 (2000).

221. Bedke, J. *et al.* A novel CXCL8 protein-based antagonist in acute experimental renal allograft damage. *Molecular Immunology* **47,** 1047–1057 (2010).

222. Catania, J. M., Chen, G. & Parrish, A. R. Role of matrix metalloproteinases in renal pathophysiologies. *Am. J. Physiol. Physiol.* **292,** F905–F911 (2007).

223. Chang, H.-R. *et al.* Relationships between circulating matrix metalloproteinase-2 and-9 and renal function in patients with chronic kidney disease. *Clin. Chim. acta* **366,** 243–248 (2006).

224. Cavaillon, J.-M. Pro-versus anti-inflammatory cytokines: myth or reality. *Cell. Mol. Biol.* **47,** 695–702 (2001).

225. Neirynck, N., Glorieux, G., Schepers, E., Verbeke, F. & Vanholder, R. Soluble tumor necrosis factor receptor 1 and 2 predict outcomes in advanced chronic kidney disease: a prospective cohort study. *PLoS One* **10,** e0122073 (2015).

226. Nauta, A. J. *et al.* Biochemical and functional characterization of the interaction between pentraxin 3 and C1q. *Eur. J. Immunol.* **33,** 465–473 (2003).

227. Tong, M. *et al.* Plasma pentraxin 3 in patients with chronic kidney disease: associations with renal function, protein-energy wasting, cardiovascular disease, and mortality. *Clin. J. Am. Soc. Nephrol.* **2,** 889–897 (2007).

228. Davies, M. R. & Hruska, K. A. Pathophysiological mechanisms of vascular calcification in end-stage renal disease. *Kidney Int.* **60,** 472–479 (2001).

229. Pichler, R. *et al.* Tubulointerstitial disease in glomerulonephritis. Potential role of osteopontin (uropontin). *Am. J. Pathol.* **144,** 915 (1994).

230. Lorenzen, J. *et al.* Circulating levels of osteopontin are closely related to glomerular filtration rate and cardiovascular risk markers in patients with chronic kidney disease. *Eur. J. Clin. Invest.* **40,** 294–300 (2010).

231. Yilmaz, M. I. *et al.* Soluble TWEAK plasma levels as a novel biomarker of endothelial function in patients with chronic kidney disease. *Clin. J. Am. Soc. Nephrol.* **4,** 1716–1723 (2009).

232. Fabriek, B. O., Dijkstra, C. D. & van den Berg, T. K. The macrophage scavenger receptor CD163. *Immunobiology* **210,** 153–160 (2005).

233. Kirkegaard-Klitbo, D. M. *et al.* Soluble CD163 predicts incident chronic lung, kidney and liver disease in HIV infection. *Aids* **31,** 981–988 (2017).

234. Field, M. *et al.* The use of NGAL and IP-10 in the prediction of early acute rejection in highly sensitized patients following HLA-incompatible renal transplantation. *Transpl. Int.* **27,** 362–370 (2014).

235. Xu, X. *et al.* Combination of IL-1 receptor antagonist, IL-20 and CD40 ligand for the prediction of acute cellular renal allograft rejection. *J. Clin. Immunol.* **33,** 280–287 (2013).

236. de Serres, S. a. *et al.* Derivation and validation of a Cytokine-based assay to screen for acute rejection in renal transplant recipients. *Clin. J. Am. Soc. Nephrol.* **7,** 1018–1025 (2012).

237. Roedder, S. *et al.* The kSORT Assay to Detect Renal Transplant Patients at High Risk for Acute Rejection: Results of the Multicenter AART Study. *PLoS Med.* **11,** (2014).

238. Luo, Y., Shi, B., Qian, Y., Bai, H. & Chang, J. Sequential monitoring of TIM-3 gene expression in peripheral blood for diagnostic and prognostic

evaluation of acute rejection in renal graft recipients. *Transplant. Proc.* **43,** 3669–3674 (2011).

239. Sawitzki, B. *et al.* Identification of gene markers for the prediction of allograft rejection or permanent acceptance. *Am. J. Transplant.* **7,** 1091–1102 (2007).

240. Famulski, K. S. *et al.* Changes in the transcriptome in allograft rejection: IFN-gamma-induced transcripts in mouse kidney allografts. *Am. J. Transplant.* **6,** 1342–1354 (2006).

241. Reeve, J. *et al.* Diagnosing rejection in renal transplants: A comparison of molecular- and histopathology-based approaches. *Am. J. Transplant.* **9,** 1802–1810 (2009).

242. Metzger, J. *et al.* Diagnosis of subclinical and clinical acute T-cell-mediated rejection in renal transplant patients by urinary proteome analysis. *Proteomics - Clin. Appl.* **5,** 322–333 (2011).

243. Ho, J. *et al.* Validation of Urinary CXCL10 As a Marker of Borderline, Subclinical, and Clinical Tubulitis. *Transplantation* **92,** 878–882 (2011).

244. Muthukumar, T. *et al.* Messenger RNA for FOXP3 in the Urine of Renal-Allograft Recipients. *N. Engl. J. Med.* **353,** 2342–2351 (2005).

245. Hu, H., Kwun, J., Aizenstein, B. D. & Knechtle, S. J. Noninvasive detection of acute and chronic injuries in human renal transplant by elevation of multiple cytokines/chemokines in urine. *Transplantation* **87,** 1814–1820 (2009).

246. Hricik, D. E. *et al.* Multicenter validation of urinary CXCL9 as a risk-stratifying biomarker for kidney transplant injury. *Am. J. Transplant.* **13,**

2634–2644 (2013).

247. Schrijvers, B. F., Flyvbjerg, A. & De Vriese, A. S. The role of vascular endothelial growth factor (VEGF) in renal pathophysiology. *Kidney Int.* **65,** 2003–2017 (2004).

248. Schwartz, R. S., Nankivell, B. J. & Alexander, S. I. Rejection of the Kidney Allograft. *N. Engl. J. Med.* **363,** 1451–1462 (2010).

249. Mackay, F., Figgett, W. A., Saulep, D., Lepage, M. & Hibbs, M. L. B-cell stage and context-dependent requirements for survival signals from BAFF and the B-cell receptor. *Immunol. Rev.* **237,** 205–225 (2010).

250. Benson, M. J. *et al.* Cutting edge: the dependence of plasma cells and independence of memory B cells on BAFF and APRIL. *J. Immunol.* **180,** 3655–3659 (2008).

251. Thibault-Espitia, A. *et al.* BAFF and BAFF-R Levels Are Associated With Risk of Long-Term Kidney Graft Dysfunction and Development of Donor-Specific Antibodies. *Am. J. Transplant.* **12,** 2754–2762 (2012).

252. Gilliet, M., Cao, W. & Liu, Y.-J. Plasmacytoid dendritic cells: sensing nucleic acids in viral infection and autoimmune diseases. *Nat. Rev. Immunol.* **8,** 594 (2008).

253. Pettersson, E., Ahonen, J. & Häyry, P. CMV infection, class II antigen expression, and human kidney allograft rejection. *Transplantation* **42,** 364–367 (1986).

254. Fishman, J. A. & Rubin, R. H. Infection in organ-transplant recipients. *N. Engl. J. Med.* **338,** 1741–1751 (1998).

255. Magnone, M. *et al.* Interferon-alpha-induced acute renal allograft rejection.

Transplantation **59,** 1068–1070 (1995).

256. Kramer, P., Bijnen, A. B., Ten Kate, F. W. J., Jeekel, J. & Weimar, W. Recombinant leucocyte interferon A induces steroid-resistant acute vascular rejection episodes in renal transplant recipients. *Lancet* **323,** 989–990 (1984).

257. Levings, M. K. *et al.* IFN-α and IL-10 Induce the Differentiation of Human Type 1 T Regulatory Cells. *J. Immunol.* **166,** 5530–5539 (2001).

258. Wells, A. D. *et al.* Requirement for T-cell apoptosis in the induction of peripheral transplantation tolerance. *Nat. Med.* **5,** 1303 (1999).

259. Noris, M. *et al.* Regulatory T cells and T cell depletion: role of immunosuppressive drugs. *J. Am. Soc. Nephrol.* **18,** 1007–18 (2007).

260. Wood, K. J., Feng, G., Wei, B., Sawitzki, B. & Bushell, A. R. Interferon Gamma: Friend or Foe? *Transplantation* **84,** S4–S5 (2007).

261. Boehm, U., Klamp, T., Groot, M. & Howard, J. C. Cellular responses to interferon-γ. *Annu. Rev. Immunol.* **15,** 749–795 (1997).

262. Hidalgo, L. G. & Halloran, P. F. Role of IFN-gamma in allograft rejection. *Crit. Rev. Immunol.* **22,** 317–349 (2002).

263. Khaira, A. *et al.* Hepatitis B virus associated focal and segmental glomerular sclerosis: Report of two cases and review of literature. *Clin. Exp. Nephrol.* **13,** 373–377 (2009).

264. Thebault, P. *et al.* Role of IFNγ in Allograft Tolerance Mediated by $CD4^+$ $CD25^+$ Regulatory T Cells by Induction of IDO in Endothelial Cells. *Am. J. Transplant.* **7,** 2472–2482 (2007).

265. Koenecke, C. *et al.* IFN-γ Production by Allogeneic Foxp3+ Regulatory T

Cells Is Essential for Preventing Experimental Graft-versus-Host Disease. *J. Immunol.* **189,** 2890–2896 (2012).

266. Hall, B. M., Tran, G. T., Robinson, C. M. & Hodgkinson, S. J. Induction of antigen specific CD4+CD25+Foxp3+T regulatory cells from na??ve natural thymic derived T regulatory cells. *Int. Immunopharmacol.* **28,** 875–886 (2015).
267. Sawitzki, B. *et al.* IFN-γ production by alloantigen-reactive regulatory T cells is important for their regulatory function in vivo. *J. Exp. Med.* **201,** 1925–1935 (2005).
268. Konieczny, B. T. *et al.* IFN-γ is critical for long-term allograft survival induced by blocking the CD28 and CD40 ligand T cell costimulation pathways. *J. Immunol.* **160,** 2059–2064 (1998).
269. Lue, H., Kleemann, R., Calandra, T., Roger, T. & Bernhagen, J. Macrophage migration inhibitory factor (MIF): mechanisms of action and role in disease. *Microbes Infect.* **4,** 449–460 (2002).
270. Loong, C. C., Chen, A., Lui, W. Y., King, K. L. & Lin, C. Y. Expression of cytokines, growth factors, and adhesion molecules in rejecting human renal allograft. in *Transplantation proceedings* **28,** 1445–1446 (1996).
271. Teppo, A.-M., Honkanen, E., Ahonen, J. & Gronhagen-Riska, C. Does increased urinary interleukin-1 receptor antagonist/interleukin-1β ratio indicate good prognosis in renal transplant recipients? *Transplantation* **66,** 1009–1014 (1998).
272. Tominaga, K. *et al.* IL-12 synergizes with IL-18 or IL-1β for IFN-γ production from human T cells. *Int. Immunol.* **12,** 151–160 (2000).

273. Wyburn, K. *et al.* Macrophage-derived interleukin-18 in experimental renal allograft rejection. *Nephrol. Dial. Transplant.* **20,** 699–706 (2005).

274. Commins, S., Steinke, J. W. & Borish, L. The extended IL-10 superfamily: IL-10, IL-19, IL-20, IL-22, IL-24, IL-26, IL-28, and IL-29. *J. Allergy Clin. Immunol.* **121,** 1108–1111 (2008).

275. Kayagaki, N. *et al.* Involvement of TNF-related apoptosis-inducing ligand in human CD4+ T cell-mediated cytotoxicity. *J. Immunol.* **162,** 2639–2647 (1999).

276. Hoffmann, S. C. *et al.* Functionally significant renal allograft rejection is defined by transcriptional criteria. *Am. J. Transplant.* **5,** 573–581 (2005).

277. Amirzargar, a. *et al.* Th1/Th2 cytokine analysis in iranian renal transplant recipients. *Transplant. Proc.* **37,** 2985–2987 (2005).

278. Davidson, C. *et al.* IL-13 prolongs allograft survival: Association with inhibition of macrophage cytokine activation. *Transpl. Immunol.* **17,** 178–186 (2007).

279. Wyburn, K. R., Jose, M. D., Wu, H., Atkins, R. C. & Chadban, S. J. The role of macrophages in allograft rejection. *Transplantation* **80,** 1641–1647 (2005).

280. Jones, S. A., Horiuchi, S., Topley, N., Yamamoto, N. & Fuller, G. M. The soluble interleukin 6 receptor: mechanisms of production and implications in disease. *FASEB J.* **15,** 43–58 (2001).

281. Du, X. & Williams, D. A. Interleukin-11: review of molecular, cell biology, and clinical use. *Blood* **89,** 3897–3908 (1997).

282. Hill, G. R. *et al.* Interleukin-11 promotes T cell polarization and prevents

acute graft-versus-host disease after allogeneic bone marrow transplantation. *J. Clin. Invest.* **102,** 115–123 (1998).

283. Teshima, T. *et al.* IL-11 separates graft-versus-leukemia effects from graft-versus-host disease after bone marrow transplantation. **104,** 317–325 (1999).

284. Loverre, A. *et al.* IL-17 Expression by Tubular Epithelial Cells in Renal Transplant Recipients with Acute Antibody-Mediated Rejection. *Am. J. Transplant.* **11,** 1248–1259 (2011).

285. Ma, L. *et al.* The imbalance between Tregs, Th17 cells and inflammatory cytokines among renal transplant recipients. *BMC Immunol.* **16,** 56 (2015).

286. Liu, Z., Fan, H. & Jiang, S. CD4 + T-cell subsets in transplantation. *China* 183–191 (2013).

287. Woltman, a M. *et al.* Interleukin-17 and CD40-ligand synergistically enhance cytokine and chemokine production by renal epithelial cells. *J. Am. Soc. Nephrol.* **11,** 2044–2055 (2000).

288. Floss, D. M., Schröder, J., Franke, M. & Scheller, J. Insights into IL-23 biology: from structure to function. *Cytokine Growth Factor Rev.* **26,** 569–578 (2015).

289. Paust, H.-J. *et al.* The IL-23/Th17 axis contributes to renal injury in experimental glomerulonephritis. *J. Am. Soc. Nephrol.* **20,** 969–979 (2009).

290. Sadeghi, M. *et al.* IL-23 plasma level is strongly associated with CMV status and reactivation of CMV in renal transplant recipients. *BMC Immunol.* **17,** 35 (2016).

291. Regateiro, F. S., Howie, D., Cobbold, S. P. & Waldmann, H. TGF-Beta in

transplantation tolerance. *Curr. Opin. Immunol.* **23,** 660–669 (2011).

292. Newell, K. A. *et al.* Identification of a B cell signature associated with renal transplant tolerance in humans. *J. Clin. Invest.* **120,** 1836–1847 (2010).

293. Witte, K., Witte, E., Sabat, R. & Wolk, K. IL-28A, IL-28B, and IL-29: Promising cytokines with type I interferon-like properties. *Cytokine Growth Factor Rev.* **21,** 237–251 (2010).

294. Mennechet, F. J. D. & Uzé, G. Interferon-λ–treated dendritic cells specifically induce proliferation of FOXP3-expressing suppressor T cells. *Blood* **107,** 4417–4423 (2006).

295. Marie, J. C., Letterio, J. J., Gavin, M. & Rudensky, A. Y. TGF-β1 maintains suppressor function and Foxp3 expression in CD4+ CD25+ regulatory T cells. *J. Exp. Med.* **201,** 1061–1067 (2005).

296. Banchereau, J., Pascual, V. & Garra, A. O. From IL-2 to IL-37 : the expanding spectrum of anti-inflammatory cytokines. *Nat. Immunol.* **13,** 925–931 (2012).

297. Hara, M. *et al.* IL-10 Is Required for Regulatory T Cells to Mediate Tolerance to Alloantigens In Vivo. *J. Immunol.* **166,** 3789–3796 (2001).

298. Collison, L. W. *et al.* The inhibitory cytokine IL-35 contributes to regulatory T-cell function. *Nature* **450,** 566–569 (2007).

299. Collison, L. W. *et al.* Interleukin-35-mediated induction of a potent regulatory T cell population. *Nat. Immunol.* **11,** 1093–1101 (2010).

300. Eller, K. *et al.* IL-9 production by regulatory T cells recruits mast cells that are essential for regulatory T cell-induced immune suppression. *J. Immunol.* **186,** 83–91 (2011).

301. Chatenoud, L. *et al.* In vivo cell activation following OKT3 administration. Systemic cytokine release and modulation by corticosteroids. *Transplantation* **49,** 697–702 (1990).

302. Gorantla, V. S. *et al.* Immunosuppressive agents in transplantation: mechanisms of action and current anti-rejection strategies. *Microsurgery* **20,** 420–429 (2000).

303. FDA. *Thymoglobulin [Anti-thymocyte Globulin (Rabbit)] Package Insert*. (2017).

304. Deeks, E. D. & Keating, G. M. Rabbit Antithymocyte Globulin (Thymoglobulin): A Review of its Use in the Prevention and Treatment of Acute Renal Rejection. **69,** 1483–1512 (2009).

305. Allison, A. C. & Eugui, E. M. Immunosuppressive and other effects of mycophenolic acid and an ester prodrug, mycophenolate mofetil. *Immunol. Rev.* **136,** 5–28 (1993).

306. Breen, E. J., Polaskova, V. & Khan, A. Bead-based multiplex immuno-assays for cytokines, chemokines, growth factors and other analytes: median fluorescence intensities versus their derived absolute concentration values for statistical analysis. *Cytokine* **71,** 188–198 (2015).

307. Vaux, D. L., Fidler, F. & Cumming, G. Replicates and repeats—what is the difference and is it significant?: A brief discussion of statistics and experimental design. *EMBO Rep.* **13,** 291–296 (2012).

308. Bolstad, N., Warren, D. J. & Nustad, K. Heterophilic antibody interference in immunometric assays. *Best Pract. Res. Clin. Endocrinol. Metab.* **27,** 647–661 (2013).

309. Browne, R. W. *et al.* Performance of multiplex cytokine assays in serum and saliva among community-dwelling postmenopausal women. *PLoS One* **8,** e59498 (2013).

310. Fang, R. *et al.* An analytical approach to reduce between-plate variation in multiplex assays that measure antibodies to Plasmodium falciparum antigens. *Malar. J.* **16,** 287 (2017).

311. Guttmann, R. D., Caudrelier, P., Alberici, G. & Touraine, J.-L. Pharmacokinetics, foreign protein immune response, cytokine release, and lymphocyte subsets in patients receiving thymoglobuline and immunosuppression. in *Transplantation proceedings* **29,** 24S–26S (Elsevier, 1997).

312. Feng, X. *et al.* In vivo effects of horse and rabbit antithymocyte globulin in patients with severe aplastic anemia. *Haematologica* **99,** 1433–1440 (2014).

313. Wu, Z. *et al.* Homeostatic proliferation is a barrier to transplantation tolerance. *Nat. Med.* **10,** 87–92 (2004).

314. Page, A., Ford, M. & Kirk, A. Memory T Cell-Specific Therapeutics in Organ Transplantation. *Curr. Opin. organ …* **14,** 643–649 (2009).

315. Wacholder, S., Chanock, S., Garcia-Closas, M., El Ghormli, L. & Rothman, N. Assessing the probability that a positive report is false: an approach for molecular epidemiology studies. *J. Natl. Cancer Inst.* **96,** 434–442 (2004).

316. Tocci, M. J. *et al.* The immunosuppressant FK506 selectively inhibits expression of early T cell activation genes. *J. Immunol.* **143,** 718–726 (1989).

317. Schreiber, S. L. & Crabtree, G. R. The mechanism of action of cyclosporin A and FK506. *Immunol. Today* **13,** 136–142 (1992).

318. Asseman, C., Mauze, S., Leach, M. W., Coffman, R. L. & Powrie, F. An essential role for interleukin 10 in the function of regulatory T cells that inhibit intestinal inflammation. *J. Exp. Med.* **190,** 995–1004 (1999).

319. Mittal, S. K., Sharma, R. K., Gupta, A., Naik, S. & Sk, M. S. K. Increased interleukin-10 production without expansion of CD4+CD25+ T-regulatory cells in early stable renal transplant patients on calcineurin inhibitors. *Transplantation* **88,** 435–441 (2009).

320. Rashad, R. H. *et al.* IL-10 Gene polymorphism and graft outcome in live-donor kidney transplantation. *African J. Nephrol.* **19,** 6–13 (2016).

321. Gregori, S. *et al.* Differentiation of type 1 T regulatory cells (Tr1) by tolerogenic DC-10 requires the IL-10 – dependent ILT4 / HLA-G pathway. *Blood* **116,** 935–944 (2010).

322. Levitsky, J. *et al.* The Human 'Treg MLR': Immune Monitoring for Foxp3+ T Regulatory Cell Generation. **88,** 1303–1311 (2010).

323. Li, X. *et al.* IL-35 is a novel responsive anti-inflammatory cytokine - a new system of categorizing anti-inflammatory cytokines. *PLoS One* **7,** (2012).

324. Collison, L. W., Pillai, M. R., Chaturvedi, V. & Vignali, D. A. A. Regulatory T cell suppression is potentiated by target T cells in a cell contact, IL-35- and IL-10-dependent manner. *J. Immunol.* **182,** 6121–8 (2009).

325. Andersson, J. *et al.* CD4+ FoxP3+ regulatory T cells confer infectious tolerance in a TGF-β–dependent manner. *J. Exp. Med.* **205,** 1975–1981 (2008).

326. Brownh, P. D., Wakefiel, L. M., Levinson, A. D. & Sporn, M. B. Physicochemical activation of recombinant latent transforming growth factor-beta's 1, 2, and 3. *Growth factors* **3,** 35–43 (1990).

327. Sakaguchi, S. *et al.* Immunologic tolerance maintained by CD25+ CD4+ regulatory T cells: their common role in controlling autoimmunity, tumor immunity, and transplantation tolerance. *Immunol Rev* **182,** 18–32 (2001).

328. Sakaguchi, S. Naturally arising Foxp3-expressing CD25+CD4+ regulatory T cells in immunological tolerance to self and non-self. *Nat. Immunol.* **6,** 345–52 (2005).

329. Sakaguchi, S., Yamaguchi, T., Nomura, T. & Ono, M. Regulatory T Cells and Immune Tolerance. *Cell* **133,** 775–787 (2008).

330. Sakaguchi, S., Sakaguchi, N., Masanao, A., Misako, I. & Masaaki, T. Immunologic Self-Tolerance Maintained by Activated T Cells Expressing 11-2 Receptor a-Chains (CD25). *J. Immunol.* **155,** 1151–64 (1995).

331. Brusko, T. M., Putnam, A. L. & Bluestone, J. A. Human regulatory T cells: Role in autoimmune disease and therapeutic opportunities. *Immunol. Rev.* **223,** 371–390 (2008).

332. Fontenot, J. D., Gavin, M. A. & Rudensky, A. Y. Foxp3 programs the development and function of CD4+ CD25+ regulatory T cells. *Nat. Immunol.* **4,** 330–336 (2003).

333. Bisikirska, B., Colgan, J., Luban, J., Bluestone, J. A. & Herold, K. C. TCR stimulation with modified anti-CD3 mAb expands CD8+ T cell population and induces CD8+ CD25+ Tregs. *J. Clin. Invest.* **115,** 2904 (2005).

334. Pillai, V., Ortega, S. B., Wang, C. K. & Karandikar, N. J. Transient regulatory

T-cells: A state attained by all activated human T-cells. *Clin. Immunol.* **123,** 18–29 (2007).

335. Read, S. *et al.* Blockade of CTLA-4 on CD4+CD25+ regulatory T cells abrogates their function in vivo. *J. Immunol.* **177,** 4376–4383 (2006).

336. McCoy, K. D. & Le Gros, G. The role of CTLA-4 in the regulation of T cell immune responses. *Immunol. Cell Biol.* **77,** 1–10 (1999).

337. Liu, W. *et al.* CD127 expression inversely correlates with FoxP3 and suppressive function of human CD4+ T reg cells. *J. Exp. Med.* **203,** 1701–11 (2006).

338. Moncrieffe, H. *et al.* High expression of the ectonucleotidase CD39 on T cells from the inflamed site identifies two distinct populations, one regulatory and one memory T cell population. *J. Immunol.* **185,** 134–143 (2010).

339. Borsellino, G. *et al.* Expression of ectonucleotidase CD39 by Foxp3+ Treg cells : hydrolysis of extracellular ATP and immune suppression. **110,** 1225–1233 (2007).

340. Deaglio, S. *et al.* Adenosine generation catalyzed by CD39 and CD73 expressed on regulatory T cells mediates immune suppression. *J. Exp. Med.* **204,** 1257–65 (2007).

341. Li, M. O., Wan, Y. Y., Sanjabi, S., Robertson, A.-K. L. & Flavell, R. A. Transforming growth factor-β regulation of immune responses. *Annu. Rev. Immunol.* **24,** 99–146 (2006).

342. Grossman, W. J. *et al.* Human T regulatory cells can use the perforin pathway to cause autologous target cell death. *Immunity* **21,** 589–601

(2004).

343. Grossman, W. J. *et al.* Differential expression of granzymes A and B in human cytotoxic lymphocyte subsets and T regulatory cells. *Analysis* **104,** 2840–2848 (2004).

344. Pandiyan, P., Zheng, L., Ishihara, S., Reed, J. & Lenardo, M. J. CD4+ CD25+ Foxp3+ regulatory T cells induce cytokine deprivation–mediated apoptosis of effector CD4+ T cells. *Nat. Immunol.* **8,** 1353–1362 (2007).

345. Wing, K. *et al.* CTLA-4 control over Foxp3+ regulatory T cell function. *Science (80-.).* **322,** 271–275 (2008).

346. Hall, B. M., Tran, G. & Hodgkinson, S. J. Alloantigen specific T regulatory cells in transplant tolerance. *Int. Immunopharmacol.* **9,** 570–574 (2009).

347. Krystufkova, E. *et al.* Regulatory T cells in kidney transplant recipients: the effect of induction immunosuppression therapy. *Nephrol. Dial. Transplant* **27,** 2576–82 (2012).

348. Hall, B. M. CD4+CD25+ T Regulatory Cells in Transplantation Tolerance. *Transplantation* **100,** 2533–2547 (2016).

349. Ramírez, E. *et al.* Peripheral Blood Regulatory T Cells in Long-Term Kidney Transplant Recipients. *Transplant. Proc.* **41,** 2360–2362 (2009).

350. Yang, J. *et al.* Allograft rejection mediated by memory T cells is resistant to regulation. *Proc. Natl. Acad. Sci.* **104,** 19954–19959 (2007).

351. Rebellato, L. M., Gross, U., Verbanac, K. M. & Thomas, J. M. A Comprehensive Definition of the Major Antibody Specificities in Polyclonal Rabbit Antithymocyte Globulin. *Transplantation* **57,** 685–693 (1994).

352. Mohty, M. Mechanisms of action of antithymocyte globulin: T-cell

depletion and beyond. *Leukemia* **21,** 1387–94 (2007).

353. Xia, C.-Q. *et al.* Anti-thymocyte globulin (ATG) differentially depletes naïve and memory T cells and permits memory-type regulatory T cells in nonobese diabetic mice. *BMC Immunol.* **13,** 70 (2012).

354. Bouvy, A. P. *et al.* The impact of induction therapy on the homeostasis and function of regulatory T cells in kidney transplant patients. *Nephrol. Dial. Transplant.* **29,** 1587–1597 (2014).

355. Feng, X. *et al.* Rabbit ATG but not horse ATG promotes expansion of functional CD4+ CD25 high FOXP3+ regulatory T cells in vitro. *Blood* **111,** 3675–3683 (2008).

356. Sewgobind, V. D. K. D. *et al.* The effect of rabbit anti-thymocyte globulin induction therapy on regulatory T cells in kidney transplant patients. *Nephrol. Dial. Transplant.* **24,** 1635–1644 (2009).

357. Tran, T. A. *et al.* Resting regulatory CD4 T cells: A site of HIV persistence in patients on long-term effective antiretroviral therapy. *PLoS One* **3,** (2008).

358. Schulze zur Wiesch, J. *et al.* Comprehensive Analysis of Frequency and Phenotype of T Regulatory Cells in HIV Infection: CD39 Expression of FoxP3+ T Regulatory Cells Correlates with Progressive Disease. *J. Virol.* **85,** 1287–97 (2011).

359. Clevers, H., Alarcon, B., Wileman, T. & Terhorst, C. The T cell receptor/CD3 complex: a dynamic protein ensemble. *Annu. Rev. Immunol.* **6,** 629–662 (1988).

360. Luckheeram, R. V., Zhou, R., Verma, A. D. & Xia, B. CD4+T Cells: Differentiation and Functions. *Clin. Dev. Immunol.* **2012,** (2012).

361. Rudolph, M. G., Stanfield, R. L. & Wilson, I. A. How TCRs bind MHCs, peptides, and coreceptors. *Annu. Rev. Immunol.* **24,** 419–466 (2006).

362. Tao, X., Constant, S., Jorritsma, P. & Bottomly, K. Strength of TCR signal determines the costimulatory requirements for Th1 and Th2 CD4+ T cell differentiation. *J. Immunol.* **159,** 5956–5963 (1997).

363. Zhu, J., Yamane, H. & Paul, W. E. Differentiation of effector CD4 T cell populations. *Annu. Rev. Immunol.* **28,** 445–489 (2009).

364. Braciale, V. L. Cytotoxic T Lymphocytes. (1998).

365. Kobata, T., Agematsu, K., Kameoka, J., Schlossman, S. F. & Morimoto, C. CD27 is a signal-transducing molecule involved in CD45RA+ naive T cell costimulation. *J. Immunol.* **153,** 5422–5432 (1994).

366. Hamann, D. *et al.* Phenotypic and functional separation of memory and effector human CD8+ T cells. *J. Exp. Med.* **186,** 1407–18 (1997).

367. Itoh, M. *et al.* Thymus and autoimmunity: production of CD25+ CD4+ naturally anergic and suppressive T cells as a key function of the thymus in maintaining immunologic self-tolerance. *J. Immunol.* **162,** 5317–5326 (1999).

368. Hori, S., Nomura, T. & Sakaguchi, S. Control of regulatory T cell development by the transcription factor Foxp3. *Science (80-.).* **299,** 1057–1061 (2003).

369. Peschon, J. J. *et al.* Early lymphocyte expansion is severely impaired in interleukin 7 receptor-deficient mice. *J. Exp. Med.* **180,** 1955–1960 (1994).

370. Puel, A., Ziegler, S. F., Buckley, R. H. & Leonard, W. J. Defective IL7R expression in T-B+ NK+ severe combined immunodeficiency. *Nat. Genet.*

20, 394–397 (1998).

371. Moncunill, G., Han, H., Doba??o, C., Mcelrath, M. J. & De Rosa, S. C. OMIP-024: Pan-leukocyte immunophenotypic characterization of PBMC subsets in human samples. *Cytom. Part A* **85,** 995–998 (2014).

372. Ayasoufi, K. *et al.* Pretransplant antithymocyte globulin has increased efficacy in controlling donor-reactive memory T cells in mice. *Am. J. Transplant.* **13,** 589–599 (2013).

373. Donckier, V. *et al.* Expansion of Memory-Type CD8+ T Cells Correlates With the Failure of Early Immunosuppression Withdrawal After Cadaver Liver Transplantation Using High-Dose ATG Induction and Rapamycin. *Transplantation* **96,** 306–315 (2013).

374. Bosch, M. *et al.* Immune reconstitution after anti-thymocyte globulin-conditioned hematopoietic cell transplantation. *Cytotherapy* **14,** 1258–75 (2012).

375. Pearl, J. P. *et al.* Immunocompetent T-cells with a memory-like phenotype are the dominant cell type following antibody-mediated T-cell depletion. *Am. J. Transplant* **5,** 465–74 (2005).

376. Ermann, J. *et al.* Only the CD62L+ subpopulation of CD4+CD25+ regulatory T cells protects from lethal acute GVHD. *Blood* **105,** 2220–6 (2005).

377. Koch, S. *et al.* Multiparameter flow cytometric analysis of CD4 and CD8 T cell subsets in young and old people. *Immun. Ageing* **5,** 6 (2008).

Appendix A - Equations

Calculation of Variation in Concentration Between Recipients % was calculated using the following equation

Equation 1:

$$\%\ variability\ due\ to\ intersubject\ variability\ = \frac{var(_{cons})^2}{var(_{cons})^2 + var(_{cyt})^2}$$

$var(_{cons})$ = β coefficient of the fixed effect

$var(_{cyt})$ = β coefficient of the random effect

Appendix B – List of Reagents Used

Supplementary Table 1. List of Reagents used

Reagent	Composition	Supplier	Details
1 x RPMI-1640 Medium (RPMI)	200mM L-glutamine,indicator	Sigma Aldrich	500ml - Cat No. : R8758
1 x Phosphate buffered Saline (PBS)	0.138M NaCl, 0.0027M KCl (pH"7.2)	Sigma Aldrich	500ml - Cat No. : R8537
Dimethly Sulfoxide (DMSO)		Sigma Aldrich	Cat. No.: D2650
Biochrom AG Fetal Bovine Serum (FBS)		Scientific Group	
Ficoll(Histopaque®)		Sigma Aldrich	
R1	1% FBS in 99% RPMI	-	-
R10	10% FBS in 99% RPMI	-	-
1% wash buffer	1% FBS in 99% PBS	-	-
Freezing media			
9ml ACD-B Tubes		Lasec	Stock code - VGRV455094R
BD Cytofix/Cytoperm™	1X stock solution	BD Biosciences	100ml - Cat No.: 554722
BD Perm/Wash™	10X stock solution + FBS + saponin	BD Biosciences	100ml - Cat No.:554723
Transcription Factor Buffer Set	Fixation/permeabilization buffer, diluent buffer, perm/wash buffer	BD Biosciences	Cat No.: 562574

Appendix C – Bland Altman Plots

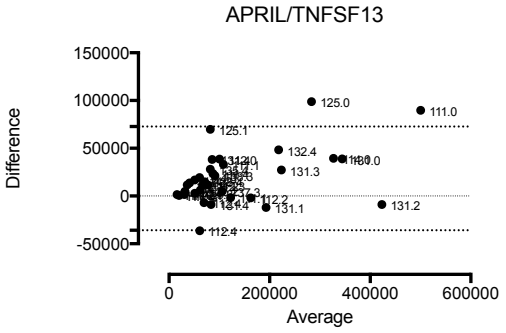

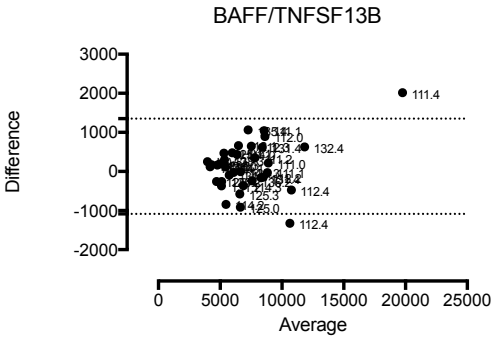

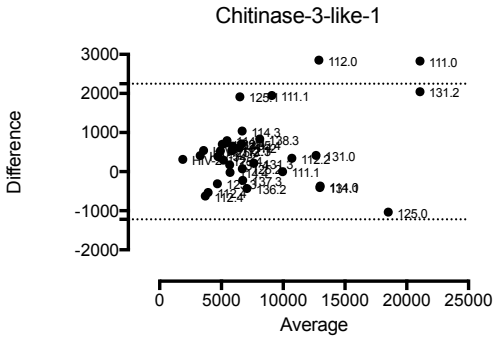

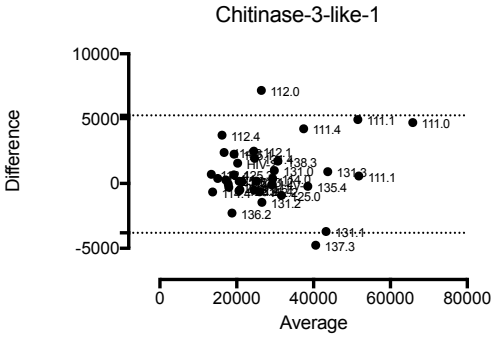

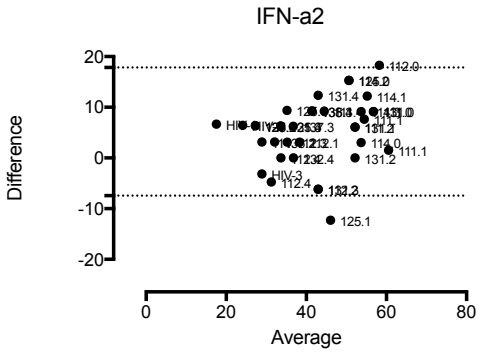

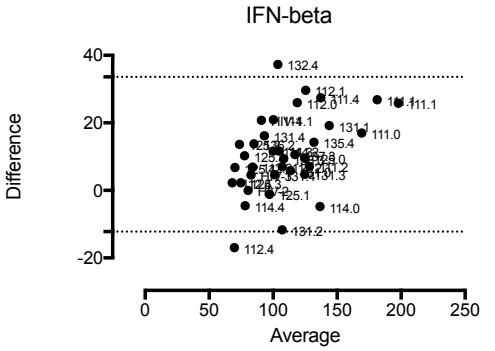

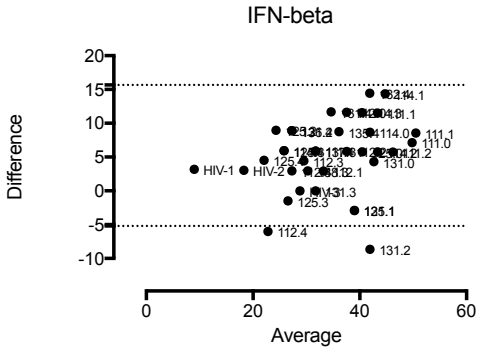

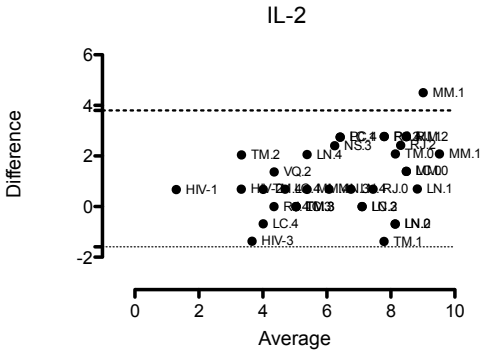

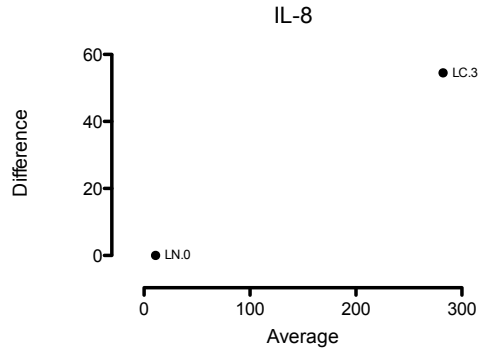
IL-8
Difference
Average
LC.3
LN.0

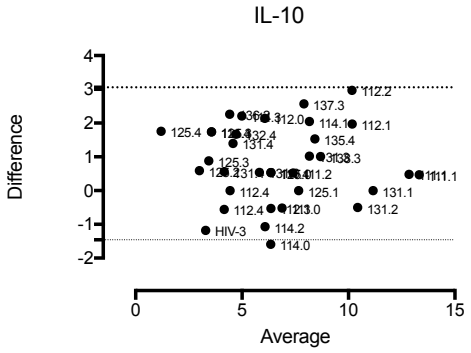
IL-10
Difference
Average
HIV-3

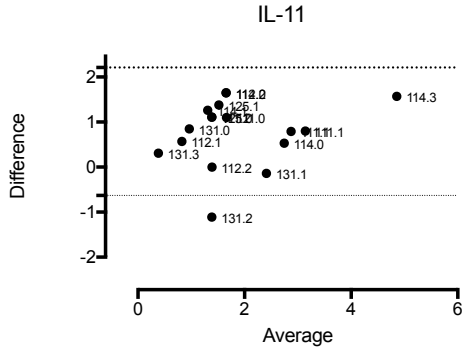
IL-11
Difference
Average
114.3

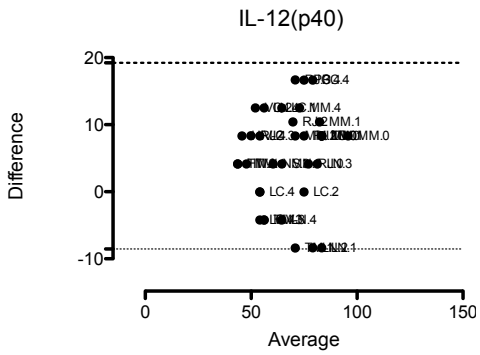
IL-12(p40)
Difference
Average
LC.4
LC.2

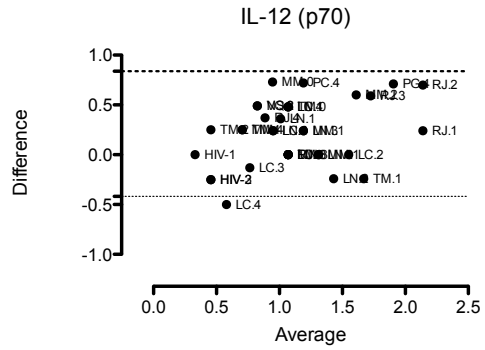
IL-12 (p70)
Difference
Average
RJ.2
RJ.1
HIV-1
LC.3
HIV-2
LC.4
TM.1

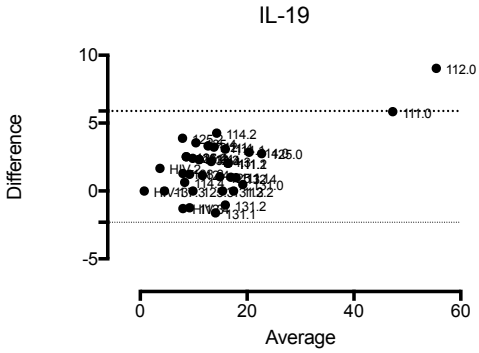
IL-19
Difference
Average
112.0
111.0

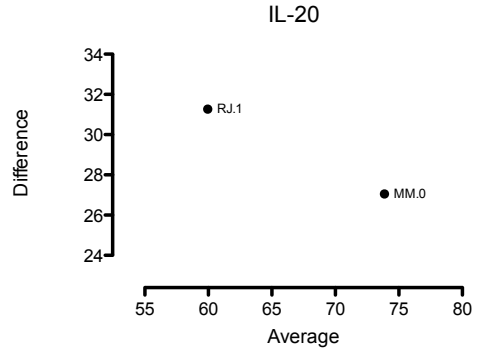
IL-20
Difference
Average
RJ.1
MM.0

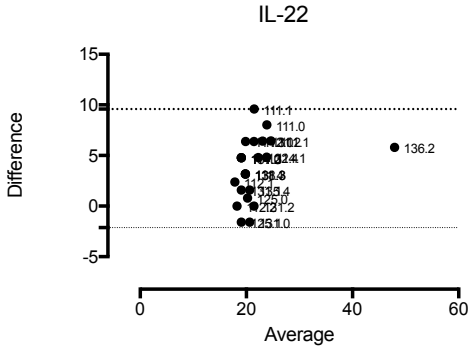
IL-22
Difference
Average
111.1
111.0
136.2

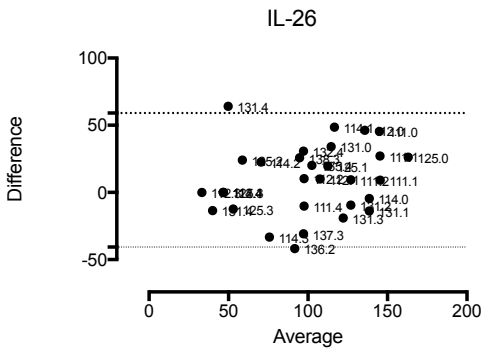
IL-26
Difference
Average

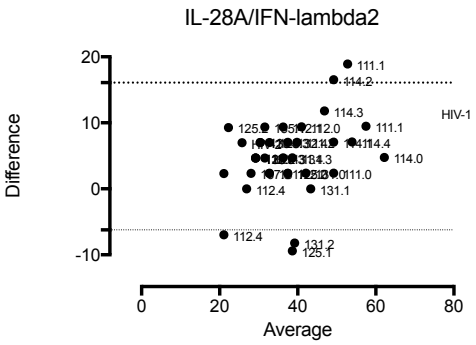
IL-28A/IFN-lambda2
HIV-1
Difference
Average

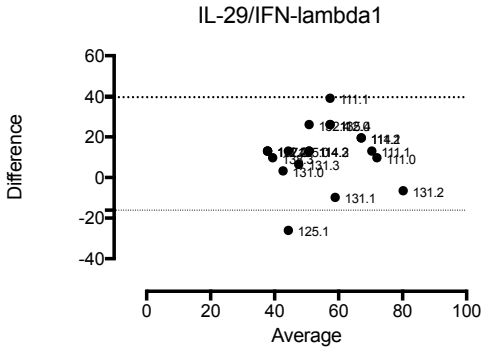
IL-29/IFN-lambda1
Difference
Average

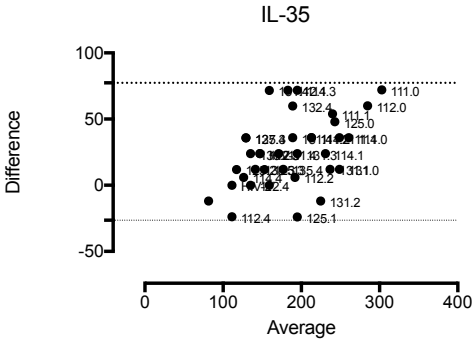
IL-35
Difference
Average

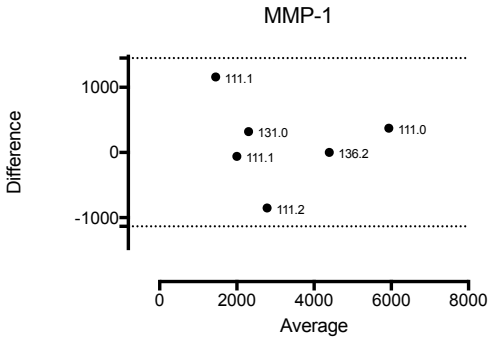
MMP-1
Difference
Average

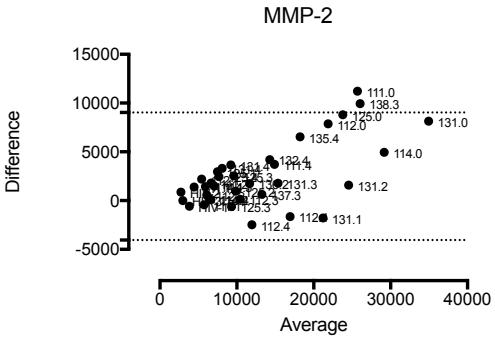
MMP-2
Difference
Average

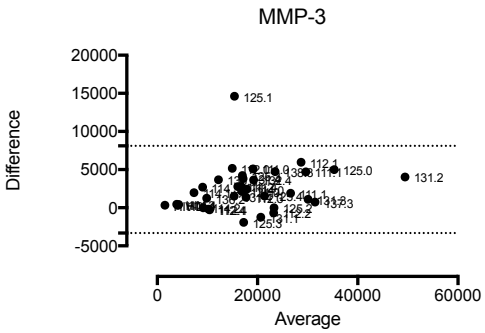
MMP-3
Difference
Average

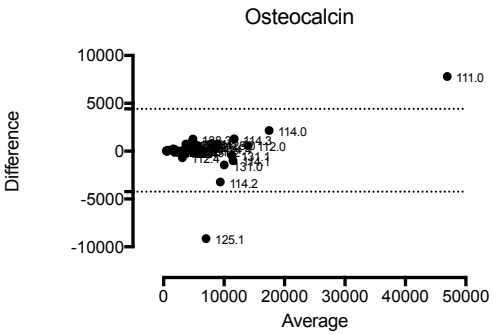
Osteocalcin
Difference
Average

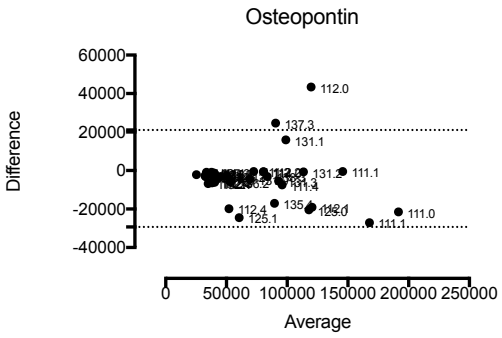
Osteopontin
Difference
Average
60000
40000
20000
0
-20000
-40000
0
50000
100000
150000
200000
250000
112.0
137.3
131.1
111.1
112.4
125.1
111.0

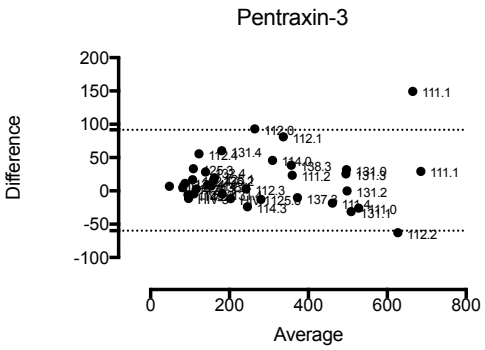
Pentraxin-3
Difference
Average
200
150
100
50
0
-50
-100
0
200
400
600
800
111.1
112.0
112.1
131.4
131.2
112.2

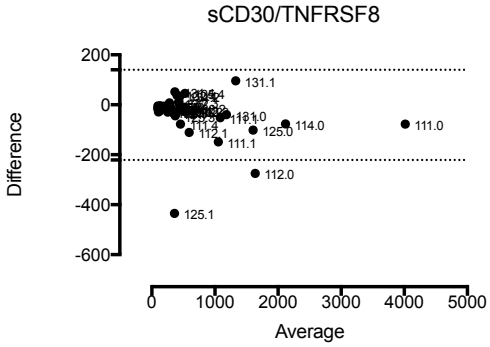
sCD30/TNFRSF8
Difference
Average
200
0
-200
-400
-600
0
1000
2000
3000
4000
5000
131.1
114.0
111.0
125.0
111.1
112.0
125.1

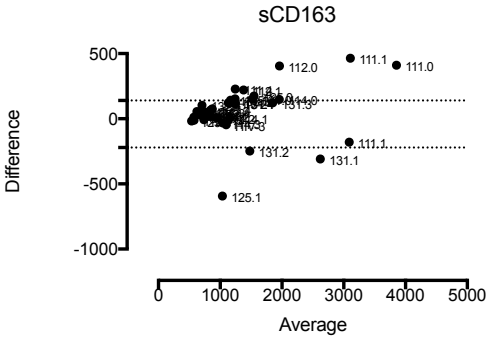
sCD163
Difference
Average
500
0
-500
-1000
0
1000
2000
3000
4000
5000
112.0
111.1
111.0
131.2
131.1
125.1

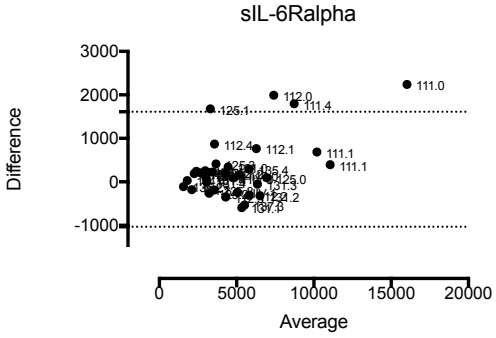
sIL-6Ralpha
Difference
Average
3000
2000
1000
0
-1000
0
5000
10000
15000
20000
111.0
112.0
111.4
125.1
112.4
112.1
111.1

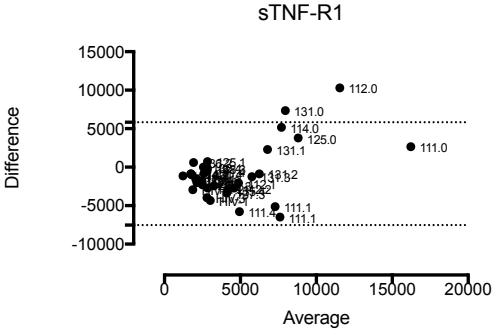
sTNF-R1
Difference
Average
15000
10000
5000
0
-5000
-10000
0
5000
10000
15000
20000
112.0
131.0
114.0
125.0
131.1
111.0
111.1

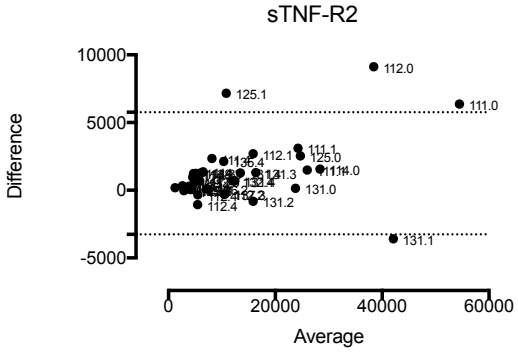
sTNF-R2
Difference
Average
10000
5000
0
-5000
0
20000
40000
60000
112.0
125.1
111.0
111.1
112.1
125.0
131.0
131.2
112.4
131.1

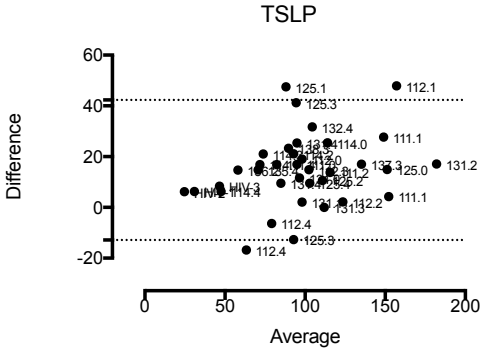
TSLP
Difference
Average
60
40
20
0
-20
0
50
100
150
200
125.1
112.1
125.3
132.4
111.1
114.0
131.2
125.0
112.4
125.3
112.4

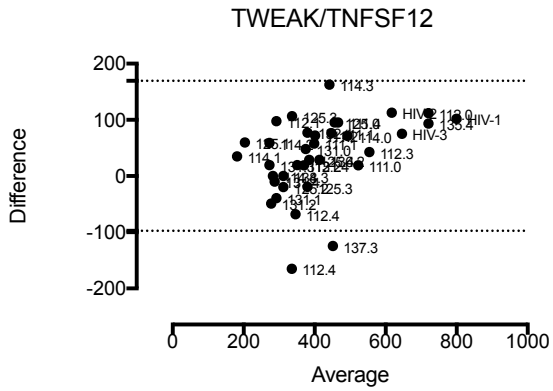

Supplementary Figure 1. Bland-Altman Plots for Intra-plate variability of all Panel 1 Plate 1 analytes Bland-Altman plots are shown for each analyte in the table. The analytes are labelled above. The mean average of two duplicates is on the x-axis (Avergage) and the difference from the mean is represented on the y-axis (Difference). The duplicates that fell outside of 2 x SD (represented as dotted line) could be excluded as an outlier with 95% confidence. The points are labelled with the KID-PID and the visit number (0-4) as KID-PID.Visit

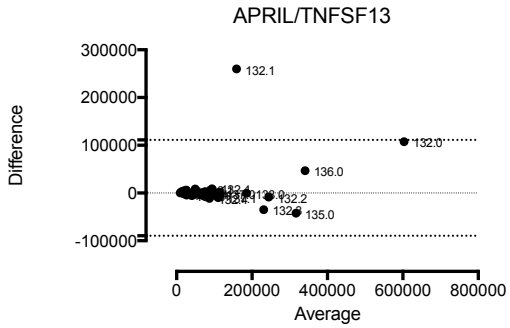
APRIL/TNFSF13
Difference
Average
300000
200000
100000
0
-100000
0
200000
400000
600000
800000
132.1
132.0
136.0
135.0

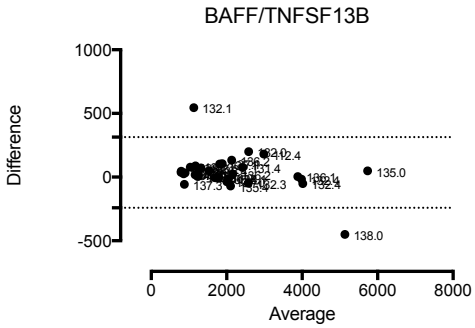
BAFF/TNFSF13B
Difference
Average
1000
500
0
-500
0
2000
4000
6000
8000
132.1
135.0
138.0

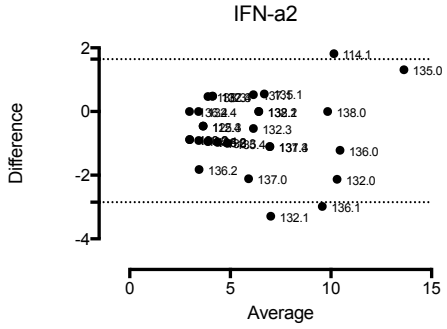
IFN-a2
Difference
Average
2
0
-2
-4
0
5
10
15
135.0
138.0
136.0
136.2
137.0
132.0
132.1

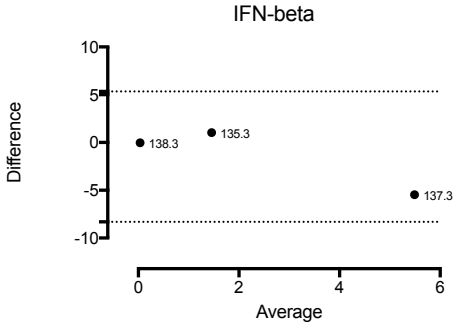
IFN-beta
Difference
Average
10
5
0
-5
-10
0
2
4
6
138.3
135.3
137.3

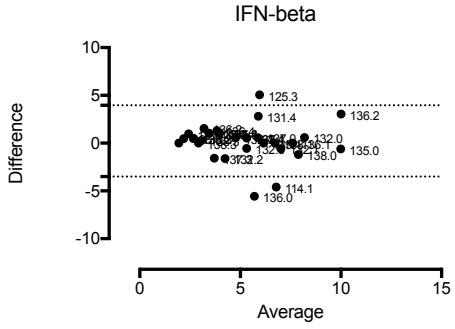
IFN-beta
Difference
Average
10
5
0
-5
-10
0
5
10
15
125.3
131.4
136.2
135.0
136.0
114.1

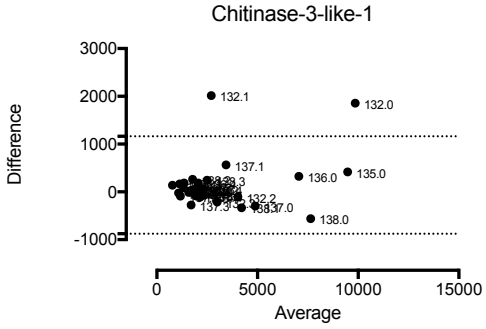
Chitinase-3-like-1
Difference
Average
3000
2000
1000
0
-1000
0
5000
10000
15000
132.1
132.0
137.1
136.0
135.0
138.0

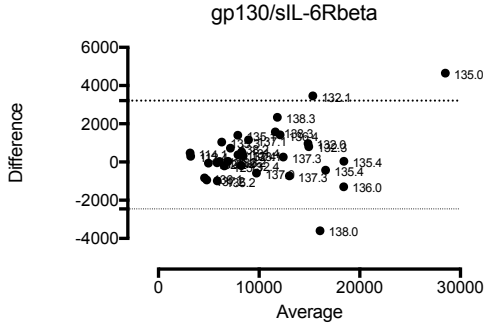
gp130/sIL-6Rbeta
Difference
Average
6000
4000
2000
0
-2000
-4000
0
10000
20000
30000
135.0
132.1
138.3
137.3
135.4
136.0
138.0

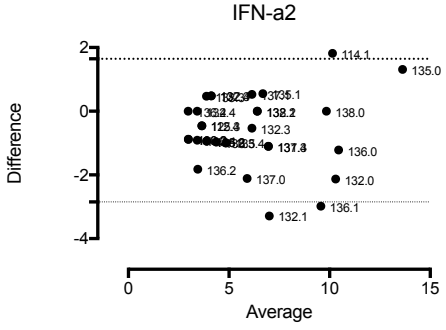
IFN-a2
Difference
Average
2
0
-2
-4
0
5
10
15
114.1
135.0
138.0
132.3
136.0
136.2
137.0
132.0
132.1
136.1

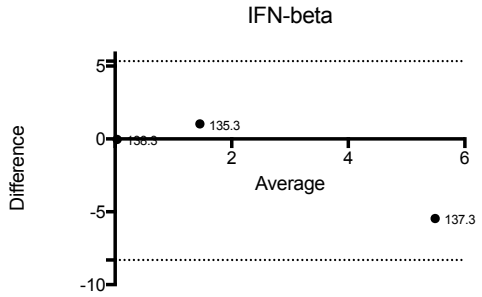
IFN-beta
Difference
Average
135.3
137.3

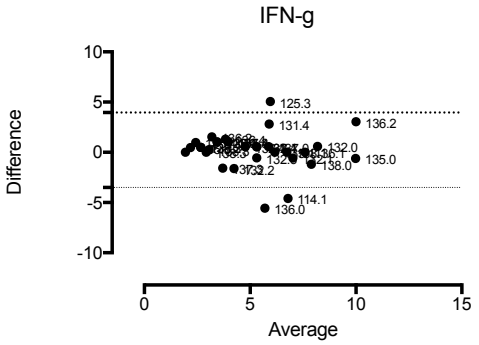
IFN-g
Difference
Average
125.3
131.4
136.2
132.0
135.0
138.0
114.1
136.0

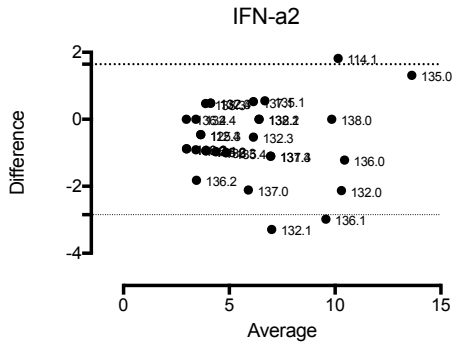
IFN-a2
Difference
Average
114.1
135.0
138.0
132.3
136.0
136.2
137.0
132.0
136.1
132.1

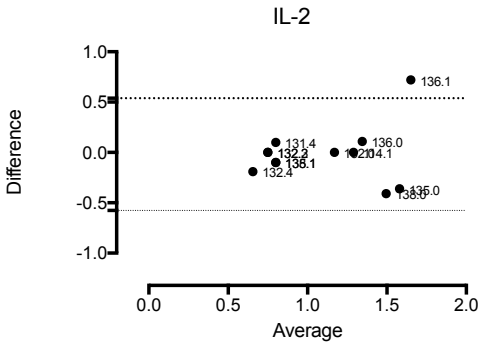
IL-2
Difference
Average
136.1
131.4
136.0
132.4
135.0

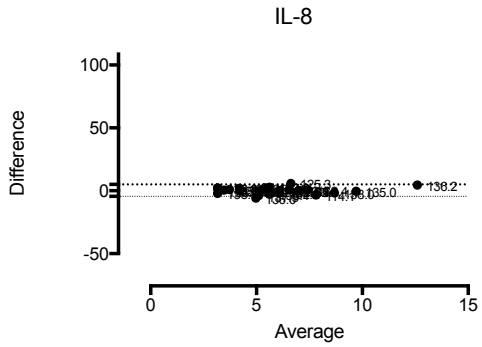
IL-8
Difference
Average

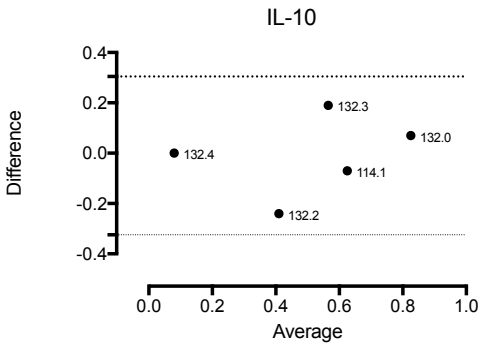
IL-10
Difference
Average
132.3
132.0
132.4
114.1
132.2

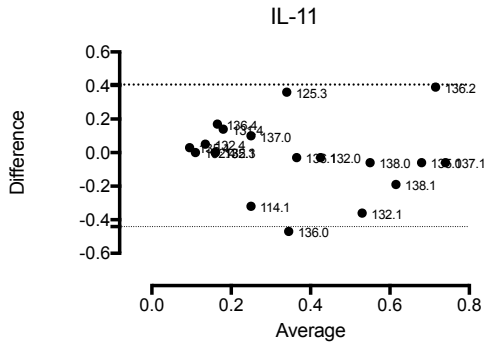
IL-11
Difference
Average
125.3
136.2
137.0
138.0
138.1
114.1
132.1
136.0

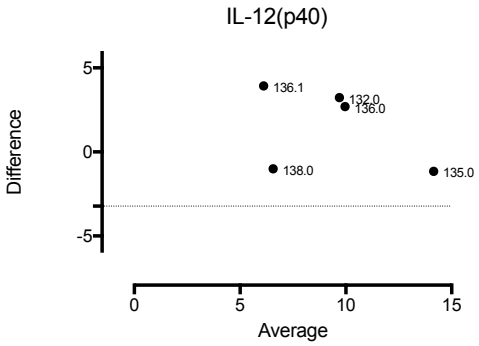
IL-12(p40)
Difference
Average
136.1
132.0
136.0
138.0
135.0

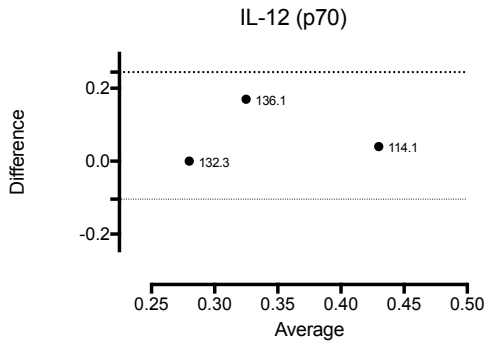
IL-12 (p70)
Difference
Average
0.2
0.0
-0.2
0.25
0.30
0.35
0.40
0.45
0.50
136.1
114.1
132.3

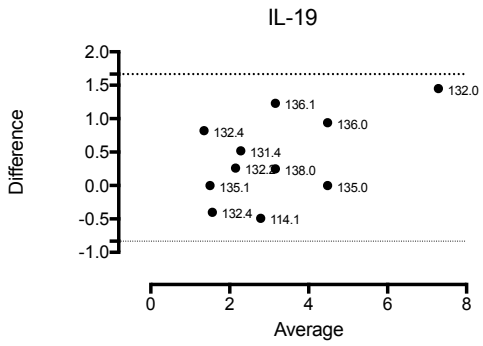
IL-19
Difference
Average
2.0
1.5
1.0
0.5
0.0
-0.5
-1.0
0
2
4
6
8
132.0
136.1
136.0
132.4
131.4
132.2
138.0
135.1
135.0
132.4
114.1

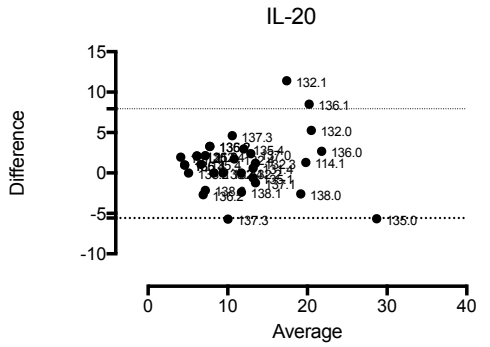
IL-20
Difference
Average
15
10
5
0
-5
-10
0
10
20
30
40
132.1
136.1
132.0
136.0
114.1
138.0
135.0

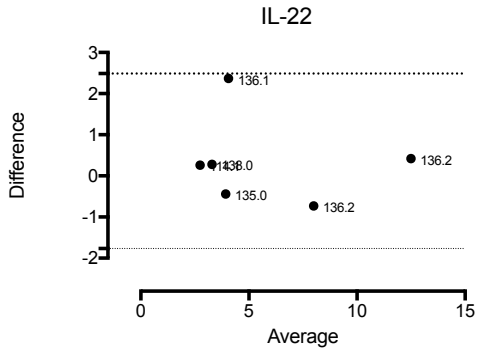
IL-22
Difference
Average
3
2
1
0
-1
-2
0
5
10
15
136.1
136.2
135.0
136.2

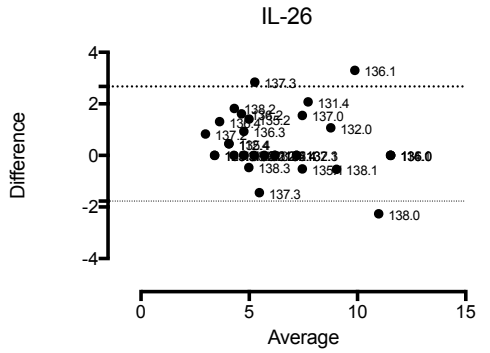
IL-26
Difference
Average
4
2
0
-2
-4
0
5
10
15
136.1
137.3
131.4
137.0
132.0
136.3
138.3
138.1
137.3
138.0

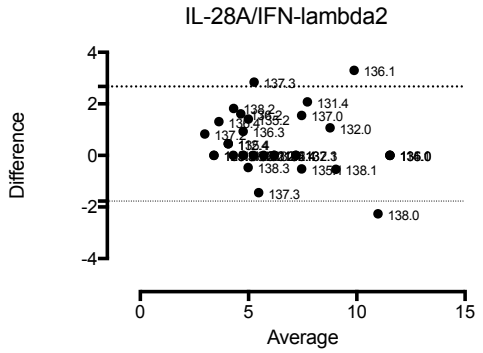
IL-28A/IFN-lambda2
Difference
Average
4
2
0
-2
-4
0
5
10
15
136.1
137.3
131.4
137.0
132.0
136.3
138.3
138.1
137.3
138.0

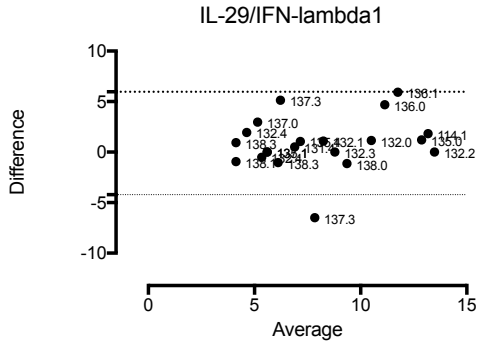
IL-29/IFN-lambda1
Difference
Average
10
5
0
-5
-10
0
5
10
15
137.3
136.0
137.0
132.4
132.0
114.1
135.0
132.2
132.3
138.0
137.3

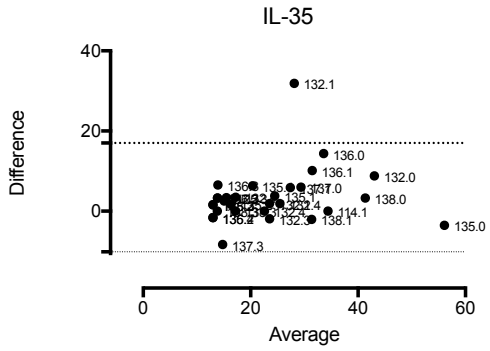
IL-35
Difference
Average
40
20
0
0
20
40
60
132.1
136.0
136.1
132.0
138.0
114.1
135.0
137.3

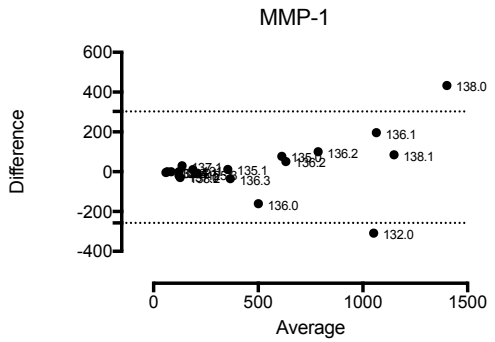
MMP-1
Difference
Average
600
400
200
0
-200
-400
0
500
1000
1500
138.0
136.1
136.2
136.2
138.1
135.1
136.3
136.0
132.0

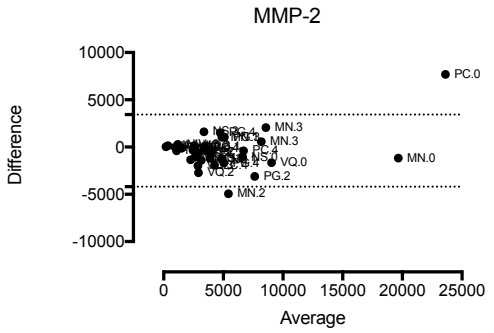
MMP-2
Difference
Average
10000
5000
0
-5000
-10000
0
5000
10000
15000
20000
25000
PC.0
MN.3
MN.3
PC.4
MN.0
VQ.0
PG.2
MN.2

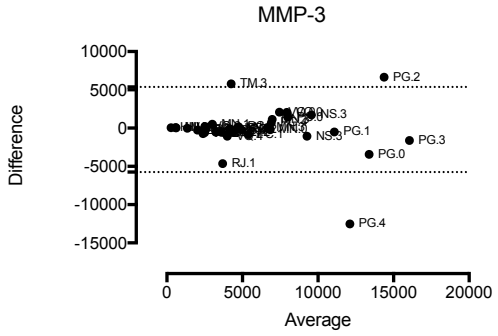
MMP-3
Difference
Average
10000
5000
0
-5000
-10000
-15000
0
5000
10000
15000
20000
PG.2
TM.3
NS.3
PG.1
NS.3
PG.3
PG.0
RJ.1
PG.4

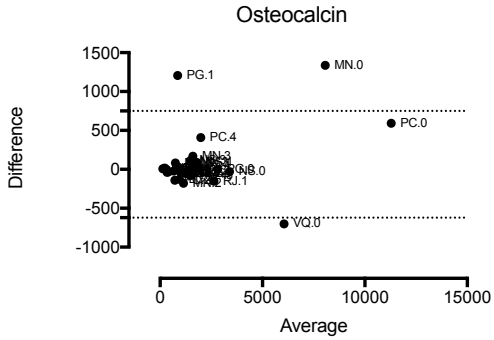
Osteocalcin
Difference
Average
1500
1000
500
0
-500
-1000
0
5000
10000
15000
MN.0
PG.1
PC.0
PC.4
VQ.0

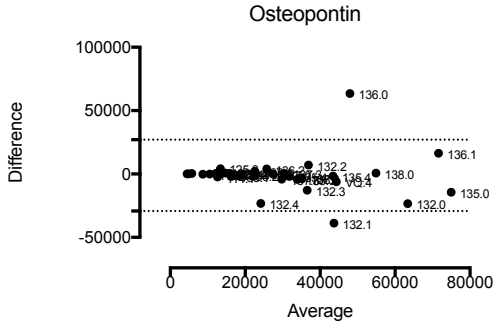
Osteopontin
Difference
Average
100000
50000
0
-50000
0
20000
40000
60000
80000
136.0
136.1
132.2
138.0
135.0
132.3
132.4
132.0
132.1

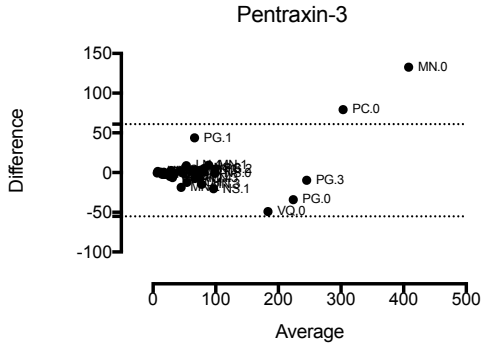
Pentraxin-3
Difference
Average
150
100
50
0
-50
-100
0
100
200
300
400
500
MN.0
PC.0
PG.1
PG.3
PG.0
NS.1
VQ.0

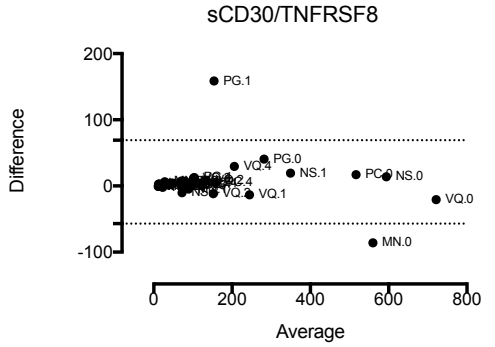
sCD30/TNFRSF8
Difference
Average
200
100
0
-100
0
200
400
600
800
PG.1
PG.0
VQ.4
NS.1
PC.0
NS.0
VQ.1
VQ.0
MN.0

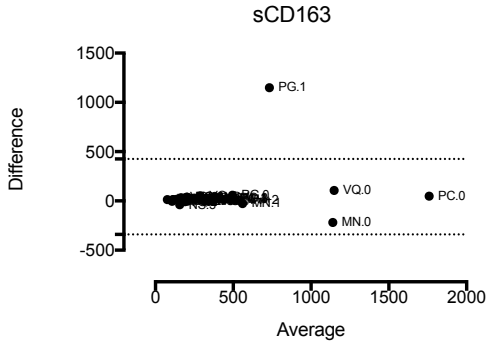
sCD163
Difference
Average
1500
1000
500
0
-500
0
500
1000
1500
2000
PG.1
VQ.0
PC.0
MN.0

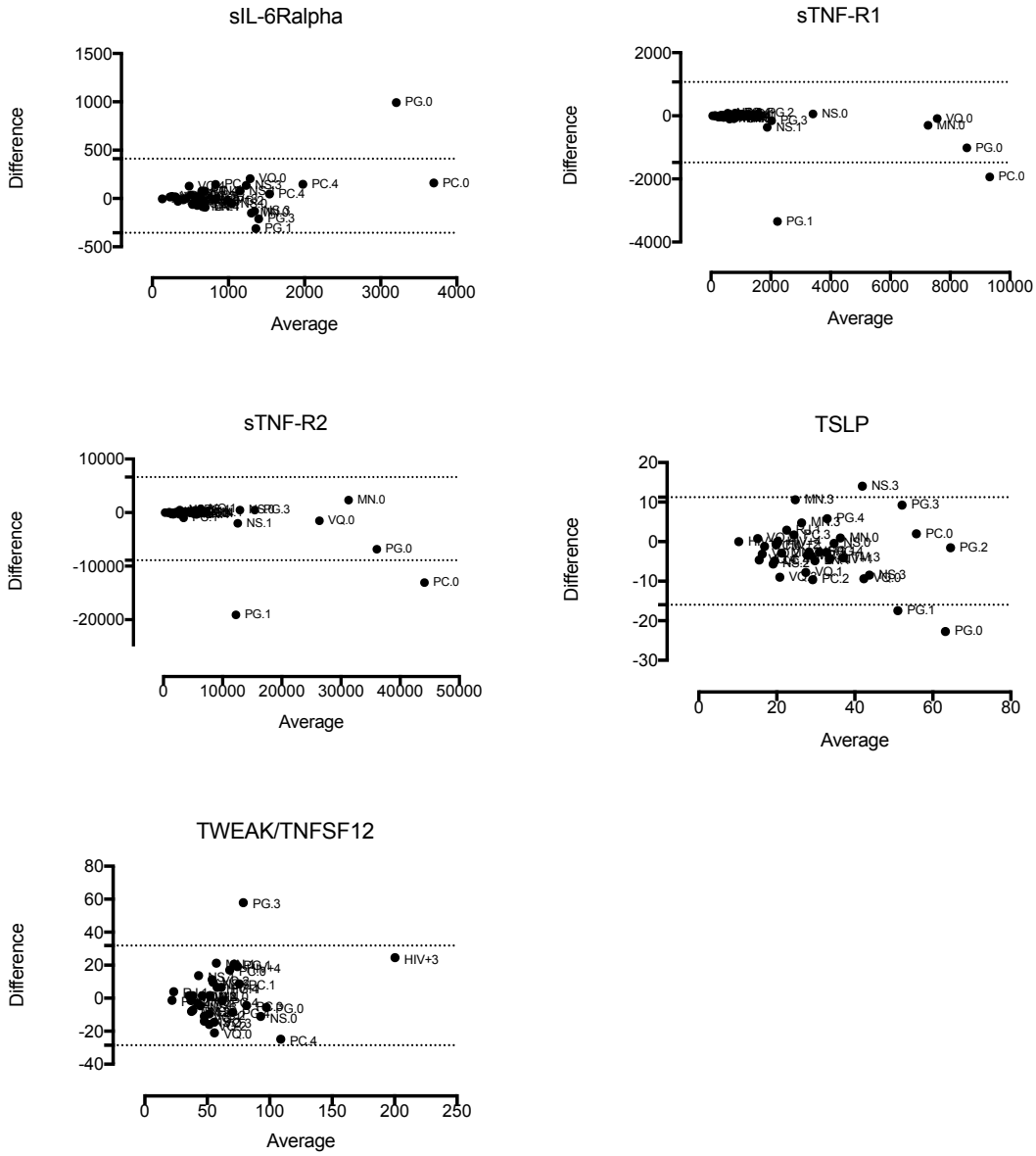

Supplementary Figure 2. Bland-Altman Plots for Intra-plate variability of all Panel 1 Plate 2 analytes Bland-Altman plots are shown for each analyte in the table. The analytes are labelled above. The mean average of two duplicates is on the x-axis (Avergage) and the difference from the mean is represented on the y-axis (Difference). The duplicates that fell outside of 2 x SD (represented as dotted line) could be excluded as an outlier with 95% confidence. The points are labelled with the KID-PID and the visit number (0-4) as KID-PID.Visit

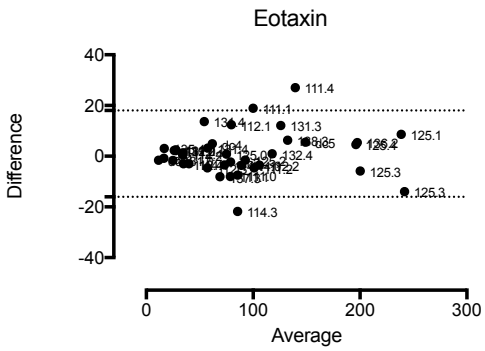
Eotaxin
Difference
Average

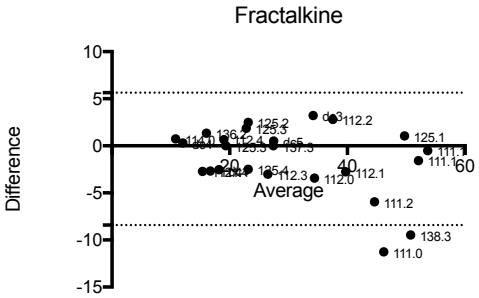
Fractalkine
Difference
Average

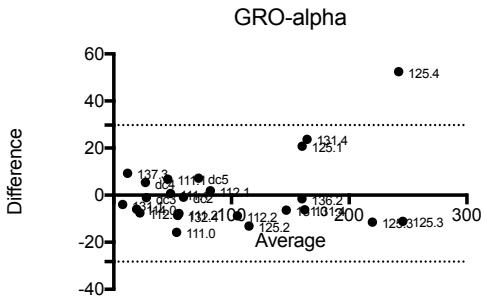
GRO-alpha
Difference
Average

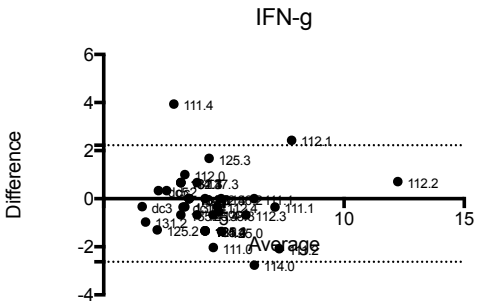
IFN-g
Difference
Average

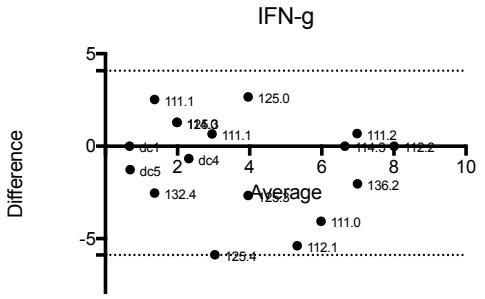
IFN-g
Difference
Average

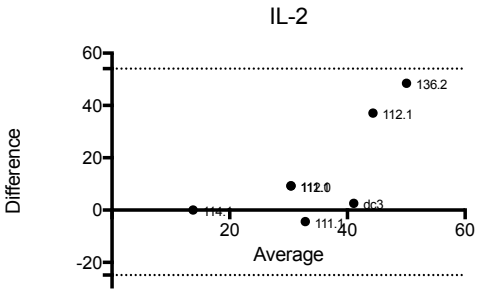
IL-2
Difference
Average

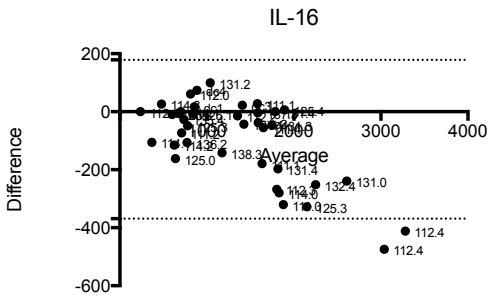
IL-16
Difference
Average

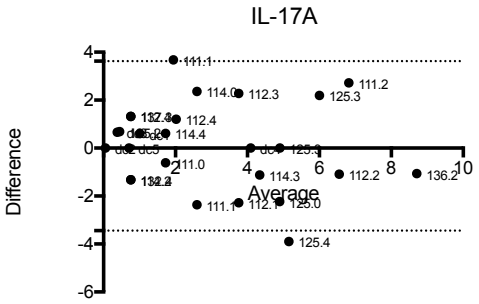
IL-17A
Difference
Average

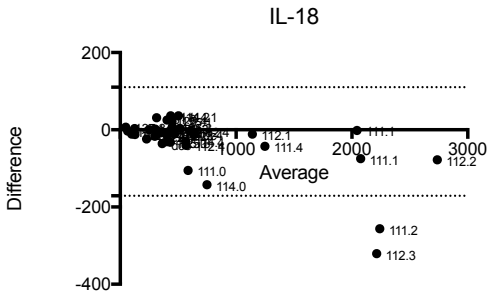
IL-18
Difference
Average
200
0
-200
-400
1000
2000
3000
111.1
112.2
111.0
114.0
111.2
112.3

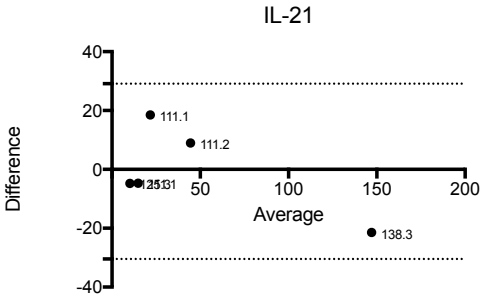
IL-21
Difference
Average
40
20
0
-20
-40
50
100
150
200
111.1
111.2
138.3

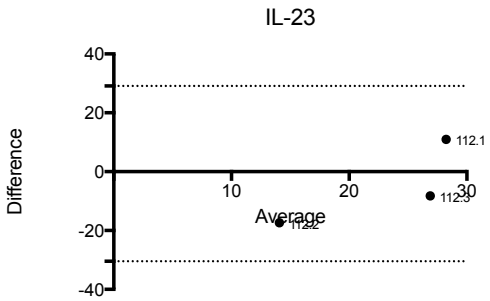
IL-23
Difference
Average
40
20
0
-20
-40
10
20
30
112.1

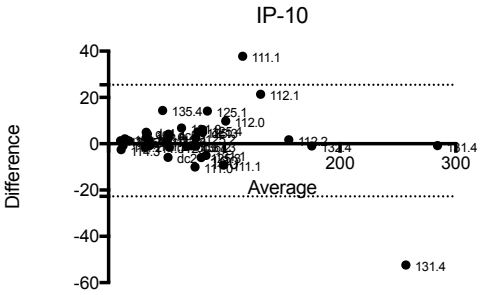
IP-10
Difference
Average
40
20
0
-20
-40
-60
200
300
111.1
112.1
135.4
125.1
112.0
131.4

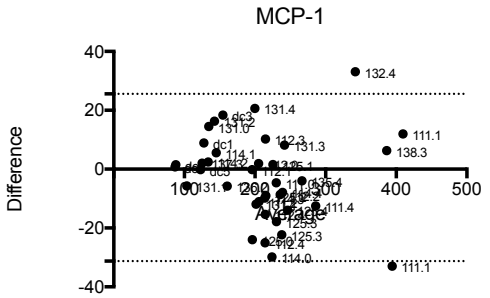
MCP-1
Difference
Average
40
20
0
-20
-40
100
400
500
132.4
131.4
111.1
138.3
111.4
125.3
111.1

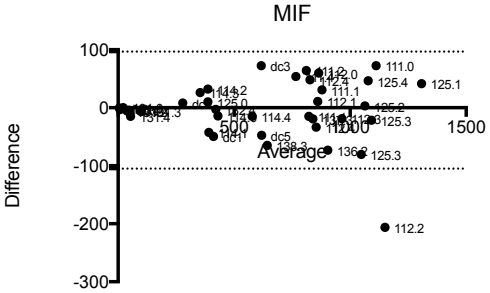
MIF
Difference
Average
100
0
-100
-200
-300
500
1000
1500
111.0
125.4
125.1
125.3
112.2

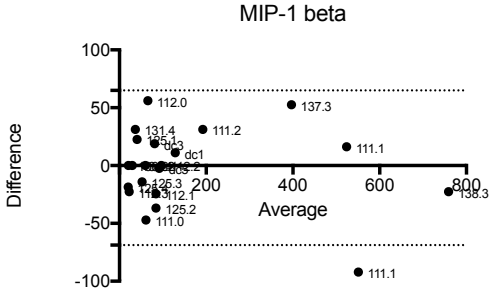
MIP-1 beta
Difference
Average
100
50
0
-50
-100
200
400
600
800
112.0
137.3
131.4
111.2
111.1
125.2
111.0
111.1

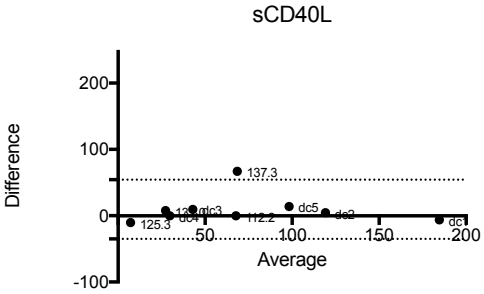
sCD40L
Difference
Average
200
100
0
-100
50
100
150
200
137.3
125.3
112.2

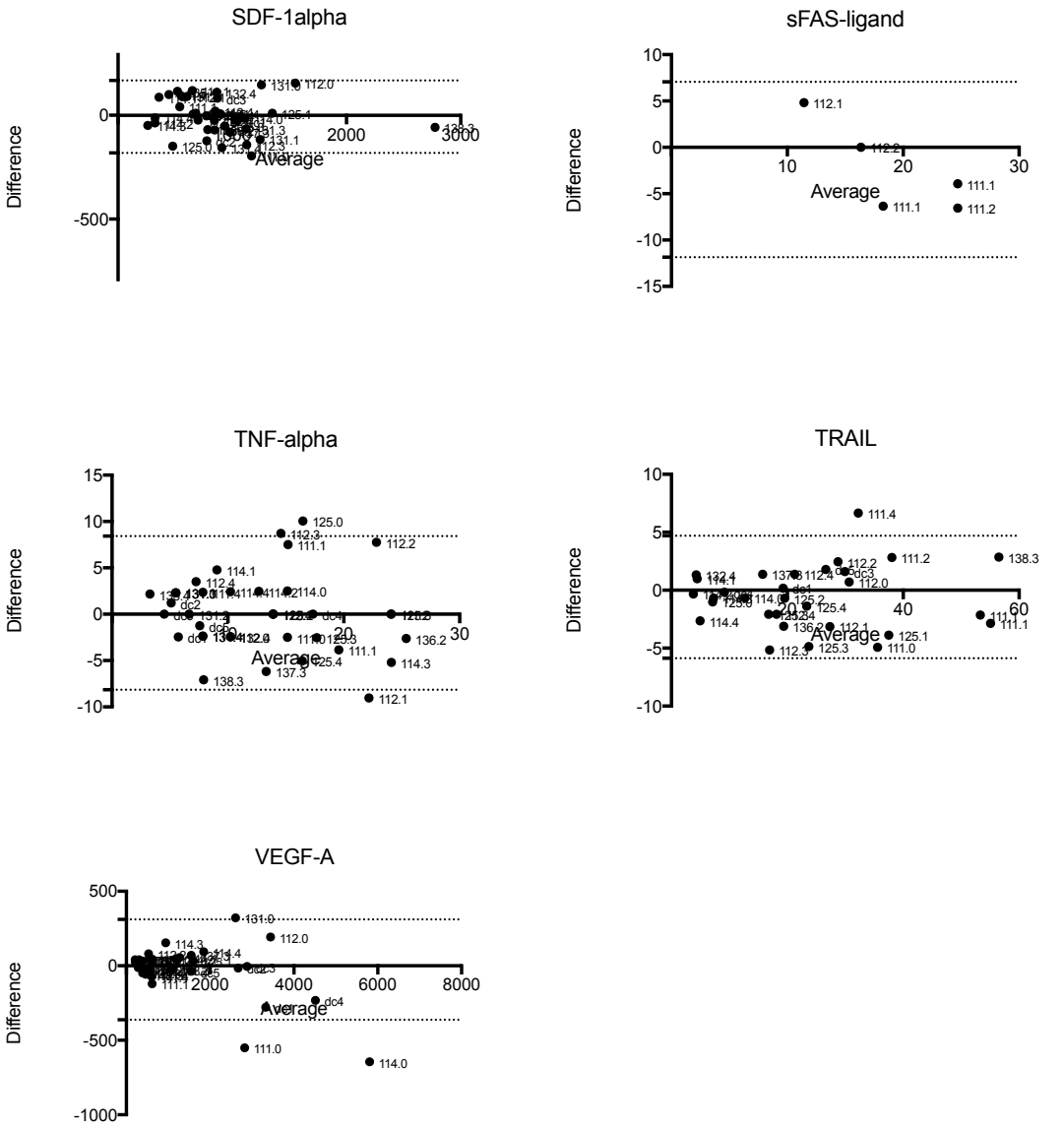

Supplementary Figure 3. Bland-Altman Plots for Intra-plate variability of all Panel 2 Plate 1 analytes Bland-Altman plots are shown for each analyte in the table. The analytes are labelled above. The mean average of two duplicates is on the x-axis (Avergage) and the difference from the mean is represented on the y-axis (Difference). The duplicates that fell outside of 2 x SD (represented as dotted line) could be excluded as an outlier with 95% confidence. The points are labelled with the KID-PID and the visit number (0-4) as KID-PID.Visit

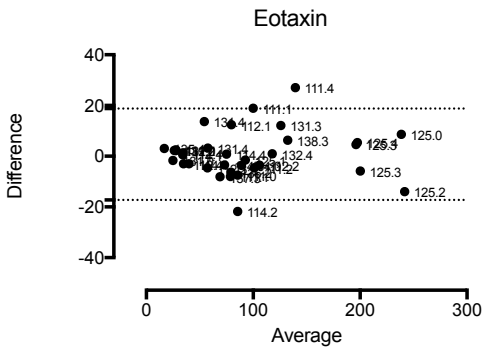
Eotaxin
Difference
Average

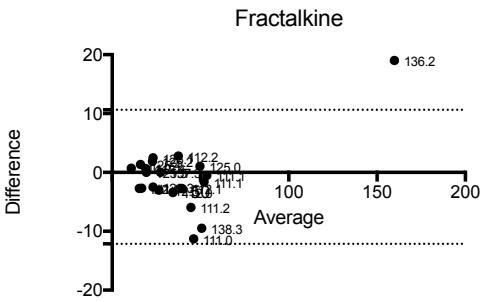
Fractalkine
Difference
Average

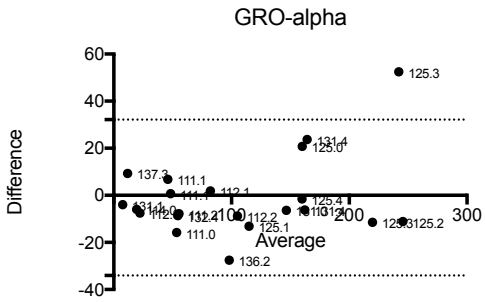
GRO-alpha
Difference
Average

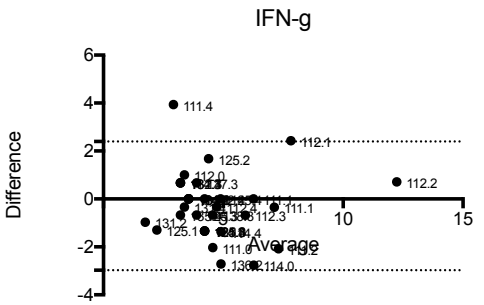
IFN-g
Difference
Average

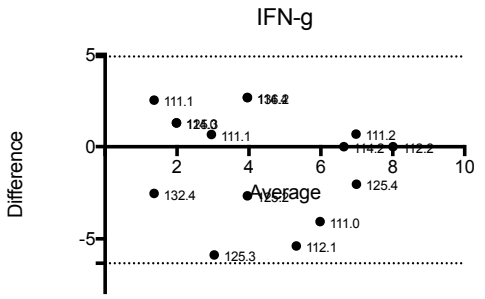
IFN-g
Difference
Average

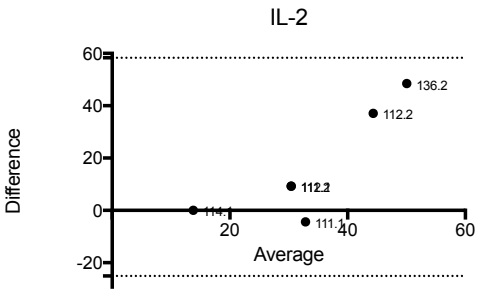
IL-2
Difference
Average

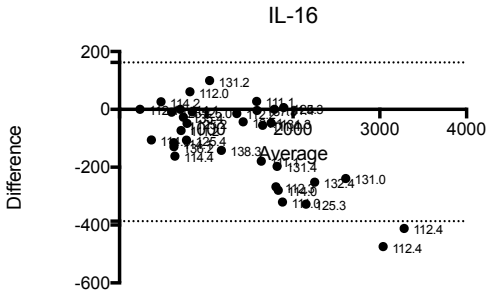
IL-16
Difference
Average

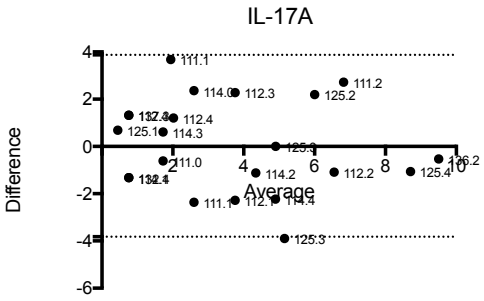
IL-17A
Difference
Average

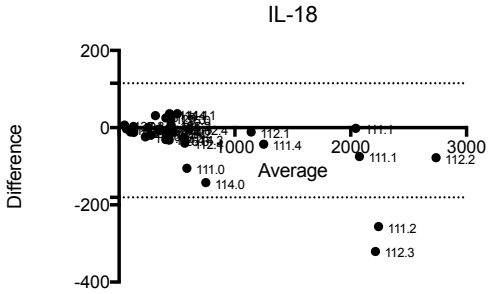
IL-18
Difference
Average

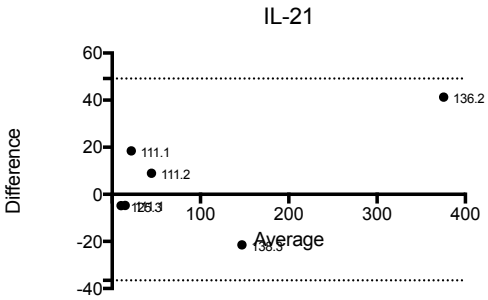
IL-21
Difference
Average

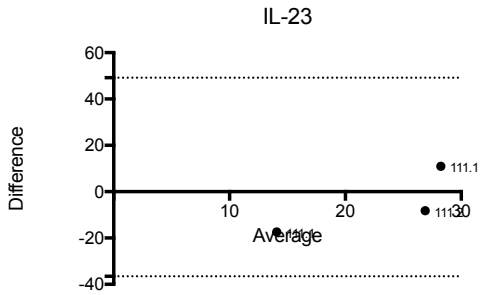
IL-23
Difference
Average

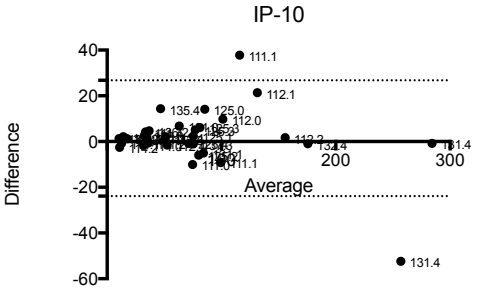
IP-10
Difference
Average

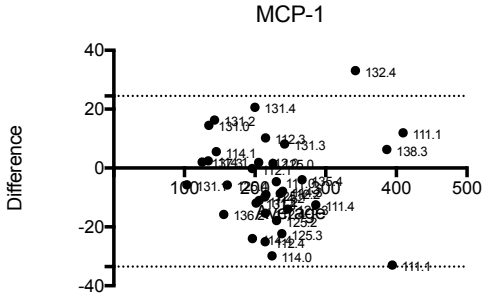
MCP-1
Difference

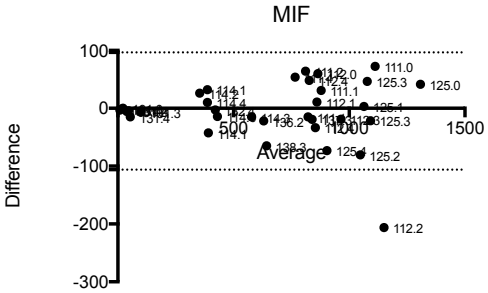
MIF
Difference
Average

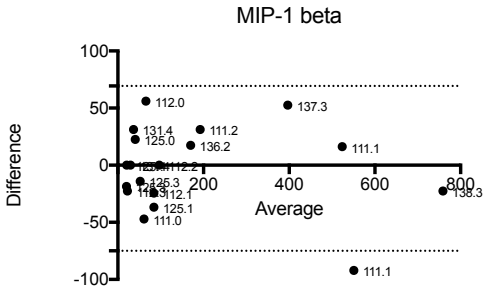
MIP-1 beta
Difference
Average

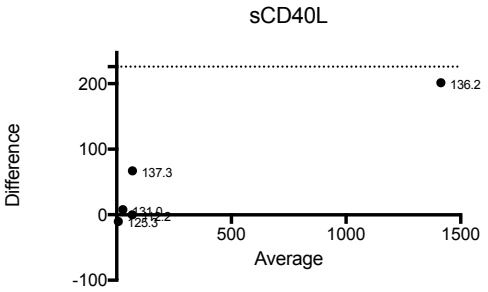
sCD40L
Difference
Average

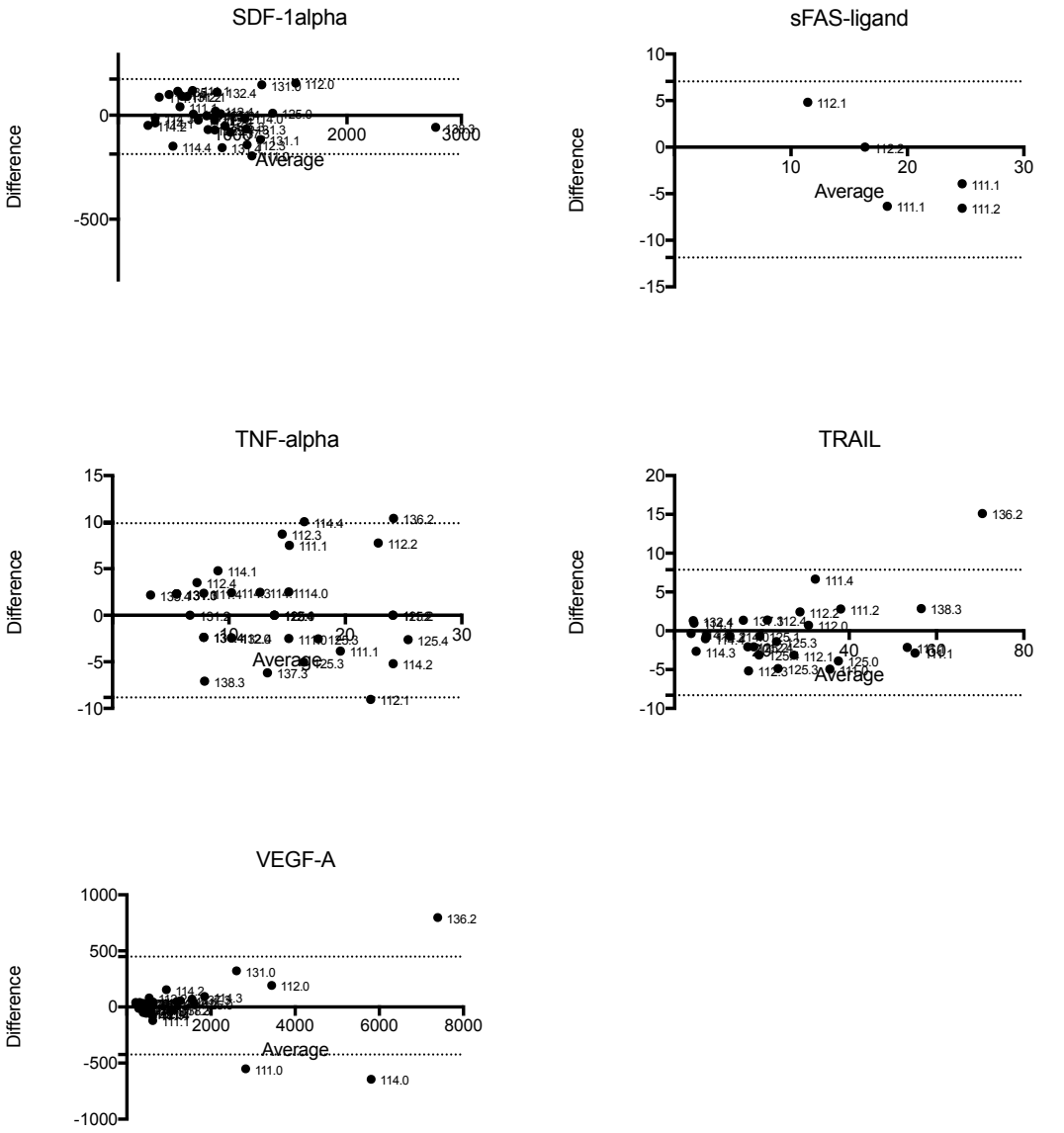

Supplementary Figure 4. Bland-Altman Plots for Intra-plate variability of all Panel 1 Plate 2 analytes Bland-Altman plots are shown for each analyte in the table. The analytes are labelled above. The mean average of two duplicates is on the x-axis (Average) and the difference from the mean is represented on the y-axis (Difference). The duplicates that fell outside of 2 x SD (represented as dotted line) could be excluded as an outlier with 95% confidence. The points are labelled with the KID-PID and the visit number (0-4) as KID-PID.Visit